**University of Strathclyde**

**Department of Pure and Applied Chemistry**

# Extraction Methods for Assessing the Bioaccessibility of Potentially Toxic Elements in Urban Airborne Particulate Matter by Inductively Coupled Plasma Mass Spectrometry

By

**Jawad Ali Hussein Alpofead**

A thesis submitted to the Department of Pure and Applied Chemistry, University of Strathclyde in partial fulfillment of the requirements for the degree of Doctor of Philosophy

August 2016

This thesis is the result of the author's original research. It has been composed by the author and has not been previously submitted for examination, which has led to the award of a degree.

## DEDICATION

To my dear parents and my family

To my teachers from primary school to the PhD

**Acknowledgements**

I would like to express my sincere gratitude to my supervisor, Dr Christine M Davidson for her supervision, support, academic guidance, expertise and patience, which has helped in different areas of my research work.

I would also like to thank my second supervisor, Professor David Littlejohn for his valuable advices and support during my study.

My appreciation also goes to the Iraqi government/Ministry of Higher Education and Scientific Research/University of Thi-Qar and Ministry of Education for funding and the opportunity to study for a PhD in the United Kingdom.

My colleagues and office mates in the Analytical Chemistry Research Group have been helpful and kind since I joined them. Special thanks goes to Dr. Pamela Allan, Alex Clunie, Matthew Palmer, Mara Knapp, and Moira McMenemy for their help.

I want also to thank Dominic Callaghan of the Glasgow City Council for supplying the exposed FDMS filters.

Thanks also to my parents who have helped me through numerous stages in life, which spans growing up, education and personal development.

Most importantly, I would like to thank my wife; my daughter, Rawasee; and my son, Mohammed, for their patience and support during my tenure on this research work.

## Table of Contents

## Abstract

Inhaled particulate matter (PM), containing bioaccessible potentially toxic elements (PTE) has attracted attention due to potential human health risk. This study was to develop and assess the suitability of simplified bioaccessibility extraction test (SBET) and the stomach phase of unified bioaccessibility method (UBMSG) to measure bioaccessible PTE in $PM_{10}$ collected on filter dynamic measurement system (FDMS) filters used worldwide. Analytes were As, Cd, Cr, Cu, Fe, Mn, Ni, Pb, and Zn and measured by ICP-MS.

The SBET and UBMSG were miniaturised for application to $PM_{10}$. Reducing sample mass and reagents volume by a factor of 10 for the SBET and by a factor of 6 for UBMSG, and presence of the FDMS filter did not affect PTE extractabilities. Bioaccessible PTE in blank FDMS filters were generally low, except for Zn. Washing acrodisc® syringe filters immediately before use with 80 mL of glycine reduced the concentration of Cu and Zn in procedural SBET blanks from 119 and 1520 to 0.129 and 14.5 μg $L^{-1}$, respectively.

New closed-loop and single-pass dynamic models for the SBET and UBMSG either coupled or not with ICP-MS were successfully applied to determine bioaccessible PTE in real and simulated $PM_{10}$ samples. Accuracy of models was ascertained by mass balance, and verified by Z-scores, which were generally acceptable. For single-pass models, rapid mobilization was observed for PTE, except for Cr.

Finally, a new artificial mucus fluid was applied sequentially with the SBET and UBMSG (gastric fluid only) to measure bioaccessible PTE in inhaled $PM_{10}$. Bioaccessible PTE concentrations, which were underestimated for As, Cr, Cu, and Pb, and overestimated for Cd, Fe, Ni and Zn using ingestion route alone, were more accurately determined. Extraction methods that are more similar to real body processes were successfully created to determine bioaccessible PTE in $PM_{10}$ that are inhaled and subsequently ingested.

# 1 Introduction

## 1.1. Airborne particulate matter (PM)

### 1.1.1. Composition of airborne PM

Airborne particulate matter (PM) is an air pollution term that refers to solid particle and liquid droplets that are suspended in the air. It is composed of elemental and organic carbon, trace elements, mineral, $SO_4^{2-}$, $NO_3^-$, $NH_4^+$, and water.

Atmospheric PM originates either as primary particles such as carbonaceous and metallic particles or as secondary particles such as sulfates, nitrates and organic aerosols.[1] The secondary particles are formed by gas-to-particles conversion processes. For example, $SO_4^{2-}$, $NO_3^-$, and secondary organic aerosols are formed from the oxidation of $SO_2$, $NO_x$ and volatile organic compounds, respectively. The primary particles are emitted directly from sources - either anthropogenic or natural sources.[2] The anthropogenic sources of airborne PM are:

- Industrial processes;
- Transportation sources (*e.g.* vehicles);
- Fuel combustion (*e.g.* coal and oil combustion); and
- Non-industrial short-term sources such as road dust, wind erosion of agricultural lands, and rebuilding processes.[1, 3]

While natural sources of airborne PM are:

- Crustal material from weathering of rock and erosion of soil;
- Activity of volcanoes *e.g.* to produce $SO_2$;
- Sea spray;
- Burning vegetation; and
- Reaction between natural gaseous emissions.[1, 3]

Airborne particles originating from natural sources represent 75 to 80% of total particles in the atmosphere. However, as a result of anthropogenic activities in a certain area, particularly in industrial sites, this percentage may change significantly.[3] During the atmospheric lifetime, processes such as condensation,

evaporation, coagulation, and chemical reaction can change both the size and the composition of airborne PM. Dry deposition (i.e. deposition at the Earth's surface) and wet deposition (i.e. following incorporation into cloud droplets) are two mechanisms that describe the removal of particles from the atmosphere.[3]

The chemical structure of airborne PM varies considerably and depends on several factors such as the climate of the region, combustion sources, season, and types of industrial or urban contamination.[4] The components of airborne PM can include:

- Volatile or semi-volatile organic compounds, which can be adsorbed onto PM, *e.g*. polycyclic aromatic hydrocarbons;
- Transition metals *e.g*. Cu, Fe, and Ni;
- Ions *e.g*. $NO_3^-$ and $SO_4^{2-}$;
- Active gases *e.g*. ozone;
- Carbonaceous material *e.g*. black carbon and organic material;
- Substances of biological origin *e.g.* bacteria, viruses, animal and plant debris); and
- Minerals *e.g*. quartz (silicon dioxide), asbestos, and soil dust.[4]

The aerodynamic diameter of airborne PM is generally from about 1 or 5 nm to 100 μm.[5] Size categories of airborne PM tabulated in Table 1.1 have been defined differently by different organizations. Typical airborne PM consists mostly (90 to 95%) of coarse particles, while only 1% to 8% of the whole mass of airborne PM is small particles.[4] Most fine and ultra-fine particles are produced by releases from vehicles. In contrast, most coarse particles are created by material that is broken down by mechanical processes.[4] Sea salt, insoluble crust-originated metals, and biological substances are the main components of coarse particles. In contrast, the composition of fine and ultrafine particles consist essentially of organic species and carbonaceous combinations with minerals.[6]

**Table 1.1. Different definitions for size categories of airborne PM***

| Categorisation system | Size particle | Definition | References (notes) |
|---|---|---|---|
| 1 | < 0.1 μm | Nuclei mode | Health effects institute (HEI) [5] |
| | 0.1μm - 1 μm | Accumulation mode | |
| | > 1 μm | Coarse mode | |
| 2 | < 0.1 μm | Ultrafine particles | HEI [5] |
| | < 1 μm | Fine particles | (Used in health effects studies) |
| 3 | < 2.5 μm | $PM_{2.5}$ | Valavanidis *et al.*, 2008 [4] |
| | < 10 μm | $PM_{10}$ | (Defined by the USEPA)** |

*Airborne particulate matter (PM); ** The US Environmental Protection Agency (USEPA)

### 1.1.2. Toxic effect of airborne PM

A correlation between daily death counts and short-term variations in PM air contamination was observed by many studies in the USA. Results suggested that a 0.5% to 1.5% rise in daily deaths was related with a 10 μg $m^{-3}$ rise in $PM_{10}$.[7, 8] Concentrations of pollutants in the $PM_{10}$ size fraction are higher than those in larger size particles because of the high surface-to-mass ratio for $PM_{10}$.[9] Similarly, pollutant levels in the $PM_{2.5}$ fraction are larger than those in the $PM_{10}$ fraction. The $PM_{2.5}$ fraction is mostly held by lung airways and alveoli, in contrast to $PM_{10}$ which does not penetrate so far into the human respiratory tract.[10] A study has demonstrated that particles less than 2.5 μm in diameter represent 96% of particles retained in the lung "parenchyma", whereas only 5% were ultra-fine particles.[11] Metals such as Cd, Ni, and Pb are one specific group of airborne PM components that cause toxic influences. These metals are related with many adverse health impacts such as cancer.[12, 13] Nevertheless, metals in urban airborne PM exert toxic effects only when they are biologically obtainable.[13] Transition metals are believed to be very important in PM cellular toxicity.[14, 15]

Moisture content of the inhaled air can change the chemical properties of inhaled airborne particles and thus determine deposition locations of airborne PM in the respiratory tract.[16] In addition, particle shape and size are significant determinants that regulate the range of permeation of inhaled airborne particles in the human respiratory tract.[12] Many researches have illustrated that the possibility of appearance of biological effects such as oxidative damage and inflammatory injury is determined by the size of the airborne particles and their surface area.[4]

The majority of inhaled smaller particles (<2.5 μm) can penetrate into the pulmonary alveoli, where they are deposited and can remain for a long time, while the majority of particles <10 μm can reach the upper airways of the respiratory tract, where they can cause adverse respiratory health effects (see Fig. 1.1).[17-19] Adverse respiratory health effects associated with concentrations of PTE in inhaled airborne PM have been strongly evidenced by recent epidemiological studies.[20] For example, one study showed that within 24 hours of a contamination incident, each of the alveolus and the lung acinus could receive about 1500 particles and 30-million particles respectively of which 50% were precipitated.[21]

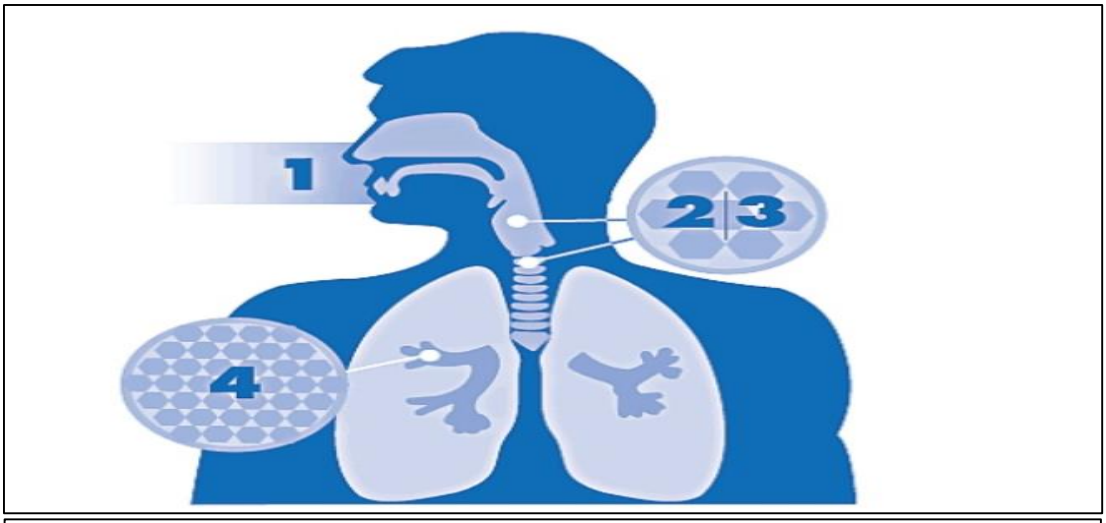


**(1)** Particulate matter enters respiratory system through the nose and throat.
**(2/3)** The larger particulate matter ($PM_{10}$) is eliminated through coughing, sneezing and swallowing.
**(4)** $PM_{2.5}$ can penetrate deep into the lungs. It can travel all the way to the alveoli, causing lung and heart problems, and delivering harmful chemicals to the blood system.

**Figure 1.1. Introduction to particulate matter and deposition in the respiratory lung system**[22]

### 1.2. Soils as a source of airborne PM

Ingestion or inhalation of dust is an important pathway for human exposure to soil. Many studies have shown that soils are a source of $PM_{10}$. For example, Mossetti *et al.*[23] found that the soil dust in the city of Milan, Italy, provided 15% of $PM_{10}$, whereas in Madrid, Spain, crustal contribution accounted for up to 67% of the $PM_{10}$.[24] Results obtained from another study[25] revealed that 69.4% of the trace elements in airborne PM originated from crustal material and road dust.

#### 1.2.1. Soil components and pollution

Soils are complicated systems with chemical, biological, and physical properties that change over time and with location. Aluminium, silicon, oxygen and iron are main components of the soil matrix.[26] A large number of additional elements with various properties and potential impacts on the environment are present in urban soils. They can accumulate in soils for decades or centuries because they cannot be decomposed by any method.[27] The environmental and health concerns from pollution of soil with metals has attracted attention because soils often act as a sink for potentially toxic elements (PTE) resulting from different anthropogenic sources.[28] Considerable pollution of soils is caused by smelting and mining activities[29] *e.g.* mining dust and the emissions and slag damps from smelters.[30, 31]

#### 1.2.2. Risks from contaminated urban soils

In the last two decades, interest in the properties of urban soils has greatly increased. Many studies have been conducted on soils of cities across the world such as Glasgow, UK,[32, 33] New Orleans, USA,[34] Gaborone, Botswana,[35] Seville, Spain,[36] Sydney, Australia,[37] Beijing, China,[38] and Turin, Italy.[39] Results of these studies show that there was a high concentration of some elements in urban soils. Over recent decades, knowledge on PTE contamination in urban soils has increased as their implication for human health has become a greater concern to the public and the media.[40] Anthropogenic activities affect urban soil properties, and the concentrations of many types of contaminants in the soil of urban areas are higher than their concentration in countryside areas.[39, 41] Polluted urban soils can cause considerable direct hazard to human health through dermal contact, dust inhalation, and soil

ingestion because of the closeness of a large number of city inhabitants.[42, 43] Soil pH, organic matter, clay-sized particles, redox conditions, carbonate minerals, and chemical speciation are the major determinants that regulate PTE bioavailability and mobility following ingestion.[44]

### 1.3. Potentially toxic elements (PTE) in $PM_{10}$

In general, urban airborne PM have higher concentrations of PTE than rural airborne PM, arising from widespread sources of contamination in cities, both natural sources such as soils and anthropogenic sources such as fuel combustion and traffic.[25, 45-47] The dominant pathway of exposure to PTE (i.e. ingestion or inhalation) is based on the nature of activities in a certain region, e.g. inhalation may be the principle route of exposure to PTE such as Ni in industrial or high traffic density areas. Chemical forms and ways of bonding of PTE in airborne PM may be various.[47] The PTE in airborne PM are mainly found in the water-soluble fraction.[47] However, PTE that combine to fractions such as carbonates, oxides, organic matter, and exchangeable portions can be partly dissolved in the acidic environment.[48] The chemistries of the PTE studied in this work are summarised in the following sections.

#### 1.3.1. Arsenic

Arsenic is a highly toxic metalloid.[49] Its concentration in the Earth's crust ranges between 0.5 and 2.5 mg $kg^{-1}$. In the air, the concentration of As varies extremely from about 0.007 ng $m^{-3}$ at the South Pole to above 50 ng $m^{-3}$ in urban regions.[50] Arsenates represent about 60% of As minerals.[51] Arsenopyrite, FeAsS; realgar, AsS; arenolite, $As_2O_3$; and orpiment $As_2S_3$, are its common minerals. Though As minerals and its compounds are readily soluble, As migration is greatly restricted in soils because it is strongly absorbed by clays, hydroxides, and organic matter.[50] The oxidation states of As are -3, 0, +3, and +5, and $As^{III}$ is more poisonous and mobile in soils than $As^{V}$. The most common mobile forms of As are the complex anions such as $AsO_2^-$, $AsO_4^{3-}$, $H_2AsO_3^-$, and $HAsO_4^{2-}$.[51] An alloy of As acts as a good solder, and some of its compounds are used as insecticides and weed killers. Arsenic minerals such as orpiment and realgar are used as golden paint and orange red pigment, respectively, and orpiment can be used as a hair remover.[49] Organic As compounds are used to produce pesticides, and they are used in glassware, wood protection, photoelectric devices, and Pb-acid batteries.[50]

Arsenic is mostly recovered from sludge after smelting of Ag, Au, Cu, Pb, and Zn ores, which are normally enriched in As. A significant source of As may be agricultural practices, as its contents may be raised in fertilizer, sludge, pesticides, and manure leading to increased contents of As in agricultural soils.[50] Dusts from soils, volcanic eruptions, sea salt aerosols and forest fires are the natural sources of As in the atmosphere. Because As and some of its compounds are easily volatile and normally escape to the gas and aerosol phases through coal combustion, a main source of As to the atmosphere is coal combustion.[50]

In low doses, As produces vomiting, diarrhea, and nausea in humans, whilst abnormal heartbeat and damage to blood vessels can result from larger doses. Redness and swelling can result when the skin contacts directly with As.[52] Long-term exposure to As and its compounds and inhaling them can cause cancer.[52]

### 1.3.2. Cadmium

Cadmium is very rare, silvery white colour, a good electrical conductor, and resistant to corrosion.[49] Mean content of Cd in the Earth's crust is between 0.1 and 0.2 mg $kg^{-1}$. Concentration of Cd in the atmosphere at urban sites varies from 2 to 150 ng $m^{-3}$, while in rural areas it ranges from 0.1 to 4 ng $m^{-3}$.[50] The global average concentration of Cd in soils ranges from 0.06 to 1.1 mg $kg^{-1}$. A pure form of Cd occurs rarely in nature.[50] Cadmium has a greater attraction for sulfur than Zn, and also a higher mobility than Zn in acid environments. During weathering, Cd moves readily into solution.[51] A strong correlation is observed for Cd with Mn and Fe contents in soils, and Cd in soils is not easily mobile at pH greater than 7.5.[51] Greenockite, CdS; monteponite, CdO; and octavite, CdSe are the common minerals of Cd. Simple Cd compounds that are easily mobile such as $Cd(OH)_2$, $CdCl_2$ and $CdF_2$ are formed during weathering processes, and between 55 and 90% of Cd in soil solution exists as free metal ion $Cd^{2+}$.[50] A rise in pH results in an increase in the sorption of Cd on humic material. Cadmium and its compounds have insignificant vapour pressures due to which they exist in the atmosphere as suspended PM. As a result, small particles containing Cd may cross a national boarder and travel for a long distance.[50]

Cadmium alloys can be used in fire discovery equipment and fire safety devices such as safety fuses and automatic water sprinklers.[49] The pure Cd metal is appropriate as control rods in atomic reactors. Cadmium is used as the anode in nickel-cadmium batteries.[49] Cadmium salts act as colouring agents for soap, glass, enamels, paper, paints, rubber, and leather printing ink. The chloride, iodide, and bromide of Cd can be used in photographic films.[49]

It has been proposed that major sources of Cd emissions to the atmosphere are coal and oil fired power plants and metal industries. However, natural sources such as forest fires, rock dusts, wind-blown soil, and volcanic activity may also contribute to Cd concentration in air.[50] Mining and refining of Zn mainly produce Cd as a byproduct.[50] Moreover, recycling of some materials such as zinc-cadmium batteries is one of the sources of Cd, whilst atmospheric depositions and P-fertilizers are considered the major sources of soil pollution with Cd. The majority of Cd contamination, up to 90%, from different sources remains in the top 15 cm layer of soil.[50]

Cadmium is one of the most ecotoxic metals that cause adverse effects on human health.[50] Coal burning, cigarette smoking, drinking polluted water, and eating certain foods such as liver and kidney lead to the entry of Cd to human body. Manufacturing plants for batteries that used Cd as a fine powder can easily be a source of Cd inhalation. Dryness of the throat, and headache can result.[52] Cadmium can escape from landfills and infiltrate the ground and groundwater, so it can become part of the food and water that humans and other animals ingest. Low levels of Cd cause vomiting, diarrhea, and nausea, while heart and kidney disease, high blood pressure, and cancer are the effects of extensive exposure to Cd.[52]

### 1.3.3. Chromium

The abundance of Cr in Earth's crust is from 100 to 300 mg $kg^{-1}$.[52] Chromium concentration in air highly varies from 0.003 ng $m^{-3}$ above the South Pole to over 1000 ng $m^{-3}$ in manufacturing areas, and from <10 ng $m^{-3}$ in rural areas in the USA to 10–30 ng $m^{-3}$ in urban areas.[50] The world median content of Cr in soils is 54 mg $kg^{-1}$.[50] Chromium does not appear as a free element.[52] It has many oxidation states from +2 to +6, and it is also well known to form complex anionic and cationic

ions *e.g.*, $CrO_4^{2-}$ and $Cr(OH)^{2+}$. Chromium compounds are considered to be very stable in soils because $Cr^{III}$ is slightly mobile only at very low pH values, and it is almost entirely precipitated at pH 5.5. In contrast, mobilization of unstable species of $Cr^{VI}$ ($HCrO_4^-$ and $CrO_4^{2-}$) is easily in either acidic or alkaline soils.[51] Greatly oxidized Cr forms ($Cr^{VI}$) are much more mobile than $Cr^{III}$ species, particularly in very acid and alkaline ranges of pH.[50]

Chromium is used in different fields such as stainless steel, chromate plating, metal finishing, colourings, wood preservatives, leather tanning, and paper production. However, it is mainly used in refractory, metallurgical and chemical industries.[50]

A major natural source of Cr in the atmosphere is continental dust flux. However, more than 70% of Cr in the atmosphere is contributed by anthropogenic sources, principally from fuel combustion and emissions of mineral industries.[50] Liquid and solid wastes from dyestuffs and leather tanning, as well as industrial and residential sewage treatment plants, are considered the main sources of Cr pollution. Elevated Cr content in surface soils is recognized due to contamination from different sources, of which the principal ones are wastes of leather manufacturing, domestic wastes, and tannery and pigments wastes.[50]

Readily soluble $Cr^{VI}$ in soils is poisonous to plants and animals.[51] Chromium is essential for human and animal nutrition.[51] Small amounts of Cr are necessary for the health of plants and animals and Cr shortage leads to diabetes-like symptoms.[52] In contrast, larger amounts of Cr are of concern, and some of its compounds are particularly hazardous, causing a rash or sores if spilled on the skin; sores in the throat and mouth if inhaled; and damage to the throat, stomach, intestines, and kidneys if swallowed. Researchers consider that an exposure to some Cr compounds on a long-term basis causes cancer.[52]

### 1.3.4. Copper

The concentration of Cu in the Earth's crust is between 25 and 75 mg $kg^{-1}$.[50] Copper content in the air varies greatly from 0.03 to 0.06 ng $m^{-3}$ around the South Pole up to 4900 ng $m^{-3}$ in manufacturing areas of Germany.[50] Copper has a strong affinity for sulfur, therefore its major minerals are chalcocite, $Cu_2S$; chalcopyrite, $CuFeS_2$;

covellite, CuS; and bornite, $Cu_5FeS_4$.[50] Copper minerals are quite readily soluble in weathering processes and liberate Cu ions, particularly in acid media.[51] Copper ions can also easily precipitate with different anions such as carbonate, hydroxide and sulfide. Hence, Cu is rather immobile in soils. However, Cu ions are very strongly bound on both organic and inorganic exchange sites.[51] The solubility of cationic and anionic forms of Cu declines above pH 7 to 8.[51] Soil texture, pH, and organic matter control the Cu solubility and consequently bioavailability.[50] Coarse structure, high pH, and a high content of organic matter each cause the deficiency of Cu in soils.[50]

Copper is utilized for the manufacture of conductor materials, wire, and rod. Copper is also extensively used in agricultural fertilizers and pesticides.[50] The pure metallic form of Cu is used in the manufacture of motors, generators, switchboards, and different household appliances. Copper sulfate is used as a blue dyestuff.[49] Copper is also used as a feed additive in livestock and poultry nutrition because of its bacteriostatic characteristics.[50]

Natural sources of Cu in the atmosphere are volcanoes, thermal springs, weathering of rocks and driven dust from earthly components. Oxide forms of Cu are frequently related with dust particles and are moderately readily dissolved in rainwater.[50] Sources of industrial contamination have a local environmental influence, and they also contribute to the universal long-distance contamination of the atmosphere.[51] Use of Cu-containing material (*e.g.* fertilizers, sprays) and agricultural or domestic wastes, as well as corrosion of Cu alloy construction materials (*e.g.*, electric wires, pipes) and industrial emissions, lead to soil pollution by Cu compounds.[51]

Copper is an important micronutrient for animals and plants. Healthy human has no more than about 2 mg of Cu for every 1 kg of body weight.[52] Copper enzymes play a role in the production of blood vessels, bones, nerves, and tendons. Animals occasionally become ill as a result of a lack of Cu, and Cu-deficiency disorders can appear with animals that live on land that lacks Cu.[52] Large concentrations of Cu in the human body generally do not cause a problem except in a condition known as Wilson's disease. However, mental illness, and death can result when the Cu level becomes too great.[52]

### 1.3.5. Iron

The average content of Fe in Earth's crust is estimated to be approximately 5 percent, and it is not considered a trace element in soils.[50] Iron concentration in air varies from 0.5 to 1.2 ng $m^{-3}$ above the South Pole, and from 166 to 171 ng $m^{-3}$ above Greenland.[50] Iron content in soils is between 0.1% and 10%, and it increases with a rise in the amounts of particles (<20 μm) in soils.[50] Forms of Fe in soils are considered to appear mainly as oxides and hydroxides associated with the surfaces of other minerals or as small particles. In soils that have high content of organic matter, Fe occurs principally in a chelated form.[51] The oxidation status of Fe in most minerals created near the Earth's surface is +3, whereas in deeper rocks it is +2.[50] Exogenic and endogenic cycles of Fe are recognized. The first takes place at the surface and includes the action of water and air; while the second one occurs underneath the surface of the Earth, and involves geological processes such as melting. Ferric oxides such as hematite are principal Fe ore minerals. In addition, pyrite, $FeS_2$; and siderite, $FeCO_3$ are composed of other Fe minerals.[50] The Eh-pH system and the oxidation state of the Fe compounds largely determine the fate of Fe in the processes of weathering. Mobilization of Fe compounds is promoted by acid and reducing conditions, whereas alkaline and oxidising conditions promote the precipitation of Fe.[50]

Both terrestrial and industrial sources are the origin of Fe in the atmosphere. A 33–38% of the weight of aerial dust in urban region is Fe.[50]

Iron is significantly important to plants, humans, and other animals. It contributes in the composition of the haemoglobin molecule that carries oxygen in the blood. Iron shortage can lead to severe health problems in humans: for example, haemoglobin molecules may not form in sufficient numbers, or lose the capability to carry oxygen. As a result, anaemia can result.[52]

### 1.3.6. Lead

The concentration of Pb in Earth's crust is assessed to be between 13 and 20 mg $kg^{-1}$. Its occurrence in the earth is rarely as a pure element.[52] Concentration of Pb in air varies greatly from about 1 ng $m^{-3}$ around the South Pole to above 10000 ng $m^{-3}$ in

industrial urban sites. Natural concentration of Pb in soils ranges from up to 40 mg $kg^{-1}$ in light sandy soils to up to 90 mg $kg^{-1}$ in heavy loam soils.[50] Oxidation states of Pb are +2 and +4, but it occurs mainly as $Pb^{II}$, and its minerals are quite insoluble in natural waters. Lead is stated to be the least mobile among the PTE, and it may be precipitated as hydroxide, phosphate, or carbonate when a soil has high pH.[51] Lead solubility may be increased with a rise in acidity, but, in organic-rich soils, accumulation is generally faster than this mobilization.[51] Remobilization of Pb in different environments can cause toxic effects to their species.[50]

Lead plates are used in acid batteries. Its compound (tetraethyl lead) is utilized as an anti-knocking substance added to petrol to reduce spark knock and to increase the efficacy and life of an engine.[49] It is also used for radiation shielding in atomic reactors, high-altitude flying aircrafts, and X-ray machines due to its high density. Lead is the appropriate material in tanks that are used for handling sulfuric acid because of its high resistance to acid corrosion.[49] Solder, an alloy of tin and Pb, is used to weld electronic parts. Some of its compounds have other uses *e.g.* Pb arsenate is used as an insecticide, oxides of Pb are utilized in processing of different products such as glass and synthetic rubber.[49]

Sources that contribute to the introduction of Pb into the atmosphere include:

- Coal and oil combustion in electric power plants;
- Roasting and smelting processes;
- Petrol combustion;
- Incineration of waste and cement production.[50]

Most Pb contamination in the eighth and ninth decades of the 20$^{th}$ century was from use of leaded petrol, but in the 1990s, strict regional regulation has effectively removed the use of Pb in petrol in developed countries.[50] Nonetheless, several countries still use it, such as in Nigeria, where Pb in petrol is approximately 0.6 g $L^{-1}$, which is the highest concentration noted in the world. Obvious soil Pb

pollution occurs in the proximity of mining and industrial activities, in urban regions, and along roads with high-traffic densities.[50]

Lead can cause immediate and long-term health problems, particularly to children, and the ingestion and inhalation of Pb results in toxicity. Children are considered the most vulnerable to Pb exposure because they can have an abnormal desire to eat materials such as dirt, paper, and chalk, and sometimes eat paint chips off walls.[52] Some symptoms of Pb toxicity involve vomiting, extreme tiredness, nausea, and high blood pressure.[52] The accumulation of Pb in the human body can occur when the duration of Pb inhalation is months or years. This type of Pb poisoning can lead to nerve harm and problems with the stomach and intestines.[52]

### 1.3.7. Manganese

Manganese always occurs as a compound in nature combined with oxygen or other elements. Its abundance in Earth's crust is from 0.085 to 0.10 percent.[52] Concentration of Mn in the air varies from <0.02 ng $m^{-3}$ above the South Pole to 900 ng $m^{-3}$ above industrial areas of the USA. Contents of Mn in soils are highly varied between 10 and 9000 mg $kg^{-1}$.[50] Its minerals include oxides, carbonates and silicates.[49] Manganese is found in a number of minerals in which it usually appears as $Mn^{II}$, $Mn^{III}$, or $Mn^{IV}$, but its +2 oxidation state is most common in the rock-forming silicate minerals. There is a high degree of association of Mn with some elements *e.g.* Cu, Ni, Pb, and Zn due to the negatively charged manganese (IV) hydroxide.[51] Manganese oxide can increase the mobilization of some metals under particular soil conditions because of its reducing and oxidizing properties. However, Mn oxides have a great influence on the immobilization of trace elements in soils.[51] During weathering and under atmospheric conditions, Mn is oxidized in minerals and may be mobilized. Manganese is concentrated in residual deposits under weathering in equatorial and semitropical conditions, whilst under wet cold environment, Mn is leached by acid solutions from soils.[50] Manganese (II) easily replaces other divalent cations *e.g.*, $Fe^{2+}$, $Mg^{2+}$.[50] The pH and redox potential highly affect the mobility of Mn in soils; generally Mn is highly mobile at acid values of pH.[50]

Steel becomes hard and resistant to corrosion when Mn is added.[52] Manganese alloys are used in electrical manufacturing *e.g.*, of dry-cell batteries. It is also extensively applied in the production of ceramics, glass and pigments. Manganese sulfate is utilized as fertilizer and as animal feed supplement.[50]

There are both natural and industrial sources for Mn in the atmosphere. In aerial particles, Mn occurs principally as various oxides that readily react with $NO_2$ and $SO_2$ then dissolve in rainwater.[50]

Manganese has positive and negative impacts on organisms. A very small amount of Mn is needed to maintain good health in plants and animals.[52] The deficiency of Mn affects the activity of enzymes, whereas an excess of Mn can cause health issues comprising sleepiness, tiredness, weakness, and emotional disturbances.[52]

### 1.3.8. Nickel

Mean concentration of Ni in the Earth's crust has been estimated at approximately 20 mg $kg^{-1}$.[50] Nickel concentration in air is 120 ng $m^{-3}$ in urban areas. The world concentration of Ni in soils ranges from 0.2 to 450 mg $kg^{-1}$, and the highest Ni contents are in clay and loamy soils.[51] There are two classes of Ni ores primarily mined - sulfides and silicates - as well as other minerals such as Niccolite, NiAs.[49] During weathering, Ni is readily mobilized and then is co-precipitated mostly with Fe and Mn oxides. Usually there is an inverse correlation between the solubility of Ni in soil and soil pH.[51] In soils with high organic matter and in polluted soils, Ni may be completely mobile.[50]

The important uses of Ni metal are: alloys (*e.g.* stainless steel), Ni-plating, coinage, magnetic shielding, white gold.[49] The common uses of stainless steel are to manufacture household appliances, kitchen sink tops, and medical equipment.[52] Nickel super alloys are also utilized in jet engine parts and gas turbines. In addition, Ni is very common in the production of batteries *e.g.* nickel-cadmium and nickel-metal hydride (NiMH) batteries, which are mainly used in electronics.[52] Nickel compounds are utilized as dyes in ceramic and glass manufacturing. Nickel has been a common catalyst for the oxidation of various organic compounds, and for hydrogenation of fats and oils.[50]

Nickel lately has become a severe atmospheric contaminant that is liberated in emissions from the combustion of coal and oil.[51] Windblown dust and volcanoes are the principal natural Ni sources, while burning residual and fuel oil, and Ni metal refining are the main anthropogenic Ni sources.[50] Important sources of Ni also may be specific phosphate fertilizers and the application of sludge. Furthermore, a significant increase in the Ni content of soils has resulted from anthropogenic sources of Ni, specifically from industrial activities.[51]

Nickel can cause health risks to humans. The most common health problem is Ni allergy, and the most usual cause of Ni allergy is body piercing.[52] Other serious health problems can be caused by Ni, for instance, cancer may be caused as a result of long term Ni exposure.[52]

### 1.3.9. Zinc

Zinc abundance is estimated at approximately 0.02% of Earth's crust.[52] Commonly, Zn levels in the air are low and fairly constant. Zinc concentration in rural air is between 10 and 200 ng $m^{-3}$, whereas in urban air it can extend 16000 ng $m^{-3}$.[50] The worldwide average concentration of Zn in soils is estimated as 64 mg $kg^{-1}$.[51] Zinc always occurs as a compound in the Earth, and its important compounds comprise zinc sulfide (ZnS); zinc oxide (ZnO); zinc carbonate ($ZnCO_3$); and zinc silicate ($ZnSiO_3$).[52] During weathering, mobile $Zn^{II}$ is produced by solubilisation of Zn minerals, particularly in acid and oxidizing environments. Zinc is very similar to Cu in terms of the important factors controlling its mobility in soils, but Zn occurs in more easily soluble forms.[51] In acid media, adsorption of Zn is associated with cation exchange sites, whereas it is highly influenced by organic ligands in alkaline medium.[51]

Zinc is mainly used to protect steel components and other metals against corrosion. It is also widely used as a catalyst in various chemical manufacturing processes, for example pigments, plastic, pesticides, rubber, and lubricants.[50] Various compounds of Zn have dental and medical applications.[50] Further, zinc sulfidosilicate is used in the inner wall of fluorescent tubes as a fluorescent substance. Zinc is also utilized to make some non-rechargeable batteries *e.g.* dry cells.[49] The second largest use of Zn

is in making alloys, and the most usual alloys of Zn are brass and bronze used in different products, including automobile parts, electrical fuses, batteries, household utensils, and building materials.[52]

Particulate forms of Zn enter the atmosphere from industrial processes, cement factories, and from fuel-fired power stations. Zinc levels in soils can be enhanced by some fertilizers, specifically super phosphate.[50] The non-ferric metal industry and agricultural practice are considered the main anthropogenic sources of Zn.[51]

Zinc is an important micronutrient for plants, humans, and animals. In humans, Zn deficiencies are more serious than deficiencies of other PTE because it is used to build DNA molecules. Loss of hair and skin lesions may happen to children whose diet does contain enough Zn.[52] In contrast, an increase of Zn can cause health problems. Inhalation of Zn dust may cause coughing, general weakness and aching, dryness in the throat, chills, fever, nausea, and vomiting.[52]

### 1.4. Risk assessment of PTE in PM

Some elements have been commonly named as PTE because, when they exist at a specific concentration, they might become hazardous for human health.[27, 53] Human health and ecosystems, particularly in urban environments, may be exposed to risks from PTE in $PM_{10}$.[45, 54] Potentially toxic elements present in different substrates enter the human body through three routes: ingestion, inhalation, and dermal contact.[42, 55] In the inhalation route, PTE enter the respiratory system associated with inhaled airborne PM, and they may cause adverse effects on human health such as cardiopulmonary diseases and lung cancer.[4, 56] The concentration of PTE in substrates can be determined by either acid digestion (to obtain the total or pseudototal concentration) or by an extraction (to obtain the extractable fraction).

#### 1.4.1. Microwave acid digestion

Recently, increased safety and reduced digestion time have made microwave-assisted digestion methods popular.[57] Three procedures for microwave digestion have been established by the US Environmental Protection Agency (USEPA): 3051 ($HNO_3$), 3051a ($HNO_3$-HCl), and 3052 ($HNO_3$-HCl-HF). The first and the second procedures

were stated by USEPA to extract metals that can potentially be available in the environment.[57] To determine total element content i.e. all fractions even those bound to the silicates, soil is digested using HF.[58] Because most of the contaminated fractions, i.e. the potentially mobile or soluble contents of elements in soils are not bound to silicates, *aqua regia* is often used instead of HF to digest soils. This digestion gives the pseudototal element content because all fractions are digested except those bound to silicates.[58, 59] Microwave assisted *aqua regia* digestion utilising Teflon bombs is considered an accelerated sample digestion method.[60]

### 1.4.2. Single and sequential extraction

An extraction is a separation technique, and its basis of separation is the selective partitioning of an analyte or an interferent between two immiscible phases.[61] Single and sequential extraction techniques have brought the principal attention of environmentalist, especially in the investigation of the fate of environmental contaminants. Many important studies - including those aiming to assess the composition and structure of soil constituents, clarify soil chemistry, and study factors influencing the mobilization and retention of toxic elements in soils - have used single and sequential extraction techniques.[59] Suitable models to mimic flooding and raining incidents are un-buffered salt solutions that are used in single extraction methods. Choice of an extractant in single extraction methods depends on the targeted phases.[59]

#### 1.4.2.1. Bioaccessibility of PTE

Measurement of total or pseudototal PTE concentrations in airborne PM generally gives a poor indication of health risk because not all PTE species present are equally labile and equally able to affect health.[62] Therefore, bioavailability and bioaccessibility tests are considered critical ways to assess these hazards.[63] Bioavailability and bioaccessibility are complicated topics that provide information of whether or not negative influences are to be expected when organisms are exposed to a pollutant.[57, 64]

A study of bioaccessibility is the first step in an evaluation of bioavailability. In the context of oral ingestion, it highlights the fraction of a trace element that is released

from its matrix in the gastrointestinal tract, and theoretically becomes available for absorption by the intestines to reach the blood stream.[29, 65, 66] In contrast, the bioavailable fraction is the amount of an element that is actually transferred across cell membranes and enters the blood (see Fig. 1.2).[67-70]

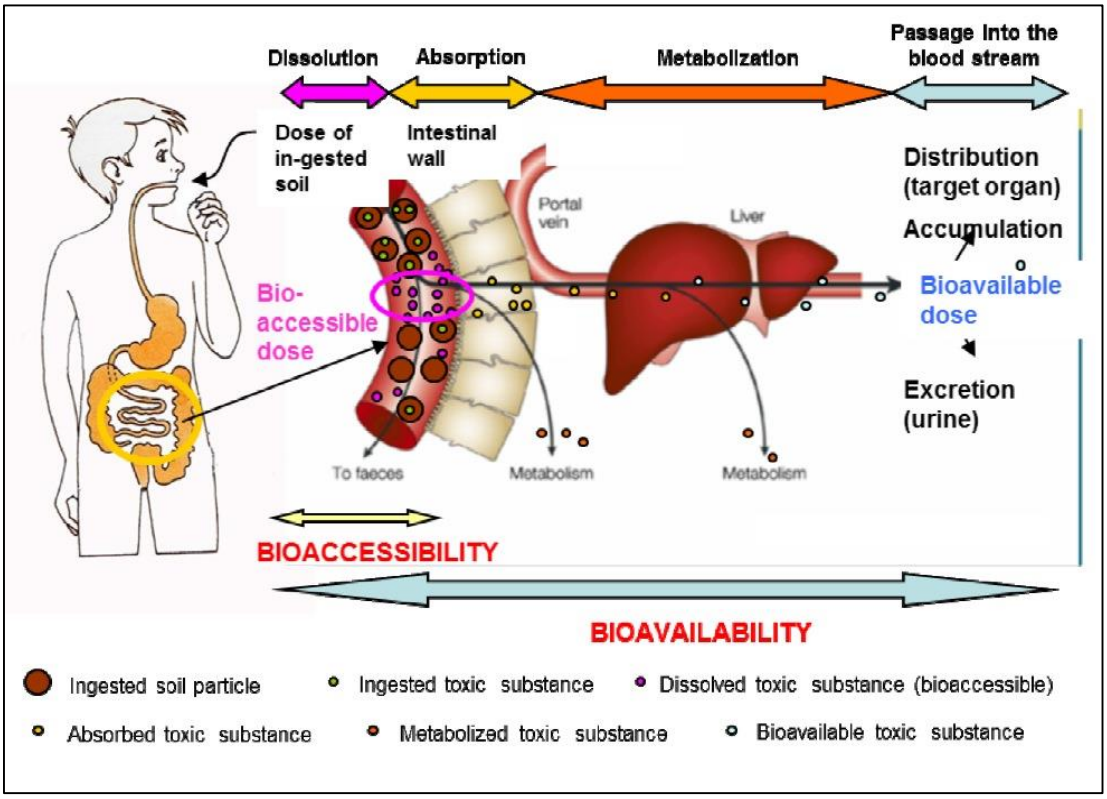


**Figure 1.2. Schematic representation of the concepts of bioavailability and bioaccessibility**[71]

The inhaled airborne PM are those ≤ 10 μm.[72] As mentioned previously in Section 1.1.2, airborne PM < 2.5 μm penetrate deep into the lungs, whilst PM 2.5-10 μm can reach the conducting airways (nose, pharynx, larynx, trachea, bronchi and bronchioles).[17-19] However, the latter are transported to the gastrointestinal tract by mucociliary clearance (clean-up of the respiratory tract from locally produced debris, unnecessary secretions and unwanted inhaled particles).[19, 73-75] Because the majority of inhaled $PM_{10}$ is eventually deposited in the gastrointestinal tract, oral bioaccessibility tests are also relevant to estimate the bioaccessibility of particle-associated PTE.

### 1.4.2.2. Methods of oral bioaccessibility assessment

Many methods have been developed to determine the oral bioaccessibility of PTE in different substrates, particularly focused on As and Pb. Methods are divided in two groups: "*in vivo*" and "*in vitro*".[27] Animals such as rats and swine are utilized in the *in vivo* method to assess bioavailability, whereas in the *in vitro* method, extraction test with fluids similar to gastric fluid are performed. Reduced costs, simplicity, reproducibility, and rapidity are the reasons that make the use of bioaccessibility for estimating bioavailability in the *in vitro* studies more common.[76] The bioavailable fraction can only be determined by using *in-vivo* methods, whilst *in-vitro* methods are used to measure the bioaccessible fraction.[63] Although the assessment of PTE hazards based on applying *in-vivo* methods is more realistic, their drawbacks such as time consumption, high costs, and ethical matters make the *in-vitro* methods preferred for assessing risks of PTE to human.[77, 78]

Various designs of *in vitro* digestion methods have been developed to estimate the human bioaccessibility of PTE in soils.[65] For example, a two stages physiologically based extraction test (PBET) was suggested to assess the solubility of metals in stomach and intestinal tract, respectively.[70] Although the PBET that mimics stomach and intestinal tract conditions has been favourably used,[70, 79] it is hard to perform with large number of samples.[80] Moreover, the mimicked intestinal phase achieved low reproducibility.[70, 81] As a result, an alternative method has been developed taking into consideration only the stomach phase.[27] Various names have been used for this modified method such as simple bioavailability extraction test[82] or simplified bioaccessibility extraction test (SBET),[63] and it has been widely used.[65]

Other methods are also used to determine bioaccessibility such as the unified BARGE method, unified bioaccessibility method (UBM),[83] *in vitro* gastrointestinal extraction method (IVG), US pharmacopoeia Method (USP), solubility bioaccessibility research consortium assay (SBRC), standardized German *in vitro* assay (DIN), simulator of human intestinal ecosystem of infants (SHIME), and TNO nutrition dynamic computer-controlled gastrointestinal model (TIM).[63, 84] The sample throughput and the fact that the method should provide conservative values are

important factors that are taken into consideration when a method for assessing bioaccessibility is chosen.

Attributes of each metal,[85] mineralogical content of samples,[86] pH of the extraction solution,[84] and the presence of other inorganic or organic components[62] significantly affected bioaccessibility.[18] Conditions of *in-vitro* methods such as a temperature, pH, time, agitation, chemical composition of the extractant(s), and presence of enzymes are intended to be similar to the conditions of digestion in the human body.[87] For example, the mimicked gastric solution in the SBET is a pH 1.5 fluid, and the extraction process is carried out for 1 hour at 37 °C.[88] Substantial compound dissolution from a sample in a mouth is not predicted because ingested matter processing in a mouth will take a very short time, a few second to minutes, and the pH of saliva is approximately neutral, 6.5.[89] As a result, it is commonly considered that the effect of saliva on a bioaccessibility of PTE is insignificant,[65] therefore only mimicked gastric and intestinal extractions are considered.[87]

***Simplified bioaccessibility extraction test (SBET)***

The SBET is a simple bioaccessibility test including only the stomach phase of the PBET.[90] In response to a request by the USEPA and other US laboratories for a rapid, easy-to-apply bioaccessibility test, Medlin[90] produced the SBET[91] by modifying the PBET of Ruby *et al.*[79] to consider only the stomach phase and use a minimal number of reagents (glycine and HCl only). An *in vivo* swine study conducted by Ruby *et al.*[64] was used to validate the SBET for Pb. In 2012, the USEPA published the most recent version of the standard operating procedure.[91] Although the SBET produces slightly higher values for bioaccessible PTE concentrations compared to other methods, a relatively short extraction time and the simplicity of the reagents used make it practically simple to perform. Hence, it is the preferred method when large batches of sample are to be processed.

***Unified bioaccessibility method (UBM)***

In contrast to the SBET, the bioaccessibility research group of Europe (BARGE) produced a complex test, the UBM.[83] This was achieved by modifying an *in-vitro* method originally created by researchers at the Netherlands National Institute for

Public Health and the Environment.[76] This test consists of two phases: a stomach phase (incorporating saliva and gastric fluids) and a "stomach and intestinal" phase (including duodenal and bile fluids). The UBM was evaluated by means of an international inter-laboratory exercise.[92] Caboche[78] and Denys *et al.*[93] validated the UBM for As, Cd, Pb and Sb in soils by conducting *in-vivo* swine studies. In 2011, the British Geological Survey (BGS) reported the methodology of the validated BARGE UBM.[94] Advantages of the UBM are the similarity of its extractants to body fluids, and it was validated for more than one element. However, the complexity of the extractants and the fact that application of the method is time consuming are serious drawbacks.

To provide a conservative estimate of risk, the International Organization for Standardization[95] recommended that the exposure route that produces the maximum amount of bioaccessible concentration should be addressed by bioaccessibility tests. In the context of the UBM, this means that only the stomach phase (UBMSG) generally needs be considered because lower values of bioaccessible PTE concentrations are usually obtained in the "stomach and intestinal" phase.[69, 96, 97]

### 1.5. Previous studies of PTE in urban airborne PM

#### 1.5.1. Studies on total and pseudototal concentration of PTE

A number of investigations were conducted to study the concentrations of PTE in PM during the last two decades. In these studies, different approaches were followed to study PTE content in PM. Some of them used the dust deposited on the ground to represent PM, while others used PM collected on filters that were located in different air quality and monitoring systems. For example, Robache *et al.* determined the concentration of eighteen elements including Cd, Cr, Cu, Fe, Mn, Ni, Pb, and Zn present in PM that were collected on polytetrafluoroethylene (PTFE) filters, and they found that recoveries for certified elements were between 95% and 105%.[98] In another example, Yongming *et al.* determined concentrations of As, Cr, Cu, Mn, Pb, and Zn in urban dusts of central China, and their results highlighted that concentrations of elements except As and Mn were high compared with Chinese background values. Result of this study also inferred that sources of Cr, Cu, Pb, and Zn were industrial, whereas soils were the main source of As and Mn.[99]

More recent studies also were conducted on this subject. For example, Huang *et al.*[100] determined the concentrations of As and the metals Cd, Cr, Cu, Mn, Ni, Pb, and Zn in outdoor and indoor particles collected from road dust and household air conditioner filter dust (using 3M$^{TM}$ membrane) in the urban centres of Guangzhou, China. Results of this study showed that %RSD values of element concentrations were high except for Mn. The results also demonstrated that concentration of Zn was the highest in road dust, whilst, in dust trapped on air-conditioning filters, the highest concentration was for Pb. In another recent study, Rueda-Holgado *et al.*[101] have studied the fractionation of trace elements including As, Cd, Cu, Mn, and Pb in total atmospheric deposition from air quality monitoring stations located at Puchuncavi, Chile. In this study, a 47 mm diameter grade QMA quartz filter Whatman (0.3 μm pore diameter) was used to collect the insoluble fraction of total atmospheric deposition. This study indicated that concentrations of elements in a quartz filter blank were very low (less than 5 μg $L^{-1}$). In the same context, Sagagi[102] investigated the pseudototal PTE content in filters loaded with $PM_{10}$. The filters used were filter dynamic measurement system (FDMS) filters (47 mm diameter) used to collect urban PM in the city of Glasgow, UK and supplied by Glasgow City Council. This study revealed that pseudototal concentrations of PTE in loaded FDMS filters were low except for Zn.

### 1.5.2. Studies on sources of PTE in airborne PM

Other studies have been conducted to investigate the source of PTE in airborne PM. For example, a study was conducted to examine the extent of PTE transportation from soils to the atmosphere. Concentrations of Cr, Cu, Ni, Pb, and Zn in five size fractions of soils from five European cities were determined. Findings revealed that fine particles ($PM_{2.5}$ and $PM_{10}$) in urban soils can be a potential source of PTE in the atmosphere.[9] In another example, Layton and Paloma[103] developed a framework of measurement and modelling to assess translocation of polluted soils and PM into a habitation, and they found that the source of approximately 60% of As input to floor dust was As in ambient air.

### 1.5.3. Studies on bioaccessibility of PTE in airborne PM

A few studies were also conducted to estimate bioaccessibility of PTE in PM in different regions throughout the world. For example, bioaccessible concentration for elements (Cd, Cu, Mn, Ni, Pb, and Zn) in PM loaded on glass fibre filters in some Greek urban sites was measured. A serum simulant (pH=7.40) was used as extractant in this study, and high bioaccessible concentration of Mn, Ni, and Zn were estimated.[104] In another example, the inhaled bioaccessible fraction of many elements including Cd, Cr, Cu, Mn, Ni, Pb, and Zn in urban $PM_{2.5}$ and $PM_{10}$ collected on GN-4 Metricel® mixed cellulose ester filters (diameter 47 mm, pore size 0.8 μm) was determined using a synthetic gastric fluid as extractant. The PM-loaded filters used were obtained using a commercial air sampler in Vienna, Austria. Results demonstrated that extractable fractions for the majority of investigated elements were over 50%.[75]

A study conducted in China in 2014, evaluated the risk to humans from elements including As, Cd, Cr, Cu, Mn, Ni, Pb, and Zn in outdoor and indoor urban particles from urban centres of Guangzhou, China. In this study, the PBET and simulated lung solution were used to assess the ingestion and inhalation bioaccessibility, respectively. Results of this study elucidated that the most hazardous element was As, although, Zn concentration was the highest among elements in road dust, whilst in household air conditioner filter dust it was Pb.[100]

By applying the SBET, Cr, Cu, Ni, Pb, and Zn were determined in five particle-size fractions separated from urban soils collected from Torino (Italy) and Seville (Spain).[105] In another study, also involving the SBET, nine elements (As, Cd, Co, Cr, Cu, Mn, Ni, Pb, and Zn) were determined in airborne PM supported on quartz microfibre filters sampled in Nanjing (China).[106] As the majority of the particles 2.5-10 μm that reach the upper airways are transported to gastrointestinal tract by mucociliary clearance, therefore assessing the risk of PTE in these particles based on inhalation route and ingestion route would be meaningful.

## 1.6. The filter dynamic measurement system (FDMS)

The FDMS is used worldwide for continuous monitoring of the concentration of $PM_{10}$ in the air.[107, 108] In this system (see Fig. 1.3), air is drawn through a $PM_{10}$ size-

selective inlet at a flow rate of 3 L $min^{-1}$, then $PM_{10}$ are dried and directed to the mass transducer, where they are accumulated on a tapered element oscillating microbalance (TEOM) filter. The mass of material is then measured based on the decrease in oscillating frequency. As the weight of a blank filter is measured previously, the weight of the $PM_{10}$ collected is calculated by subtracting the weight of the blank filter from the loaded filter. The concentration of the $PM_{10}$ in the air then can be expressed as the mass of $PM_{10}$ calculated (ng, μg, and mg) per the volume of air drawn ($m^3$).[109]

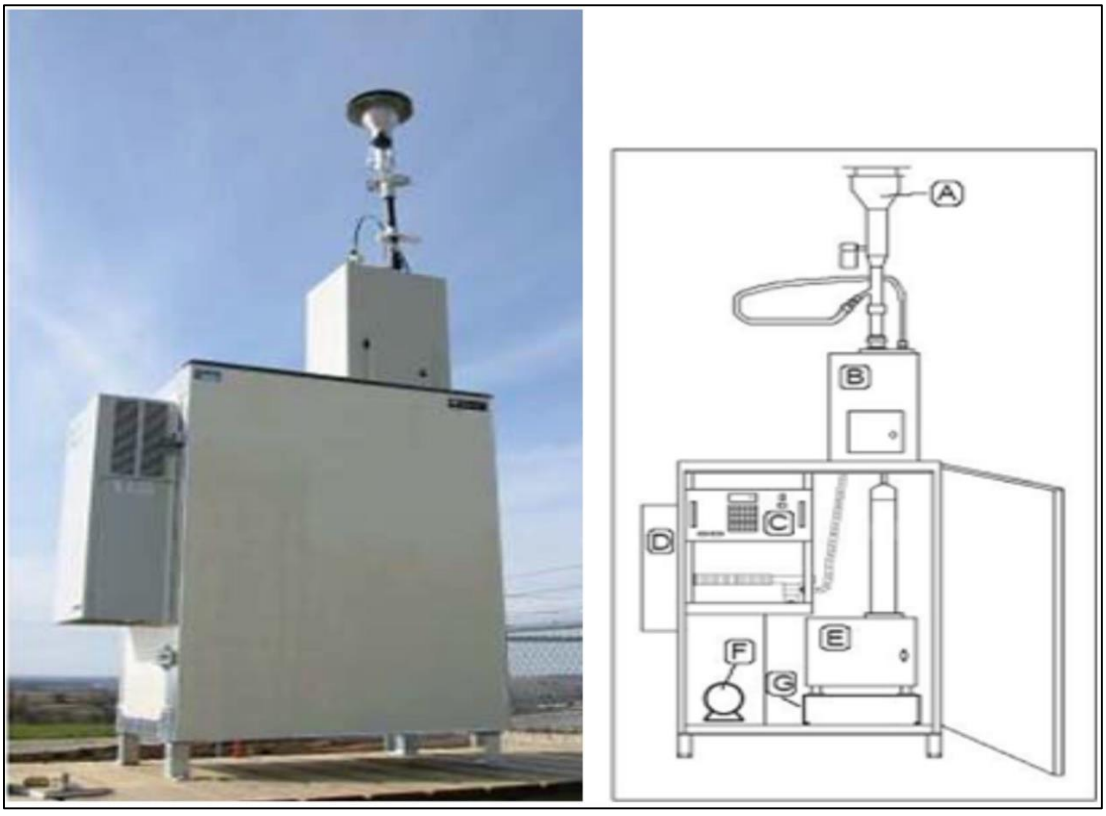


**Figure 1.3. A picture and schematic diagram of the filter dynamic measurement system (FDMS): (A) sample inlet, (B) FDMS enclosure, (C) control unit, (D) air conditioner, (E) sensor unit, (F) pump, and (G) spacer**[110]

In the FDMS, an alternative reference flow path incorporating a chiller unit and a 47 mm Teflon-coated borosilicate TX40 filter (see Fig. 1.4) is used to correct for loss of semi-volatile material. The media of this filter is borosilicate glass microfiber reinforced with woven glass cloth and bonded with PTFE.[111] After use, these loaded filters are not kept for further analysis and they are discard.[108] As risk-assessment studies for PTE in $PM_{10}$ need real samples, loaded FDMS filters represent a valuable, but hitherto unexploited, source of real $PM_{10}$ samples for assessment studies.

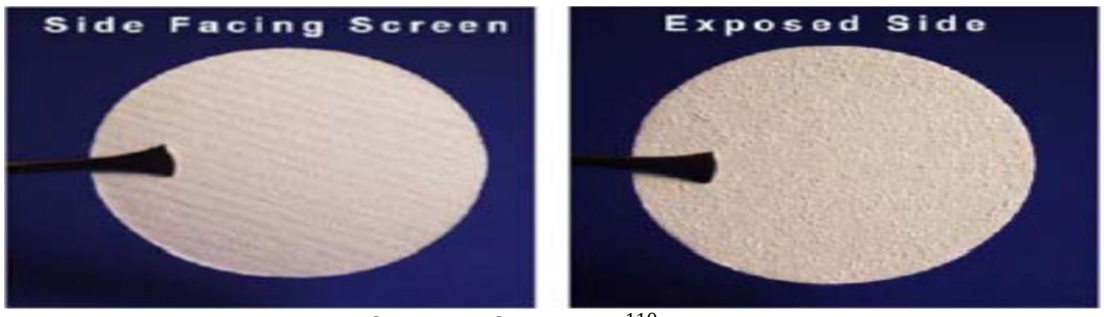


**Figure 1.4. The two sides of the Pallflex TX40**[110]

### 1.7. Scope and aim of the study

The overall aim of this project was to evaluate, develop, modify and optimize bioaccessibility extraction tests protocols to assess risk to human health from exposure to PTE in the urban PM so that they are more representative of the human body and can be applied to real samples collected in routine air quality monitoring. Based on the literature mentioned in Section 1.5, it was noted that bioaccessibility of PTE in $PM_{10}$ loaded on FDMS filters had not been investigated. As the nature of the digestion process in the gastrointestinal tract is dynamic, so the dynamic extraction would be more representative to the real process. Also no study was conducted estimating risk to human health from exposure to PTE in $PM_{10}$ taking account of potential absorption en route to deposition in the stomach. The specific objectives selected were thus:

a) To miniaturise the SBET and UBM methods to make them more suitable for application to the small amount of $PM_{10}$ typically available so that they could be applied to real $PM_{10}$ samples collected on FDMS filters (Chapter 4).
b) Creation of dynamic models for the SBET and the stomach phase of the UBM to measure the bioaccessible concentration of PTE in $PM_{10}$, to represent a more appropriate simulator than batch extraction for the real digestion process in the human body (Chapter 5).
c) To establish a new, two steps sequential extraction method for determining the bioaccessible concentration of PTE in $PM_{10}$ transported to the gastrointestinal tract by mucociliary clearance, to more closely mimic the routes by which PTE in inhalable $PM_{10}$ are absorbed (Chapter 6).

# 2 Theory of applied approaches and techniques

## 2.1. Microwave assisted digestion

In the 1980s, a major development in sample preparation methods occurred using microwave-heating methods instead of conventional methods such as hot plates or sand baths.[112, 113] Common and wide use of microwave-assisted digestion methods has increased since the 1980s.[114, 115] Sample digestion using microwave assisted digestion is now the most frequently applied approach in the environmental chemistry.[116]

Microwaves are in the region of the electromagnetic spectrum between infrared radiation and radio frequencies, and they have a typical wavelength of 1 mm to 100 cm (see Fig. 2.1). Potential interferences with radio transmissions are prevented by operating domestic and industrial microwaves at around 12.2 cm wavelength.[117]

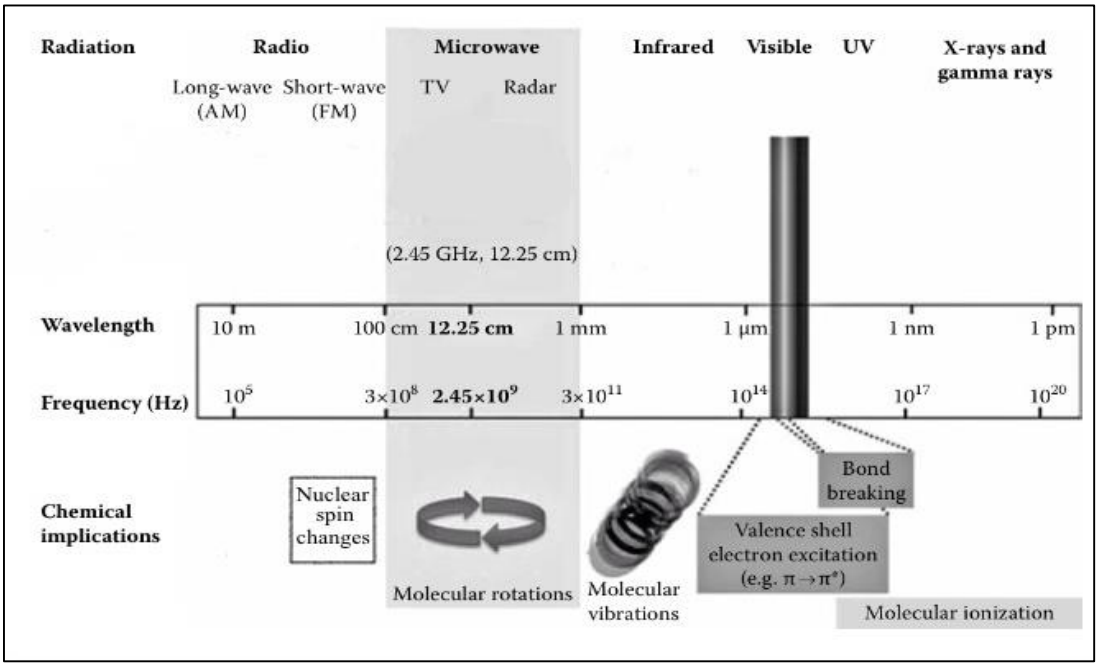


**Figure 2.1. Regions of the electromagnetic spectrum with chemical implications for selected wavelength regions (after[118])**

Fast heating is achieved by using microwave radiation compared to conventional methods, as the energy is absorbed directly by only a solution present in the microwave vessels, which do not absorb the radiation (see Fig. 2.2).[117]

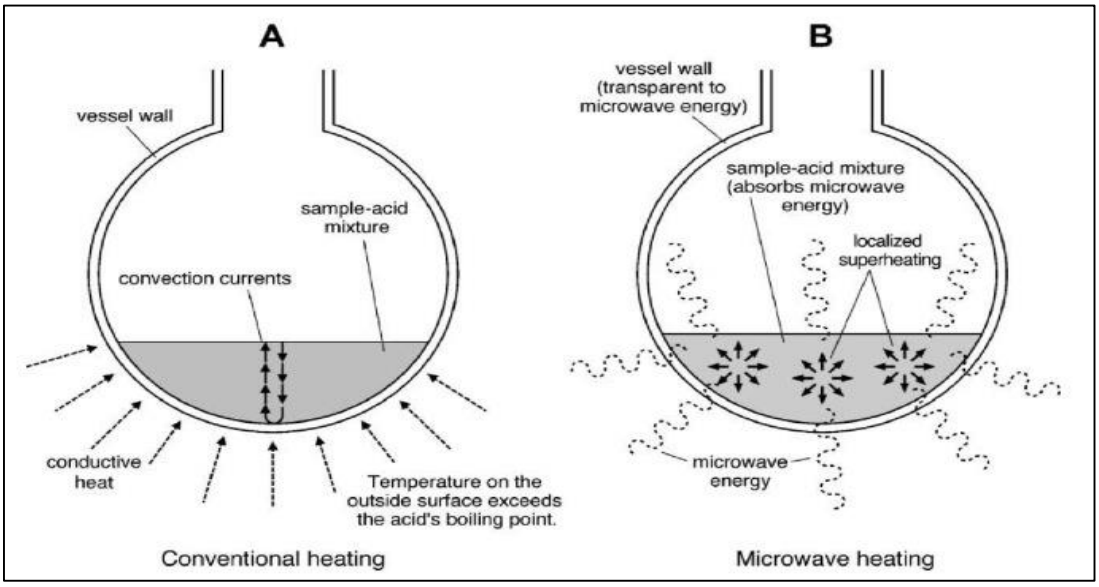


**Figure 2.2. A schematic diagram of sample heating by (A) conventional heating and (B) microwave heating**[119]

Microwave energy is more strongly absorbed by polar molecules and ionic solutions such as acids, relative to non-polar molecules. This is because polar molecules have a permanent dipole moment that is affected by the microwaves.[117] Microwave irradiation heats polar solvents, such as water, methanol and acetone, but it does not heat non-polar solvents, such as toluene and hexane.[117] Microwave energy is absorbed by the liquid phase, but it is not absorbed by the vapour phase. Thus, only the liquid phase is heated by microwave energy. Therefore, the temperature of the liquid phase is higher than the temperature of the vapour phase and vapour condensation on cool vessel walls occurs.[119] As a result, the predicted vapour pressure is higher than the actual vapour pressure. Thus, very high temperatures can be reached at relatively low pressures.[119]

Microwaves are classified as nonionizing energy (photon energies in the range 0.004-0.4 meV) that is not enough to break chemical bonds (*e.g.* the energy of the H-O bond in $H_2O$ is 5.2 eV; and for the H-C bond in $CH_4$ is 4.5 eV). Microwaves are split into two parts, the electric-field component and the magnetic-field component (see Fig. 2.3).[120] Generally, materials can transmit, reflect, and/or absorb microwaves. Transparent materials can transmit microwaves when they pass through them, without any effects.[120] Reflective materials are not affected by microwaves, which are reflected by the surface. Absorption occurs when the material partially or completely absorbs the microwaves.[120]

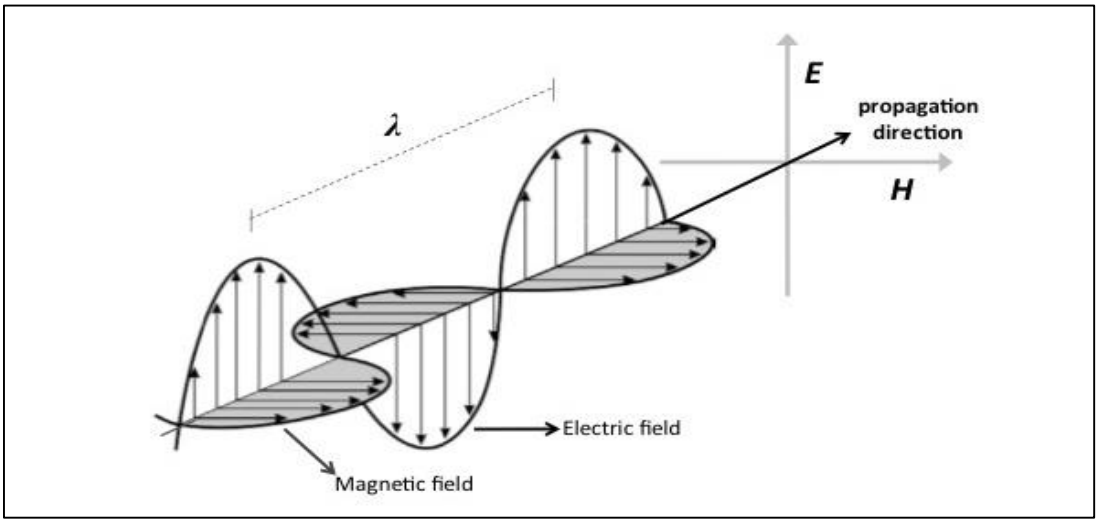


**Figure 2.3. A schematic representation of an electromagnetic wave (E=electric field; H=magnetic field; λ=wavelength)**[120]

Microwaves are able to interact with many materials, such as solids and liquids. Metals are not heated by microwaves, and they are normally good reflectors.[120] The behaviour of materials when exposed to microwaves is tabulated in Table 2.1.

**Table 2.1. Classes of materials considering their interaction with microwaves**[120]

| Material | Class of material | Interaction with microwaves |
|---|---|---|
| Metals | Reflective | Reflection; no heating |
| Polytetrafluoroethylene (PTFE), quartz | Transparent | Without interaction; no heating |
| Water, nitric acid and other polar liquids | Absorptive | Absorption; heating is produced to different extents according to the dielectric properties |

There are two mechanisms to describe the energy transfer in the microwave heating process: ionic conduction and dipolar rotation. In ionic conduction, a solution is heated as a result of friction between its ions that are affected by the electromagnetic field applied and other species. In dipole rotation, heating of the solution is produced as a result of the molecular friction caused by alignment of dipolar molecules with the applied electric field and their return to a disordered state.[120] The degree of penetration of microwaves affects the capacity of each material to absorb microwave energy. For transparent materials such as quartz and PTFE, this penetration is infinite and it is null for reflective materials *e.g.* metals.[120]

When absorption occurs, the conversion of electromagnetic energy into heat depends on the dissipation factor (or loss tangent, tan δ) i.e. the relation between the dielectric constant ($\mathcal{E}'$) and dielectric loss factor ($\mathcal{E}''$) for a given material. This relation is presented in Equation 2.1:[117]

$$\tan \delta = \mathcal{E}'' / \mathcal{E}'$$

**Equation 2.1**

A measure of the ability of a material to be polarized by an external electric field is represented by the dielectric constant ($\boldsymbol{\mathcal{E}'}$). In contrast, the dielectric loss factor ($\boldsymbol{\mathcal{E}''}$) "represents the ability of the material to convert the absorbed electromagnetic energy into heat" i.e. dissipation capacity.[117] There is reverse correlation between the penetration of microwaves into the sample and its dissipation capacity. From 1 to 12 GHz the $\boldsymbol{\mathcal{E}''}$ is increased, whereas the $\boldsymbol{\mathcal{E}'}$ is decreased. Thus, at high frequencies, values of tan **δ** are appreciable. However, in order to allow a deeper penetration of microwaves into the materials, microwave ovens for laboratory applications normally use work at 2.45 GHz.[120]

An open-focused and a closed-vessel system are two types of microwave heating systems commercially available. Loss of volatile analytes is one of the disadvantages of the open microwave digestion.[121] The majority of environmental sample digestion is currently performed in closed vessels. Figure 2.4 shows the main components of closed-vessel microwave assisted digestion.[119]

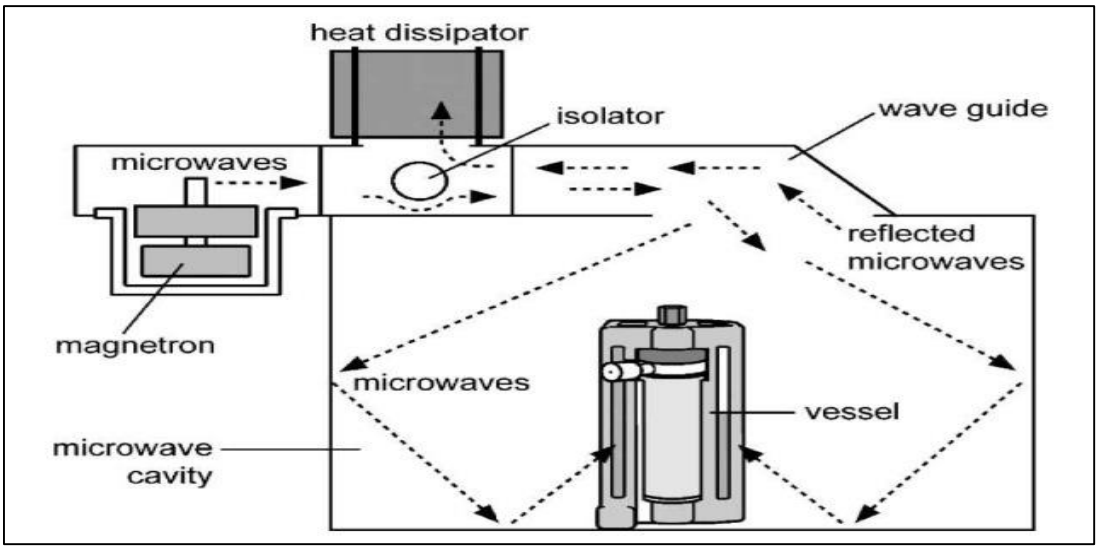


**Figure 2.4. A schematic diagram of a closed vessel microwave assisted digestion system**[119]

Microwave energy is generated by a magnetron tube (see Fig. 2.5). The magnetron is a cylindrical diode with an anode and a cathode. Electrons must flow from the cathode to the anode in order to operate the magnetron.[119] The direct path of electrons is curved by a magnetic field generated by a magnet.[119]

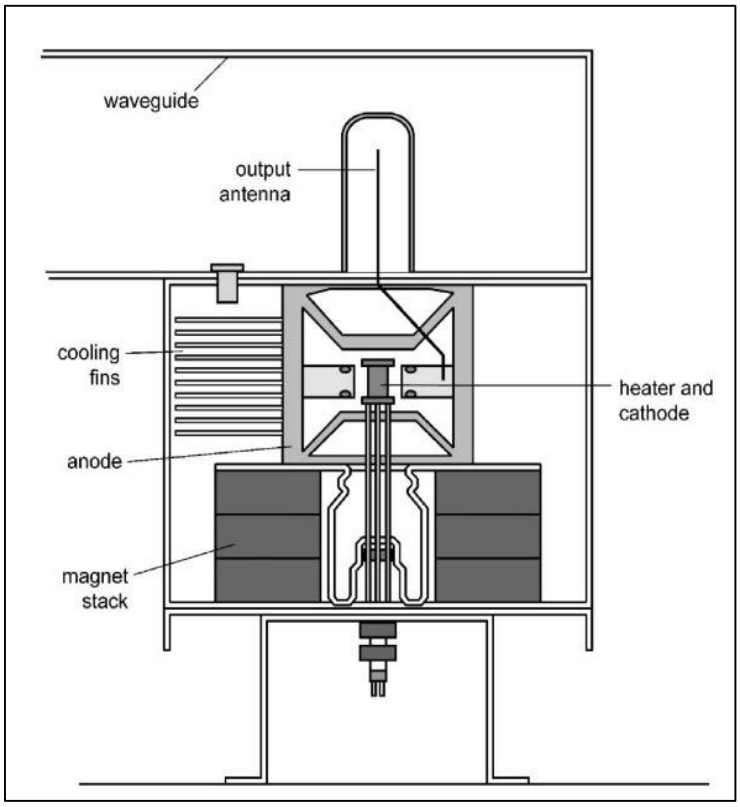


**Figure 2.5. A schematic diagram of a magnetron tube**[119]

From the magnetron, energy is transferred to the microwave cavity by a metallic rectangular enclosure (i.e. waveguide).[119] The waveguide collects and transfers the microwave energy through constructive interference of the waves and launches the energy into the microwave cavity with minimal loss. Between the walls of the cavity, standing wave patterns are established by repeated reflections of the microwaves.[119] The interaction of microwaves within the cavity continues until the waves are totally dissipated. The samples and sample components that are placed in the cavity repeatedly interact with the microwave reflections and are heated.[119]

An accelerated, a secure, and an adequate digestion are the main advantages of microwave assisted digestion as well as lack of vulnerability to losses of volatile metals.[26] Not only these but a reduction in digestion time and decrease in solvent volume and contaminants are also typical features of microwave heating (i.e. microwave assisted digestion).[113, 122]

### 2.2. Inductively coupled plasma mass spectrometry (ICP-MS)

The wide acceptance of inductively coupled plasma mass spectrometry (ICP-MS) is due to properties such as outstanding sensitivity, ability to produce isotope ratio data, multi-element capacity, rapid analysis, and flexibility of connectivity to different sample introduction systems such as electro-thermal vaporization (ETV), laser ablation, high performance liquid chromatography (HPLC), and gas chromatography (GC).[121, 123, 124]

#### 2.2.1. Inductively coupled plasma (ICP)

A plasma is "the co-existence, in a confined space, of positive ions, and electrons" in addition to "neutral species of an inert gas" such as argon or helium.[121] The most common plasma source in commercial use is the ICP.[121] Other commercial plasma sources are the direct-current plasma (DCP), the helium microwave induced plasma (MIP), and the glow discharge.[121] Plasmas are electrically conductive because they consist of a hot, partially ionized gas, containing an abundant concentration of cations and electrons.[61]

##### 2.2.1.1. Sample introduction systems

Liquid samples are usually introduced into ICP by the combination of a nebulizer and spray chamber,[121] whereas solid samples can be injected directly into the plasma by using other systems such as lasers, sparks, and graphite furnaces to generate gaseous samples from solids.[117] The nebulizer is used to convert an aqueous sample into an aerosol of small droplets by the physical interaction of argon gas and liquid sample.[117] Inert polymers are used to manufacture some nebulizers in order for the latter to become more resistant to corrosive samples, such as those containing HF.[119] A peristaltic pump is used in most ICP systems to eliminate alterations of sample

uptake due to viscosity differences and permits rapid washing out of the nebulizer and spray chamber.[125] The concentric nebulizer, the cross-flow nebulizer, and the Babington nebulizer are commonly used as pneumatic nebulizers,[125] and the most common in use among them is the concentric nebulizer (see Fig. 2.6 A).[121]

In order to produce an aerosol of sufficient particle size, the aerosol is passed through a spray chamber to remove large droplets where the latter would extinguish or induce cooling of the plasma, consequently leading to severe matrix interferences.[119] Figure 2.6 B shows the double-pass spray chamber.

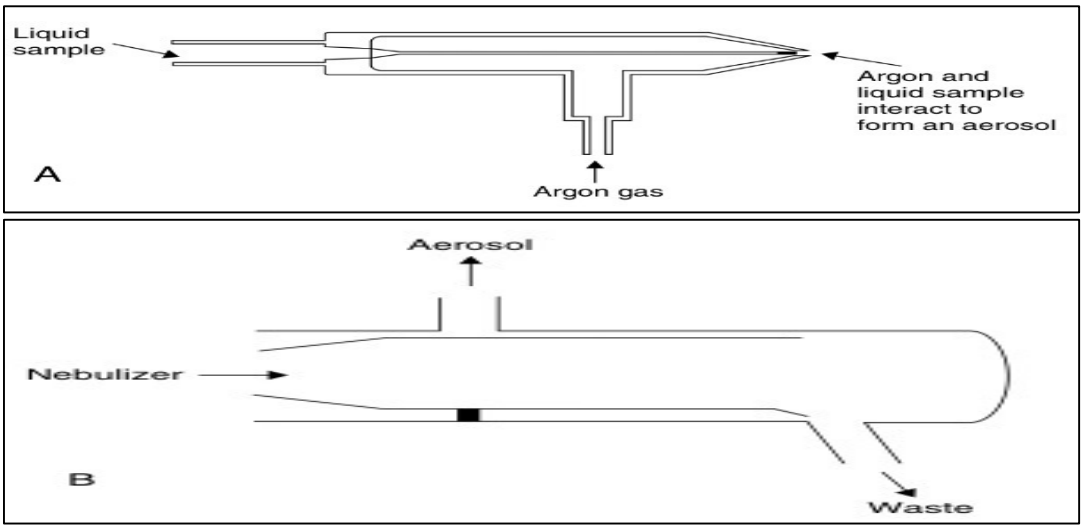


**Figure 2.6. Schematic diagram of the (A) pneumatic concentric nebulizer and (B) double-pass spray chamber**[121]

### 2.2.1.2. Inductively coupled plasma torch

The plasma is formed in a torch, which is a concentric arrangement of quartz tubes (see Fig. 2.7).[125] The ICP torch consists of three concentric quartz tubes, and it has three entry points: one (accessing the intermediate tube) for introducing the plasma gas; a second (accessing the external tube) for introducing the coolant gas; and a third (accessing the inner tube) for introducing sample aerosols.[117] Located around the outer glass tube is a water-cooled copper load coil. The latter generates the power required for the ICP, typically in the range 500–1500 W at a frequency of 27 or 40 MHz.[125]

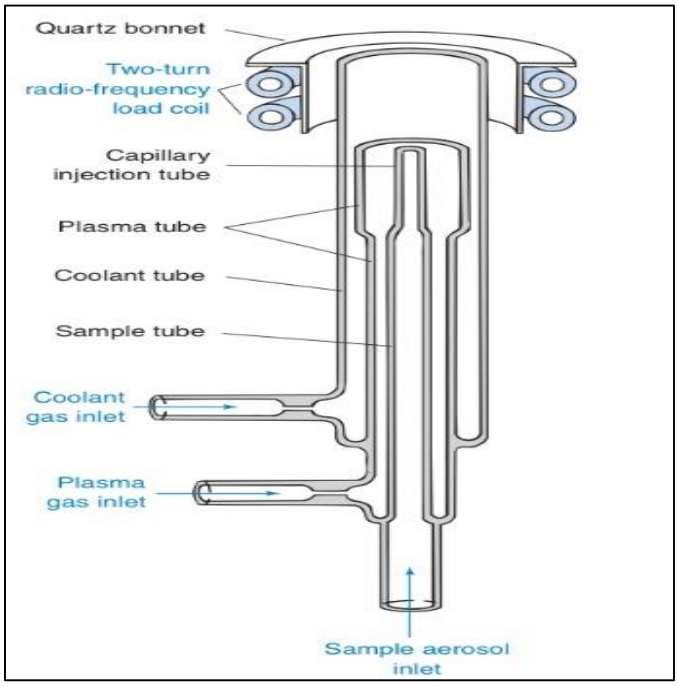


**Figure 2.7. Inductively coupled plasma torch**[126]

The coolant gas in the outer tube keeps the quartz tube walls cool and centres the plasma.[119] A typical flow rate for coolant gas is 7–15 L argon/min.[125] The flow rate for plasma gas in the middle channel, which is called the auxiliary gas, can be 0–3 L argon/min, and this gas flow reduces organic deposits at the injector tip, hence preventing the plasma from sitting too low in the torch and melting the injector (inner tube).[119, 125] In the inner tube, sample aerosols are carried into the plasma by the gas flow. The latter is called the sample flow or nebulizer flow and is typically about 1 L argon/min.[125]

Ionized argon, which forms the plasma, has a first ionization potential (IP) of 15.76 eV. An element that has an IP less than this value will be partly ionized in the Ar ICP.[119] For example, As, with its first IP of 9.81 eV, will be only 30-40% ionized, whereas cesium will be 100% ionized because its first IP is 3.89 eV. In contrast, fluorine will not be ionized because its a first IP, 17.42 eV, is higher than the first IP of argon.[119] An analyte atom (A) in the ICP is excited by collisions with electrons or with an excited (metastable)-state argon atom ($Ar^*$) (Equations 2.2 and 2.3):

$$A + e^- \longrightarrow A^+ + 2e^-$$

**Equation 2.2**

$$Ar^* + A \longrightarrow Ar + A^+ + e^-$$

**Equation 2.3**

Analyte also can be ionised by charge transfer collision with $Ar^+$ (Equation 2.4).[121]

$$Ar^+ + A \longrightarrow Ar + A^+$$

**Equation 2.4**

### 2.2.2. Interfacing an inductively coupled plasma with a mass spectrometer

The ICP act as an ionization source (i.e. producing ions from the elements introduced into the plasma) for MS, and these ions can be extracted into a mass analyser. To extract the ions directly from the ICP into the mass spectrometer, the torch of ICP is positioned axially (see Fig. 2.8).[125] The plasma gas is directed onto a metal cone with a small orifice (typically 1 mm in diameter). This water-cooled cone is made of Ni, and it is called the sampling cone.[126] A portion of the gas passes into the evacuated mass analyser through another cone located behind the sampling cone. This cone is called a skimmer cone, and it has a smaller orifice (typically 0 .75 mm in diameter).[125]

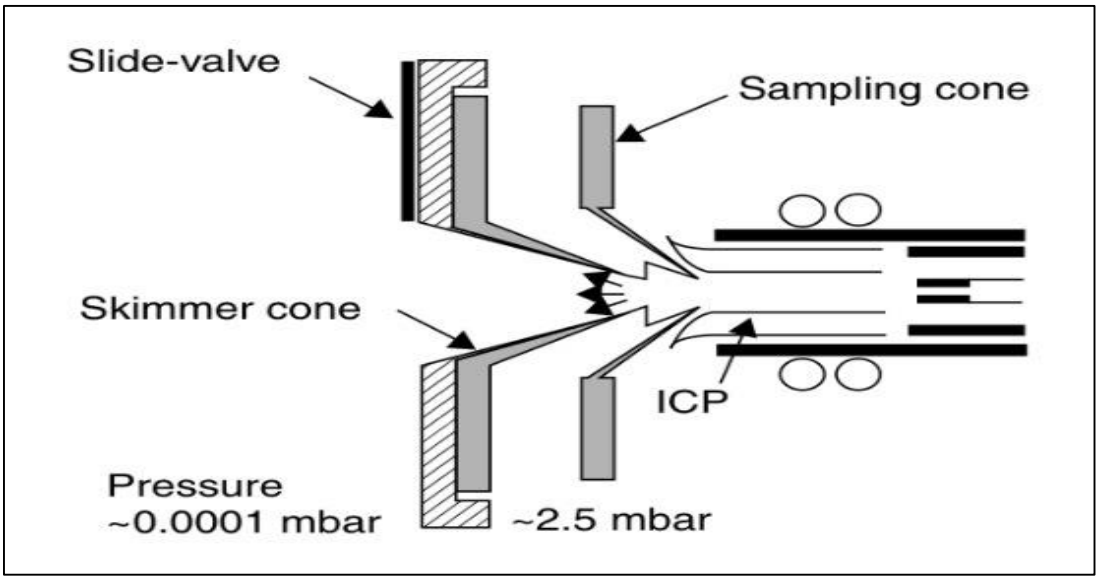


**Figure 2.8. Schematic diagram of inductively coupled plasma mass spectrometer interface**[117]

The cones that are used to interface ICP with MS are usually made of Ni.[121] A series of electrostatic lenses are then used to focus the extracted ions into MS. In recent instruments, after the lenses, ions are guided through collision or reaction cells to the entrance of MS.[126]

### 2.2.3. Mass spectrometer (MS)

The MS is an instrument that separates gaseous ionized atoms and molecules or its fragments according to their mass-to-charge ratio (m/z), where the mass, m, is expressed in unified atomic mass units and z is the number of charges on the ion.[126] A sample introduction system, an ionization source, a mass analyser, and a detector are the main parts of mass spectrometers (see Fig. 2.9). These components are under high vacuum except sample input systems or ion source.[125] High vacuum is applied to avoid collisions between ions and background gas molecules that divert the ions from their path. The components of recent MS are controlled by software programs.[125]

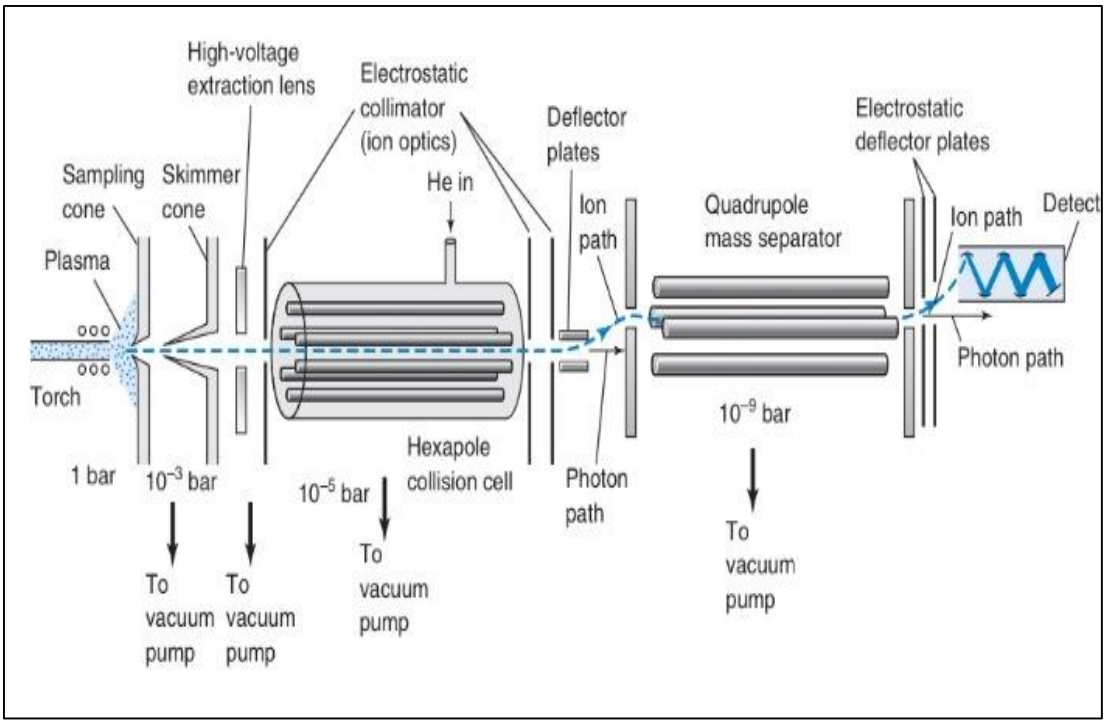


**Figure 2.9. Schematic diagram of an ICP-MS instrument[126]**

### 2.2.3.1. Mass analysers

After dissociation in the collision cell, ions are separated according to their mass-to-charge ratio by a mass analyser located at the core of the MS.[117] There are many types of mass analysers such as the quadrupole, sector field, ion trap, and time of flight.[121] The most common mass analyser in ICP-MS is the quadrupole because it is inexpensive and very fast. However, its resolution is low which is *ca.* 300 (i.e. 0.7-1.0 amu)[127]. This analyser consists of four parallel metal rods to which are applied both a constant voltage (up to 200 V) and a radio- frequency oscillating voltage (up to 1200 V).[117, 119] Figure 2.10 shows the opposite pairs of rods are each linked to the opposite ends of a DC source: as a result, at any particular time, one of the pairs is positive and the other is negative.[125] A magnetic field is not used to separate ions in the quadrupole mass analyser. The latter uses an electric field to separate ions. The ion path is directed axially between the analyser rods.[125] Separated ions are then directed towards the detector, and a signal is generated.[126]

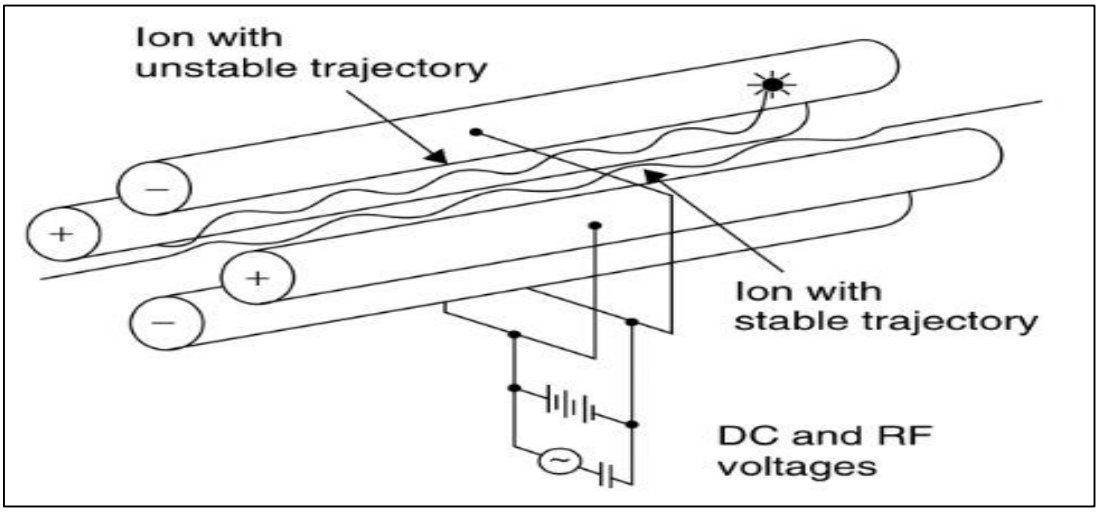


**Figure 2.10. Schematic arrangement of the quadrupole analyser**[121]

### 2.2.4. Detector

There are several types of detector available for ICP-MS instruments. The continuous dynode electron multiplier (see Figure 2.11) is the most common of detectors.[121] This detector consists of a curved open glass tube. The tube has a wide conical entrance, and its inside is coated with a semiconducting material. The tube is curved so that positive ions can not return "upstream", as a result, electrical noise is reduced.[125] The tube ends are subjected to a different potential, where the wide end is

highly negative, to detect the positive ions resulting from a mass analyser, and the second end is earthed.[121] Once the positive ions impinge on the coated surface of the tube, one or more secondary electrons are ejected. As there is a difference in the potential between the ends of the tube, these secondary electrons are attracted towards the earthed end.[127] When these electrons move through the tube, they can hit it again, resulting in more electrons. This process continues until up to $10^8$ electrons are generated from a single ion are collected, as a discrete pulse.[121, 125] The pulse is then amplified and recorded as a number of counts per second.[127]

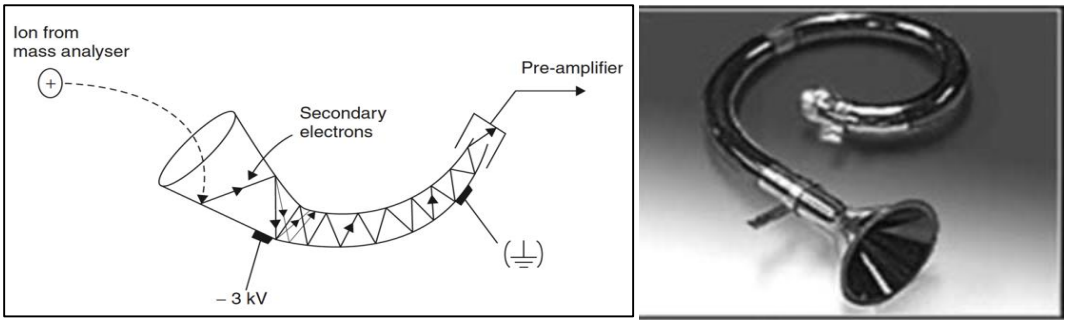


**Figure 2.11. Schematic diagram of operating principle (left)[121] and a photo (right)[125] of a continuous electron multiplier**

### 2.2.5. Interferences

#### 2.2.5.1. Physical interferences

In ICP-MS, existence of, for example, elevated concentrations of an acid, or higher than the typical level of total dissolved solids (TDS) (i.e. < 0.2%) in a sample means that it will not be nebulized with the same efficiency as a standard prepared in 2% nitric acid. As a result, a variant signal may be obtained for the same concentration of an analyte. Furthermore, when the ion current in a sampled analyte beam exceeds the capability of ionic lens systems, space charge interferences may be elevated.[119, 127] The use of at least one internal standard may partly overcome the effects where the signal obtained per unit concentration over a mass range may alter with time, whereas the utilization of more than one internal standard may lead to greater long-term instrument stability. An internal standard should not exist at significant concentration in a sample, and it should match, as closely as possible, the ionization energy and mass of an analyte.[119] In addition to use of an internal standard, these interferences can be reduced or removed by: using a nebuliser specified for high

TDS levels (e.g. V-groove high solid nebulizer); preparing standards that are matrix-matched; separation of an analyte from its matrix by coupling ICP-MS with separation techniques (e.g. chromatographic techniques); and dilution of the matrix to an extent that does not affect the sensitivity for measurement of an analyte of interest.[121] Another approach was created by Agilent Technologies to reduce the high TDS level effect (up to 3%) by integrating a high matrix introduction (HMI) accessory with the sample introducing system of ICP-MS. In the HMI mode, sample aerosols are diluted using dry argon gas, thus resolving the dilution effect problem arising from use of aqueous dilution.[128]

#### 2.2.5.2. Spectroscopic interferences

The presence of argon ions and argon-containing polyatomic species in high abundance in the argon plasma can cause spectral interferences in ICP-MS. Although there are three isotopes for argon, the ion of most interest is $^{40}Ar^{+}$ because the abundance of $^{40}Ar$ is 99.6%.[125] It overlaps with $^{40}Ca^{+}$ because they have the same theoretical mass. As a result, a quadruple MS cannot differentiate between them. This kind of spectral interferences is called isobaric.[125] These interferences can be prevented by using an alternative analyte isotope for quantification. However, this solution may lead to decrease in sensitivity when the abundance of the alternative isotope is low. An example is the use $^{60}Ni$ (26.2% abundant) instead of $^{58}Ni$ (67.9% abundant) to prevent isobaric interference with $^{58}Fe$. In this situation, use of the collision/reaction cell is preferred for removal of these interferences.[121, 125]

Commonly formed polyatomic ions in the plasma are $^{40}Ar^{16}OH^{+}$, $^{40}Ar^{15}N^{+}$, $^{38}ArH^{+}$, $^{40}Ar_2^{+}$, and $^{40}Ar^{35}Cl^{+}$, which interfere with various analytes. Interference is very complex to overcome with a mono-isotopic element, *e.g.* $^{55}Mn$ and $^{75}As$, or with an element that has an isotope with abundance more than 90%, *e.g.* $^{40}Ca$, $^{51}V$, $^{39}K$, and $^{56}Fe$. In addition to plasma, polyatomic species such as $^{48}Cu^{16}OH^{+}$, $^{40}Ar^{16}O$, and $^{48}Cu^{16}O^{+}$ also arise from solvents, air, acids, and matrix components such as oxides of metals.[125, 127] This type of spectral interferences is called polyatomic, and they can be reduced or removed using a correction method (i.e. mathematical equations), cold plasma or a collision/reaction cell.[127]

Cold plasma is used when mathematical equations are not ideal for correction the polyatomic interferences, particularly when the intensity of an analyte is extremely low compared with the intensity of interferences. This approach involves changing the normal plasma conditions (i.e. 1-1.4 kW RF power and 0.8-1.0 L $min^{-1}$ of nebuliser gas flow rate) to cool conditions (i.e. 0.5-0.8 kW RF power and 1.5-1.8 L $min^{-1}$ of nebuliser gas flow rate).[121, 127] Since the ionization temperature for the majority of elements is lower than normal condition of plasma, cold plasma is limited to few elements that are affected by argon-based polyatomic interferences such as $^{40}Ar_2^+$, $^{38}ArH^+$, and $^{40}Ar^{16}O$.[121, 127] In addition to this limitation, a poor detection limits for some elements and potential increase in matrix suppression effect are the disadvantages of this approach, although the matrix effect can be compensated using an internal standard.[125] The use of collision/reaction cells can resolve these problems.

In the late 1990s, collision/reaction cells have been developed as a result of the limitation of the cold plasma approach to remove or reduce polyatomic interferences. A collision or reaction cell consists of a multipole that is located between the ion optics and the mass analyser.[125, 127] The ions that enter the collision/ reaction cells collide or react with the collision/reaction gas, which is usually He for collision cells or $H_2$ for reaction cells.[127] In the collision/reaction cells, polyatomic interfering ions can be converted to noninterfering ions, or analytes ions to those that are not interfered with, by different mechanisms of reactions or collisions between ions and a collision/reaction gas.[127] One of these mechanisms is proton transfer,[121, 127] and an example is the use of this reaction to remove the polyatomic ion ($^{38}Ar\ H^+$), which interferes with $^{39}K^+$, as shown in Equations 2.5 and 2.6.

$$^{38}ArH^+ + H_2 \rightarrow H_3^+ + Ar$$

**Equation 2.5**

$$^{39}K^+ + H_2 \rightarrow {}^{39}K^+ + H_2 \quad (no\ reaction)$$

**Equation 2.6**

For the collision cells, kinetic energy discrimination (KED) is the typical approach that is used to remove the polyatomic interferences. Since the size of polyatomic ions is higher than the size of analytes ions, the collision gas collides with polyatomic ions more than with analytes ions. Thus, the kinetic energy of polyatomic ions will be lowered to the extent that they can not be transmitted to the mass analyser, while the analytes ions are transmitted.[127] The KED is considered the best way for removing polyatomic interferences compared to reactive interference removal because there are no new interferences observed and it works for multiple interferences. However, analyte sensitivity may be affected.

In addition to the methods mentioned above, use of high mass resolution ICP-MS (HR-ICP-MS) is considered one of the primary instrumental approaches and the best way that can be used to remove or reduce interferences in atomic mass spectrometry. However, its cost is high compared with other approachs.[125] As is the case with high-resolution molecular mass spectrometers, this magnetic sector based instrument permits accurate mass determination.[125]

## 2.3. Data handling approaches

### 2.3.1. Precision and accuracy of analysis[61, 126, 129]

Determination of precision and accuracy is a significant part of environmental chemical analyses because it reveals the extent of bias or any mistake in the measurements. Precision "determines the reproducibility or repeatability of the analytical data". It measures the closeness of number of measurements of an analyte from each other. If a sample is repeatedly analysed under identical circumstances, the results of each measurement, $x_i$, may differ from each other due to experimental error or reasons outside control. These results will be distributed randomly about a mean value ($\bar{x}$) that is the sum of all measurements divided by the number of measurements (n). The mean is calculated using Equation 2.7:

$$\bar{x} = \frac{\sum x_i}{n}$$

**Equation 2.7**

Standard deviation, which relates to "the width of the normal distribution, consists of a fixed fraction of the values making up the curve". Standard deviation, s, can be calculated using Equation 2.8:

$$s = \sqrt{\frac{\sum(x_i - \bar{x})^2}{n - 1}}$$

**Equation 2.8**

In a normal distribution curve, 68.27% of the area lies between $\bar{x} \pm 1s$, 95.45% between $\bar{x} \pm 2s$, and 99.70% between $\bar{x} \pm 3s$. Therefore, 3s about the mean is often taken as the upper and lower control limits (UCL and LCL) in control charts.

Other scales are used to express the precision, one such scale is the relative standard deviation (RSD) or the coefficient of variance (CV), which can be calculated by using Equation 2.9.

$$RSD = \frac{s}{\bar{x}} \times 100\%$$

**Equation 2.9**

In most tests of environmental samples, performing many repeat analyses of sample aliquots is not feasible. So the precision can be estimated from duplicate and multiple analyses of the sample aliquots and expressed as the relative percent difference (RPD). The RPD is determined from the duplicate analysis carried out under identical circumstances on two aliquots of one of the samples in a batch and is calculated by using Equation 2.10.

$$RPD = \left[\frac{|x_1 - x_2|}{\{(x_1 + x_2)/2\}}\right] \times 100$$

**Equation 2.10**

Where $x_1$ and $x_2$ are the results of the duplicate analysis of a sample.

Accuracy of the mean defines the closeness of the measured mean value to the true value (u), it is calculated using Equation 2.11.

$$\% \text{ Accuracy} = \frac{\bar{x} - u}{u} \times 100$$

**Equation 2.11**

### 2.3.2. Uncertainty analysis[61, 126, 130, 131]

Uncertainty is used to assess the doubt about the results for any measurement quantitatively. The standard uncertainty of the mean has usually also been named the standard error of the mean. An estimated uncertainty, u, of the mean of replicates, n, can be calculated using Equation 2.12.

$$u = \frac{s}{\sqrt{n}}$$

**Equation 2.12**

Where, s, is the one standard deviation of replicates. An expanded uncertainty, U, can be calculated using Equation 2.13.

$$U = k \times u$$

**Equation 2.13**

Where, k, is a coverage factor, equal to 2 when the level of confidence is 95%. Combined uncertainty, $u_c$, when two or more means (X, Y,…) are added, subtracted, divided, or multiplied, can be calculated using Equation 2.14 for addition and subtraction and Equation 2.15 for division and multiplication.

$$u_c = \sqrt{u_A^2 + u_B^2 + \cdots}$$

**Equation 2.14**

$$u_c = P \times \sqrt{\left(\frac{u_A}{A}\right)^2 + \left(\frac{u_B}{B}\right)^2 + \cdots}$$

**Equation 2.15**

Where, P, the product of mathematical calculations applied to means (A, B); $u_A$ and $u_B$ are the estimated uncertainties of the means A and B, respectively.

### 2.4. Detection limit[61, 125, 132]

A detection limit (DL) is the lowest concentration level that can be measured to be statistically different from an analyte blank. It is calculated based on the standard deviation, s, of the response and the slope or sensitivity, S, of the calibration curve.
To calculate the instrumental detection limit (IDL), Equation 2.16 is used.

$$\mathrm{IDL} = \frac{3 \times s}{\text{slope of calibration curve}(S)}$$

**Equation 2.16**

Equation 2.17 is used to calculate the procedural detection limit (PDL) that represents the lowest concentration of analyte, which could be measured in a solid environmental substrate, allowing for the method of sample preparation.

$$\mathrm{PDL}(\mathrm{mg\ kg^{-1}}) = \frac{\mathrm{IDL}(\mu\mathrm{g\ L^{-1}}) \times \text{final volume of extract}(\mathrm{mL}) \times \left(\frac{1\mathrm{L}}{1000\mathrm{mL}}\right) \times \text{dilution factor}}{\text{weight of sample}(\mathrm{g})}$$

**Equation 2.17**

## 2.5. Statistical analysis of data

### 2.5.1. Significance testing[125, 126, 133]

A significance test is a statistical test that is used to determine if a difference between two or more values is significant. A null hypothesis ("an indeterminate error is sufficient to explain any difference in values being compared") and an alternative hypothesis ("a difference between values is too great to be explained by a random error and, therefore, must be real") detect whether a difference is or is not significant. A one-tailed significance test is a significance test in which the null hypothesis is rejected for values at only one end of a normal distribution, while a two-tailed test is a significance test in which the null hypothesis is rejected for values at either end of a normal distribution.

#### 2.5.1.1. F-test

The F-test is a statistical test that is used for comparing two variances to see if their difference is too large to be explained by indeterminate error. It is used to determine

the difference between true variance ($\sigma^2$) and measured variance value ($s^2$) for an analyte in an unknown sample. Equation 2.18 is used to calculate $F_{expected}$ ($F_{exp}$) when $s^2 > \sigma^2$:

$$F_{exp} = \frac{s^2}{\sigma^2}$$

**Equation 2.18**

While Equation 2.19 is used when $\sigma^2 > s^2$:

$$F_{exp} = \frac{\sigma^2}{s^2}$$

**Equation 2.19**

Also the F-test can be used to compare variances for two samples, and it is calculated by using Equation 2.20:

$$F_{exp} = \frac{s_A^2}{s_B^2}$$

**Equation 2.20**

Where $s_A$, $s_B$ are standard deviation for values obtained from analysis of samples A and B respectively where $s_A$ is larger than $s_B$.

A critical F value, $F_{crtical}$ ($\alpha$, $\nu_{numerator}$ , $\nu_{denominator}$ ) gives the largest value of F that can be explained by indeterminate error, where $\alpha$ is a significance level and $\nu$ is a degree of freedom for $s^2$ ($\nu = n-1$), where n is the number of replicates. Expected F values, $F_{exp}$, were compared with $F_{crtical}$ values at two-tailed 0.05 $\alpha$ (i.e. at 95% confidence level). If $F_{exp}$ is less than or equal $F_{crtical}$, the F-test is passed (i.e. the difference is not significant), while when $F_{exp}$ is larger than $F_{crtical}$, the F-test is failed (i.e. the difference is significant).

#### 2.5.1.2. T-test

The T-test is a statistical test that is used for comparing two mean values to determine if their difference is too large to be explained by indeterminate error. It can be used to determine a difference between a true mean value ($\mu$) and a measured mean value ( $\bar{x}$ ) for an analyte in a sample, and $t_{expected}$ ($t_{exp}$) is calculated by Equation 2.21:

$$t_{exp} = \frac{|\mu - \bar{x}| \times \sqrt{n}}{s}$$

**Equation 2.21**

Where n is a number of replicates, and s is a standard deviation.

Also t-test can be used for comparing two samples means, where Equation 2.22 is used when the F-test is passed:

$$t_{exp} = \frac{|\bar{x}_A - \bar{x}_B|}{s_{pool} \times \sqrt{(1/n_A) + (1/n_B)}}$$

**Equation 2.22**

Where $\bar{x}_A$ and $\bar{x}_B$ are measured means of an analyte in samples A and B respectively; $n_A$, $n_B$ are a number of replicates; $s_{pool}$ is the pooled standard deviation and it is calculated by Equation 2.23:

$$s_{pool} = \sqrt{\frac{(n_A - 1)s_A^2 + (n_B - 1)s_B^2}{n_A + n_B - 2}}$$

**Equation 2.23**

Where $s_A$, $s_B$ are standard deviation.

Equation 2.24 is used to calculate the t-test when the F-test is failed:

$$t_{exp} = \frac{|\bar{x}_A - \bar{x}_B|}{\sqrt{(s_A^2/n_A) + (s_B^2/n_B)}}$$

**Equation 2.24**

Critical values ($t_{critical}$), t (α, ν), at two-tailed 0.05 α, were compared with $t_{exp}$ values. Where ν is calculated using Equation 2.25 when F-test is passed, whilst Equation 2.26 is used when F-test is failed, where n is a number of replicates.

$$\nu = n_A + n_B - 2$$

**Equation 2.25**

$$\nu = \frac{((s_A^2/n_A) + (s_B^2/n_B))^2}{(\frac{(s_A^2/n_A)^2}{n_A + 1}) + (\frac{(s_B^2/n_B)^2}{n_B + 1})} - 2$$

**Equation 2.26**

### 2.5.1.3. Analysis of variance (ANOVA)[134, 135]

The significant tests (F-test and t-test) described in the sections 2.5.1.1 and 2.5.1.2 as well as the one-way ANOVA in this section are considered parametric tests as analysing data is assumed under the normal distribution. However, this is not valid for the small number of samples normally used in analytical research. In the case of that the normal distribution cannot be assumed, and so non-parametric test such as Levene's F test, Welch, Games-Howell and Tukey honestly significant difference (HSD) tests are used. Although not ideal, parametric tests are used more commonly in the literature and hence, were used here at times for easier comparison. However, some of the data was analysed by using non-parametric tests as the number of samples was small and the distribution was not normal.

This is a method that can be used for comparing more than two means, as the t-test in this case cannot be used. The comparison can be based on one dependent variable (i.e. one-way ANOVA) or more dependent variables (i.e. two-way ANOVA). Homogeneity of variance for compared means should be tested before conducting these analyses. This is most commonly performed using the Levene's F test (a statistic test used for assessing the variances equality of a variable between the groups). When there is no a significant difference between variances, one-way ANOVA can be used, otherwise, the Welch test is usually used. One-way ANOVA and the Welch tests are conducted to evaluate whether mean values of a dependent variable are significantly different among the groups. Between which two groups that significant difference is present, this can be determined by conducting one of the Post Hoc tests. For this purpose, Games-Howell and Tukey HSD tests are usually used when the variances are, or are not, significantly different, respectively. These statistical calculations were performed using the official package IBM SPSS version 23 (see Chapter 5).

### 2.5.2. Z-score[61, 126, 136]

A Z-score is a simple statistical method that is used for comparing data. It is the number of standard deviations or standard errors from a certified or measured mean

for a certain data point or a certain test mean. It can be positive, zero, or negative indicating that an experimental value is above, equal to, or below a certified or measured mean, respectively. Equation 2.27 is used to calculate the Z-score when a data point is compared to a certified or measured mean, while Equation 2.28 is used to compare a test mean to a certified or measured mean.

$$Z_{score} = \frac{x - \bar{x}}{s}$$

**Equation 2.27**

Where x, $\bar{x}$ and s are a data point, a certified or measured mean, and a standard deviation, respectively.

$$Z_{score} = \frac{\bar{x}_1 - \bar{x}_2}{s/\sqrt{n}}$$

**Equation 2.28**

Where, $\bar{x}_1$, $\bar{x}_2$, and n are a measured mean, certified mean, and a number of replicates of the test sample, respectively. The Z-score can be used to assess, to rank, and to validate results obtained from a certain test compared with a certified or measured value of a certified reference material. Equation 2.26 is used for this situation, taking into account that the n here is a number of independent replicates, and the s is a predicted standard deviation calculated according to the Horwitz equation (see Equation 2.29).

$$s = \frac{C}{100} \times 2^{1-0.5\log(C \times f)}$$

**Equation 2.29**

Where, C, is the concentration (e.g. a certified or measured mean), and f is a fraction factor (e.g. for mg $kg^{-1}$, i.e. ppm, it is $10^{-6}$). Since, $2^{1-0.5 \log (C \times f)}$, represents a RSD value in the formula of the Horwitz equation, therefore, under worst case scenario (i.e. 10% RSD), the Horwitz equation can be written in the formula of Equation 2.30.

$$s = \frac{C}{10}$$

**Equation 2.30**

Values of Z-score between 2 and -2 are considered acceptable and between 2 and 3 or -2 and -3 are questionable. Z-scores are considered not satisfactory when they are > 3 or < -3.

# 3 General experimental procedures

The experimental procedures described in this chapter were used throughout the thesis. Experimental procedures specific to individual chapters are contained in the relevant chapters.

## 3.1. Cleaning procedure

For all experiments conducted, an acid bath containing 10% (*v/v*) nitric acid was used to soak all glassware and plastic-ware overnight before use. Glassware and plastic-ware were then washed three times using distilled water. After that they were rinsed in deionized water then dried in a clean air environment.

## 3.2. Simulation of $PM_{10}$ samples

Samples of $PM_{10}$ were simulated by smearing blank FDMS filters using a plastic spatula (see Fig. 3.1) with 100 mg of a BGS RM 102 Ironstone Soil, produced by BGS. This material was used partly due to its small particle size (< 40 μm, where the fraction of airborne PM collected on FDMS filters is < 10 μm); also because soil particles typically constitute a major component of airborne $PM_{10}$; and finally because it has certified values for the bioaccessible concentration of As, Cd, and Pb when the stomach phase of the UBM is applied.

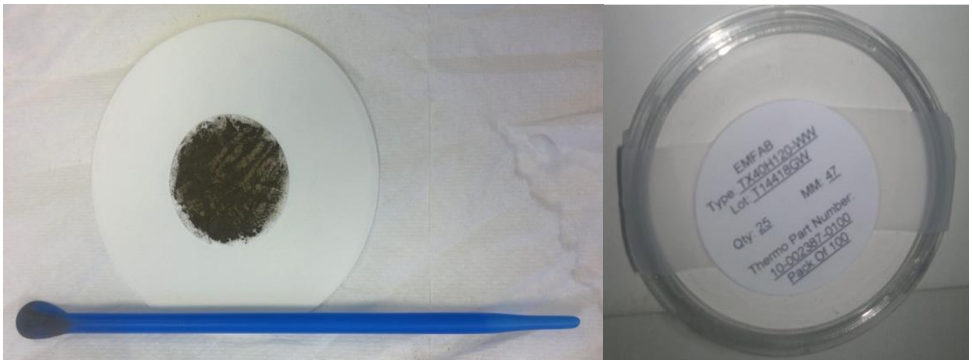


**Figure 3.1. Blank and loaded Pallflex TX40 FDMS filters**

## 3.3. Pseudototal digestion

### 3.3.1. Apparatus

Glassware and plastic-ware were pre-cleaned as described in Section 3.1. Blank Pallflex TX40 FDMS filters, mass 5 mg $cm^{-2}$, diameter 47 mm, were supplied by Air

Monitors Ltd. (Gloucestershire, UK). A MARSXpress microwave assisted digestion system (CEM, Buckingham, UK), was utilized to digest samples. Digests obtained were analysed by ICP-MS (Model 7700x, Agilent Technologies, Cheshire, UK).

### 3.3.2. Reagents

All chemicals were of analytical grade. Hydrochloric acid (HCl) (36.5-38%) and nitric acid ($HNO_3$) (≥ 69% Trace SELECT® for trace analysis) were obtained from Sigma Aldrich (Gillingham, UK). *Aqua regia* was made freshly each time it was required by addition of 1 volume of concentrated $HNO_3$ to 3 volumes of concentrated HCl ($1HNO_3$: 3HCl, *v/v*).

### 3.3.3. Procedure

Triplicate 0.1 g soil samples were weighed, together with three simulated $PM_{10}$ samples as described in Section 3.2. The soil samples and simulated $PM_{10}$ samples, as well as three blank FDMS filters, were placed into clean microwave vessels then 5 mL of *aqua regia*, was added to the soil samples, loaded and blank filters. A reagent blank was also prepared. The vessels were loosely closed and placed in a rack inside a fume hood overnight. After that the vessels were tightly sealed and put inside the rotor of the microwave assisted digestion system. The microwave was operated according to the conditions shown in Table 3.1. Low power (800 W) was applied because the small volumes of extractant used may be vented when a high power is applied.

When the holding time was finished, the vessels were left for 1 hour inside the fume hood to cool. Digests were filtered using Whatman filter paper into 100 mL pre-cleaned volumetric flasks and were washed several times with deionized water. Filtered digests were then diluted to the mark with deionized water. Required dilutions were performed to obtain the analyte in 2% *aqua regia.* The solutions obtained were stored in polypropylene tubes in a fridge at 4 °C prior to analysis by ICP-MS (see Section 3.6).

**Table 3.1. The operating conditions of the microwave assisted digestion system**

| Parameters | Values |
|---|---|
| Number of vessels | 22 |
| Power (watts) | 800 |
| Temperature (°C) | 160 |
| Ramping time (min) | 20 |
| Holding time (min) | 20 |

## 3.4. Original procedure of the simplified bioaccessibility extraction test (SBET)[91]

### 3.4.1. Apparatus

Glassware and plastic-ware were pre-cleaned as was described in Section 3.1. Acrodisc® cellulose acetate membrane syringe filters (pore size 0.45 μm, diameter 25 mm) were purchased from Sigma Aldrich (Gillingham, UK). The pH of solutions was measured by using a Mettler-Toledo (SevenGo™) pH meter supplied by Mettler-Toledo Ltd., Leicester, UK. Suspensions were shaken and incubated by using an end-over-end rotator placed inside an incubator (Stuart® SI500 shaking incubator) manufactured by Barloworld Scientific Ltd., Staffordshire, UK (see Fig. 3.2). The ICP-MS, mentioned in Section 3.3.1, was used to analyse extracts obtained.

### 3.4.2. Reagents

Hydrochloric acid was as described in Section 3.3.2. A 0.4 M glycine solution, pH 1.5 ± 0.05, was prepared by dissolving 60.060 g glycine (analytical reagent grade, Fisher scientific, Loughborough, UK) in 1900 mL of deionized water. Hydrochloric acid was then utilized to adjust the pH of the solution using a Mettler-Toledo (SevenGo™) pH meter to 1.5 ± 0.05 at 37 ± 2°C. The solution was then made up to 2 L with deionised water.


**Figure 3.2. Stuart® SI500 shaking incubator**

### 3.4.3. Procedure

Soil samples (1.0 g) were placed into 125 mL wide mouth high-density polyethylene (HDPE) bottles. A 100 mL aliquot of the extractant (0.4 M glycine solution at pH 1.5 ± 0.05) was added to the sample bottles as well as to an empty HDPE bottle as a procedural blank. The bottles were tightly sealed and placed on an end-over-end rotator inside a pre-heated incubator at 37±2°C. Samples were extracted at a rotator speed of 30 rpm, for 1 hour, at 37±2°C. The HDPE bottles were then removed from the incubator. A 20 mL disposable syringe was used to remove the supernatant fluids from the extraction bottles. Supernatant fluids were filtered through a 0.45 µm luer-lok cellulose acetate disk filter (25 mm diameter) attached to a disposable syringe (see Fig. 3.3). The pH of the fluid was measured at the end of extraction, to check that it was within ± 0.5 pH units of the starting pH. The total extraction time also did not exceed 90 minutes. Obtained extracts were stored in polypropylene tubes in a fridge at 4 °C prior to analysis within a week by ICP-MS (see Section 3.6).

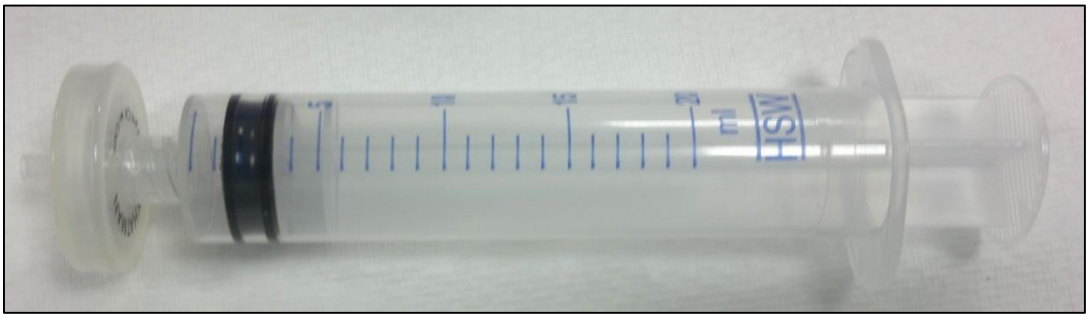

**Figure 3.3. Luer-lok cellulose acetate disk filter attached to the disposable syringe**

## 3.5. Original procedure of the stomach phase of the unified bioaccessibility method (UBM)[94]

### 3.5.1. Apparatus

Glassware and plastic-ware were pre-cleaned as was described in Section 3.1. A pH meter as described in Section 3.4.1, was used to measure pH. An end-over-end rotator placed inside an incubator, described in Section 3.4.1, was used to incubate and agitate suspensions. Suspensions were centrifuged using an Eppendorf centrifuge 5804R (Hamburg, Germany). The ICP-MS, described in Section 3.3.1, was used to analyse extracts obtained.

### 3.5.2. Reagents

All chemicals were of analytical grade. Bovine serum albumin, $NaH_2PO_4$, KCl, urea, $CaCl_2.2H_2O$, and pepsin (porcine) were purchased from Merck (Poole, UK). Glucose, NaCl, $Na_2SO_4$, $NH_4Cl$, and NaOH were supplied by VWR International, Lutterworth, UK. Glucuronic acid, KSCN, glucosamine hydrochloride, alpha amylase, mucin (porcine), and uric acid were obtained from Sigma Aldrich (Gillingham, UK). Hydrochloric acid (HCl) and nitric acid ($HNO_3$) were as described in Section 3.3.2.

### 3.5.3. Preparation of the digestive fluids

The reagents required for the stomach phase of the UBM were prepared one day before conducting the experiments. These reagents were saliva and gastric fluids, and the details of their preparation are shown in Fig. 3.4.

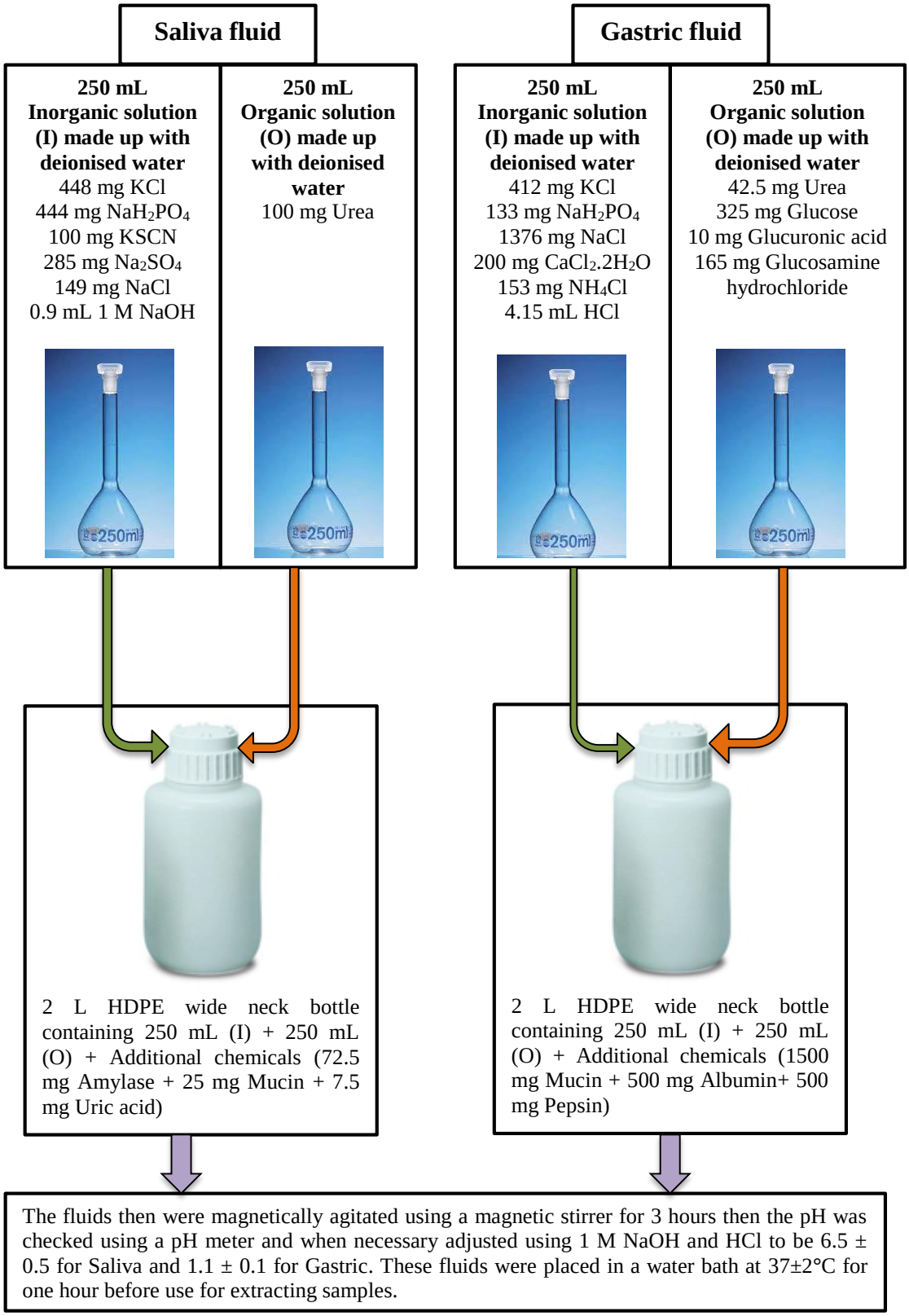


**Figure 3.4. Schematic diagram of the preparation of digestive fluids of the stomach phase of the unified bioaccessibility method (UBM)**

### 3.5.4. Controlling the pH of the stomach fluids

The pH of fluids was controlled by putting 9.0 mL of the saliva fluid into a 50 mL centrifuge tube then 13.5 mL of the gastric fluid was added. The pH was then checked to be 1.20 ± 0.05 and when necessary the gastric or saliva fluid was adjusted with HCl or 1 M NaOH to obtain the pH required.

### 3.5.5. Procedure of the stomach phase extraction

Soil samples (0.6 g) were placed into extraction tubes then 9.0 mL of the saliva fluid was added using a pipette. For approximately 10 seconds, the suspensions were manually shaken then 13.5 mL of the gastric fluid was added by pipette. The pHs of suspensions were then checked to be 1.20 ± 0.05 and, when necessary, they were adjusted with HCl or 1 M NaOH to achieve the pH required. The closed tubes of the pH-checked suspensions were then placed on an end-over-end rotator inside a pre-heated incubator at 37±2°C. Samples were extracted at a rotator, for 1 hour, at 37±2°C. The tubes were then removed from the incubator. The pHs of suspensions was checked to ensure they were less than 1.50, and the extraction was repeated when the pH was ≥ 1.50. The samples were then centrifuged at 4500 g for 15 minutes. The supernatants were carefully pipetted into polypropylene tubes and acidified with 0.5 mL $HNO_3$. Obtained extracts were stored in polypropylene tubes in a fridge at 4 °C prior to analysis by ICP-MS (see Section 3.6).

## 3.6. Analysis of extracts and digests

The ICP-MS system, mentioned in Section 3.3.1, was used to determine concentrations of PTE in extracts and digests obtained. Spectrum analysis (multi tune) mode was used for performing data acquisition. The parameters of this mode and the operation conditions of the ICP-MS are tabulated in Table 3.2. A constant amount of sample at a rate of 1 mL $min^{-1}$ was introduced using an auto-sampler and a peristaltic pump. To calibrate the ICP-MS, four matrix-matched standard solutions, prepared by serial dilution of multi-element standard stock solution (10 mg $L^{-1}$ of As, Cd, Cr, Cu, Mn, Ni, Pb, and Zn) and Fe standard stock solution (1003 mg $L^{-1}$) obtained from Qmx Laboratories, Essex, UK, were used. A calibration blank was also prepared in reagents similar to those used for preparing standard solutions.

**Table 3.2. Operation conditions of the ICP-MS and parameters of the spectrum analysis (multi tune) mode**

| **ICP-MS conditions** | |
|---|---|
| Power (watt) | 1550 |
| Quadrupole bias (V) | -15 |
| Octopole bias (V) | -18 |
| Nebulizer gas flow (L $min^{-1}$) | 0.85 |
| Plasma gas flow (L $min^{-1}$) | 15 |
| Auxiliary gas flow (L $min^{-1}$) | 0.9 |
| Collision cell gas (L $min^{-1}$) | He (4.5) for all masses determined, except for $^{111}Cd$, $^{114}Cd$, $^{206}Pb$, $^{207}Pb$ and $^{208}Pb$, where no gas mode was chosen |
| Sample uptake rate (mL $min^{-1}$) | 1 |
| **Spectrum (multi tune) mode parameters** | |
| Number of peaks | 1 |
| Number of points per peak | 3 |
| Integration time (sec) | 0.1 For all masses determined, except $^{75}As$, $^{111}Cd$, $^{114}Cd$, $^{52}Cr$, $^{53}Cr$, $^{60}Ni$ and $^{61}Ni$, where the value was 1.0 |
| Total acquisition time of analysis per sample (sec) | 170 |
| Rinse time between analysis of samples (sec) | 60 |
| Type of run | Running a sequence |

To check for interferences, two or three isotopes were measured for each element, except As and Mn that are monoisotopic (see Table 3.3). Based on this, one isotope was chosen for each element to determine the bioaccessible concentration of PTE tested (see Table 3.3). A 3 mg $L^{-1}$ internal standard solution was prepared by using an internal standard stock solution for ICP-MS containing 100 mg $L^{-1}$ of Bi, In, Ge, Li, Lu, Rh, Sc, and Tb (Agilent Technologies, USA). This solution was introduced to the instrument on-line, by means of a peristaltic pump, to compensate for physical interferences. To remove spectroscopic interferences, the He collision cell mode was operated.

The computer software (ICP-MS MassHunter 4.1 Workstation software) was used to process the data. For checking instrumental draft, concentration of PTE in one of the calibration standards was measured every ten analyses, and also at the end of sample analysis.

### 3.7. Data handling

Mean, standard deviation, RSD, and RPD were calculated using Equations 2.7, 2.8, 2.9, and 2.10 respectively (see Section 2.3). Equation 3.1 was used to convert the analyte concentration obtained by ICP-MS, which is usually in μg $L^{-1}$, to mg $kg^{-1}$ that is commonly used to express the concentration of an analyte in soils.

$$\text{Conc.}\,(\text{mg kg}^{-1}) = \frac{\text{analyte conc.}\,(\mu\text{g L}^{-1}) \times \text{ final volume of extract(mL)} \times \left(\frac{1\text{L}}{1000\text{mL}}\right) \times \text{dilution factor}}{\text{dry weight of sample(g)}}$$

**Equation 3.1**

### 3.8. Moisture content

In order to be able to express the concentrations of PTE measured based on the dry weight of samples, moisture content was determined. A 1 g soil sample was weighed into a dry pre-cleaned and pre-weighed crucible then placed in an oven for 24 hours at 105 °C. Equation 3.2 was used to calculate the moisture content.

$$\text{Moisture (\%)} = \frac{\text{initial weight} - \text{dry weight}}{\text{initial weight}} \times 100$$

**Equation 3.2**

### 3.9. Detection limits

Equation 2.16 and 2.17 mentioned in Section 2.4 were used to calculate the IDL and the PDL.

### 3.10. Statistical analysis of data

The F-test and t-test statistics were calculated using Equations 2.18 - 2.26 (see Section 2.5), while Equations 2.28 and 2.30 were used to calculate Z-score.

**Table 3.3. Determined and chosen isotopes, their natural abundances and internal standards of potentially toxic elements (PTE)**

| PTE | Determined Isotopes | % Natural Abundance | Chosen isotope | Internal standard |
|---|---|---|---|---|
| **As** | $^{75}$As | 100 | $^{75}$As | $^{72}$Ge |
| **Cd** | $^{111}$Cd | 12.8 | $^{111}$Cd | $^{115}$In |
| | $^{114}$Cd | 28.7 | | |
| **Cr** | $^{52}$Cr | 83.8 | $^{52}$Cr | $^{45}$Sc |
| | $^{53}$Cr | 9.50 | | |
| **Cu** | $^{63}$Cu | 69.2 | $^{63}$Cu | $^{45}$Sc |
| | $^{65}$Cu | 30.9 | | |
| **Fe** | $^{56}$Fe | 91.7 | $^{56}$Fe | $^{45}$Sc |
| | $^{57}$Fe | 2.20 | | |
| **Mn** | $^{55}$Mn | 100 | $^{55}$Mn | $^{45}$Sc |
| **Ni** | $^{60}$Ni | 26.2 | $^{60}$Ni | $^{45}$Sc |
| | $^{61}$Ni | 1.14 | | |
| **Pb** | $^{206}$Pb | 24.1 | $^{208}$Pb | $^{209}$Bi |
| | $^{207}$Pb | 22.1 | | |
| | $^{208}$Pb | 52.4 | | |
| **Zn** | $^{64}$Zn | 48.6 | $^{66}$Zn | $^{72}$Ge |
| | $^{66}$Zn | 27.9 | | |

### 3.11. Safety

Experimental hazard assessments were applied with all apparatus and chemicals used in this work. Table 3.4 shows the classification of substances used in terms of their risk to health in relation to the "Control of Substances Hazardous to Health" regulations. Gloves, safety glasses, and laboratory coats were used for personal protection. Unused chemicals were sealed and kept in appropriate cupboards, and excess acids, digests, and extracts were disposed off as highlighted in the relevant COSHH assessments.

**Table 3.4. Hazardous substances used in this research work**

| Substance | Very toxic | Toxic | Harmful | Corrosive | Irritant |
|---|---|---|---|---|---|
| HCl | | ✔ | ✔ | ✔ | ✔ |
| $HNO_3$ | ✔ | ✔ | ✔ | ✔ | ✔ |
| Glycine | | | ✔ | | ✔ |
| Glucosamine hydrochloride | | | | | ✔ |
| Pepsin | | | | | ✔ |
| $MgCl_2.6H_2O$ | | | ✔ | | ✔ |
| KSCN | | | ✔ | | ✔ |
| NaOH (solution) | | | ✔ | ✔ | |
| $CaCl_2.2H_2O$ | | | | | ✔ |
| $NH_4Cl$ | | | ✔ | | |
| $NaHCO_3$ | | | | | ✔ |
| Multi element stock solution | | ✔ | ✔ | ✔ | ✔ |

# 4 Miniaturization of two oral bioaccessibility tests to measure potentially toxic elements in inhalable particulate matter collected during routine air quality monitoring

## 4.1. Introduction

Many studies applying the UBM[69, 78, 95-97, 137-139] and the SBET[28,29, 65, 82, 105, 137, 140-145] have been conducted to measure the bioaccessible PTE concentration in soils. In contrast, to date, no work has been reported for the application of the UBM to $PM_{10}$ and few studies have been observed in the literature for application of the SBET to $PM_{10}$, either for particles extracted from soil and dust or those collected on filters. For particles extracted from soils, the SBET was applied to determine Cr, Cu, Ni, Pb, and Zn in five particle-size fractions separated from urban soils collected from Torino (Italy) and Seville (Spain).[105] Based on Stokes' Law, particles of soils were fractionated. These fractions ranged from the finest particles (i.e. < 2 μm) to the coarse particles (> 50 μm). Centrifugation followed by filtration using Whatman filter paper number 2 was adopted to obtain a clear extract.

For airborne PM collected on filters, only one study has reported the application of the SBET to real samples.[106] In the study, nine elements (As, Cd, Co, Cr, Cu, Mn, Ni, Pb, and Zn) were determined in airborne PM supported on quartz microfibre filters sampled in Nanjing (China). Limitations of this study were that the method for extraction of PM collected on filters was not analytically optimised. In addition, the protocol of the SBET was not followed exactly: instead of using acrodisc® cellulose acetate membrane syringe filters to obtain a clear extract, centrifugation followed by filtration through a filter paper was used. Moreover, the fractions investigated did not have close similarity to those transported to the gastrointenstinal tract by mucocillary clearance, which is generally between 2.5 and 10 μm. Furthermore, airborne PM were sampled using a large-volume air sampler which is not similar to those normally used in routine air quality monitoring.

The aim of this part of thesis was to develop versions of the SBET and the stomach phase of the UBM applicable for the determination of bioaccessible PTE concentrations in $PM_{10}$ collected on FDMS filters, as used in routine air quality monitoring in the UK.

## 4.2. Experimental

### 4.2.1. Apparatus and reagents

Blank Pallflex TX40 FDMS filters, as described in Section 3.3.1, were used. The apparatus and reagents used for the SBET and the stomach phase of the UBM were as described in Sections 3.4.1-3.4.2 and 3.5.1-3.5.2, respectively.

### 4.2.2. Simulation of $PM_{10}$ samples

Simulated $PM_{10}$ samples were prepared as described in Section 3.2. To investigate whether the presence of the FDMS filters affected the extractability of PTE from $PM_{10}$, samples of 100 mg BGS RM 102 Ironstone Soil alone and blank FDMS filters were also involved in this experiment.

### 4.2.3. Procedures of the original SBET and stomach phase of the UBM

When the SBET[91] was applied, three 1.0 g test portions of BGS RM 102 Ironstone Soil were placed into three 125 mL wide-mouth HDPE bottles, then the procedure was conducted as described in Section 3.4.3. Extracts were stored in polyethylene bottles at 4 °C prior to analysis by ICP-MS as described in Section 3.6.

The validated BARGE UBM (stomach phase) methodology[94] was implemented in this study. Three 0.6 g test portions of BGS RM 102 Ironstone Soil were placed into three centrifuge tubes; the procedure was then conducted as described in Section 3.5.5. A 2.5 mL aliquot of each supernatant was collected by pipetting and diluted 4-fold with 2% $HNO_3$. Extracts were stored in polyethylene bottles at 4 °C prior to analysis by ICP-MS as described in Section 3.6.

### 4.2.4. Modification of procedures of the SBET and stomach phase of the UBM

#### 4.2.4.1. The miniaturised SBET procedure

To maintain the same ratio between the sample mass and the extractant volume as in the original procedure (1.0 g : 100 mL), these were each reduced ten-fold (to 0.1 g and 10 mL). Three replicated extractions of BGS RM 102 Ironstone Soil were carried out and results compared with those obtained using the original method (described in Section 4.2.3).

Three simulated PM samples were prepared by loading BGS RM 102 Ironstone Soil onto FDMS filters as described in Section 3.2, and the miniaturised SBET was performed. A wide neck heavy-duty polypropylene bottle (150 mL) was used as the extraction vessel. The original bottle (a narrow neck 125 mL bottle) was changed because it was found that folding FDMS filters reduced the efficiency of analyte extraction. This was likely because of reduced contact between sample and extractant. The suspension obtained at the end of the extraction period was filtered through a pre-washed acrodisc® syringe filter (see Section 4.3.1) to separate the extract. Three blank FDMS filters and three samples of 0.1 g BGS RM 102 Ironstone Soil alone (i.e. not loaded on FDMS filters) were extracted in parallel to the three simulated $PM_{10}$ samples.

#### 4.2.4.2. The miniaturised UBM (stomach phase) procedure

Similarly, for the stomach phase of the UBM, the ratio between the sample mass and the volume of extractant was maintained by reducing the original values (0.6 g soil : 9 mL simulated saliva fluid : 13.5 mL simulated gastric fluid) six times (to be 0.1 g soil : 1.5 mL saliva : 2.25 mL gastric fluid). Three replicated extractions of BGS RM 102 Ironstone Soil were carried out and results compared with those obtained using the original method (described in Section 4.2.3).

Three simulated PM samples were prepared by loading BGS RM 102 Ironstone Soil onto FDMS filters as described in Section 3.2, and the miniaturised UBM (stomach phase) was performed. Recoveries of PTE were very low (between 17% for Fe and 48% for As) when a 15 mL centrifuge tube was used for extracting samples with respect to those achieved by using the larger vessel, although the volume of the

vessel is adequate for the maximum reagent volume used (i.e. 3.75 mL). Therefore, a wide neck heavy-duty polypropylene bottle (150 mL) was used as the extraction vessel. The suspension obtained at the end of the extraction time was then decanted into a 15 mL centrifuge tube for isolation of the extract by centrifugation. The pH was adjusted using 25 or 50% *v/v* HCl and 0.1 M NaOH as well as a micro pH electrode because the extractant volume was small (< 4 mL). Three blank FDMS filters and three samples of 0.1 g BGS RM 102 Ironstone Soil alone (not loaded on filters) were extracted in parallel to the three simulated $PM_{10}$ samples.

### 4.2.5. Analyte quantification

Extracts obtained were analysed by ICP-MS as described in Section 3.6. The IDL and PDL, shown in Table 4.1, were calculated using Equations 2.16 and 2.17.

**Table 4.1. Instrumental (IDL) and procedural (PDL) detection limits for the simplified bioaccessibility extraction test (SBET) and the stomach phase of the unified bioaccessibility method (UBM) by ICP-MS**

| Isotopes | SBET | | UBM | |
|---|---|---|---|---|
| | IDL (µg $L^{-1}$) | PDL (mg $kg^{-1}$) | IDL (µg $L^{-1}$) | PDL (mg $kg^{-1}$) |
| $^{75}As$ | 0.019 | 0.002 | 0.025 | 0.001 |
| $^{111}Cd$ | 0.010 | 0.001 | 0.006 | 0.0002 |
| $^{52}Cr$ | 0.028 | 0.003 | 0.161 | 0.006 |
| $^{63}Cu$ | 0.135 | 0.014 | 0.057 | 0.002 |
| $^{56}Fe$ | 0.955 | 0.096 | 8.55 | 0.321 |
| $^{55}Mn$ | 0.708 | 0.071 | 0.230 | 0.009 |
| $^{60}Ni$ | 0.027 | 0.003 | 0.043 | 0.002 |
| $^{208}Pb$ | 0.031 | 0.003 | 0.018 | 0.001 |
| $^{66}Zn$ | 0.189 | 0.019 | 0.686 | 0.026 |

### 4.2.6. Quality control

No certified reference material is currently available for bioaccessible PTE in airborne PM. Therefore, performance of the extraction was assessed by using spike recovery tests and by extracting triplicate sample. Extractants were spiked to known concentrations of analytes (10020 μg $L^{-1}$ for Fe and 250 μg $L^{-1}$ for other PTE), and taken through the complete extraction procedure. The percentage spike recovery was calculated using Equation 1.

$$\%\ \boldsymbol{spike\ recovery} = \left(\frac{|\boldsymbol{measured\ conc.\ of\ PTE\ in\ spiked\ reagent - measured\ conc.\ of\ PTE\ in\ unspiked\ reagent}|}{\boldsymbol{known\ conc\ of\ PTE\ in\ spiked\ reagent}}\right) \times \mathbf{100}$$

**Equation 4.1**

For the miniaturised and original experiment, all RSDs values were less than 10%, except for Zn, where they were larger than 10% when the SBET (miniaturised and original) was conducted (see Fig. 4.1). When the miniaturised versions of the SBET and the stomach phase of the UBM were applied to simulated $PM_{10}$ samples, the RSD values were < 10 %, except 8% of the values ranged from 10 to 15 % and one value was 24% (see Fig. 4.2). The spike recoveries were between 86.8 and 114% (see Fig. 4.3).

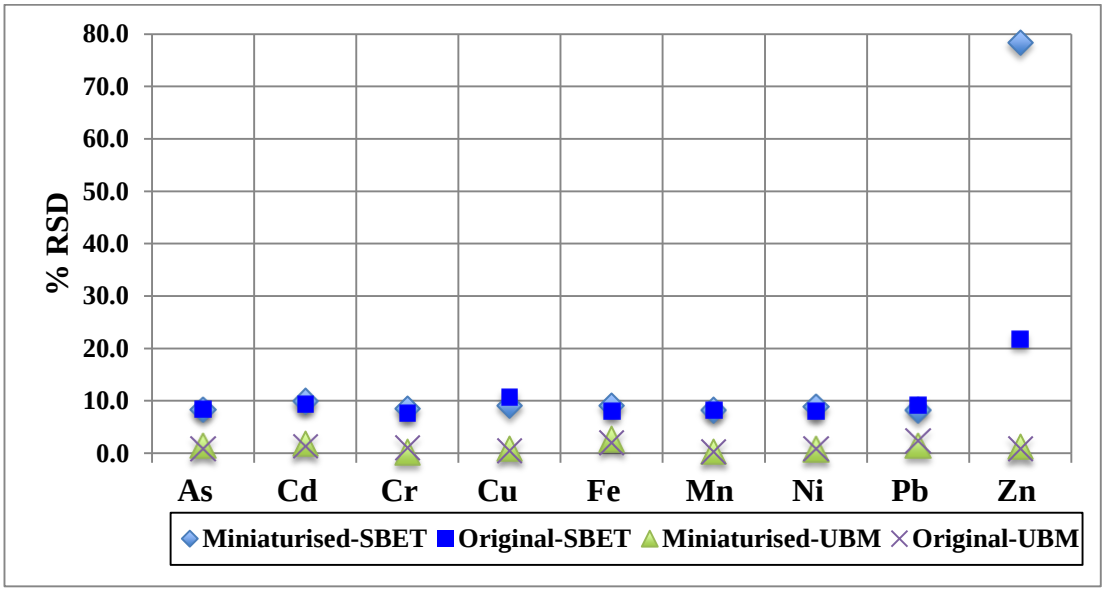


**Figure 4.1. Values of the percentage relative standard deviation (RSD) for the triplicate extractions of the BGS RM 102 Ironstone Soil for the miniaturised and original simplified bioaccessibility extraction test (SBET) and stomach phase of the unified bioaccessibility method (UBM)**

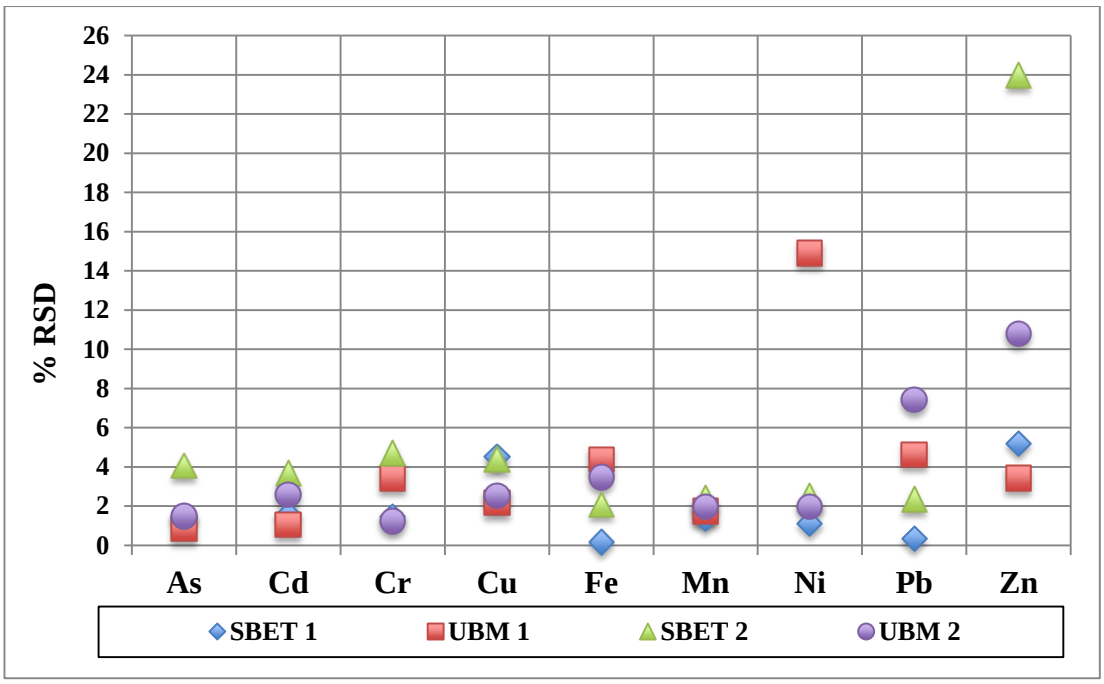


**Figure 4.2. Values of the percentage relative standard deviation (RSD) for the triplicate extractions of BGS RM 102 Ironstone Soil (1) alone and (2) when smeared on FDMS filters to simulated $PM_{10}$ samples, as obtained with the miniaturised simplified bioaccessibility extraction test (SBET) and stomach phase of the unified bioaccessibility method (UBM)**

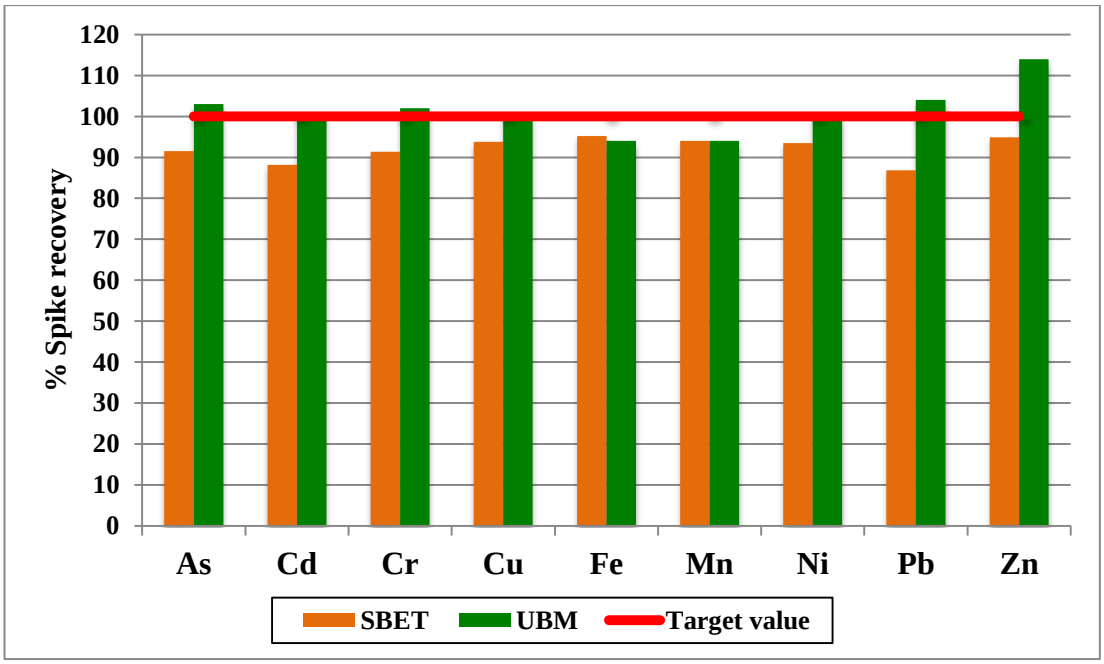


**Figure 4.3. The percentage of PTE spike recovery in the reagent blank of the miniaturised simplified bioaccessibility extraction test (SBET) and stomach phase of the unified bioaccessibility method (UBM)**

## 4.3. Results and discussion

### 4.3.1. Washing regime to reduce Cu and Zn blanks arising from acrodisc® filters

Results obtained initially from the SBET revealed that procedural blanks contained high concentrations of Cu (119 μg $L^{-1}$) and Zn (1520 μg $L^{-1}$). As a result, poor precision for these analytes was obtained (RSD values of 9.2% for Cu and 78% for Zn, when triplicate extractions were performed). The acrodisc® syringe filters used to separate the supernatant from the suspension, were recognised as a source for Cu and Zn in procedural blanks. Previous SBET studies[141, 143, 144] have not highlighted this problem. That may be not only because the SBET is mostly used to determine As and Pb but also due to the fact that centrifugation was used instead of filtration to obtain clear extracts for analysis in some studies in which Cu and Zn were the analytes of interest.[105] However, a study conducted by Falta *et al.*[75] to assess gastric bioaccessibility using a US Pharmacopeia methodology mentioned that, although pre-cleaned cellulose acetate filters were used for filtration, higher blank levels were obtained compared to centrifugation of sample extracts.

To find an appropriate washing regime, sequential 10 mL aliquots of either glycine (0.4 mol $L^{-1}$, pH 1.5), HCl (pH 1.5) or deionized water were passed through three new acrodisc® filters and the filtrates analysed using ICP-MS. Concentration of Cu and Zn were lower than detectable concentrations when deionized water was used for washing syringe filters, whereas they were leached from the syringe filters when other reagents (i.e. glycine and HCl) were used (see Figures 4.4-4.7). When the volume of washing solution was increased, the concentrations of Cu and Zn decreased. After 80 mL of glycine or HCl had been passed through, the concentrations of Cu in the filtrates were 0.217 and 0.154 μg $L^{-1}$, respectively, and for Zn, they were 38.9 and 29.2 μg $L^{-1}$, respectively. No significant decrease in concentration of Cu or Zn was observed on further washing. Although both glycine and HCl were able successfully to remove the Cu and Zn contribution to the procedural blank result from the syringe filters, glycine was selected for use in the washing regime because glycine is used as the extractant in the SBET and also because of the matrix-matched calibration standards for ICP-MS.

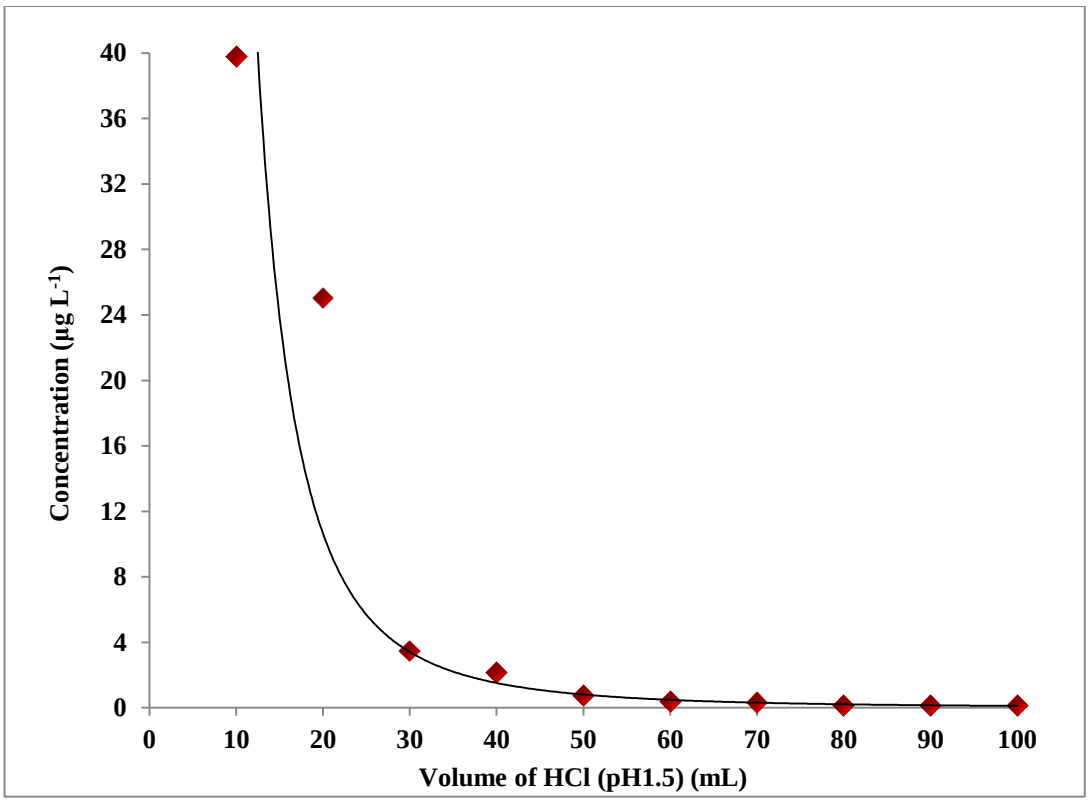


**Figure 4.4. Release of Cu from blank acrodisc® syringe filters washed with HCl (pH 1.5)**

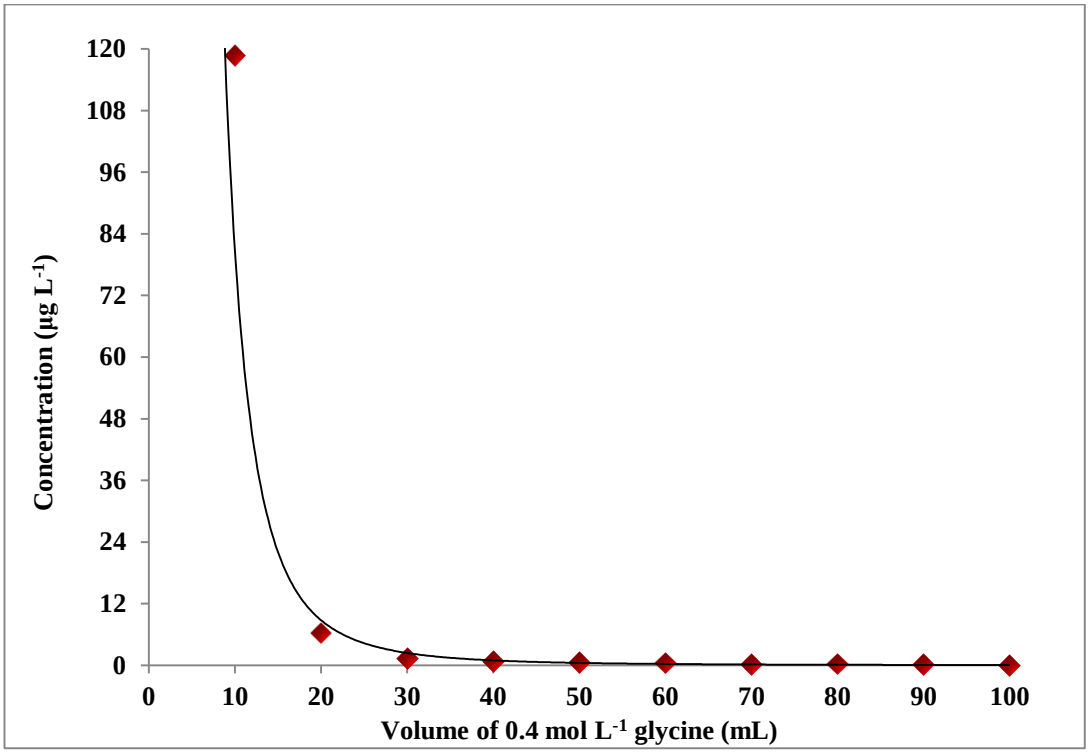


**Figure 4.5. Release of Cu from blank acrodisc® syringe filters washed with glycine (0.4 mol $L^{-1}$ pH 1.5)**

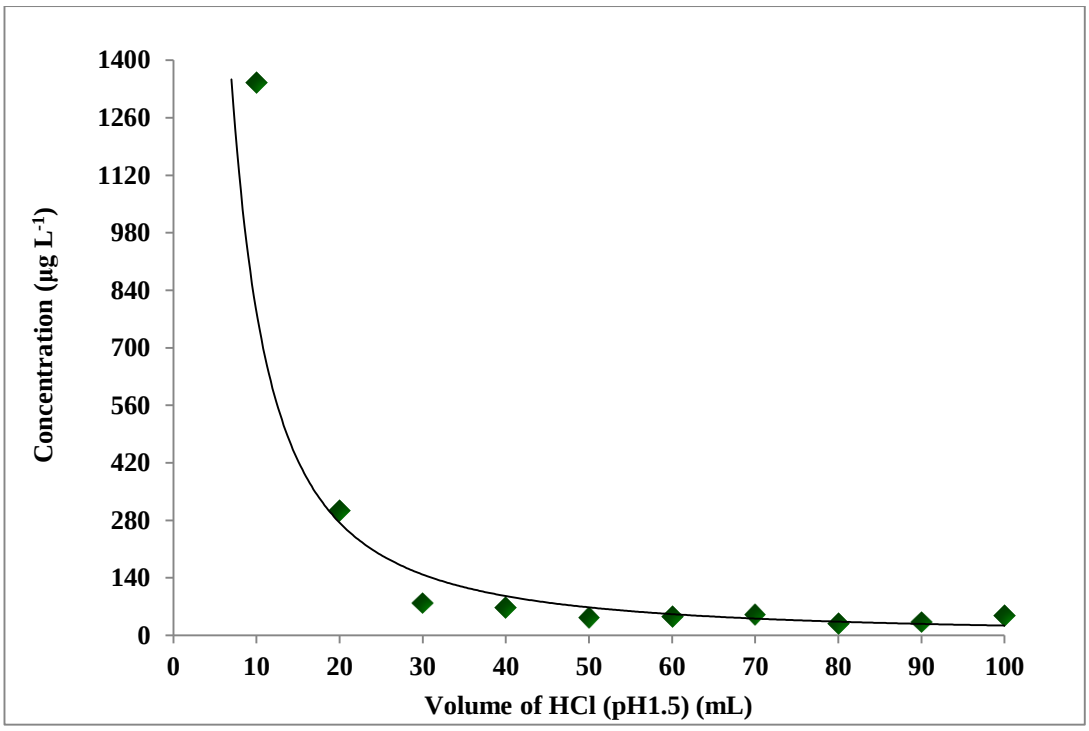


**Figure 4.6. Release of Zn from blank acrodisc® syringe filters washed with HCl (pH 1.5)**

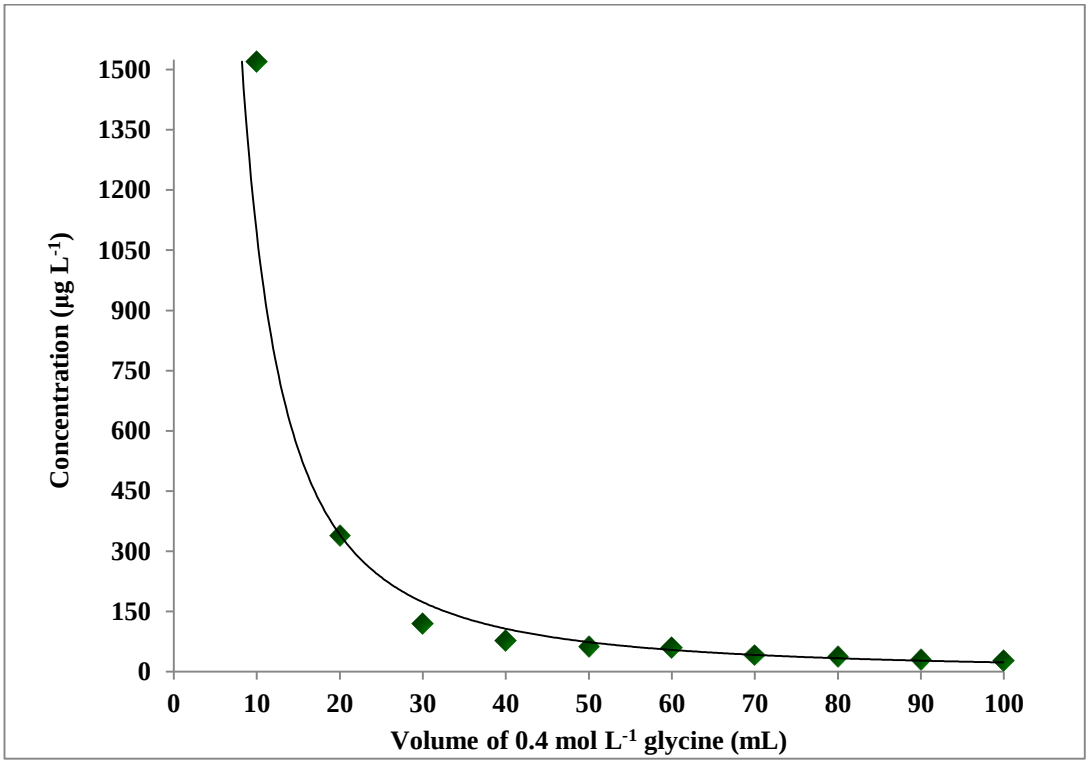


**Figure 4.7. Release of Zn from blank acrodisc® syringe filters washed with glycine (0.4 mol $L^{-1}$ pH 1.5)**

Since normally triplicates of a sample should be used when the SBET test is conducted, repeatability of the washing regime procedure was investigated. This was performed by applying the SBET to three procedural blank samples (i.e. 0.4 mol $L^{-1}$ glycine only). During the hour in which the samples were being extracted, three acrodisc syringe filters were washed as described at the beginning of this Section (i.e. 4 x 20 mL of glycine). After the end of the sample extraction time, the three procedural blank samples were injected through the three washed acrodisc syringe filters, and filtrates then analysed by ICP-MS. Results obtained showed that the concentrations (mean ± SD) of Cu and Zn in the filtrates collected from the washed acrodisc filters were 0.129 ± 0.012 and 164 ± 17.9 μg $L^{-1}$, respectively.

Although the previous washing process resulted in the concentration of Cu being low in procedural blank samples passing through pre-washed acrodisc syringe filters, the concentration of Zn was still relatively high, as was its RSD (10.9%). That may be because of the time elapsed between the injection of the last 20 mL of washing solution and use of the acrodisc syringe filters for filtration of samples (*ca.* 20 minutes, when 10 acrodisc syringe filters were washed). This could cause an increase in the amount of Zn released, which could contaminate the filtrate. Therefore, the washing method was slightly modified. This modification involved washing the acrodisc syringe filters three times (3 x 20 mL) with the washing solution (0.4 mol $L^{-1}$ glycine) whilst sample extraction was being performed. The acrodisc syringe filters were then attached with 20 $cm^3$ disposable syringes filled with the last 20 mL of washing solution (see Fig. 4.8). Once sample extraction was complete, the last 20 mL of washing solution was injected through the acrodisc syringe filters and then immediately the filters were used for filtration of the samples themselves. Filtrates were then analysed by ICP-MS. Results obtained indicated that the concentration (mean ± SD) of Zn in the procedural blank of the SBET decreased to 14.5 ± 1.29 μg $L^{-1}$ (i.e. the RSD was 8.90%). This modified washing regime substantially reduced the Zn blank contribution from the acrodisc filters and so it was adopted for the rest of this work.

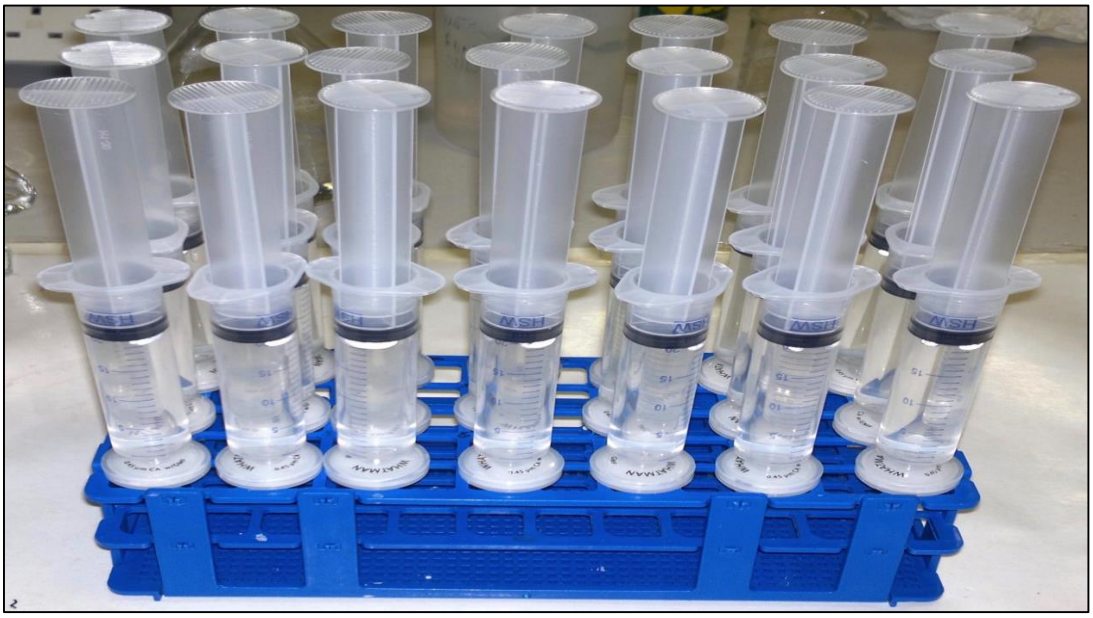

**Figure 4.8. The acrodisc syringe filters each attached with a 20 $cm^3$ disposable syringe filled with 20 mL of 0.4 mol $L^{-1}$ glycine**

### 4.3.2. Miniaturisation of the SBET and UBM (stomach phase)

Bioaccessible concentration of PTE obtained by applying the original and the miniaturised versions of both the SBET and the stomach phase of the UBM to BGS RM 102 Ironstone Soil are summarised in Table 4.2. Results revealed that the bioaccessible PTE concentration obtained by applying the miniaturised methods are similar to those achieved when the original methods were applied. Recoveries for the miniaturised SBET were within 100 ± 10% (except for Fe and Pb, where values of 119 and 115% were obtained), while they were within 100 ± 4% for the miniaturised UBM. Statistical results obtained by conducting the Student's t-test (at 0.05 significance level) showed that there was no significant difference between the results obtained using original and miniaturised SBET for all PTE tested whereas, for the stomach phase of the UBM, the t-test failed for Cr, Mn, Ni, and Zn. The bioaccessible As, Cd, and Pb concentrations in the stomach phase of the UBM were within the certified and guideline values[83] of 4.52 ± 1.28, 0.281 ± 0.170, and 13.0 ± 6.0 mg $kg^{-1}$, respectively, in both original and miniaturised versions of the procedure (Figures 4.9-4.11). For the SBET, no indicative values are available for bioaccessible concentration of PTE in BGS RM 102 Ironstone Soil.

**Table 4.2. Comparison between bioaccessible concentrations obtained by the original and the miniaturised simplified bioaccessibility extraction test (SBET) and the stomach phase of the unified bioaccessibility method (UBM)**

| PTE | Mean ± SD (mg kg$^{-1}$, n=3) | | | | Recovery (%) | | % RPD | |
|---|---|---|---|---|---|---|---|---|
| | SBET | | UBM (stomach phase) | | SBET | UBM (stomach phase) | SBET | UBM (stomach phase) |
| | Original | Miniaturised | Original | Miniaturised | | | | |
| **As** | 2.31 ± 0.20 | 2.16 ± 0.18 | 4.88 ± 0.04 | 5.01 ± 0.07 | 93.8 | 103 | 6.44$^{P}$ | 2.54$^{P}$ |
| **Cd** | 0.199 ± 0.019 | 0.196 ± 0.020 | 0.220 ± 0.003 | 0.214 ± 0.004 | 99 | 97.5 | 1.41$^{P}$ | 2.56$^{P}$ |
| **Cr** | 23.8 ± 1.8 | 26.2 ± 2.3 | 37.7 ± 0.4 | 36.9 ± 0.1 | 110 | 97.8 | 9.68$^{P}$ | 2.21$^{F}$ |
| **Cu** | 7.30 ± 0.78 | 7.29 ± 0.67 | 7.91 ± 0.04 | 7.78 ± 0.07 | 99.9 | 98.4 | 0.138$^{P}$ | 1.59$^{P}$ |
| **Fe** | 1130 ± 91 | 1350 ± 123 | 1490 ± 30 | 1560 ± 42 | 119 | 104 | 17.5$^{P}$ | 4.32$^{P}$ |
| **Mn** | 2060 ± 170 | 1920 ± 158 | 3010 ± 12 | 2900 ± 10 | 93.3 | 96.3 | 6.98$^{P}$ | 3.82$^{F}$ |
| **Ni** | 8.61 ± 0.69 | 8.37 ± 0.74 | 12.5 ± 0.1 | 12.2 ± 0.1 | 97 | 97.6 | 2.74$^{P}$ | 2.46$^{F}$ |
| **Pb** | 15.1 ± 1.4 | 17.3 ± 1.4 | 19.5 ± 0.5 | 19.1 ± 0.3 | 115 | 97.8 | 13.7$^{P}$ | 2.22$^{P}$ |
| **Zn** | 21.2 ± 4.6 | 20.2 ± 15.8 | 36.9 ± 0.3 | 35.7 ± 0.4 | 95 | 96.8 | 5.25$^{P}$ | 3.24$^{F}$ |

n: number of replicates; Recovery (%) = ([mean measured value in the miniaturised procedure]/[mean measured value in the original procedure]) × 100; RPD: Relative percent difference = $\{|x_1 - x_2|/((x_1+x_2)/2)\}\times 100$ where $x_1$: values in the original procedure and $x_2$: values in in the miniaturised procedure; P: means that t test (0.05 significance level) passed; F: means that t test failed

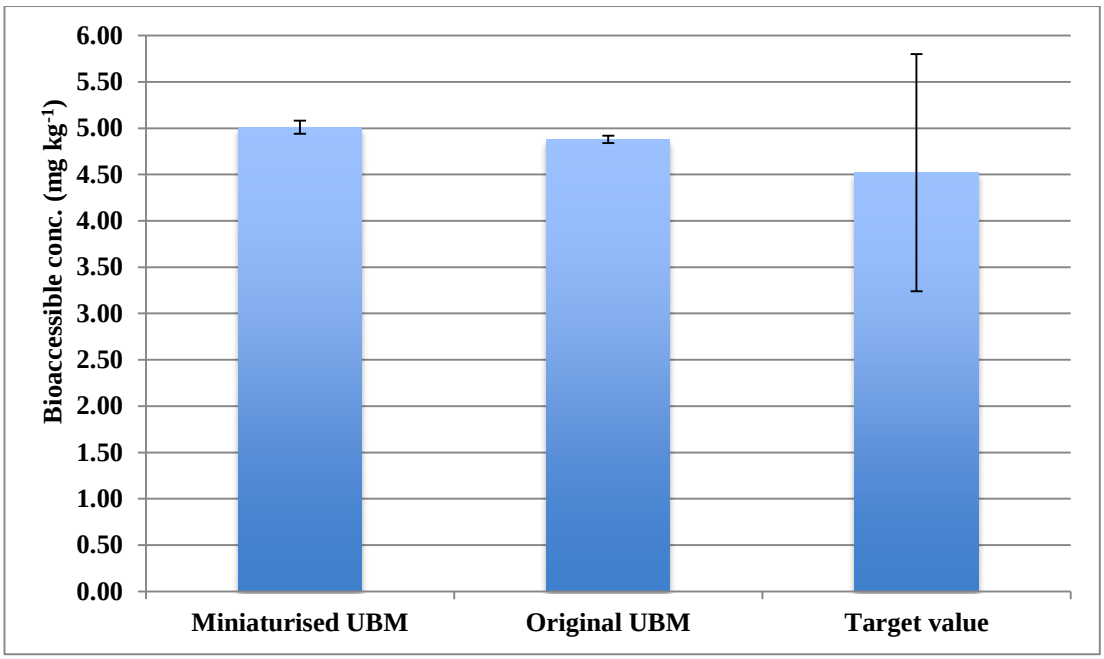


**Figure 4.9. Comparison of the bioaccessible concentration of As in the BGS RM 102 Ironstone Soil obtained by using the miniaturised and original procedure of the stomach phase of the unified bioaccessibility method (UBM) with the target value; error bars represent one standard deviations (SD) (repeatability) (n = 3) and inter-laboratory reproducibility SD (n = 7) for measured and target value, respectively**

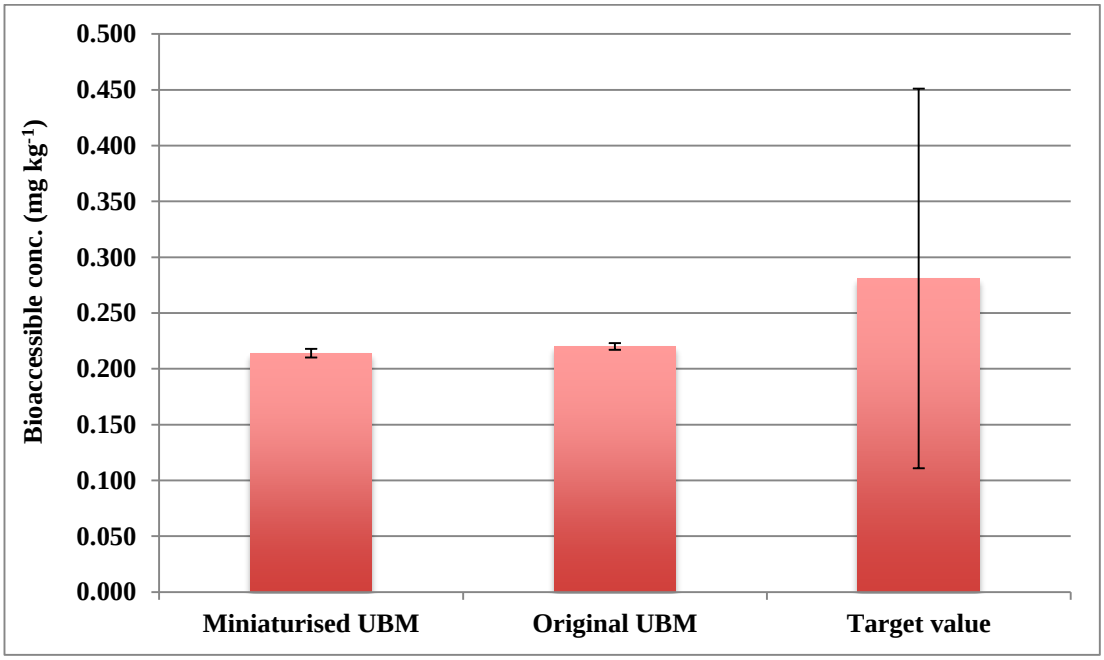


**Figure 4.10. Comparison of the bioaccessible concentration of Cd in the BGS RM 102 Ironstone Soil obtained by using the miniaturised and original procedure of the stomach phase of the unified bioaccessibility method (UBM) with target value; error bars represent one standard deviations (SD) (repeatability) (n = 3) and inter-laboratory reproducibility SD (n = 7) for measured and target value, respectively**

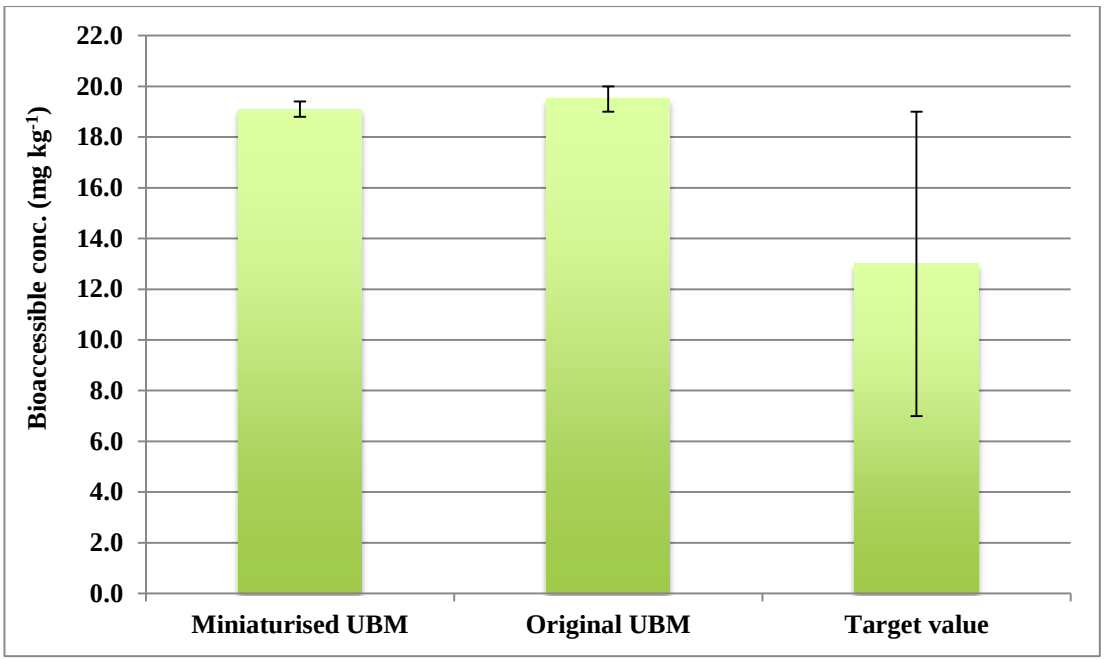


**Figure 4.11. Comparison of the bioaccessible concentration of Pb in the BGS RM 102 Ironstone Soil obtained by using the miniaturised and original procedure of the stomach phase of the unified bioaccessibility method (UBM) with target value; error bars represent one standard deviations (SD) (repeatability) (n = 3) and inter-laboratory reproducibility SD (n = 6) for measured and target value, respectively**

Generally, the bioaccessible PTE concentrations obtained with the stomach phase of the UBM, either its original or miniaturised version, were higher than those achieved when the two versions of the SBET were applied. This was in agreement with previous studies conducted for comparing PTE extractability using different oral bioaccessibility tests. One such example, a study carried out by Oomen *et al*. revealed that different bioaccessible PTE values were obtained when five bioaccessibility test (included the SBET) were applied to the same samples.[65] The differences between the methods applied in the current study are in terms of the pH value of the extractants (1.2 for the stomach phase of the UBM and 1.5 for the SBET) and the reagents. These factors can be responsible for the differences observed. Mucin, for example, has been reported to be responsible for increasing the bioaccessible concentration of Cr, Cu, Ni, Pb, and Zn when the stomach phase of the UBM was applied to a soil sample.[95] Another study has reported that the solubility of elements is affected principally by the pH specified for oral bioaccessibility tests.[84]

### 4.3.3. Effect of PTE bioaccessibility in blank FDMS filters on those measured in soil

Table 4.3 shows the bioaccessible concentration of PTE in blank FDMS filters extracted using the miniaturised SBET and the stomach phase of the UBM. In general, the extractability of PTE was very low or less than IDL for all PTE determined, except for Zn, it was significantly high. This may be due to the fact that Zn is used as a binder in the production of FDMS filters.[146] Approximately 3 μg of Zn was leached from each FDMS filter. This amount was similar to the amount extracted from 100 mg of soil sample (35 mg $kg^{-1}$) that had been loaded. Since the repeatability represented by RSD for the bioaccessible Zn in blank FDMS filters was relatively low (< 19% for the SBET and < 9% for the UBM, n=3), thus, blank-correct results was reasonable.

**Table 4.3. Bioaccessible concentrations of potentially toxic elements (PTE) in blank FDMS filters extracted using the miniaturised simplified bioaccessibility extraction test (SBET) and the stomach phase of the unified bioaccessibility method (UBM)**

| PTE | SBET (n = 3) | | UBM (stomach phase) (n = 3) | |
|---|---|---|---|---|
| | μg $L^{-1}$ Mean ± SD | μg per filter Mean ± SD | μg $L^{-1}$ Mean ± SD | μg per filter Mean ± SD |
| **As** | < IDL | < IDL | < IDL | < IDL |
| **Cd** | < IDL | < IDL | < IDL | < DL |
| **Cr** | 0.100 ± 0.060 | 0.001 ± 0.001 | < IDL | < IDL |
| **Cu** | 5.60 ± 0.39 | 0.056 ± 0.004 | 20.8 ± 0.3 | 0.078 ± 0.001 |
| **Fe** | < IDL | < IDL | < IDL | < IDL |
| **Mn** | < IDL | < IDL | 6.96 ± 0.97 | 0.026 ± 0.004 |
| **Ni** | 0.400 ± 0.260 | 0.004 ± 0.003 | < IDL | < IDL |
| **Pb** | 0.200 ± 0.060 | 0.002 ± 0.001 | 0.416 ± 0.127 | 0.002 ± 0.001 |
| **Zn** | 284 ± 53 | 2.84 ± 0.53 | 986 ± 88 | 3.70 ± 0.33 |

< IDL indicates a value less than the instrumental detection limit; n: number of replicates

### 4.3.4. Application of the miniaturised tests to simulated $PM_{10}$ samples

Figures 4.12-4.20 show the comparisons of bioaccessible PTE concentration obtained by applying the miniaturised SBET and the stomach phase of the UBM to soil samples (SBET 1 and UBM 1) with those obtained when these tests were applied to simulated $PM_{10}$ samples (SBET 2 and UBM 2) (see Appendix A). The soil samples were the BGS RM 102 Ironstone Soil, and the simulated $PM_{10}$ samples were prepared by smearing the BGS RM 102 Ironstone Soil onto blank FDMS filters. Statistical results represented by t-test at 95% confidence level indicated that the presence of the FDMS filter with the soil was similar to its absence in terms of its effect on the bioaccessible PTE concentrations measured. No significant differences appeared between these two cases for the two miniaturised tests, except for Fe (see Table 4.4). In addition to significance testing, RDP values between soil alone and soil on a FDMS filter were <2% for the miniaturised SBET method, except for Zn (10.2%) and < 5% for the miniaturised stomach phase of the UBM except for Ni and Pb (11.7 and 6.2%, respectively). The bioaccessible concentration of As, Cd, and Pb (4.41 ± 0.07, 0.217 ± 0.006, and 18.4 ± 1.4 mg $kg^{-1}$, respectively) in BGS RM 102 Ironstone Soil loaded on a FDMS filter for the miniaturised stomach phase of the UBM were within the ranges of guidance values.

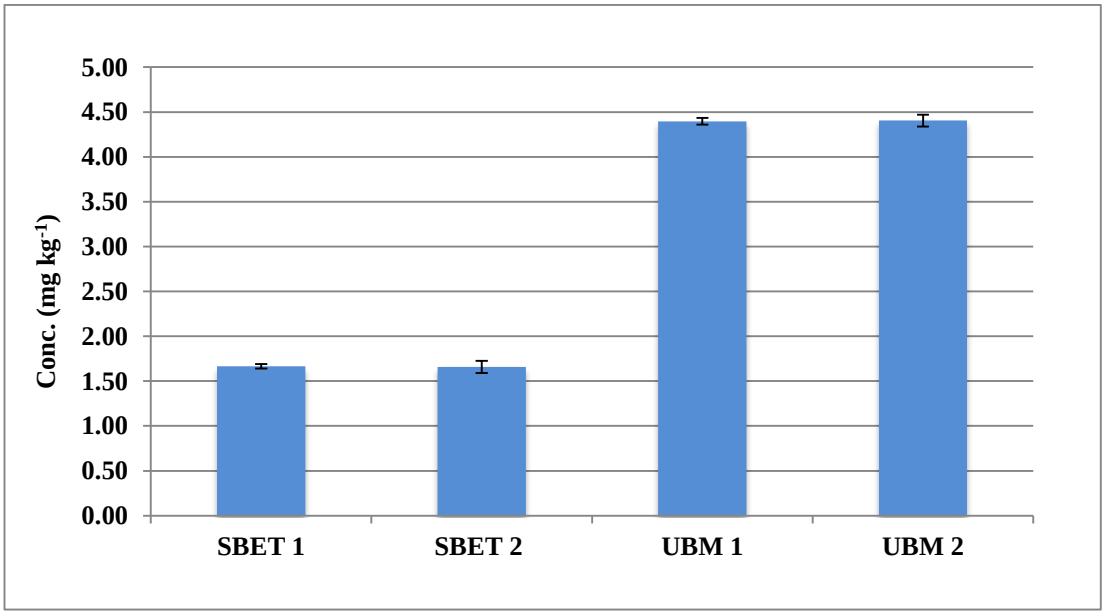


**Figure 4.12. The bioaccessible concentrations of As in BGS RM 102 Ironstone Soil (1) alone and (2) when smeared on FDMS filters to simulated $PM_{10}$ samples, as obtained with the miniaturised simplified bioaccessibility extraction test (SBET) and stomach phase of the unified bioaccessibility method (UBM); error bars represent one standard deviations (n=3)**

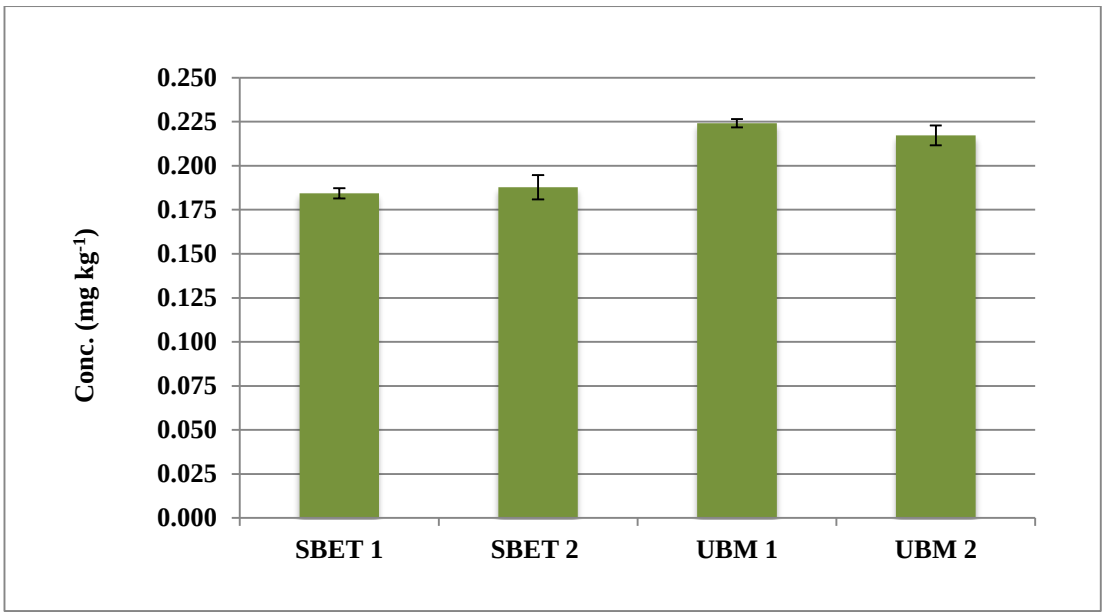


**Figure 4.13. The bioaccessible concentrations of Cd in BGS RM 102 Ironstone Soil (1) alone and (2) when smeared on FDMS filters to simulated $PM_{10}$ samples, as obtained with the miniaturised simplified bioaccessibility extraction test (SBET) and stomach phase of the unified bioaccessibility method (UBM); error bars represent one standard deviations (n=3)**

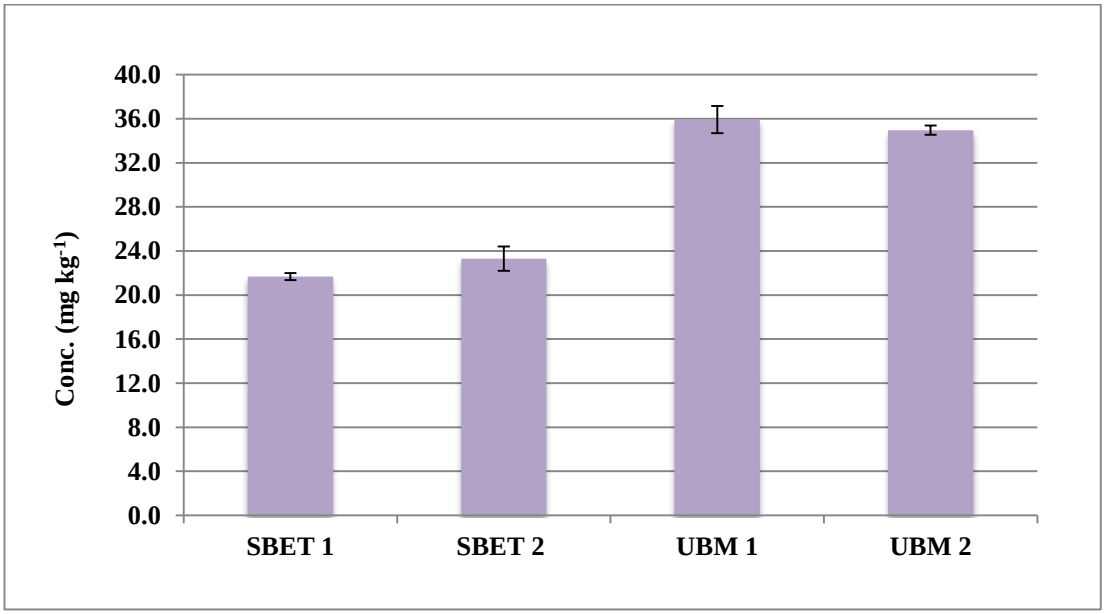


**Figure 4.14. The bioaccessible concentrations of Cr in BGS RM 102 Ironstone Soil (1) alone and (2) when smeared on FDMS filters to simulated $PM_{10}$ samples, as obtained with the miniaturised simplified bioaccessibility extraction test (SBET) and stomach phase of the unified bioaccessibility method (UBM); error bars represent one standard deviations (n=3)**

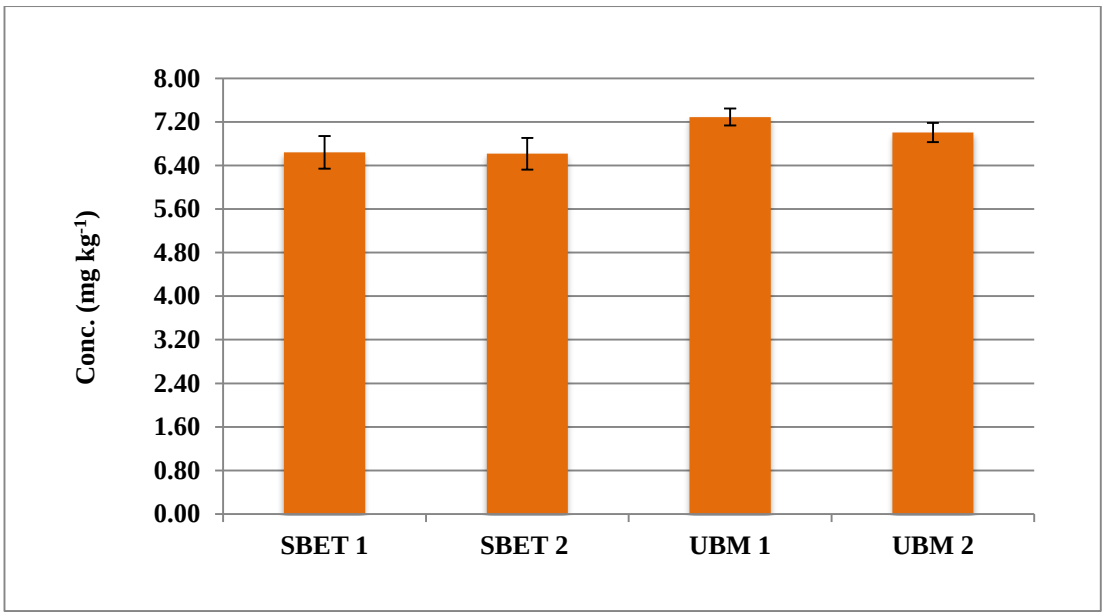


**Figure 4.15. The bioaccessible concentrations of Cu in BGS RM 102 Ironstone Soil (1) alone and (2) when smeared on FDMS filters to simulated $PM_{10}$ samples, as obtained with the miniaturised simplified bioaccessibility extraction test (SBET) and stomach phase of the unified bioaccessibility method (UBM); error bars represent one standard deviations (n=3)**

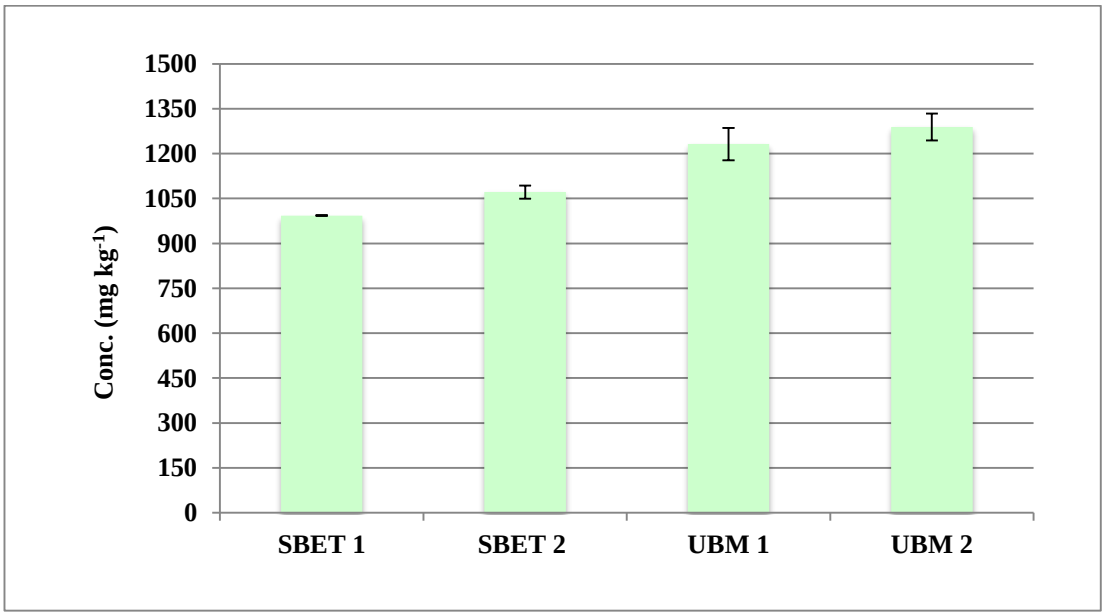


**Figure 4.16. The bioaccessible concentrations of Fe in BGS RM 102 Ironstone Soil (1) alone and (2) when smeared on FDMS filters to simulated $PM_{10}$ samples, as obtained with the miniaturised simplified bioaccessibility extraction test (SBET) and stomach phase of the unified bioaccessibility method (UBM); error bars represent one standard deviations (n=3)**

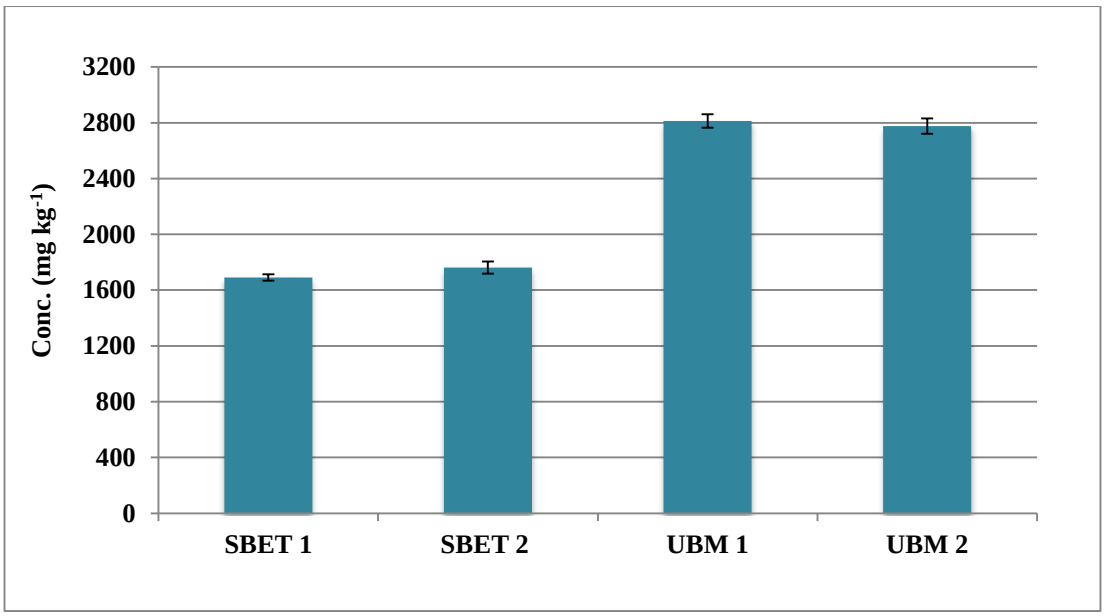


**Figure 4.17. The bioaccessible concentrations of Mn in BGS RM 102 Ironstone Soil (1) alone and (2) when smeared on FDMS filters to simulated $PM_{10}$ samples, as obtained with the miniaturised simplified bioaccessibility extraction test (SBET) and stomach phase of the unified bioaccessibility method (UBM); error bars represent one standard deviations (n=3)**

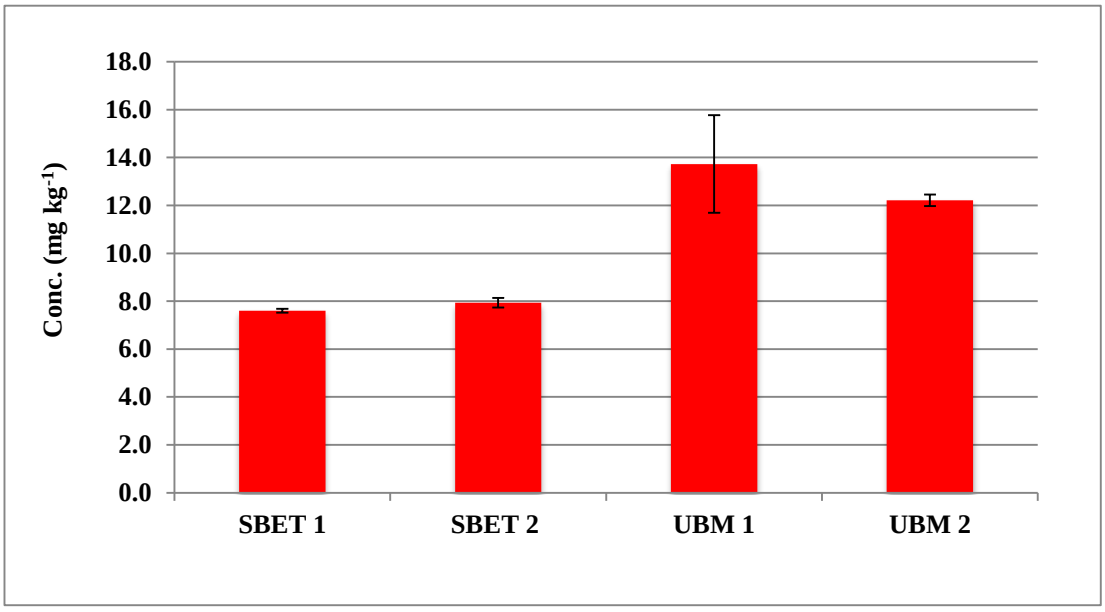


**Figure 4.18. The bioaccessible concentrations of Ni in BGS RM 102 Ironstone Soil (1) alone and (2) when smeared on FDMS filters to simulated $PM_{10}$ samples, as obtained with the miniaturised simplified bioaccessibility extraction test (SBET) and stomach phase of the unified bioaccessibility method (UBM); error bars represent one standard deviations (n=3)**

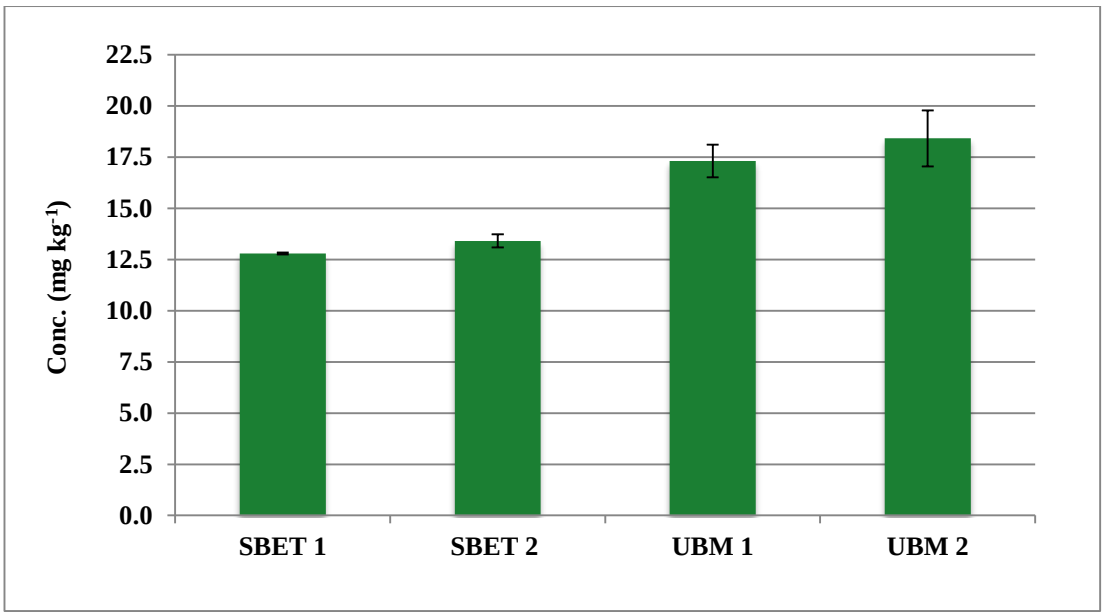


**Figure 4.19. The bioaccessible concentrations of Pb in BGS RM 102 Ironstone Soil (1) alone and (2) when smeared on FDMS filters to simulated $PM_{10}$ samples, as obtained with the miniaturised simplified bioaccessibility extraction test (SBET) and stomach phase of the unified bioaccessibility method (UBM); error bars represent one standard deviations (n=3)**

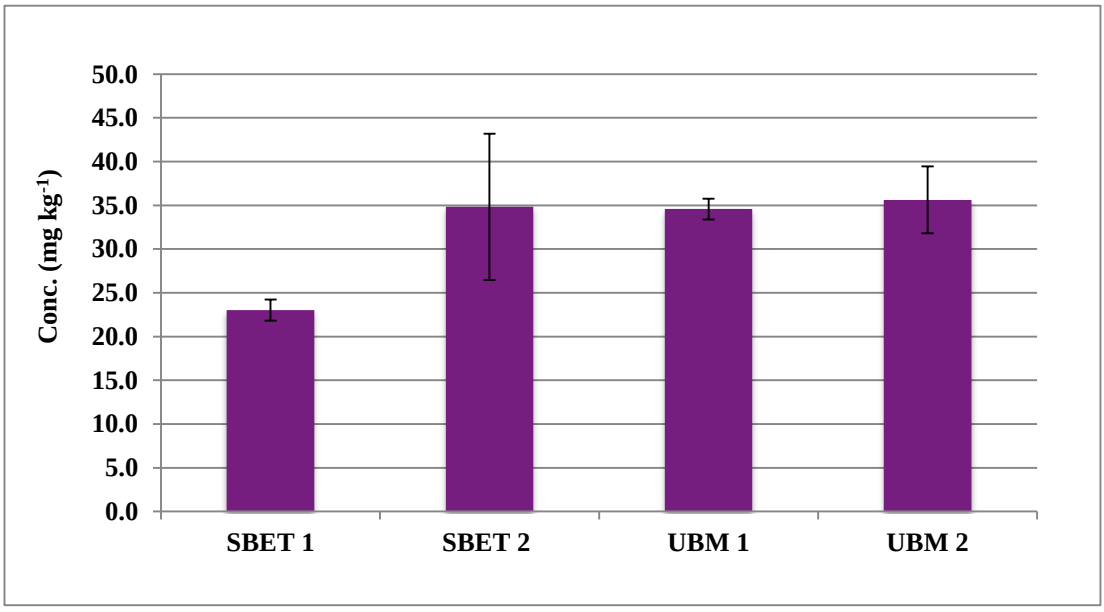


**Figure 4.20. The bioaccessible concentrations of Zn in BGS RM 102 Ironstone Soil (1) alone and (2) when smeared on FDMS filters to simulated $PM_{10}$ samples, as obtained with the miniaturised simplified bioaccessibility extraction test (SBET) and stomach phase of the unified bioaccessibility method (UBM); error bars represent one standard deviations (n=3)**

**Table 4.4. T test and relative percent difference (RPD) of the bioaccessible concentrations of potentially toxic elements (PTE) in the simulated $PM_{10}$ (soil on FDMS filters) and in soil alone using the simplified bioaccessibility extraction test (SBET) and the stomach phase of the unified bioaccessibility method (UBM)**

| PTE | T test (between soil alone and soil on FDMS filters) | | | | %RPD | |
|---|---|---|---|---|---|---|
| | SBET ($\nu = 4^a, 2^b$) | | UBM (stomach phase) ($\nu = 4^a, 2^b$) | | | |
| | t calculated | t critical | t calculated | t critical | SBET | UBM (stomach phase) |
| **As** | 0.24 | $2.78^a$ | 0.24 | $2.78^a$ | 0.108 | 0.216 |
| **Cd** | 0.91 | $2.78^a$ | 0.91 | $2.78^a$ | 0.467 | 3.10 |
| **Cr** | 2.42 | $2.78^a$ | 2.42 | $2.78^a$ | 1.82 | 2.72 |
| **Cu** | 0.08 | $2.78^a$ | 0.08 | $2.78^a$ | 0.083 | 3.97 |
| **Fe** | **6.01** | $4.30^b$ | **6.01** | $4.30^b$ | 1.90 | 4.53 |
| **Mn** | 2.51 | $2.78^a$ | 2.51 | $2.78^a$ | 1.03 | 1.31 |
| **Ni** | 2.60 | $2.78^a$ | 2.60 | $2.78^a$ | 1.07 | 11.7 |
| **Pb** | 3.25 | $4.30^b$ | 3.25 | $4.30^b$ | 1.17 | 6.20 |
| **Zn** | 2.42 | $4.30^b$ | 2.42 | $4.30^b$ | 10.2 | 2.98 |

$\nu$: degree of freedom; A significance level ($\alpha$) =0.05; RPD: Relative percent difference = $\{|x_1 - x_2|/((x_1+x_2)/2)\}\times 100$ where $x_1$: values in soil alone and $x_2$: values in soil loaded on FDMS filter

### 4.4. Conclusion

In this work, the SBET and the stomach phase of the UBM have been successfully miniaturised to determine the bioaccessible PTE concentration in $PM_{10}$ collected on FDMS filters. This was performed by reducing the sample size to near the amount of $PM_{10}$ that could be collected during routine air sampling. To maintain the solid to liquid ratio, the volume of reagents was also reduced. Samples were simulated using BGS RM 102 Ironstone Soil, with more than 50% of its particles less than 10 μm in diameter. Use of wide mouth bottles as extraction vessels enhanced the extractability of PTE, which was affected when the filters were folded. Washing the acrodisc filters, used for filtration stage of the SBET, immediately before the use, by 80 mL of glycine acidified to pH 1.5 with HCl, led to minimise the procedural blank of the Cu and Zn. Results obtained indicated that the use a small amount of a sample and the presence of FDMS filters did not affect the extractability of PTE when the SBET or the stomach phase of the UBM was applied. This was ascertained by comparing results obtained from soil alone with those obtained when the soil was supported on FDMS filters as well as between the original sample mass and the small adapted mass. Either when the SBET or the stomach phase of the UBM was applied, the amount of PTE extracted from blank FDMS filters was low or non-detectable with the exception of relatively high bioaccessible Zn as it is used as a binder for FDMS filters. The high Zn blank concentration is a consequence of the filter composition and so cannot be eliminated, but would be corrected by blank subtraction. Thus, the miniaturised SBET and stomach phase of the UBM were applicable to measure PTE in $PM_{10}$.

# 5 Use of dynamic models of the simplified bioaccessibility extraction test and the unified bioaccessibility method to measure the bioaccessible concentration of potentially toxic elements in airborne particulate matter using off-line and on-line analysis by ICP-MS

## 5.1. Introduction

The physical properties of airborne PM such as size and shape as well as their chemical properties influence risk of PM to human health. For chemical properties, the fraction that can be dissolved and then available for absorption (i.e. the bioaccessible fraction) should be considered when human health effects caused by PTE in different substrates need to be assessed,[62] many methods for measuring the bioaccessible concentration have been created, both *in vitro* and *in vivo* methods. Advantages of the *in vitro* methods such as short laboratory work time, low costs, and avoidance of ethical issues associated with animal testing make them preferred for assessing risks of PTE to human.[77, 78] These methods, which were mentioned in Section 1.4.2.2, are generally batch (static) gastric or gastrointestinal models, except for limited dynamic models such as the TIM.[63, 147, 148] In addition to their disadvantages such as, laborious work, technologically complicated experimental procedures, high costs, and the fact that they are time consuming, the latter are considered as equilibrium batch models.[149-151] This is because only data at certain time points can be obtained with these models.

The reactions that occur between substrates, whether ingested or mucociliary transported and subsequently ingested, and constituents of the gastrointestinal tract (i.e. acids and others) are non-equilibrium reactions as the PTE released permeate across membranes once liberated.[95] Therefore, non-equilibrium dynamic models (i.e. continuous on-line leaching) of the *in vitro* bioaccessibility methods would be a good way to represent the real conditions that substrates are subjected to in the body.

Many non-equilibrium dynamic models of extraction methods have been developed. The majority of these methods were based on sequential extraction. Some of these studies used a stirred-flow chamber as an extraction unit for fractionation or speciation of PTE in soil,[152-154] in corrosion products from natural gas pipelines,[155]

and in solid biofuels.[156] Other dynamic sequential extraction models used a rotating coiled column for fractionation of PTE in soils, sludge, and sediments.[157-163] In addition to these extraction units, a column machined out of two polyoxymethylene end-caps was used as an extraction unit for fractionation of PTE either in soils and sludge[164-166] or in environmental and bio-shielding concrete samples.[167] Beside sequential extraction, dynamic models for some single extraction methods have also been investigated. For example, mobility of trace elements in soil and sediments was dynamically studied by using the rotating coiled column approach coupled with ICP-MS.[168] In another example, bioavailable Cr in soil was investigated using a dynamic model where a bi-conical micro column was adopted as an extraction unit.[169, 170] A recent study conducted by Fedotov *et al*.[171] concluded that a dynamic extraction model involving a rotating coiled column could be used to measure the water-soluble fraction of As, Cd, Cu, Ni, Pb, S, Sb, and Zn in dust samples that were atmospherically deposited on window sills of a building near a copper smelter in Chelyabinsk region, Russia.

Dynamic leaching has not only been studied for single and sequential extraction methods but also has been investigated for bioaccessibility extraction methods such as studies shown in Table 5.1. Conclusions of the studies, both those conducted for single and sequential extraction methods and those for bioaccessibility extraction methods, have pointed out that the advantages of non-equilibrium dynamic models compared with batch models are that they:

1. are simple and easy to apply;
2. offer short procedure time;
3. are less susceptible to potential contamination;
4. represent best simulators of the gastrointestinal or environmental conditions;
5. are a good source for data on real time element mobilisation;
6. involve less probability of the occurrence of readsorption or redistribution of elements; and
7. have less likelihood for analyte losses.

However, a few disadvantages have also been concluded such as the long time required for analysis and dilution effects.[153]

**Table 5.1. Studies on dynamic models of bioaccessibility extraction methods**

| Bioaccessibility method | Substrates | Analytes | Extraction unit (Sample container) | Analysis mode (sample uptake rate) | Digestive fluids used | Reagents driven by | References |
|---|---|---|---|---|---|---|---|
| USP XXIII (without enzymes) | Food (NIST SRM-8433 corn bran) | Pb and Zn | Micro-column (4-cm long and 3.17 mm ID PTFE tube) | ICP-MS on-line (1.2 mL $min^{-1}$) | Artificial saliva, gastric juice, and intestinal juice | Flow injection | Chu, M. Y. and Beauchemin, D., 2004[149] |
| USP XXIII | Seafood reference materials and real sample of seafood | As | Mini-column (8-cm long and 3.17 mm ID PTFE tube) | ICP-MS on-line (1.2 mL $min^{-1}$) | Artificial saliva, gastric juice, and intestinal juice | Peristaltic pump | Dufailly *et al*., 2008[172] |
| USP XXIII | Rice reference material (SRM 1568a) and real sample of white rice | As | Mini-column (8-cm long and 3.17 mm ID PTFE tube) | ICP-MS on-line (0.8 mL $min^{-1}$) | Artificial saliva, gastric juice, and intestinal juice | Peristaltic pump | Horner, N. S. and Beauchemin, D., 2012[173] |
| USP XXIII for preparing the gastric juice and intestinal juice; In vitro digestion (RIVM) method for artificial saliva | Seafood reference materials and real sample of seafood | As | Mini-column (5-cm stainless steel tube) | ICP-MS on-line (1 mL $min^{-1}$) | Artificial saliva, gastric juice, and intestinal juice | High pressure liquid chromatography pump | Leufroy *et al*., 2012[147] |

USP: US pharmacopoeia Method

**Table 5.1. Studies on dynamic models of bioaccessibility extraction methods continued …**

| Bioaccessibility method | Substrates | Analytes | Extraction unit (Sample container) | Analysis mode (sample uptake rate) | Digestive fluids used | Reagents driven by | References |
|---|---|---|---|---|---|---|---|
| USP XXIII for preparing the gastric juice and intestinal juice; In vitro digestion (RIVM) method for artificial saliva | Seafood reference materials and real sample of seafood | Al, Cd, Cu, Hg, Mn, Pb, V, and Zn | Mini-column (5-cm stainless steel tube) | ICP-MS on-line, (1 mL $min^{-1}$) | Artificial saliva, gastric juice, and intestinal juice | High pressure liquid chromatography pump | Leufroy *et al*., 2012[174] |
| UBM-like test | Forest and residential garden soils | Cr, Cu, Ni, Pb, and Zn | Stirred flow chamber | Hybrid flow ICP-AES off-line, (1.5 mL $min^{-1}$) | Gastric juice alone without saliva | Bi-directional syringe pump | Rosende *et al*., 2014[95] |
| USP XXIII with no enzyme was added to artificial saliva | Bread | As, Cd, Cr, and Pb | A mini-column (10-cm long and 3.17 mm ID PTFE tube) | On-line by ICP-MS | Artificial saliva, gastric juice, and intestinal juice | Instrument's built-in peristaltic pump | Lamsal, R. P. and Beauchemin, D., 2015[175] |

USP: US pharmacopoeia Method

**Table 5.1. Studies on dynamic models of bioaccessibility extraction methods continued …**

| Bioaccessibility method | Substrates | Analytes | Extraction unit (Sample container) | Analysis mode (Sample uptake rate) | Digestive fluids used | Reagents driven by | References |
|---|---|---|---|---|---|---|---|
| Simulate Lung fluid | $PM_{10}$ collected by an automated sampler on mixed cellulose ester filters 47 mm | Zn | A Chromafix® SPE column (12 mm diameter and 14 mm length) | On-line by Flame atomic absorption spectrometry (1.0 mL $min^{-1}$) | High purity water | FI (a peristaltic pump + a six port injection valve) | Mukhtar A. and Limbeck A., 2010[176] |
| Simulated Lung fluid | $PM_{10}$ collected by a digital high volume sampler on Pallflex Tissue Quartz 2500 QAT-UP filters | Ba, Cr, Cu, Fe, Mn, and Ni | A Chromafix® SPE column (12 mm diameter and 14 mm length) | On-line by ICP-AES (0.8 mL $min^{-1}$) | High purity water | FI (a syringe pump + a six port injection valve) | Limbeck *et al*., 2012[177] |

Some of the advantages of dynamic models - such as shortened extraction time – are not feasible when the gastrointestinal or inhalation bioaccessibility methods are applied, because the aim is to create the best simulator of the body tracts. The conditions of these tracts - such as the residence time of a substrate and volume of fluids - should be maintained at physiologically relevant levels. For the gastrointestinal tract, one hour is typically adopted by several bioaccessibility methods as the residence time of a substrate in the stomach. For the volume of fluids, different volumes of fluids were used depending on which solid to fluid ratio was adopted by a method. However, a review conducted in 2013, stated that in the fasted state, the volume of gastric fluid in the human body must be near 50 mL.[151] Therefore, reduction of procedure time should not be the overriding aim when a new dynamic model for a bioaccessibility method is conducted.

**Off-line and on-line analysis**

Extracts obtained by applying dynamic extraction models could be analysed by collecting subfractions with a defined volume or by interfacing a dynamic extraction system to an atomic spectrometer. These modes of detection are called off-line and on-line analysis, respectively. Advantages that make off-line analysis preferable compared with on-line analysis were reviewed in Ref 178.[178] They include the following.

1. A single detection spectrometer can be used for multi-element analysis;
2. Measurements can be reproduced;
3. Measurement of other parameters such as pH are applicable;
4. Leachates can be pre-treated before detection;
5. They are suitable for multistage extraction systems; and
6. They are simple to use because complex interfaces between the spectrometers and extraction system are not required compared with on-line analysis.

However, on-line analysis provides real time extraction with insignificant contamination risks. As a result, extraction time can be reduced. It is also suitable when the purpose of a dynamic method is to monitor the leaching profile of elements that are extracted easily.[178]

Although the simulation of the digestion process by using the dynamic extraction models more closely resembles the real conditions of the gastrointestinal tract than the batch models, no study has been conducted to date for dynamic models of the SBET and the stomach phase of the UBM. Although a study was carried out by Rosende *et al.*[95] to establish a dynamic model for the UBM, it was for a UBM-like extraction test where the saliva fluid was not included and mucin was excluded from the reagents. Also, the substrate was soil not $PM_{10}$ on filters.

Therefore, in this chapter, three experiments are reported:

1. Use of an equilibrium-based closed-loop (CL) dynamic extraction model of the SBET (CL-SBET) and the stomach phase of the UBM (CL-UBM) along with their batch models to measure the bioaccessible concentration of PTE in $PM_{10}$ using off-line analysis by ICP-MS.

2. Use of a (non-equilibrium)-based single-pass (SP) dynamic extraction model with fraction collection (FC) for the SBET (SPFC-SBET) and the stomach phase of the UBM (SPFC-UBM) to measure the bioaccessible concentration of PTE in $PM_{10}$ using off-line analysis by ICP-MS.

3. On-line determination of the bioaccessible concentration of PTE in airborne $PM_{10}$ using the SP model of the SBET with direct coupling (DC) to ICP-MS (SPDC-SBET).

## 5.2. Experiment 1: Closed-loop dynamic extraction model (CL)

The batch models of the SBET and the stomach phase of the UBM involve many stages after extraction such as centrifuging and filtrations. This experiment was conducted to develop a simple equilibrium dynamic model as an alternative to these batch models, avoiding stages after the extraction. The CL-SBET and the CL-UBM were used to determine the bioaccessible concentration of PTE in inhaled and subsequently ingested $PM_{10}$ under biological conditions using off-line analysis by ICP-MS.

### 5.2.1. Experimental

#### 5.2.1.1. Apparatus and reagents

Blank Pallflex TX40 FDMS filters, as described in Section 3.3.1, were used. The apparatus and reagents used for the batch model of the SBET and the stomach phase of the UBM were as described in Sections 3.4.1-3.4.2 and 3.5.1-3.5.2 respectively. For others models, the reagents were as described in Sections 3.4.1-3.4.2 and 3.5.1-3.5.2 respectively. The apparatus were:

1. a multichannel peristaltic pump, REGLO ICC and 47 mm in-line polycarbonate filter holder.
2. 0.51 mm 3-stop cartridge tubing Tygon® LMT-55;
3. 0.51 mm extension tubing Tygon® LMT-55; and
4. plastic connector tube 0.51 mm internal diameter.

These apparatus were purchased from VWR International, Lutterworth, UK. The pH meter was as described in Section 3.4.1.

#### 5.2.1.2 Simulation of $PM_{10}$ samples

In addition to those described in Section 3.2, simulated $PM_{10}$ samples were also prepared by smearing the blank FDMS filters with NIST SRM 2711A Montana II Soil. As this SRM has recommended bioaccessible value for Pb using the SBET, it is considered as a control material for the standard procedure of the SBET.[91]

### 5.2.1.3. Analytical procedures

The extraction device used for the CL extraction is shown in Fig 5.1. The device consists of a multichannel peristaltic pump, a 47 mm in-line polycarbonate filter holder (see Fig. 5.2), an extractant tube (50 mL centrifuge tube), a water bath, a pH meter, a plastic rack, and a thermometer. A four-channel peristaltic pump was chosen because it has three channels that can be individually controlled either from its keypad or from a PC. As a result, the throughput of the method is increased. The polycarbonate filter holder was chosen as extraction cell because it has diameter that is suitable for FDMS filters. In addition, it can be vented, allowing for the volume required from a reagent to be added before passage the leachate through the filters.

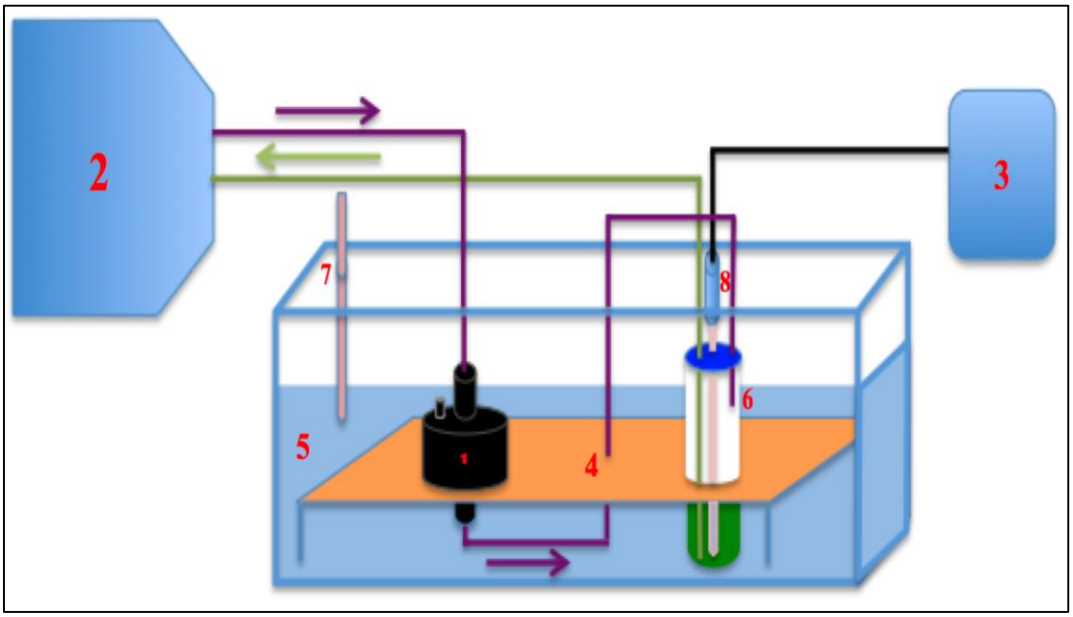


(1) Polycarbonate filter holder (2) Peristaltic pump (3) pH meter (4) Plastic rack (5) Water bath (6) Extractant tube (7) Thermometer (8) pH electrode

**Figure 5.1. Schematic diagram of the closed-loop dynamic extraction device**

The cap of the 50 mL centrifuge tube (extractant tube) was holed as shown in Fig 5.1. A wider hole in the middle of the cap was used for inserting the pH electrode and also for introducing reagents, while the two small holes were used to insert the tubing. The wider hole of the cap was covered by laboratory Para-film during the extraction to prevent contamination of the reagents. A simulated $PM_{10}$ sample was placed into the pre-cleaned filter holder and the holder was then tightly closed by hand. The filter holder and the extractant tube were then fixed on the plastic rack

using elastic bands. The inlet of the filter holder was connected to the outlet of the peristaltic pump using the 0.51 mm extension tubing (50 cm long). The outlet of the filter holder was connected to the extractant tube (33 cm long from 0.51 mm extension tubing). A 58 cm long section of tubing (from the 0.51 mm extension tubing) was used to connect the inlet of the pump to the extractant tube. That means the total volume of fluid in the CL system was 0.288 mL.

For the CL-SBET, 10 mL of the 0.4 M glycine (37 °C, pH 1.5 ± 0.05) was transferred to the extractant tube by means of a micropipette. The pump flow rate was set at 1.5 mL $min^{-1}$ for 5 min. The vent cap of the filter holder was opened to ensure that the sample was covered completely before passing the extractant through the filter. To deliver the volume required to fill the holder (*ca.* 7.5 mL), the pump was then run for 5 min. Then the vent cap was closed. The flow rate then was changed to 1 mL $min^{-1}$. The plastic rack containing the filter holder and extractant tube was then placed into the pre-thermostated water bath at 37 °C. The pump was then run for 1 hour. The pH of extract obtained was checked to ensure that it was 1.5 ± 0.5 (i.e. ≤ 2.0). Finally, the extract was stored in polyethylene bottles at 4 °C prior to analysis by ICP-MS as described in Section 3.6.

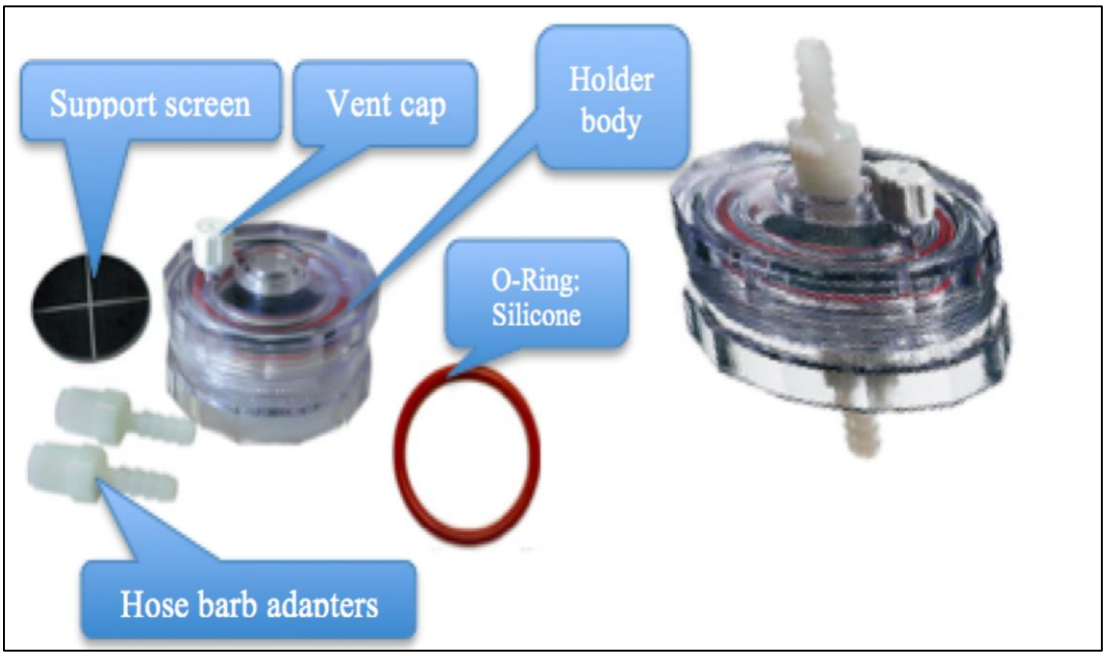


**Figure 5.2. Constituents of 47 mm in-line polycarbonate filter holder**

For the CL-UBM, 1.5 mL of saliva fluid (37 °C, pH 6.5 ± 0.5), prepared as described in Section 3.5.3, was transferred to the extractant tube by means of the micropipette. The pump flow rate was set at 1 mL $min^{-1}$ for 1.5 min. The vent cap of the filter holder was opened. The pump was then run for 1.5 min to deliver the saliva fluid. A 2.25 mL aliquot of gastric fluid (37 °C, pH 1.1 ± 0.1), prepared as described in Section 3.5.3, was pipetted into the extractant tube. The pump was then run for 2.25 min to deliver the gastric fluid, and the vent cap was then closed. The pump was then run for 4 min, and the pH of the extractant was checked to ensure that it was within 1.20 ± 0.05. When necessary it was adjusted by addition of different concentrations of HCl or NaOH solutions. The pump was then run for 1 hour, and the pH of the extract obtained was checked to ensure it was < 1.5. The extract was finally diluted four-fold with 2 % $HNO_3$, and then stored in polyethylene bottles at 4 °C prior to analysis by ICP-MS as described in Section 3.6.

When either the CL-SBET or the CL-UBM was applied, three simulated PM10 samples prepared by using BGS RM 102 Ironstone Soil, three simulated PM10 samples prepared by using NIST SRM 2711A Montana II Soil, and three blank FDMS filter, were used. In addition, a method blank was performed by running the extractant only through the complete procedure. A spike recovery test was also conducted by running the extractant, spiked at 10020 μg $L^{-1}$ for Fe and 250 μg $L^{-1}$ for other PTE, through the complete procedure.

A washing process for filter holders was performed between samples when the system was used many times. This process was conducted after removing an extracted simulated $PM_{10}$ sample from the filter holder. The process involved pumping 10 mL of 5% $HNO_3$, 15 mL deionised water, and 5 mL of the extractant used, sequentially, through the filter holder at a flow rate 1.5 mL $min^{-1}$. The filter holder then was air-dried before re-using.

#### 5.2.1.4. Batch models

The batch model of the SBET and the stomach phase of the UBM were also conducted, as described in Section 4.2.4.1 and 4.2.4.2. For assessing the efficiency of dynamic models of these methods, results obtained from their batch models were

compared to results achieved from their dynamic models. Extracts obtained from the batch models were analysed as described in Section 5.2.1.6.

#### 5.2.1.5. Digestion of residues and mass balance

Mass balance of the CL-SBET, the CL-UBM, and the batch models of the methods was checked by comparing the pseudototal PTE content with the sum of the bioaccessible PTE concentration and the PTE concentration remaining following extraction of samples. The latter was obtained by digesting the residues remaining after sample leaching.

For the batch model of the SBET, this was performed by taking out an extracted loaded FDMS filter (i.e. a simulated $PM_{10}$ sample) or an extracted blank FDMS filter from an extraction bottle using plastic disposable forceps. The filter was then transferred to a pre-cleaned digestion tube. In order to obtain the residue separate from any remaining leachate, the bottle containing the extracted loaded FDMS filter was washed three times with deionised water. The suspension obtained was then transferred to a 50 mL centrifuge tube. The suspension was then centrifuged at 4500 g for 10 min, and the supernatant was discarded by decantation. A 5 mL of aliquot freshly prepared *aqua regia* was added to the residues remaining in the 50 mL centrifuge tube. The 50 mL centrifuge tube was then shaken by hand. The suspension obtained was then transferred to the digestion tube containing the extracted loaded FDMS filter. The microwave digestion was then completed as described in Section 3.3.3. For the stomach phase of the UBM, the digestion procedure for the residues was similar to the SBET, except those 50 mL centrifuge tubes used for centrifuging the residues were the same ones that were used for centrifuging suspensions after the extraction for obtaining the extracts.

In the dynamic models of the SBET and the stomach phase of the UBM, the digestion of residues was performed by disconnecting the filter holder from the system. An extracted loaded FDMS filter (i.e. a simulated $PM_{10}$ sample) or an extracted blank FDMS filter was taken out from the filter holder using a plastic disposable forceps, and was then transferred to a pre-cleaned digestion tube.

For comparison to the sum of fractions, each batch of digestion involved non-extracted three simulated $PM_{10}$ samples using BGS RM 102 Ironstone Soil, three simulated $PM_{10}$ samples using NIST SRM 2711A Montana II Soil, and three blank FDMS filters. For assessing the accuracy of digestion, three samples of BCR CRM 143R Sewage Sludge Amended Soil were also digested. Digests obtained were analysed as described in Section 5.2.1.6.

#### 5.2.1.6. Analyte quantification

Extracts and digests obtained from the batch and CL extraction models, and from microwave digestion were analysed by ICP-MS as described in Section 3.6. The IDL and PDL, shown in Table 5.2, were calculated using Equations 2.16 and 2.17.

#### 5.2.1.7. Quality control and reference materials

No certified reference material is currently available for bioaccessible PTE in airborne PM. Analytical performance was therefore assessed by processing triplicate samples and by use of spike recovery tests. Extractants were spiked to known concentrations of analytes (10020 μg $L^{-1}$ for Fe and 250 μg $L^{-1}$ for other PTE) and taken through the complete extraction procedure. The percentage spike recovery was calculated using Equation 4.1. A recommended value of bioaccessible Pb concentration in NIST SRM 2711A Montana II Soil and guidance values of bioaccessible concentration of As, Cd, and Pb in BGS RM 102 Ironstone Soil were used to assess the accuracy of extraction models for the SBET and the stomach phase of the UBM, respectively. Mass balance was verified by a Z-score calculated using Equations 2.28 and 2.30. The performance of the microwave digestion for pseudototal PTE content was ascertained by using BCR CRM 143R Sewage Sludge Amended Soil.

**Table 5.2. Instrumental (IDL) and procedural (PDL) detection limits for the batch and closed-loop dynamic models (CL) and pseudototal content of the simplified bioaccessibility extraction test (SBET) and the stomach phase of the unified bioaccessibility method (UBM) by ICP-MS**

| Isotope | Batch-SBET and CL-SBET | | Batch-UBM and CL-UBM | |
|---|---|---|---|---|
| | IDL (µg $L^{-1}$) | PDL (mg $kg^{-1}$) | IDL (µg $L^{-1}$) | PDL (mg $kg^{-1}$) |
| $^{75}As$ | 0.008 | 0.001 | 0.009 | 0.0003 |
| $^{111}Cd$ | 0.017 | 0.002 | 0.017 | 0.001 |
| $^{52}Cr$ | 0.036 | 0.004 | 0.031 | 0.001 |
| $^{65}Cu$ | 1.04 | 0.104 | 0.097 | 0.004 |
| $^{56}Fe$ | 0.458 | 0.046 | 7.61 | 0.285 |
| $^{55}Mn$ | 0.021 | 0.002 | 0.068 | 0.003 |
| $^{60}Ni$ | 0.012 | 0.001 | 0.040 | 0.002 |
| $^{208}Pb$ | 0.008 | 0.001 | 0.020 | 0.001 |
| $^{66}Zn$ | 0.499 | 0.050 | 0.177 | 0.007 |

**SBET-UBM-Pseudototal for all models**

| PTE | $^{75}As$ | $^{111}Cd$ | $^{52}Cr$ | $^{65}Cu$ | $^{56}Fe$ | $^{55}Mn$ | $^{60}Ni$ | $^{108}Pb$ | $^{66}Zn$ |
|---|---|---|---|---|---|---|---|---|---|
| IDL-SBET (µg $L^{-1}$) | 0.011 | 0.004 | 0.003 | 0.150 | 0.370 | 0.068 | 0.187 | 0.003 | 0.152 |
| PDL-SBET (mg $kg^{-1}$) | 0.011 | 0.004 | 0.003 | 0.150 | 0.370 | 0.068 | 0.187 | 0.003 | 0.152 |
| IDL-UBM (µg $L^{-1}$) | 0.009 | 0.003 | 0.009 | 0.376 | 0.582 | 0.046 | 0.022 | 0.010 | 0.412 |
| PDL-UBM (mg $kg^{-1}$) | 0.009 | 0.003 | 0.009 | 0.376 | 0.582 | 0.046 | 0.022 | 0.010 | 0.412 |

### 5.2.2. Results and discussion

#### 5.2.2.1. Optimisation of extractant flow rate

The first step in this study was assessing the effect of the flow rate of extractant on the amount of PTE that could be extracted. For this purpose, three flow rates for each method (i.e. the CL-SBET and the CL-UBM) were investigated. The flow rates for the CL-SBET were 0.166, 1.0, and 10.0 ml $min^{-1}$, while for the CL-UBM, they were 0.0625, 1.0, and 3.75 ml $min^{-1}$. These flow rates were chosen based on the number of cycles of the entire volume of extractant (i.e. 10 mL for the CL-SBET and 3.75 mL for CL-UBM) through the extraction system over 60 min. These were 1, 6, and 60 cycles for the CL-SBET, whilst they were 1, 16, and 60 cycles for the CL-UBM.

The device described in Section 5.2.1.3 (Fig. 5.1) was used for this optimisation. Three simulated $PM_{10}$ samples prepared using BGS RM 102 Ironstone Soil were extracted for each method. The experiment was conducted by following the procedure described in Section 5.2.1.3, either for the CL-SBET or the CL-UBM. For blank corrections, blank filters and reagent blank were processed for each flow rate. Results obtained are summarised in Tables 5.3 and 5.4. Guidance values for BGS RM 102 in both methods were not available to compare with results obtained, except for As, Cd, and Pb in the stomach phase of the UBM. Therefore, the results were statistically compared using ANOVA (see Appendices B and C) with the bioaccessible PTE concentration obtained by applying the batch model of the SBET to simulated $PM_{10}$ samples (see Chapter 4). For the SBET, statistical analysis demonstrated that there was no significant difference between the results obtained by the three flow rates of the CL-SBET and those obtained using the batch model for Cr, Cu, Fe, Pb, and Zn. One flow rate gave a significant difference for the rest of analytes. This flow rate was 10.0 mL $min^{-1}$ for As and 0.166 mL $min^{-1}$ for Cd, Mn, and Ni. Since the best precision was generally achieved when the extractant flowed at 1.0 mL $min^{-1}$ (see Table 5.3), this was adopted as the preferred flow rate for the CL-SBET.

For the stomach phase of the UBM, statistical results showed that there was a significant difference between the results obtained by the three flow rates of the CL-UBM and those obtained using the batch model for Fe, Mn, Ni, and Pb. No

significant difference was observed between the three flow rates of the CL-UBM and the batch model for As, while two flow rates gave a significant difference for Cd, Cr, and Cu. These two flow rates were 0.0625 and 3.75 mL $min^{-1}$ for Cu and 1.0 and 3.75 mL $min^{-1}$ for Cd and Cr. For Zn, only a flow rate of 3.75 mL $min^{-1}$ showed a significant difference. As a significant difference was observed for the Cu, Fe, Mn, Ni, and Pb for the three flow rates, except for 1.0 mL $min^{-1}$ for Cu, and no significant difference was noted for As, 1.0 mL $min^{-1}$ flow rate was chosen for the rest of experiment. This was because the best precision (represented by the RSD) was achieved when this flow rate was used and because the bioaccessible concentration obtained was closer to the guidance value (for Pb) or the batch value (for Zn) (see Table 5.4). Although the flow rate that showed no significant difference for Cd and Cr was 0.0625 mL $min^{-1}$, the best RSD was achieved with the 1.0 mL $min^{-1}$ flow rate. Also, the bioaccessible concentration of Cd was within the guidance value ($0.281 \pm 0.170$ mg $kg^{-1}$).

**Table 5.3. Effect of the flow rate of extractant on the bioaccessible concentration (mg $kg^{-1}$) of PTE measured in simulated $PM_{10}$ samples prepared using BGS RM 102 Ironstone Soil and extracted using the closed-loop dynamic model (CL) of the simplified bioaccessibility extraction test (SBET) (CL-SBET)**

| PTE | Flow rate (0.166 mL $min^{-1}$) | | Flow rate (1.0 mL min-1) | | Flow rate (10.0 mL min-1) | |
|---|---|---|---|---|---|---|
| | Mean ± SD (n=3) | %RSD | Mean ± SD (n=3) | % RSD | Mean ± SD (n=3) | % RSD |
| **As** | 1.77 ± 0.09 | 5.28 | 1.70 ± 0.06 | 3.66 | 2.00 ± 0.09 | 4.26 |
| **Cd** | 0.225 ± 0.007 | 2.93 | 0.204 ± 0.009 | 4.5 | 0.206 ± 0.008 | 3.8 |
| **Cr** | 24.3 ± 1.5 | 5.98 | 24.2 ± 0.6 | 2.48 | 24.7 ± 1.7 | 6.93 |
| **Cu** | 8.15 ± 1.13 | 13.8 | 6.78 ± 0.24 | 3.49 | 7.04 ± 0.26 | 3.68 |
| **Fe** | 1020 ± 114 | 11.1 | 1080 ± 17 | 1.55 | 1120 ± 72 | 6.48 |
| **Mn** | 2000 ± 57 | 2.86 | 1870 ± 58 | 3.09 | 1840 ± 115 | 6.25 |
| **Ni** | 9.27 ± 0.26 | 2.85 | 8.09 ± 0.14 | 1.78 | 7.89 ± 0.55 | 6.95 |
| **Pb** | 15.2 ± 1.2 | 7.7 | 14.7 ± 0.5 | 3.06 | 15.0 ± 1.0 | 6.33 |
| **Zn** | 46.9 ± 21.4 | 45.7 | 22.3 ± 4.6 | 20.7 | 37.5 ± 5.3 | 14 |

SD: standard deviation; RSD: relative standard deviation

**Table 5.4. Effect of the flow rate of extractant on the bioaccessible concentration (mg $kg^{-1}$) of PTE measured in simulated $PM_{10}$ samples prepared using BGS RM 102 Ironstone Soil and extracted using the closed-loop dynamic model (CL) of the stomach phase of the unified bioaccessibility method (UBM) (CL-UBM)**

| PTE | Flow rate (0.0625 mL $min^{-1}$) | | Flow rate (1.0 mL min-1) | | Flow rate (3.75 mL min-1) | |
|---|---|---|---|---|---|---|
| | Mean ± SD (n=3) | %RSD | Mean ± SD (n=3) | % RSD | Mean ± SD (n=3) | % RSD |
| **As** | 4.24 ± 0.39 | 9.16 | 3.82 ± 0.14 | 3.76 | 3.99 ± 0.20 | 5.11 |
| **Cd** | 0.206 ± 0.025 | 12.2 | 0.154 ± 0.011 | 7.08 | 0.139 ± 0.013 | 9.05 |
| **Cr** | 31.4 ± 3.4 | 10.9 | 25.9 ± 0.4 | 1.57 | 26.8 ± 1.5 | 5.72 |
| **Cu** | 5.65 ± 0.53 | 9.34 | 6.46 ± 0.31 | 4.83 | 5.88 ± 0.40 | 6.8 |
| **Fe** | 847 ± 114 | 13.4 | 1040 ± 130 | 12.5 | 781 ± 58 | 7.39 |
| **Mn** | 2090 ± 267 | 12.7 | 1840 ± 106 | 5.76 | 1860 ± 127 | 6.83 |
| **Ni** | 9.53 ± 1.16 | 12.1 | 7.90 ± 0.44 | 5.56 | 8.24 ± 0.64 | 7.76 |
| **Pb** | 11.7 ± 1.6 | 13.4 | 13.1 ± 1.4 | 10.9 | 10.3 ± 1.1 | 10.3 |
| **Zn** | 24.9 ± 1.6 | 6.51 | 30.4 ± 10.5 | 34.5 | 19.6 ± 3.4 | 17.1 |

SD: standard deviation; RSD: relative standard deviation

#### 5.2.2.2. Bioaccessible concentration of PTE in blank FDMS filters

The bioaccessible and residual fractions of PTE in extracted blank FDMS filters as well as pseudototal content of PTE in non-extracted blank FDMS filters using the batch models, the CL-SBET, and the CL-UBM are summarised in Tables 5.5 and 5.6. For all models, either those for the SBET or the stomach phase of the UBM, bioaccessible PTE concentrations in blank FDMS filters were very low, except for Zn, where they were comparatively high. This may due to the fact that Zn is used as a binder for FDMS filters. The extent of agreement between the sum of PTE fractions (bioaccessible + residual fractions) and the measured pseudototal PTE values (i.e. % mass balance) was assessed by application of the Student's t-test at 95% confidence level. In general, no significant difference was observed between the sum of the PTE fractions and their measured pseudototal values (see Tables 5.5 and 5.6), indicating that the performance and the accuracy of these dynamic extraction models were acceptable.

**Table 5.5. Concentrations of potentially toxic elements (PTE) in the bioaccessible and residual fractions, together with pseudototal content and mass balance in blank FDMS filters using the batch and closed-loop dynamic (CL) models of the simplified bioaccessibility extraction test (SBET) (CL-SBET)**

| PTE | Models | Bioaccessible fraction (µg filter$^{-1}$) Mean (n=3) ± SD | Residual fraction (µg filter$^{-1}$) Mean (n=3) ± SD | Sum ± $SD_C$ (µg filter$^{-1}$) | Pseudototal (µg filter$^{-1}$) Mean (n=3) ± SD | % Mass balance ± $SD_C$ | Student's t-test at 95% confidence level | |
|---|---|---|---|---|---|---|---|---|
| | | | | | | | $t_{calculated}$ | $t_{critical}$ |
| **As** | **Batch** | < RB | 0.318 ± 0.039 | 0.318 ± 0.039 | 0.251 ± 0.027 | 127 ± 21 | 2.44 | 2.78 |
| | **CL** | < RB | 0.300 ± 0.060 | 0.300 ± 0.060 | 0.290 ± 0.036 | 103 ± 24 | 0.25 | 2.78 |
| **Cd** | **Batch** | < IDL | < RB | NC | < RB | NC | NC | NC |
| | **CL** | < IDL | < RB | NC | 0.002 ± 0.0004 | NC | NC | NC |
| **Cr** | **Batch** | 0.001 ± 0.0003 | 2.80 ± 0.03 | 2.81 ± 0.03 | 2.72 ± 0.11 | 103 ± 4 | 1.05 | 3.18 |
| | **CL** | < RB | 2.56 ± 0.24 | 2.56 ± 0.24 | 2.93 ± 0.18 | 87.4 ± 9.8 | 2.14 | 2.78 |
| **Cu** | **Batch** | < IDL | < RB | NC | < RB | NC | NC | NC |
| | **CL** | < IDL | 0.360 ± 0.120 | 0.360 ± 0.120 | 0.540 ± 0.116 | 66.6 ± 26.4 | 1.87 | 2.78 |
| **Fe** | **Batch** | 0.422 ± 0.148 | 83.0 ± 6.1 | 83.4 ± 6.1 | 60.5 ± 2.3 | 138 ± 11 | **6.31** | 3.18 |
| | **CL** | < RB | 63.8 ± 3.3 | 63.8 ± 3.3 | 62.3 ± 3.3 | 102 ± 8 | 0.57 | 2.78 |
| **Mn** | **Batch** | 0.076 ± 0.039 | 1.42 ± 0.44 | 1.49 ± 0.45 | 0.932 ± 0.114 | 160 ± 52 | 2.24 | 3.18 |
| | **CL** | < RB | 1.16 ± 0.07 | 1.16 ± 0.07 | 0.920 ± 0.095 | 126 ± 15 | **3.52** | 2.78 |
| **Ni** | **Batch** | 0.002 ± 0.0005 | 0.053 ± 0.018 | 0.054 ± 0.018 | 0.084 ± 0.007 | 64.5 ± 22.3 | 2.76 | 3.18 |
| | **CL** | 0.004 ± 0.001 | < IDL | 0.004 ± 0.001 | < IDL | NC | NC | NC |
| **Pb** | **Batch** | < RB | 0.530 ± 0.048 | 0.530 ± 0.048 | 0.456 ± 0.027 | 116 ± 13 | 2.31 | 2.78 |
| | **CL** | 0.002 ± 0.0003 | 0.520 ± 0.020 | 0.522 ± 0.020 | 0.490 ± 0.029 | 107 ± 8 | 1.35 | 3.18 |
| **Zn** | **Batch** | 2.07 ± 0.10 | 1010 ± 28 | 1010 ± 28 | 867 ± 154 | 117 ± 21 | 1.26 | 3.18 |
| | **CL** | 1.75 ± 0.11 | 875 ± 168 | 877 ± 168 | 693 ± 197 | 127 ± 43 | 1.08 | 3.18 |

n= number of replicates; $SD_C$: combined standard deviation; Sum = (Bioaccessible fraction + Residual fraction); % Mass balance = $\frac{\text{Sum}}{\text{pseudototal}} \times 100$; < IDL: less than instrumental detection limit; < RB: less than reagent blank; NC: not calculated

**Table 5.6. Concentrations of potentially toxic elements (PTE) in the bioaccessible and residual fractions, together with pseudototal content and mass balance in blank FDMS filters using the batch and closed-loop dynamic (CL) models of the stomach phase of the unified bioaccessibility method (UBM) (CL-UBM)**

| PTE | Models | Bioaccessible fraction (µg filter$^{-1}$) Mean (n=3) ± SD | Residual fraction (µg filter$^{-1}$) Mean (n=3) ± SD | Sum ± $SD_C$ (µg filter$^{-1}$) | Pseudototal (µg filter$^{-1}$) Mean (n=3) ± SD | % Mass balance ± $SD_C$ | Student's t-test at 95% confidence level | |
|---|---|---|---|---|---|---|---|---|
| | | | | | | | $t_{calculated}$ | $t_{critical}$ |
| **As** | **Batch** | < RB | 0.288 ± 0.025 | 0.288 ± 0.025 | 0.276 ± 0.016 | 104 ± 11 | 0.69 | 2.78 |
| | **CL** | < RB | 0.334 ± 0.011 | 0.334 ± 0.011 | 0.331 ± 0.003 | 101 ± 3 | 0.45 | 2.78 |
| **Cd** | **Batch** | < RB | < RB | NC | < RB | NC | NC | NC |
| | **CL** | < IDL | < RB | NC | < RB | NC | NC | NC |
| **Cr** | **Batch** | < IDL | 2.58 ± 0.07 | 2.58 ± 0.07 | 2.59 ± 0.05 | 99.6 ± 3.3 | 0.21 | 2.78 |
| | **CL** | < IDL | 2.70 ± 0.05 | 2.70 ± 0.05 | 2.59 ± 0.02 | 104 ± 2 | **3.51** | 2.78 |
| **Cu** | **Batch** | 0.061 ± 0.047 | < RB | 0.061 ± 0.047 | < RB | NC | NC | NC |
| | **CL** | 0.035 ± 0.005 | 0.573 ± 0.322 | 0.608 ± 0.322 | < RB | NC | NC | NC |
| **Fe** | **Batch** | < IDL | 64.6 ± 4.1 | 64.6 ± 4.1 | 60.1 ± 2.2 | 107 ± 8 | 1.67 | 2.78 |
| | **CL** | < IDL | 65.0 ± 3.0 | 65.0 ± 3.0 | 61.3 ± 1.2 | 106 ± 5 | 1.98 | 2.78 |
| **Mn** | **Batch** | 0.060 ± 0.040 | 1.02 ± 0.09 | 1.08 ± 0.10 | 1.08 ± 0.01 | 100 ± 9 | 0.06 | 12.7 |
| | **CL** | < RB | 1.26 ± 0.11 | 1.28 ± 0.11 | 1.11 ± 0.05 | 113 ± 11 | 2.22 | 2.78 |
| **Ni** | **Batch** | < IDL | 0.208 ± 0.006 | 0.208 ± 0.006 | 0.241 ± 0.006 | 86.4 ± 3.2 | **6.88** | 2.78 |
| | **CL** | < IDL | 0.322 ± 0.017 | 0.322 ± 0.017 | 0.315 ± 0.009 | 102 ± 6 | 0.62 | 2.78 |
| **Pb** | **Batch** | < IDL | 0.474 ± 0.006 | 0.474 ± 0.006 | 0.473 ± 0.007 | 100 ± 2 | 0.25 | 2.78 |
| | **CL** | < IDL | 0.543 ± 0.022 | 0.543 ± 0.022 | 0.512 ± 0.006 | 106 ± 5 | 2.36 | 2.78 |
| **Zn** | **Batch** | 3.10 ± 1.03 | 985 ± 6 | 988 ± 6 | 898 ± 79 | 110 ± 10 | 1.54 | 3.18 |
| | **CL** | 1.11 ± 0.68 | 952 ± 62.5 | 953 ± 63 | 934 ± 23 | 102 ± 7 | 0.51 | 3.18 |

n= number of replicates; $SD_C$: combined standard deviation; Sum = (Bioaccessible fraction + Residual fraction); % Mass balance = $\frac{\text{Sum}}{\text{pseudototal}} \times 100$; < IDL: less than instrumental detection limit; < RB: less than reagent blank; NC: not calculated

### 5.2.2.3. Closed-loop dynamic model of the SBET (CL-SBET)

Figures 5.3-5-10 display the bioaccessible and residual PTE fractions, as well as their sum with respect to the pseudototal contents, in simulated $PM_{10}$ samples, prepared using BGS RM 102 Ironstone Soil and NIST SRM 2711A Montana II Soil, extracted by applying the batch model and the CL-SBET. Generally, when the batch model or the CL-SBET was applied, the concentration of PTE in the bioaccessible fraction in BGS RM 102 or NIST SRM 2711A was smaller compared to the residual fraction. This was the case for all PTE tested, except As, Cd, Cu, and Pb in NIST SRM 2711A, where the PTE concentration in the bioaccessible fraction was the higher, particularly for Cd and Pb (95.5%, 89.8%, and 84.0%, 83.1%, respectively). This different trend may be because forms of these PTE present in NIST SRM 2711A are more available than in BGS RM 102. This generally was in agreement with the results of a sequential-extraction study[179] conducted using NIST SRM 2711. Recoveries of the bioaccessible PTE concentration for the CL-SBET with respect to those obtained by the batch model ranged from 70.2 ± 9.0% for Fe in BGS RM 102 to 107 ± 11% for Cu in NIST SRM 2711A. The recovery of bioaccessible Pb for the CL-SBET based on the recommended value was 97.3 ± 5.3% (see Table 5.7).

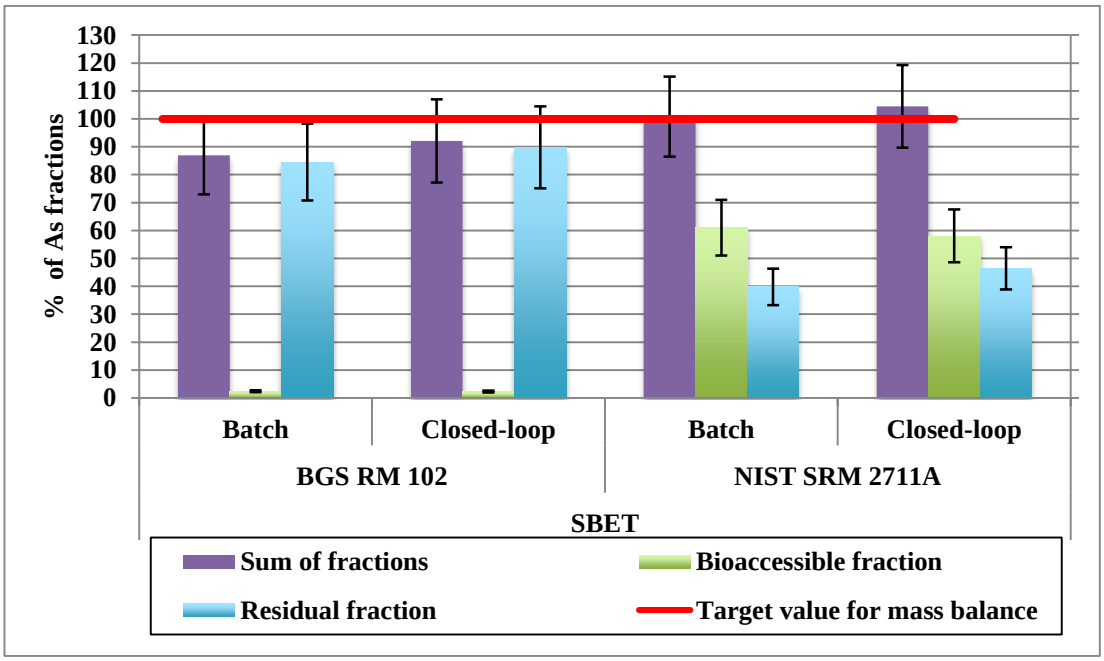


**Figure 5.3. Arsenic fractions and their sum (mass balance) as a percentage of pseudototal content, released from simulated $PM_{10}$ samples using BGS RM 102 Ironstone Soil and NIST SRM 2711A Montana II Soil by applying the batch and closed-loop dynamic (CL) models of the simplified bioaccessibility extraction test (SBET) (CL-SBET)**

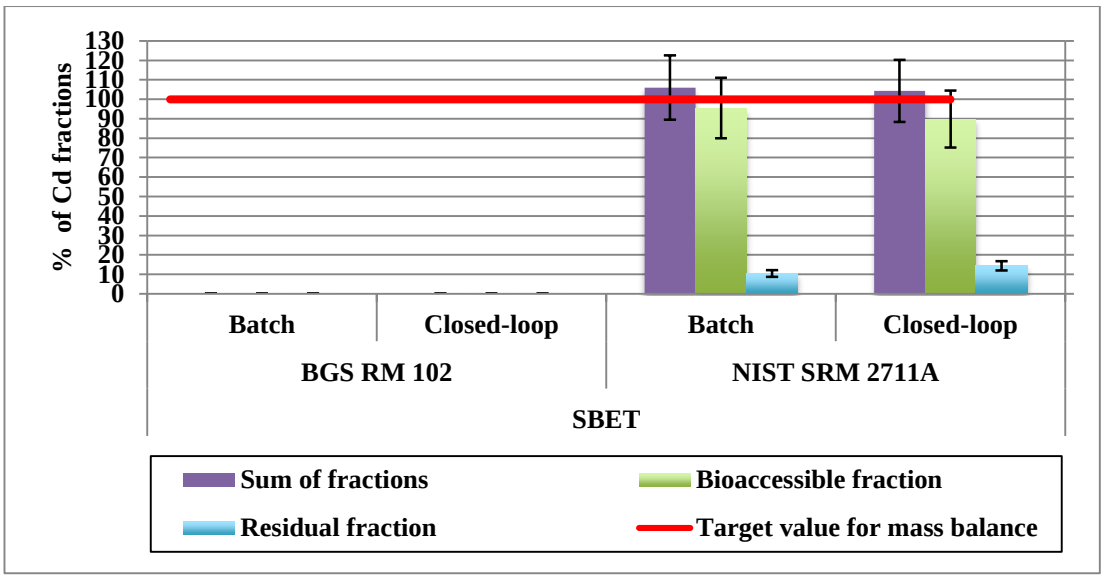


**Figure 5.4. Cadmium fractions and their sum (mass balance) as a percentage of pseudototal content, released from simulated $PM_{10}$ samples using BGS RM 102 Ironstone Soil and NIST SRM 2711A Montana II Soil by applying the batch and closed-loop dynamic (CL) models of the simplified bioaccessibility extraction test (SBET) (CL-SBET)**

The bioaccessible and residual fraction for Zn in both materials and also for Cd in BGS RM 102 Ironstone Soil with respect to the pseudototal contents were not calculated. This was because the concentration of PTE in the residual fraction or pseudototal PTE content was less than the reagent blank (for Cd) or the FDMS filter blank (for Zn). Results obtained from the Student's t-test at 95% confidence level (see Table 5.7) demonstrated that there was no significant difference between the bioaccessible concentration obtained by applying the batch model of the SBET and those obtained using the CL-SBET for all PTE tested, except for Fe and Mn in both materials and for Cr, Ni, Pb, and Zn in BGS RM 102 Ironstone Soil. However, good recoveries relative to the batch values were obtained for Fe (90.4 ± 4.9%) and Mn (91.5 ± 4.5%) in NIST SRM 2711A, while the others were within 100.0 ± 20%. These significant differences may be because the batch model (open system) is more prone to contamination than the CL model (closed system), particularly for ubiquitous elements such as Pb.[175] Also, the weight of sample (100 mg) adopted for this study (to more closely represent the amount of airborne PM typically collected in real quality monitoring campaigns) was less than the minimum recommended for each material. Therefore, lack of homogeneity between samples may also be a reason for these differences.

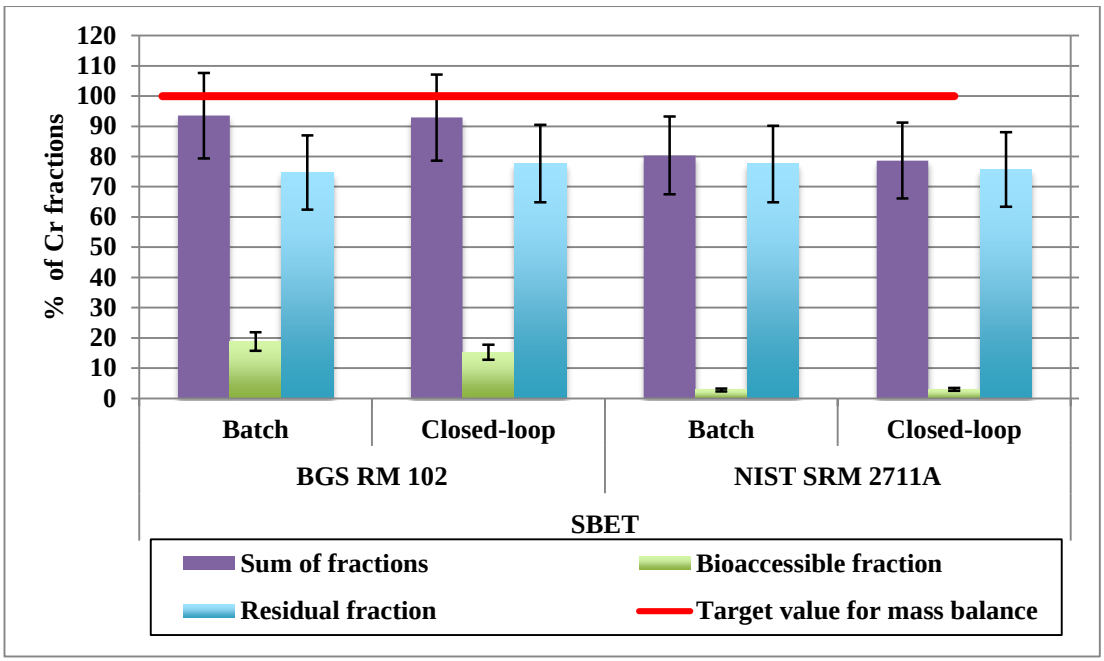


**Figure 5.5. Chromium fractions and their sum (mass balance) as a percentage of pseudototal content, released from simulated $PM_{10}$ samples using BGS RM 102 Ironstone Soil and NIST SRM 2711A Montana II Soil by applying the batch and closed-loop dynamic (CL) models of the simplified bioaccessibility extraction test (SBET) (CL-SBET)**

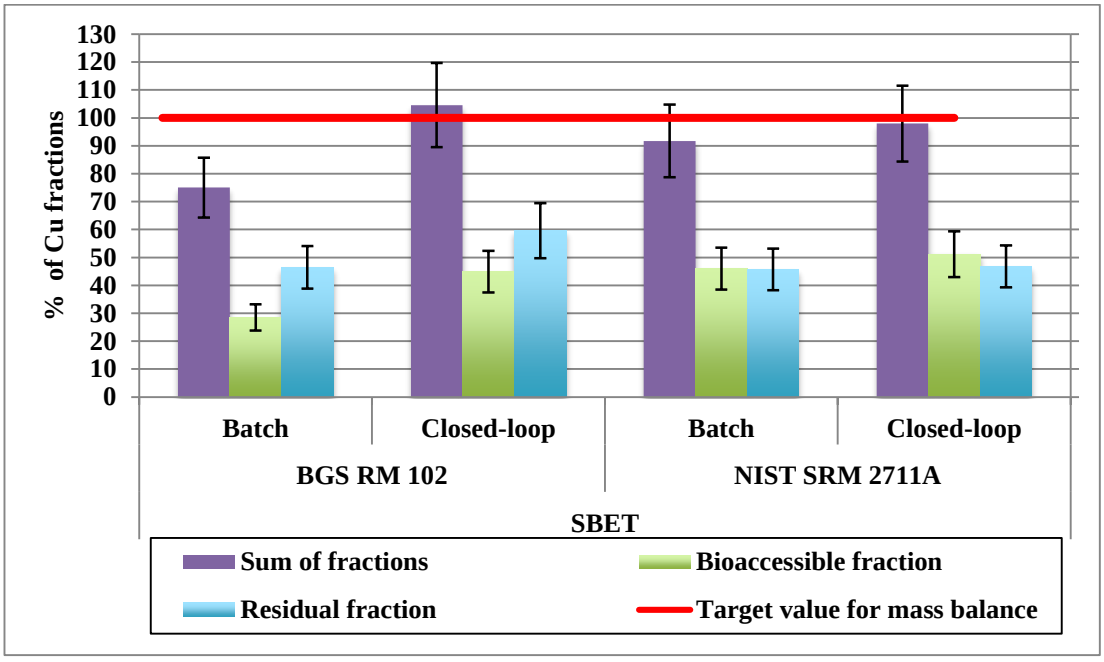


**Figure 5.6. Copper fractions and their sum (mass balance) as a percentage of pseudototal content, released from simulated $PM_{10}$ samples using BGS RM 102 Ironstone Soil and NIST SRM 2711A Montana II Soil by applying the batch and closed-loop dynamic (CL) models of the simplified bioaccessibility extraction test (SBET) (CL-SBET)**

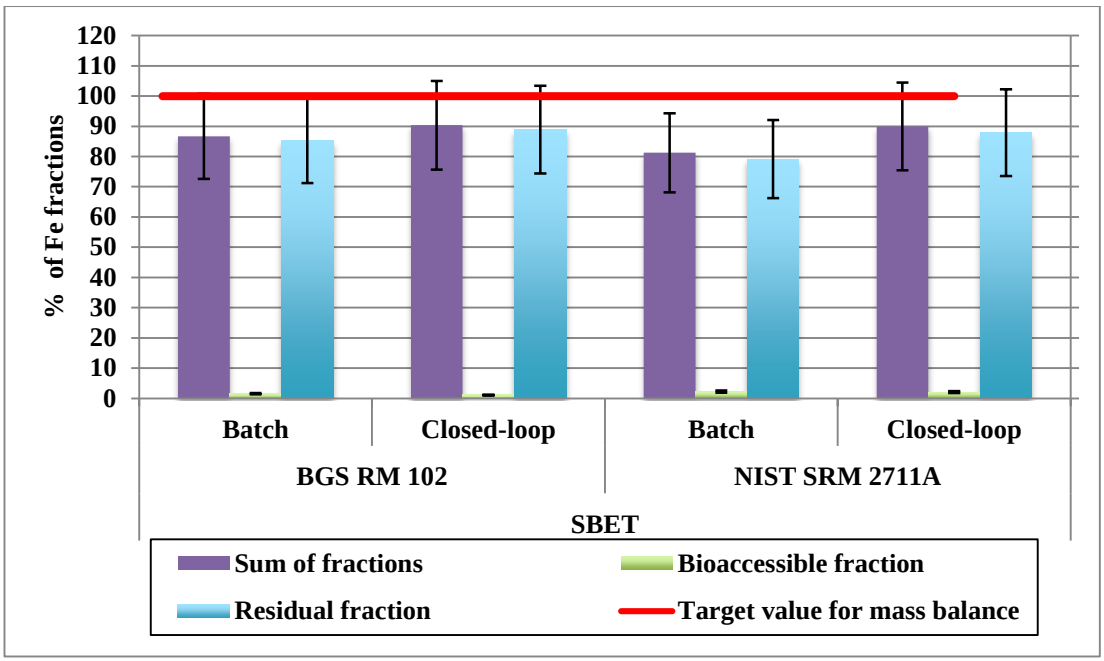


**Figure 5.7. Iron fractions and their sum (mass balance) as a percentage of pseudototal content, released from simulated $PM_{10}$ samples using BGS RM 102 Ironstone Soil and NIST SRM 2711A Montana II Soil by applying the batch and closed-loop dynamic (CL) models of the simplified bioaccessibility extraction test (SBET) (CL-SBET)**

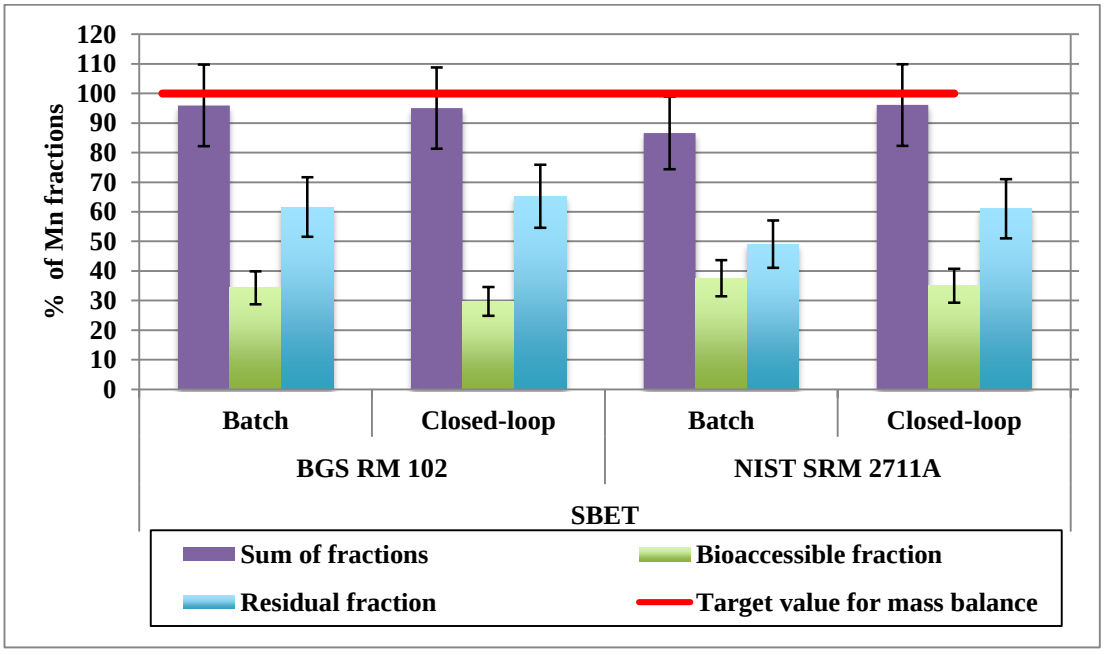


**Figure 5.8. Manganese fractions and their sum (mass balance) as a percentage of pseudototal content, released from simulated $PM_{10}$ samples using BGS RM 102 Ironstone Soil and NIST SRM 2711A Montana II Soil by applying the batch and closed-loop dynamic (CL) models of the simplified bioaccessibility extraction test (SBET) (CL-SBET)**

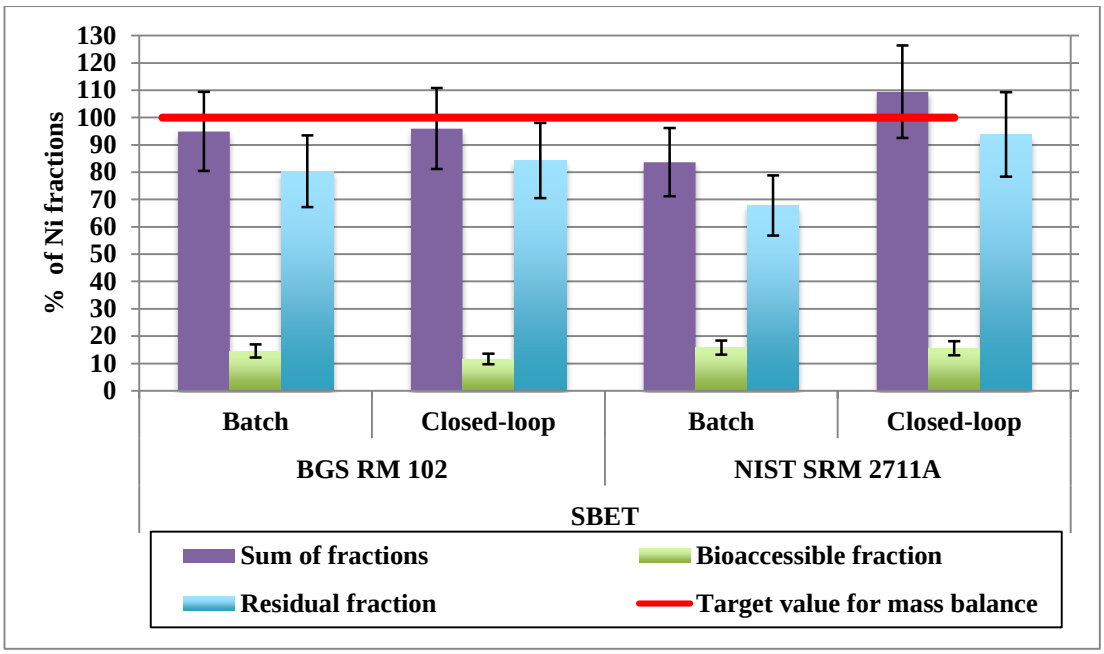


**Figure 5.9. Nickel fractions and their sum (mass balance) as a percentage of pseudototal content, released from simulated $PM_{10}$ samples using BGS RM 102 Ironstone Soil and NIST SRM 2711A Montana II Soil by applying the batch and closed-loop dynamic (CL) models of the simplified bioaccessibility extraction test (SBET) (CL-SBET)**

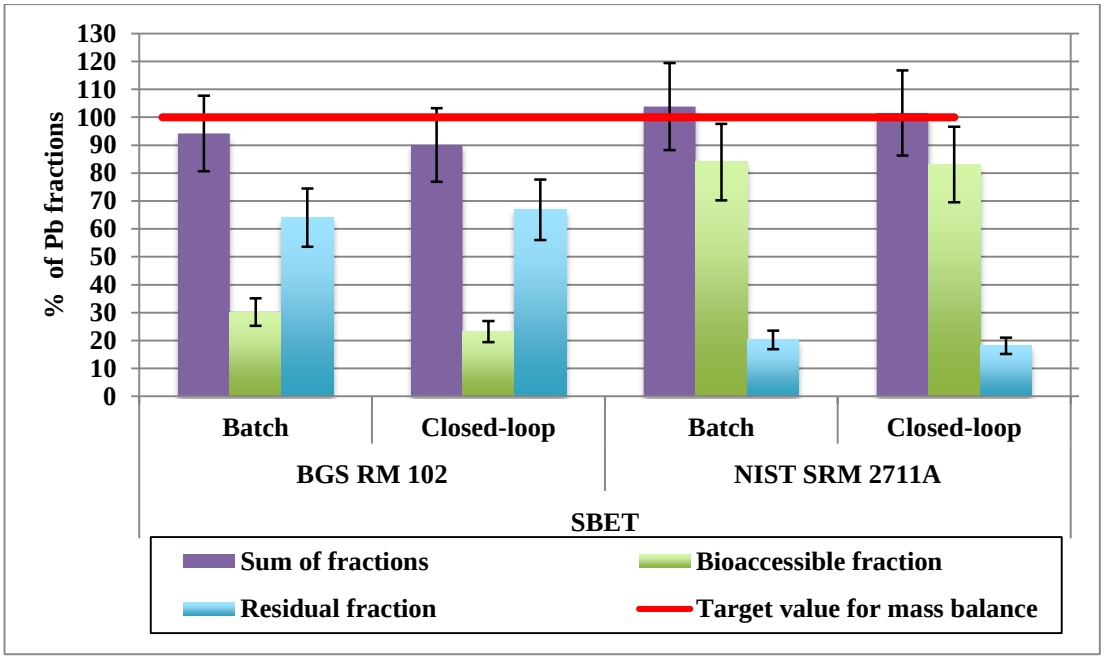


**Figure 5.10. Lead fractions and their sum (mass balance) as a percentage of pseudototal content, released from simulated $PM_{10}$ samples using BGS RM 102 Ironstone Soil and NIST SRM 2711A Montana II Soil by applying the batch and closed-loop dynamic (CL) models of the simplified bioaccessibility extraction test (SBET) (CL-SBET)**

**Table 5.7. Recoveries of bioaccessible fraction of potentially toxic elements (PTE) in simulated $PM_{10}$ samples, prepared using BGS RM 102 Ironstone Soil and NIST SRM 2711A Montana II Soil, obtained by applying the closed-loop (CL) dynamic model of the simplified bioaccessibility extraction test (SBET) (CL-SBET) with respect to those obtained using its batch model or to available recommended bioaccessible values**

| PTE | Models | Bioaccessible fraction (mg $kg^{-1}$)(n=3) | | %Recovery[a] | Recommended value Mean (n=35) ± SD | %Recovery[b] | Student's t-test[c] at 95% confidence level | | Student's t-test[d] at 95% confidence level | |
|---|---|---|---|---|---|---|---|---|---|---|
| | | Batch Mean ± SD | CL Mean ± SD | | | | $t_{calculated}$ | $t_{critical}$ | $t_{calculated}$ | $t_{critical}$ |
| **As** | **BGS102** | 2.36 ± 0.01 | 2.25 ± 0.14 | 95.4 ± 6.0 | NA | - | - | - | 1.32 | 4.30 |
| | **NIST2711A** | 57.8 ± 0.7 | 55.4 ± 1.4 | 95.9 ± 2.7 | NA | - | - | - | 2.59 | 2.78 |
| **Cd** | **BGS102** | 0.208 ± 0.003 | 0.208 ± 0.009 | 100 ± 4.5 | NA | - | - | - | 0.08 | 2.78 |
| | **NIST2711A** | 47.1 ± 1.1 | 44.3 ± 1.7 | 94.1 ± 4.3 | NA | - | - | - | 2.34 | 2.78 |
| **Cr** | **BGS102** | 35.4 ± 1.0 | 28.5 ± 2.8 | 80.5 ± 8.3 | NA | - | - | - | **4.00** | 2.78 |
| | **NIST2711A** | 0.899 ± 0.023 | 0.822 ± 0.055 | 91.4 ± 6.6 | NA | - | - | - | 2.25 | 2.78 |
| **Cu** | **BGS102** | 7.84 ± 0.04 | 8.36 ± 0.54 | 107 ± 7 | NA | - | - | - | 1.64 | 4.30 |
| | **NIST2711A** | 59.9 ± 1.6 | 64.0 ± 6.1 | 107 ± 11 | NA | - | - | - | 1.15 | 2.78 |
| **Fe** | **BGS102** | 2100 ± 2 | 1470 ± 189 | 70.2 ± 9.0 | NA | - | - | - | **5.73** | 4.30 |
| | **NIST2711A** | 544 ± 15 | 492 ± 24 | 90.4 ± 4.9 | NA | - | - | - | **3.27** | 2.78 |
| **Mn** | **BGS102** | 2200 ± 32 | 1910 ± 82 | 86.6 ± 3.9 | NA | - | - | - | **5.84** | 2.78 |
| | **NIST2711A** | 215 ± 4 | 197 ± 9 | 91.5 ± 4.5 | NA | - | - | - | **3.23** | 2.78 |
| **Ni** | **BGS102** | 10.6 ± 0.3 | 8.47 ± 0.47 | 79.9 ± 4.9 | NA | - | - | - | **6.68** | 2.78 |
| | **NIST2711A** | 2.92 ± 0.07 | 2.79 ± 0.14 | 95.7 ± 5.4 | NA | - | - | - | 1.37 | 2.78 |
| **Pb** | **BGS102** | 22.6 ± 0.8 | 17.8 ± 2.0 | 78.8 ± 9.2 | NA | - | - | - | **3.91** | 2.78 |
| | **NIST2711A** | 1100 ± 30 | 1080 ± 34 | 98.0 ± 4.1 | 1110 ± 49 | 97.3 ± 5.3 | 1.03 | 2.03 | 0.84 | 2.78 |
| **Zn** | **BGS102** | 39.7 ± 3.2 | 28.4 ± 3.5 | 71.6 ± 10.6 | NA | - | - | - | **4.08** | 2.78 |
| | **NIST2711A** | 130 ± 5 | 124 ± 5 | 95.6 ± 4.9 | NA | - | - | - | 1.52 | 2.78 |

SD: standard deviation; n= number of replicates; [c]: t-test for difference between the bioaccessible fraction by closed-loop (CL) model and recommended values; [d]: t-test for difference between the bioaccessible fraction by CL and batch models; $\%\,Recovery^{\,a} = \left(\frac{Bioaccessible\ fraction\ for\ CL\ model}{Bioaccessible\ fraction\ for\ batch\ model}\right) \times 100$; $\%\,Recovery^{\,b} = \left(\frac{Bioaccessible\ fraction\ for\ CL\ model}{Certified\ value}\right) \times 100$

### 5.2.2.4. Closed-loop dynamic model of the stomach phase of the UBM (CL-UBM)

Figures 5.11-5.18 present the bioaccessible and residual PTE fractions, as well as their sum relative to the pseudototal contents, in simulated $PM_{10}$ samples, prepared using BGS RM 102 Ironstone Soil and NIST SRM 2711A Montana II Soil, extracted by applying the batch model and the CL-UBM. Similar to the SBET, when the batch model and CL-UBM were applied, the PTE concentration in the bioaccessible fraction was smaller than the residual fraction in most of the cases. However, for As, Cd, Mn, and Pb in NIST SRM 2711A and for Cd in BGS RM 102 Ironstone Soil, the bioaccessible concentration was the higher. Based on the Student's t-test at 95% confidence level (see Table 5.8), there was a significant difference between the bioaccessible concentrations obtained using the batch model and those obtained from the CL-UBM for all PTE determined, except for Cr, Cu, and Fe in BGS RM 102 Ironstone Soil, and Cd and Zn in both materials, where no significant difference was observed. However, no significant difference was also shown between the bioaccessible concentration of As, Cd, and Pb and their guidance values in BGS RM 102 Ironstone Soil. Recoveries of the bioaccessible PTE concentration with respect to the batch values for the CL-UBM were, in most cases, within 100 ± 20%.

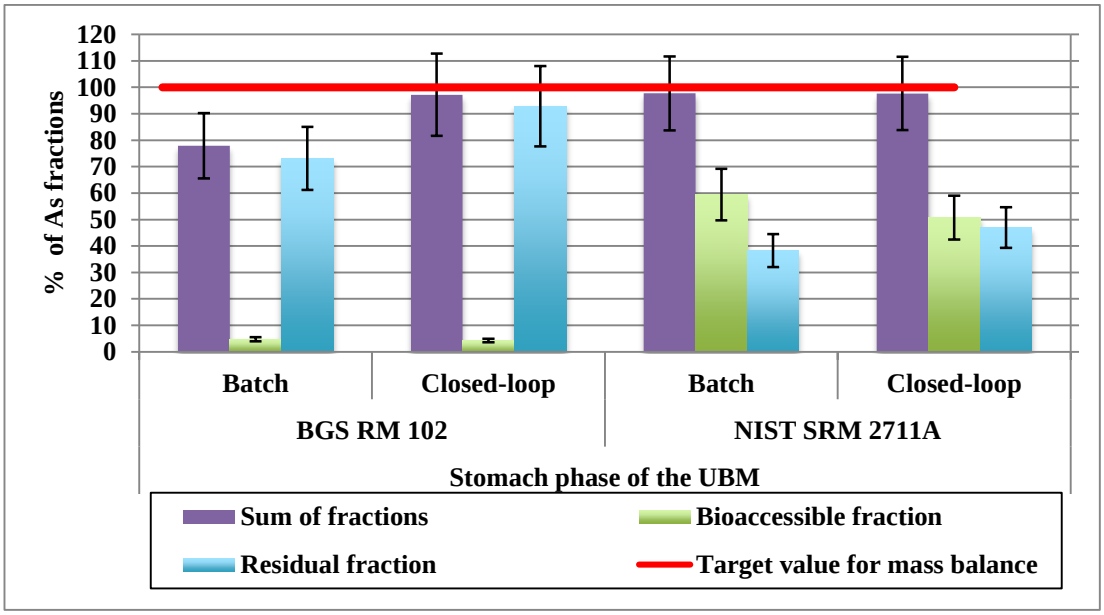


**Figure 5.11. Arsenic fractions and their sum (mass balance) as a percentage of pseudototal content, released from simulated $PM_{10}$ samples using BGS RM 102 Ironstone Soil and NIST SRM 2711A Montana II Soil by applying the batch and closed-loop dynamic (CL) models of the stomach phase of the unified bioaccessibility method (UBM) (CL-UBM)**

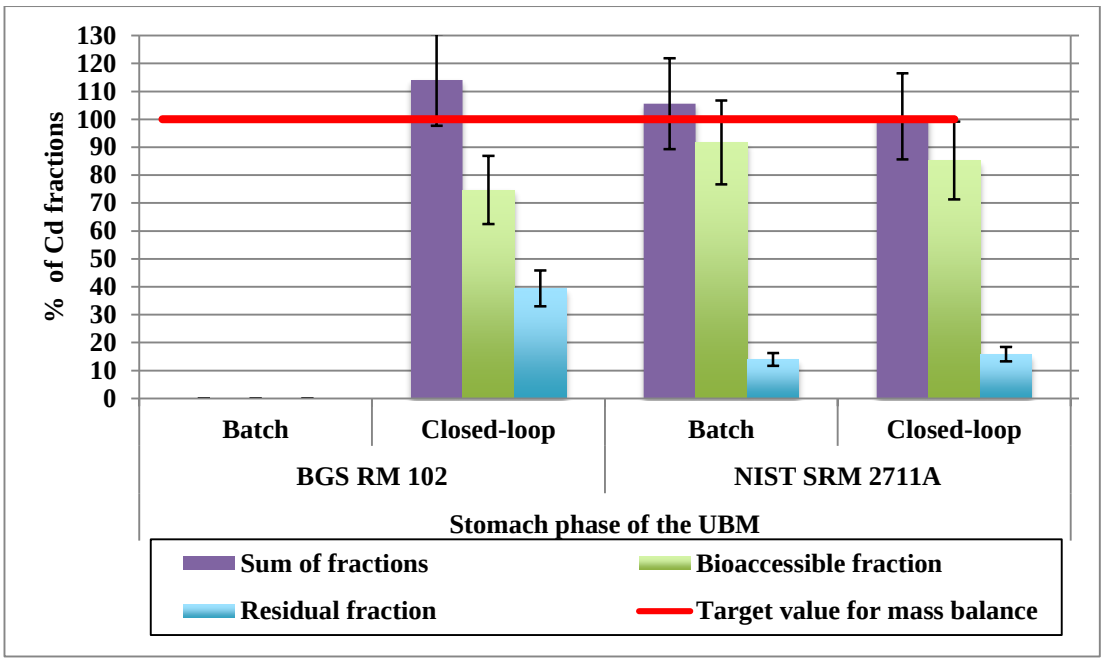


**Figure 5.12. Cadmium fractions and their sum (mass balance) as a percentage of pseudototal content, released from simulated $PM_{10}$ samples using BGS RM 102 Ironstone Soil and NIST SRM 2711A Montana II Soil by applying the batch and closed-loop dynamic (CL) models of the stomach phase of the unified bioaccessibility method (UBM) (CL-UBM)**

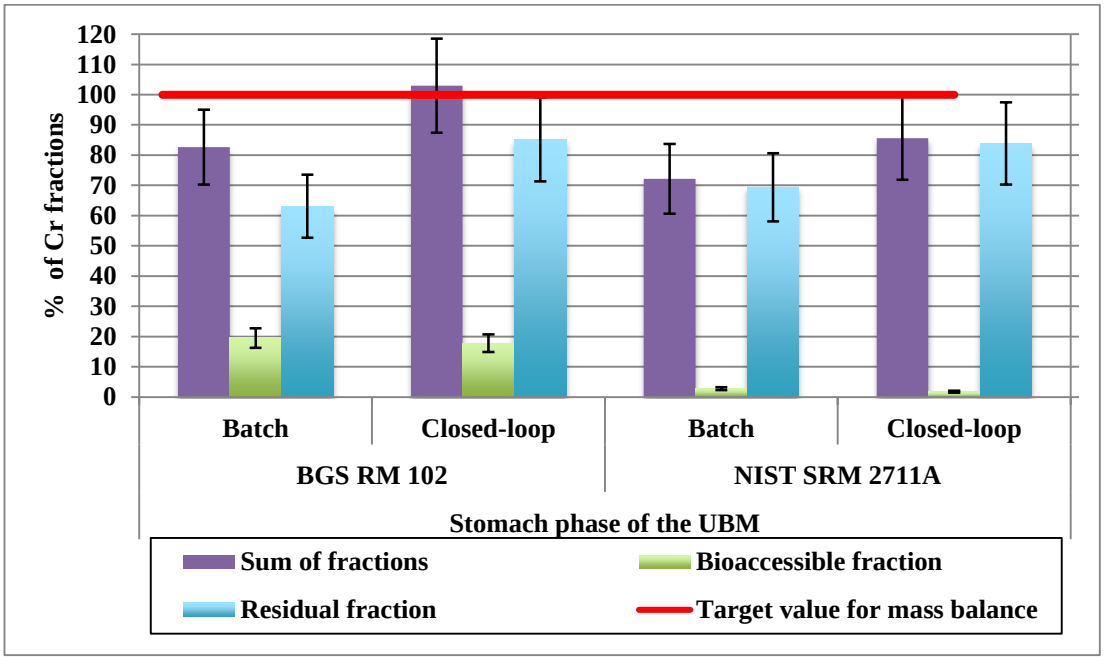


**Figure 5.13. Chromium fractions and their sum (mass balance) as a percentage of pseudototal content, released from simulated $PM_{10}$ samples using BGS RM 102 Ironstone Soil and NIST SRM 2711A Montana II Soil by applying the batch and closed-loop dynamic (CL) models of the stomach phase of the unified bioaccessibility method (UBM) (CL-UBM)**

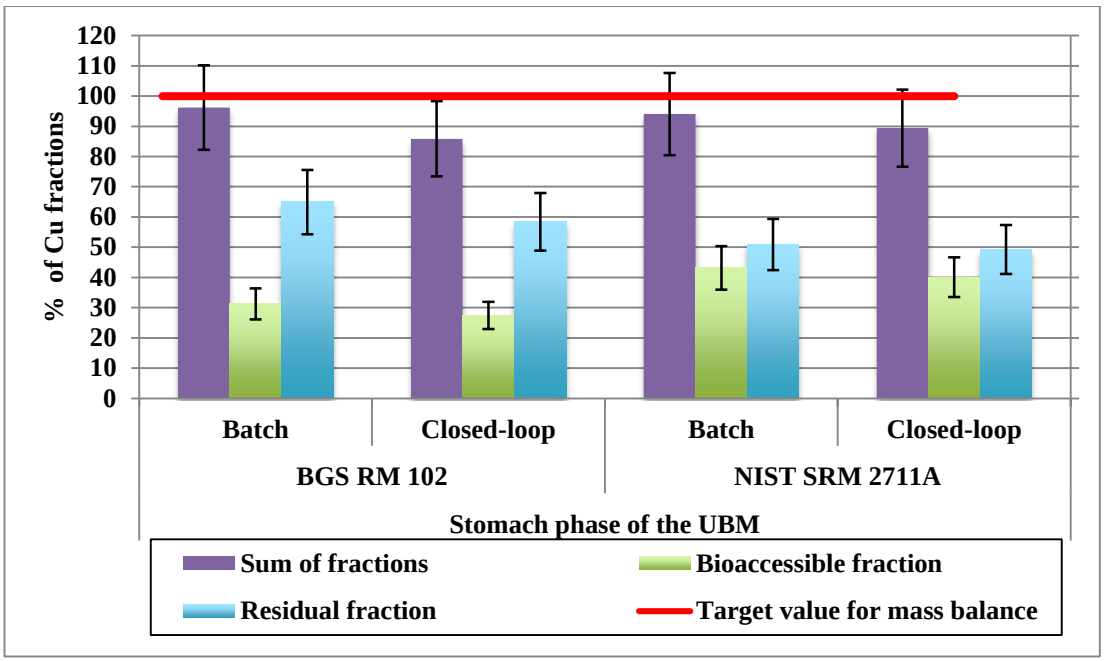


**Figure 5.14. Copper fractions and their sum (mass balance) as a percentage of pseudototal content, released from simulated $PM_{10}$ samples using BGS RM 102 Ironstone Soil and NIST SRM 2711A Montana II Soil by applying the batch and closed-loop dynamic (CL) models of the stomach phase of the unified bioaccessibility method (UBM) (CL-UBM)**

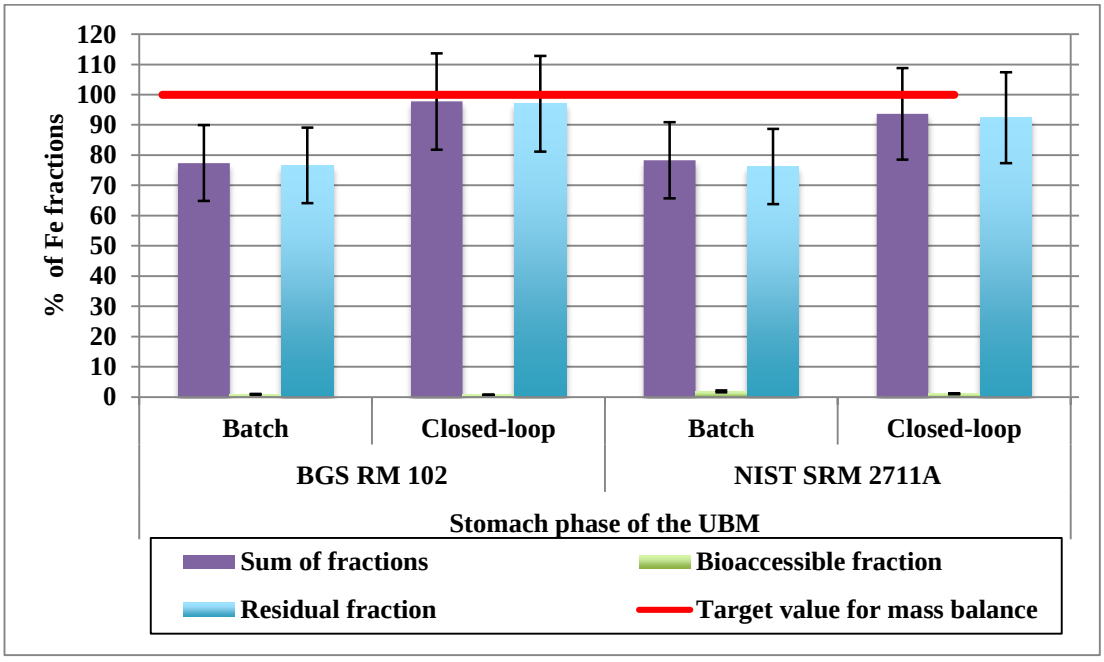


**Figure 5.15. Iron fractions and their sum (mass balance) as a percentage of pseudototal content, released from simulated $PM_{10}$ samples using BGS RM 102 Ironstone Soil and NIST SRM 2711A Montana II Soil by applying the batch and closed-loop dynamic (CL) models of the stomach phase of the unified bioaccessibility method (UBM) (CL-UBM)**

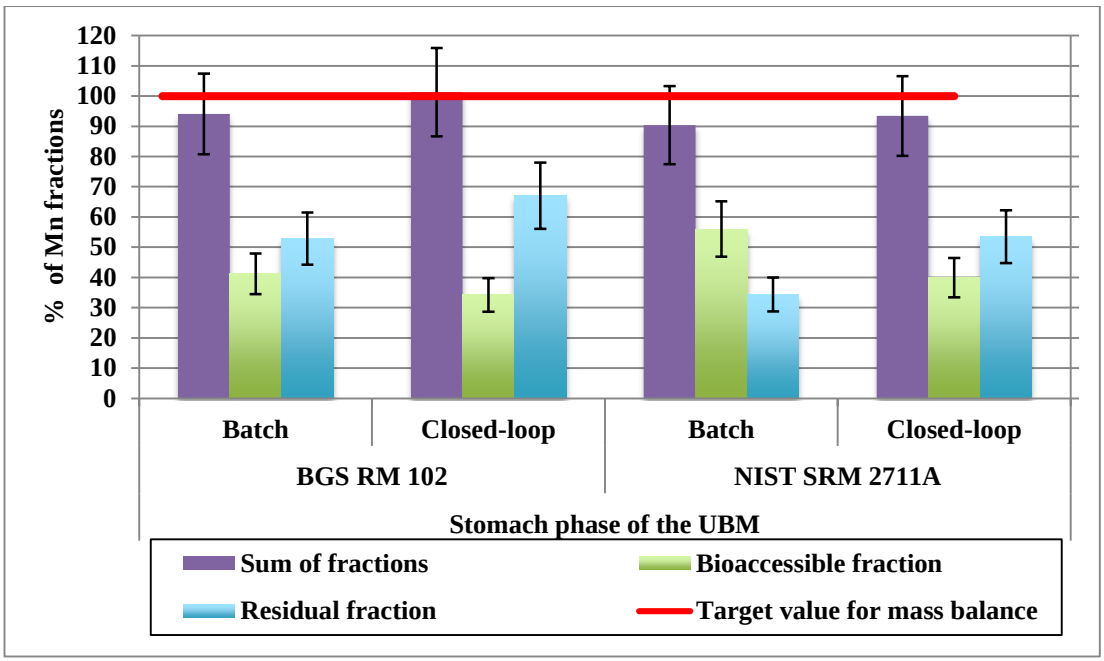


**Figure 5.16. Manganese fractions and their sum (mass balance) as a percentage of pseudototal content, released from simulated $PM_{10}$ samples using BGS RM 102 Ironstone Soil and NIST SRM 2711A Montana II Soil by applying the batch and closed-loop dynamic (CL) models of the stomach phase of the unified bioaccessibility method (UBM) (CL-UBM)**

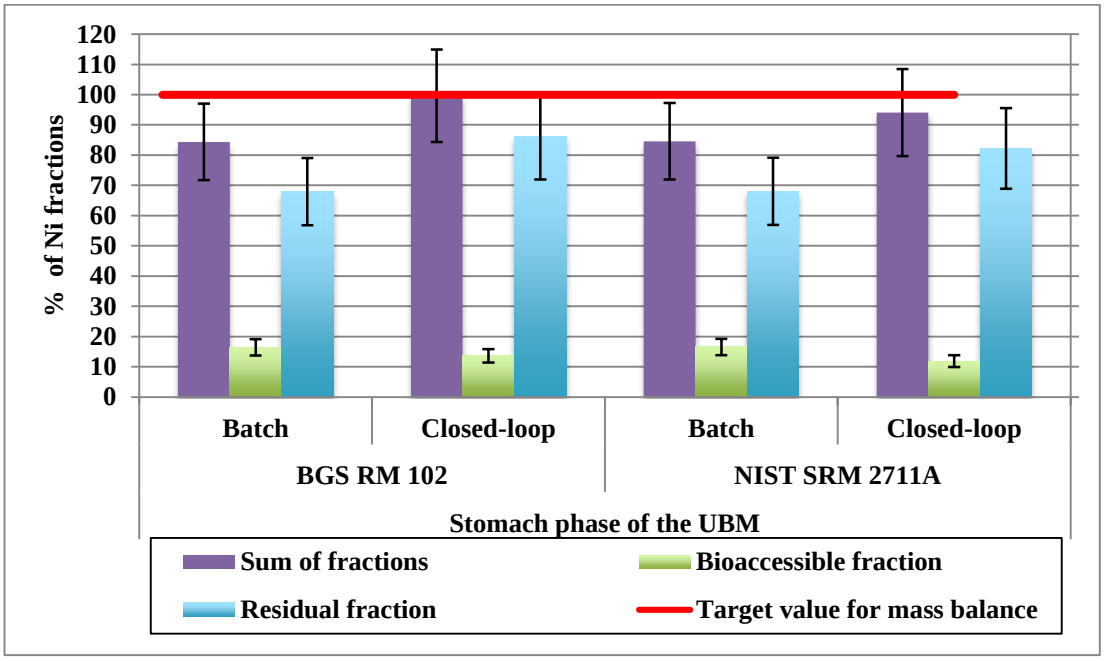


**Figure 5.17. Nickel fractions and their sum (mass balance) as a percentage of pseudototal content, released from simulated $PM_{10}$ samples using BGS RM 102 Ironstone Soil and NIST SRM 2711A Montana II Soil by applying the batch and closed-loop dynamic (CL) models of the stomach phase of the unified bioaccessibility method (UBM) (CL-UBM)**

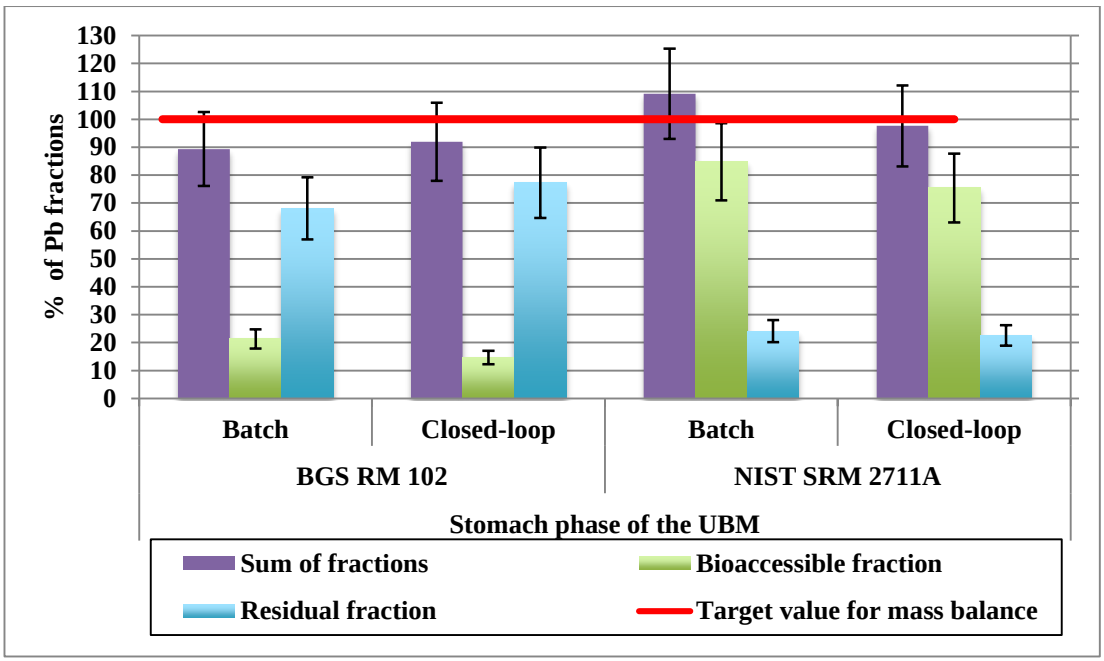


**Figure 5.18. Lead fractions and their sum (mass balance) as a percentage of pseudototal content, released from simulated $PM_{10}$ samples using BGS RM 102 Ironstone Soil and NIST SRM 2711A Montana II Soil by applying the batch and closed-loop dynamic (CL) models of the stomach phase of the unified bioaccessibility method (UBM) (CL-UBM)**

### 5.2.2.5. Mass balance

The bioaccessible and residual fraction as well as the pseudototal content of PTE in simulated $PM_{10}$ samples, prepared using BGS RM 102 Ironstone Soil and NIST SRM 2711A Montana II Soil, extracted by applying the batch models, the CL-SBET and the CL- UBM and also mass balance are illustrated in Tables 5.9-5.12. Validation of mass balance was verified by Z-scores calculated using Equations 2.28 and 2.30. For the batch model of the SBET, 73% of Z-scores were acceptable, while 20%, and 7% were satisfactory and not satisfactory, respectively. However, for the CL-SBET, 93% of Z-scores were acceptable and 7% were satisfactory. For the batch model of the stomach phase of the UBM, 53%, 27%, and 20% of Z-scores were acceptable, satisfactory, and not satisfactory, respectively. However, Z-scores for the CL-UBM were all acceptable. Nonetheless, recoveries of mass balance with respect to pseudototal PTE content, either for the models of the SBET or the stomach phase of the UBM, were in most cases within 100 ± 10%.

**Table 5.8. Recoveries of bioaccessible fraction of potentially toxic elements (PTE) in simulated $PM_{10}$ samples, prepared using BGS RM 102 Ironstone Soil and NIST SRM 2711A Montana II Soil, obtained by applying the closed-loop dynamic (CL) model of the stomach phase of the unified bioaccessibility method (UBM) (CL-UBM) with respect to those obtained using its batch model or to available recommended bioaccessible values**

| PTE | Sample | Bioaccessible fraction (mg $kg^{-1}$) (n=3) | | %Recovery[a] | Recommended value Mean ± SD (n=7 for x, 6 for y) | %Recovery[b] | Student's t-test[c] at 95% confidence level | | Student's t-test[d] at 95% confidence level | |
|---|---|---|---|---|---|---|---|---|---|---|
| | | Batch Mean ± SD | CL Mean ± SD | | | | $t_{calculated}$ | $t_{critical}$ | $t_{calculated}$ | $t_{critical}$ |
| **As** | **BGS102** | 4.97 ± 0.05 | 4.25 ± 0.29 | 85.6 ± 5.9 | 4.52 ± 1.28[x] | 94.0 ± 27.4 | 0.35 | 2.31 | **4.21** | 2.78 |
| | **NIST2711A** | 57.5 ± 0.8 | 47.2 ± 2.3 | 82.0 ± 4.1 | NA | - | - | - | **7.38** | 2.78 |
| **Cd** | **BGS102** | 0.221 ± 0.003 | 0.212 ± 0.008 | 96.1 ± 4.0 | 0.281 ± 0.170[x] | 75.4 ± 45.7 | 1.07 | 2.45 | 1.69 | 2.78 |
| | **NIST2711A** | 45.0 ± 0.1 | 41.3 ± 1.8 | 91.7 ± 4.1 | NA | - | - | - | 3.57 | 4.30 |
| **Cr** | **BGS102** | 36.5 ± 0.1 | 32.4 ± 3.2 | 88.7 ± 8.8 | NA | - | - | - | 2.22 | 4.30 |
| | **NIST2711A** | 0.876 ± 0.003 | 0.551 ± 0.042 | 62.9 ± 4.8 | NA | - | - | - | **13.3** | 4.30 |
| **Cu** | **BGS102** | 7.76 ± 0.50 | 6.86 ± 0.49 | 88.4 ± 8.5 | NA | - | - | - | 2.21 | 2.78 |
| | **NIST2711A** | 57.8 ± 0.5 | 51.7 ± 2.8 | 89.5 ± 4.9 | NA | - | - | - | **3.70** | 2.78 |
| **Fe** | **BGS102** | 1170 ± 23 | 866 ±151 | 74.4 ± 13.0 | NA | - | - | - | 3.39 | 4.30 |
| | **NIST2711A** | 449 ± 8 | 257 ± 15 | 57.3 ± 3.5 | NA | - | - | - | **19.3** | 2.78 |
| **Mn** | **BGS102** | 2720 ± 16 | 2160 ± 121 | 79.4 ± 4.7 | NA | - | - | - | **7.95** | 4.30 |
| | **NIST2711A** | 324 ± 1 | 223 ± 13 | 68.6 ± 4.9 | NA | - | - | - | **14.0** | 4.3 |
| **Ni** | **BGS102** | 12.4 ± 0.1 | 9.85 ± 0.58 | 79.6 ± 4.7 | NA | - | - | - | **7.48** | 4.30 |
| | **NIST2711A** | 3.16 ± 0.04 | 2.17 ± 0.15 | 68.6 ± 4.9 | NA | - | - | - | **10.8** | 2.78 |
| **Pb** | **BGS102** | 16.6 ± 0.2 | 11.8 ± 0.4 | 71.1 ± 2.5 | 13.0 ± 6.0[y] | 90.8 ± 42.0 | 0.49 | 2.57 | **18.4** | 2.78 |
| | **NIST2711A** | 1110 ± 12 | 957 ± 51 | 86.7 ± 4.7 | NA | - | - | - | **4.91** | 2.78 |
| **Zn** | **BGS102** | 36.0 ± 9.2 | 37.6 ± 3.6 | 104 ± 28 | NA | - | - | - | 0.27 | 2.78 |
| | **NIST2711A** | 120 ± 6 | 105 ± 8 | 87.4 ± 8.3 | NA | - | - | - | 2.52 | 2.78 |

SD: standard deviation; n= number of replicates; [c]: t-test for difference between the bioaccessible fraction by closed-loop (CL) model and recommended values; [d]: t-test for difference between the bioaccessible fraction by CL and batch models; $\%\,Recovery^{\,a} = \left(\frac{Bioaccessible\ fraction\ for\ CL\ model}{Bioaccessible\ fraction\ for\ batch\ model}\right) \times 100$ ; $\%\,Recovery^{\,b} = \left(\frac{Bioaccessible\ fraction\ for\ CL\ model}{Certified\ value}\right) \times 100$

**Table 5.9. Concentrations of potentially toxic elements (PTE) in the bioaccessible and residual fractions, together with pseudototal content and mass balance in simulated $PM_{10}$ samples (BGS RM 102 Ironstone Soil on FDMS filters) using the closed-loop (CL) dynamic model of the simplified bioaccessibility extraction test (SBET) (CL-SBET) with off-line analysis**

| PTE | Models | Bioaccessible fraction (mg $kg^{-1}$) Mean (n=3) ± U (% RSD) | Residual fraction (mg $kg^{-1}$) Mean (n=3) ± U | Sum ± $U_C$ (mg $kg^{-1}$) | Pseudototal (mg $kg^{-1}$) Mean (n=3) ± U | % Mass balance ± $U_C$ | %Spike recovery | Z-Score |
|---|---|---|---|---|---|---|---|---|
| **As** | **Batch** | 2.36 ± 0.27 **(0.314)** | 82.9 ± 9.6 | 85.3 ± 9.6 | 98.1 ± 11.3 | 86.9 ± 14.0 | 100 | -1.8 |
| | **CL** | 2.25 ± 0.26 **(6.31)** | 89.1 ± 10.3 | 91.4 ± 10.3 | 99.2 ± 11.5 | 92.1 ± 14.9 | 86 | -1.1 |
| **Cd** | **Batch** | 0.208 ± 0.024 **(1.27)** | < RB | NC | < RB | NC | 100 | NC |
| | **CL** | 0.208 ± 0.024 **(4.56)** | < RB | NC | 0.340 ± 0.039 | NC | 90 | NC |
| **Cr** | **Batch** | 35.4 ± 4.1 **(2.74)** | 140 ± 16 | 176 ± 17 | 188 ± 22 | 93.6 ± 14.0 | 101 | -0.9 |
| | **CL** | 28.5 ± 3.3 **(9.92)** | 145 ± 17 | 174 ± 17 | 187 ± 22 | 93.0 ± 14.1 | 89 | -1.0 |
| **Cu** | **Batch** | 7.84 ± 0.91 **(0.514)** | 12.8 ± 1.5 | 20.6 ± 1.7 | 27.5 ± 3.2 | 75.0 ± 10.7 | 104 | -3.5 |
| | **CL** | 8.36 ± 0.97 **(6.50)** | 11.1 ± 1.3 | 19.5 ± 1.6 | 18.6 ± 2.2 | 104 ± 15 | 89 | 0.6 |
| **Fe** | **Batch** | 2100 ± 242 **(0.073)** | 115000 ± 13300 | 117000 ± 13300 | 135000 ± 15600 | 86.4 ± 14.0 | 103 | -1.9 |
| | **CL** | 1470 ± 170 **(12.8)** | 120000 ± 13900 | 122000 ± 13900 | 135000 ± 15600 | 90.2 ± 14.6 | 88 | -1.4 |
| **Mn** | **Batch** | 2200 ± 254 **(1.45)** | 3950 ± 456 | 6150 ± 522 | 6410 ± 740 | 96.0 ± 13.8 | 104 | -0.6 |
| | **CL** | 1910 ± 221 **(4.29)** | 4190 ± 484 | 6100 ± 532 | 6420 ± 741 | 95.1 ± 13.8 | 90 | -0.7 |
| **Ni** | **Batch** | 10.6 ± 1.2 **(2.77)** | 58.4 ± 6.7 | 69.0 ± 6.9 | 72.7 ± 8.4 | 95.0 ± 14.5 | 103 | -0.7 |
| | **CL** | 8.47 ± 0.98 **(5.53)** | 61.3 ± 7.1 | 69.8 ± 7.1 | 72.7 ± 8.4 | 96.0 ± 14.8 | 87 | -0.6 |
| **Pb** | **Batch** | 22.6 ± 2.6 **(3.42)** | 47.9 ± 5.5 | 70.5 ± 6.1 | 74.9 ± 8.6 | 94.2 ± 13.6 | 101 | -0.8 |
| | **CL** | 17.8 ± 2.1 **(11.1)** | 51.2 ± 5.9 | 69.0 ± 6.3 | 76.6 ± 8.8 | 90.1 ± 13.2 | 89 | -1.4 |
| **Zn** | **Batch** | 39.7 ± 4.6 **(8.17)** | < FB | NC | < FB | NC | 87 | NC |
| | **CL** | 28.4 ± 3.3 **(12.4)** | 2330 ± 269 | 2360 ± 269 | < FB | NC | 80 | NC |

$U = \frac{(K \times Mean \times \%RSD)}{100 \times \sqrt{n}}$ , K = 2, % RSD = 10, n= number of replicates; $Z - Score = \frac{(Sum - Pseudototal)}{SD_R/\sqrt{n}}$, $SD_R = \frac{Mean\ of\ pseudototal \times 10}{100}$, n= number of independent replicates; $U_C$: combined uncertainty; $Sum = (Bioaccessible\ fraction + Residual\ fraction)$; $\%\ Mass\ balance = \frac{Sum}{pseudototal} \times 100$

**Table 5.10. Concentrations of potentially toxic elements (PTE) in the bioaccessible and residual fractions, together with pseudototal content and mass balance in simulated $PM_{10}$ samples (NIST SRM 2711A Montana II Soil on FDMS filters) using the closed-loop (CL) dynamic model of the simplified bioaccessibility extraction test (SBET) (CL-SBET) with off-line analysis**

| PTE | Models | Bioaccessible fraction (mg $kg^{-1}$) Mean (n=3) ± U (% RSD) | Residual fraction (mg $kg^{-1}$) Mean (n=3) ± U | Sum ± $U_C$ (mg $kg^{-1}$) | Pseudototal (mg $kg^{-1}$) Mean (n=3) ± U | % Mass balance ± $U_C$ | Z-Score |
|---|---|---|---|---|---|---|---|
| **As** | **Batch** | 57.8 ± 6.7 **(1.26)** | 37.7 ± 4.4 | 95.4 ± 8.0 | 94.7 ± 10.9 | 101 ± 14 | 0.1 |
| | **CL** | 55.4 ± 6.4 **(2.52)** | 44.3 ± 5.1 | 99.7 ± 8.2 | 95.4 ± 11.0 | 104 ± 15 | 0.6 |
| **Cd** | **Batch** | 47.1 ± 5.4 **(2.32)** | 5.18 ± 0.60 | 52.2 ± 5.5 | 49.3 ± 5.7 | 106 ± 17 | 0.8 |
| | **CL** | 44.3 ± 5.1 **(3.93)** | 7.10 ± 0.82 | 51.4 ± 5.2 | 49.3 ± 5.7 | 104 ± 16 | 0.6 |
| **Cr** | **Batch** | 0.899 ± 0.104 **(2.57)** | 24.9 ± 2.9 | 25.8 ± 2.9 | 32.1 ± 3.7 | 80.3 ± 12.9 | -2.8 |
| | **CL** | 0.822 ± 0.095 **(6.63)** | 21.2 ± 2.4 | 22.0 ± 2.4 | 28.0 ± 3.2 | 78.5 ± 12.6 | -3.0 |
| **Cu** | **Batch** | 59.9 ± 6.9 **(2.69)** | 59.4 ± 6.9 | 119 ± 10 | 130 ± 15 | 91.7 ± 13.0 | -1.2 |
| | **CL** | 64.0 ± 7.4 **(9.45)** | 58.5 ± 6.8 | 123 ± 10 | 125 ± 14 | 97.8 ± 13.8 | -0.3 |
| **Fe** | **Batch** | 544 ± 63 **(2.67)** | 19400 ± 2240 | 19900 ± 2240 | 24500 ± 2830 | 81.3 ± 13.1 | -2.6 |
| | **CL** | 492 ± 57 **(4.77)** | 21000 ± 2430 | 21500 ± 2430 | 23900 ± 2750 | 90.1 ± 14.6 | -1.4 |
| **Mn** | **Batch** | 215 ± 25 **(1.97)** | 281 ± 32 | 496 ± 41 | 573 ± 66 | 86.7 ± 12.3 | -1.9 |
| | **CL** | 197 ± 23 **(4.47)** | 343 ± 40 | 540 ± 46 | 562 ± 65 | 96.1 ± 13.8 | -0.5 |
| **Ni** | **Batch** | 2.92 ± 0.34 **(2.34)** | 12.5 ± 1.4 | 15.4 ± 1.5 | 18.4 ± 2.1 | 83.9 ± 12.6 | -2.3 |
| | **CL** | 2.79 ± 0.32 **(5.13)** | 16.8 ± 1.9 | 19.6 ± 2.0 | 17.9 ± 2.1 | 109 ± 17 | 1.3 |
| **Pb** | **Batch** | 1100 ± 127 **(2.75)** | 265 ± 31 | 1360 ± 131 | 1310 ± 151 | 104 ± 16 | 0.5 |
| | **CL** | 1080 ± 125 **(3.11)** | 235 ± 27 | 1320 ± 128 | 1300 ± 150 | 102 ± 15 | 0.2 |
| **Zn** | **Batch** | 130 ± 15 **(3.53)** | < FB | NC | < FB | NC | NC |
| | **CL** | 124 ± 14 **(3.72)** | 1088 ± 666 | 1212 ± 666 | < FB | NC | NC |

$U = \frac{(K \times Mean \times \%RSD)}{100 \times \sqrt{n}}$ , K = 2, % RSD = 10, n= number of replicates; $Z - Score = \frac{(Sum - Pseudototal)}{SD_R/\sqrt{n}}$, $SD_R = \frac{Mean\ of\ pseudototal \times 10}{100}$, n= number of independent replicates; $U_C$: combined uncertainty; $Sum = (Bioaccessible\ fraction + Residual\ fraction)$; $\%\ Mass\ balance = \frac{Sum}{pseudototal} \times 100$

**Table 5.11. Concentrations of potentially toxic elements (PTE) in the bioaccessible and residual fractions, together with pseudototal content and mass balance in simulated $PM_{10}$ samples (BGS RM 102 Ironstone Soil on FDMS filters) using the closed-loop (CL) dynamic model of the stomach phase of the unified bioaccessibility method (UBM) (CL-UBM) with off-line analysis**

| PTE | Models | Bioaccessible fraction (mg kg$^{-1}$) Mean (n=3) ± U (% RSD) | Residual fraction (mg kg$^{-1}$) Mean (n=3) ± U | Sum ± $U_C$ (mg kg$^{-1}$) | Pseudototal (mg kg$^{-1}$) Mean (n=3) ± U | % Mass balance ± $U_C$ | %Spike recovery | Z-Score |
|---|---|---|---|---|---|---|---|---|
| **As** | **Batch** | 4.97 ± 0.57 **(0.945)** | 76.0 ± 8.8 | 81.0 ± 8.8 | 104 ± 12 | 77.6 ± 12.3 | 98 | -3.2 |
| | **CL** | 4.25 ± 0.49 **(6.85)** | 92.3 ± 10.7 | 96.6 ± 10.7 | 99.4 ± 11.5 | 97.1 ± 15.5 | 90 | -0.4 |
| **Cd** | **Batch** | 0.221 ± 0.026 **(1.28)** | < RB | NC | < RB | NC | 99 | NC |
| | **CL** | 0.212 ± 0.024 **(3.97)** | 0.112 ± 0.013 | 0.324 ± 0.028 | 0.284 ± 0.033 | 114 ± 16 | 91 | 2.0 |
| **Cr** | **Batch** | 36.5 ± 4.2 **(0.383)** | 118 ± 14 | 155 ± 14 | 187 ± 22 | 82.8 ± 12.2 | 97 | -2.4 |
| | **CL** | 32.4 ± 3.7 **(9.86)** | 155 ± 18 | 187 ± 18 | 182 ± 21 | 103 ± 16 | 90 | 0.4 |
| **Cu** | **Batch** | 7.76 ± 0.90 **(6.48)** | 16.1 ± 1.9 | 23.9 ± 2.1 | 24.8 ± 2.9 | 96.1 ± 13.9 | 94 | -0.5 |
| | **CL** | 6.86 ± 0.79 **(7.16)** | 14.6 ± 1.7 | 21.5 ± 1.9 | 25.0 ± 2.9 | 86.0 ± 12.4 | 86 | -2.0 |
| **Fe** | **Batch** | 1170 ± 135 **(2.00)** | 105000 ± 12100 | 106000 ± 12100 | 137000 ± 15800 | 77.4 ± 12.6 | 87 | -3.2 |
| | **CL** | 866 ±100 **(17.4)** | 128000 ± 14800 | 129000 ± 14800 | 132000 ± 15200 | 97.9 ± 15.9 | 83 | -0.3 |
| **Mn** | **Batch** | 2720 ± 314 **(0.571)** | 3490 ± 403 | 6210 ± 511 | 6600 ± 762 | 94.2 ± 13.4 | 101 | -0.8 |
| | **CL** | 2160 ± 249 **(5.60)** | 4230 ± 488 | 6390 ± 548 | 6310 ± 729 | 101 ± 15 | 90 | 0.2 |
| **Ni** | **Batch** | 12.4 ± 1.4 **(0.378)** | 51.3 ± 5.9 | 63.7 ± 6.1 | 75.5 ± 8.7 | 84.4 ± 12.7 | 98 | -2.2 |
| | **CL** | 9.85 ± 1.14 **(5.90)** | 62.4 ± 7.2 | 72.3 ± 7.3 | 72.5 ± 8.4 | 99.7 ± 15.3 | 91 | 0.0 |
| **Pb** | **Batch** | 16.6 ± 1.9 **(1.44)** | 53.1 ± 6.1 | 69.7 ± 6.4 | 78.0 ± 9.0 | 89.3 ± 13.2 | 100 | -1.5 |
| | **CL** | 11.8 ± 1.4 **(3.25)** | 62.3 ± 7.2 | 74.1 ± 7.3 | 80.6 ± 9.3 | 91.9 ± 14.0 | 91 | -1.1 |
| **Zn** | **Batch** | 36.0 ± 4.2 **(1.44)** | < FB | NC | < FB | NC | 112 | NC |
| | **CL** | 37.6 ± 4.3 **(3.25)** | < FB | NC | < FB | NC | 82 | NC |

$U = \frac{(K \times Mean \times \%RSD)}{100 \times \sqrt{n}}$ , K = 2, % RSD = 10, n= number of replicates; $Z - Score = \frac{(Sum - Pseudototal)}{SD_R/\sqrt{n}}$, $SD_R = \frac{Mean\ of\ pseudototal \times 10}{100}$, n= number of independent replicates; $U_C$: combined uncertainty; $Sum = (Bioaccessible\ fraction + Residual\ fraction)$; $\%\ Mass\ balance = \frac{Sum}{pseudototal} \times 100$

**Table 5.12. Concentrations of potentially toxic elements (PTE) in the bioaccessible and residual fractions, together with pseudototal content and mass balance in simulated $PM_{10}$ samples (NIST SRM 2711A Montana II Soil on FDMS filters) using the closed-loop (CL) dynamic model of the stomach phase of the unified bioaccessibility method (UBM) (CL-UBM) with off-line analysis**

| PTE | Models | Bioaccessible fraction (mg $kg^{-1}$) Mean (n=3) ± U (% RSD) | Residual fraction (mg $kg^{-1}$) Mean (n=3) ± U | Sum ± $U_C$ (mg $kg^{-1}$) | Pseudototal (mg $kg^{-1}$) Mean (n=3) ± U | % Mass balance ± $U_C$ | Z-Score |
|---|---|---|---|---|---|---|---|
| **As** | **Batch** | 57.5 ± 6.6 **(1.40)** | 37.0 ± 4.3 | 94.6 ± 7.9 | 96.8 ± 11.2 | 97.7 ± 13.9 | -0.3 |
| | **CL** | 47.2 ± 5.4 **(4.86)** | 43.7 ± 5.0 | 90.9 ± 7.4 | 93.1 ± 10.8 | 97.6 ± 13.8 | -0.3 |
| **Cd** | **Batch** | 45.0 ± 5.2 **(0.284)** | 6.84 ± 0.79 | 51.9 ± 5.3 | 49.1 ± 5.7 | 106 ± 16 | 0.8 |
| | **CL** | 41.3 ± 4.8 **(4.41)** | 7.65 ± 0.88 | 48.9 ± 4.8 | 48.4 ± 5.6 | 101 ± 15 | 0.1 |
| **Cr** | **Batch** | 0.876 ± 0.101 **(0.393)** | 21.9 ± 2.5 | 22.7 ± 2.5 | 31.5 ± 3.6 | 72.1 ± 11.6 | -3.9 |
| | **CL** | 0.551 ± 0.064 **(7.65)** | 26.5 ± 3.1 | 27.1 ± 3.1 | 31.6 ± 3.6 | 85.6 ± 13.8 | -2.0 |
| **Cu** | **Batch** | 57.8 ± 6.7 **(0.946)** | 68.2 ± 7.9 | 126 ± 10 | 134 ± 16 | 93.7 ± 13.3 | -0.9 |
| | **CL** | 51.7 ± 6.0 **(5.42)** | 63.6 ± 7.3 | 115 ± 9 | 129 ± 15 | 89.4 ± 12.7 | -1.5 |
| **Fe** | **Batch** | 449 ± 52 **(1.84)** | 18600 ± 2150 | 19100 ± 2150 | 24400 ± 2810 | 78.4 ± 12.6 | -3.0 |
| | **CL** | 257 ± 30 **(5.88)** | 21800 ± 2520 | 22100 ± 2520 | 23600 ± 2720 | 93.8 ± 15.2 | -0.9 |
| **Mn** | **Batch** | 324 ± 37 **(0.263)** | 199 ± 23 | 523 ± 44 | 579 ± 67 | 90.4 ± 12.9 | -1.4 |
| | **CL** | 223 ± 26 **(5.64)** | 298 ± 34 | 521 ± 43 | 558 ± 64 | 93.4 ± 13.3 | -0.9 |
| **Ni** | **Batch** | 3.16 ± 0.37 **(1.30)** | 13.0 ± 1.5 | 16.1 ± 1.5 | 19.1 ± 2.2 | 84.6 ± 12.7 | -2.2 |
| | **CL** | 2.17 ± 0.25 **(7.08)** | 15.0 ± 1.7 | 17.2 ± 1.8 | 18.3 ± 2.1 | 94.1 ± 14.5 | -0.8 |
| **Pb** | **Batch** | 1110 ± 128 **(1.05)** | 316 ± 36 | 1430 ± 133 | 1310 ± 151 | 109 ± 16 | 1.3 |
| | **CL** | 957 ± 111 **(5.28)** | 286 ± 33 | 1240 ± 115 | 1270 ± 147 | 97.4 ± 14.5 | -0.4 |
| **Zn** | **Batch** | 120 ± 14 **(5.26)** | < FB | NC | < FB | NC | NC |
| | **CL** | 105 ± 12 **(7.88)** | < FB | NC | < FB | NC | NC |

$U = \frac{(K \times Mean \times \%RSD)}{100 \times \sqrt{n}}$ , K = 2, % RSD = 10, n= number of replicates; $Z - Score = \frac{(Sum - Pseudototal)}{SD_R/\sqrt{n}}$, $SD_R = \frac{Mean\ of\ pseudototal \times 10}{100}$, n= number of independent replicates; $U_C$: combined uncertainty; $Sum = (Bioaccessible\ fraction + Residual\ fraction)$; $\%\ Mass\ balance = \frac{Sum}{pseudototal} \times 100$

#### 5.2.2.6. Quality control

Precision of the extraction models was ascertained by calculating the RSDs for three replicates (see Tables 5.9-5.12). All RSDs for the batch model of the SBET and the stomach phase of the UBM were less than 10%. Some 84% of RSDs for the CL-SBET were below 10%, and the remaining 16% were less than 13%. For the CL-UBM, all RSD values were less than 10%, except for Fe in BGS RM 102 Ironstone Soil, where it was 17.4%.

Recoveries of known additions of PTE to the reagents of the methods were 87-104% and 80-90% for the batch model and the CL-SBET, respectively, whereas for the batch model and the CL-UBM, they were 87-112% and 82-91, respectively (see Tables 5.9 and 5.11).

In addition to the spike recovery test, accuracy of the extraction models was assessed using the guidance values of As, Cd, and Pb in BGS RM 102 Ironstone Soil for the the stomach phase of the UBM, and a recommended value of Pb in NIST SRM 2711A for the SBET. The bioaccessible PTE concentration obtained by applying the CL-SBET and the CL-UBM were in agreement with the recommended Pb value and guidance values of As, Cd, and Pb, respectively (see Tables 5.7 and 5.8). For the bioaccessible Pb concentration in NIST SRM 2711A achieved using the batch model of the SBET, the recovery with respect to the recommended value was 99.1 ± 5.1%. Recoveries with respect to guidance values for bioaccessible concentration of As, Cd, and Pb obtained using the batch model of the stomach phase of the UBM were 110 ± 31, 78.6 ± 47.6, and 128 ± 59%, respectively. The efficiency of microwave digestion was assessed using BCR CRM 143R Sewage Sludge Amended Soil and results obtained agreed with available certified values as shown in Table 5.13.

**Table 5.13. Comparison between determined and certified values for BCR CRM 143R Sewage Sludge Amended Soil subjected to microwave assisted *aqua regia* digestion in parallel to residual material from the batch and closed-loop (CL) models of the simplified bioaccessibility extraction test (SBET) and the stomach phase of the unified bioaccessibility method (UBM)**

| PTE | Cd | Cr | Mn | Ni | Pb | Zn |
|---|---|---|---|---|---|---|
| **Certified pseudototal values (Mean ± SD)** | 72.0 ± 1.8 | 426 ± 12 | 858 ± 11 | 296 ± 4 | 174 ± 5 | 1063 ± 16 |
| **Measured pseudototal PTE content for the SBET models** | | | | | | |
| **Batch model (Mean ± SD)** | 69.6 ± 0.6 | 449 ± 11 | 884 ± 18 | 294 ± 5 | 170 ± 3 | 1020 ± 9 |
| **% Recovery** | 96.7 ± 2.5 | 105 ± 4 | 103 ± 2 | 99.4 ± 2.1 | 97.8 ± 3.4 | 96.2 ± 1.7 |
| **CL model (Mean ± SD)** | 70.0 ± 1.2 | 450 ± 10 | 872 ± 10 | 292 ± 0.4 | 170 ± 1 | 1020 ± 6 |
| **% Recovery** | 97.2 ± 2.9 | 106 ± 4 | 102 ± 2 | 98.7 ± 1.3 | 97.8 ± 2.9 | 95.6 ± 1.6 |
| **Measured pseudototal PTE content for the stomach phase of the UBM models** | | | | | | |
| **Batch model (Mean ± SD)** | 67.3 ± 0.5 | 437 ± 5 | 864 ± 9 | 288 ± 2 | 166 ± 3 | 996 ± 4 |
| **% Recovery** | 93.4 ± 2.4 | 103 ± 3 | 101 ± 2 | 97.4 ± 1.5 | 95.2 ± 3.1 | 93.7 ± 1.4 |
| **CL model (Mean ± SD)** | 67.3 ± 0.4 | 437 ± 16 | 856 ± 17 | 289 ± 5 | 164 ± 1 | 991 ± 7 |
| **% Recovery** | 93.4 ± 2.4 | 103 ± 5 | 99.8 ± 2.3 | 97.7 ± 2.2 | 94.5 ± 2.8 | 93.2 ± 1.5 |

SD: standard deviation

## 5.3. Experiment 2: Single-pass dynamic extraction model with fraction collection (SPFC)

This experiment was carried out to establish a new non-equilibrium-based continuous dynamic extraction model for the SBET and the stomach phase of the UBM for determining the bioaccessible concentration of PTE in inhaled and subsequently ingested $PM_{10}$ under biological condition using off-line analysis by ICP-MS.

### 5.3.1. Experimental

#### 5.3.1.1. Apparatus and reagents

As was described in Section 5.2.1.1.

#### 5.3.1.2 Simulation of $PM_{10}$ samples

As was described in Section 5.2.1.2.

#### 5.3.1.3. Analytical procedure

A single-pass flow-through system is schematically illustrated in Fig 5.19. This system was similar to the system described in Section 5.2.1.3، except that the outlet of the filter holder was connected to the leachate tube instead of the extractant tube using the 0.51 mm extension tubing (75 cm long). The preparation of the filter holders containing simulated $PM_{10}$ samples was as described in Section 5.2.1.3.

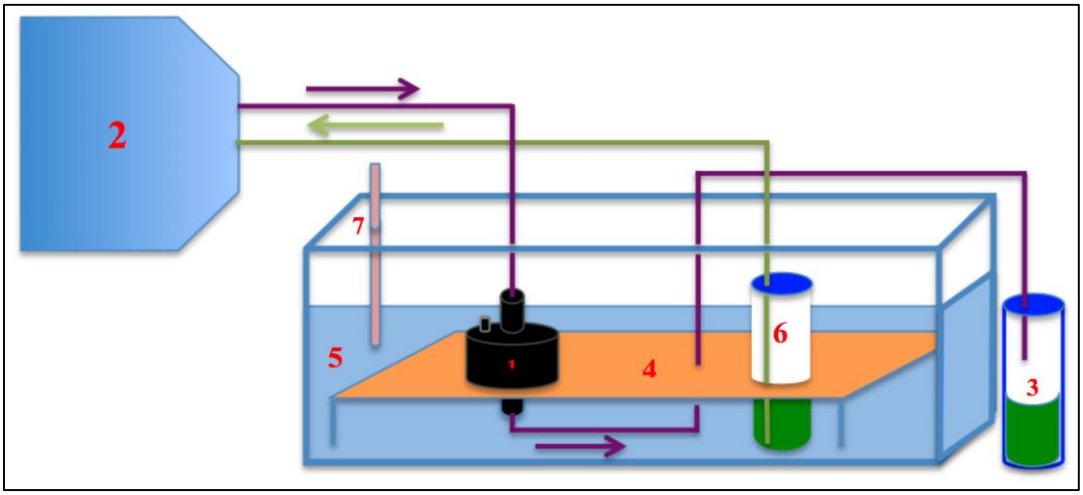


(1) Polycarbonate filter holder (2) Peristaltic pump (3) Leachate tube (4) Plastic rack (5) Water bath (6) Extractant tube (7) Thermometer

**Figure 5.19. Schematic diagram of the single-pass dynamic extraction model with fraction collection device**

The procedure for the SPFC-SBET was: 50 mL of the 0.4 M glycine (37 °C, pH 1.5 ± 0.05) was transferred to the extractant tube by means of a micropipette. The pump flow rate was set at 1.5 mL $min^{-1}$ for 5 min. The vent cap of the filter holder was then opened. To fill the filter holder, the pump was then run for 5 min, and the vent cap was then closed. The pump flow rate was then set at 1 mL $min^{-1}$ and run for 5 min to pass 5 mL of extractant through the loaded filter. This was repeated 12 times, with a 15-second pause between delivery of each extractant volume, allowing for subfraction collection tubes (extract tubes) to be changed after each cycle. The plastic rack containing the filter holder and the extractant tube was then placed into the pre-thermostated water bath at 37 °C. The pump was then run for 1 hour, and the last 10 mL of the 0.4 M glycine was added to the extractant tube during the extraction. The extracts were collected as subfractions every 5 min with a 5 mL volume. The pH of extracts obtained was checked to ensure that they were within 1.5 ± 0.5 (i.e. ≤ 2.0). The extracts were finally stored in polyethylene bottles at 4 °C prior to analysis by ICP-MS as described in Section 3.6.

For the SPFC-UBM, 1.5 mL of saliva fluid (37 °C, pH 6.5 ± 0.5), prepared as described in Section 3.5.3, was transferred to the extractant tube by means of a micropipette. The pump flow rate was set at 1 mL $min^{-1}$ for 1.5 min. The vent cap of the filter holder was then opened. To deliver the saliva fluid, the pump was then run for 1.5 min. A 48.5 mL aliquot of gastric fluid (37 °C, pH 1.1 ± 0.1), prepared as described in Section 3.5.3, was pipetted into the extractant tube. The pump was run for 2.25 min. The vent cap was then closed. The flow rate was then set at 1 mL $min^{-1}$ and the pump was run for 16 × 3.75 min periods with a 15-second pause time between for receiving tube changeover. The plastic rack containing the filter holder and extractant tube was then placed into the pre-thermostated water bath at 37 °C. The pump was then run for 1 hour, and during the extraction, the last 10 mL of gastric fluid was added to the extractant tube. The extracts were collected as subfractions every 3.75 min with a 3.75 mL volume. The pH of extracts obtained was checked to ensure that were < 1.5. The extracts were then diluted four-fold with 2 % $HNO_3$. Finally, the extracts were stored in polyethylene bottles at 4 °C prior to analysis by ICP-MS as described in Section 3.6.

Three simulated $PM_{10}$ samples prepared using BGS RM 102 Ironstone Soil, three simulated $PM_{10}$ samples prepared using NIST SRM 2711A Montana II Soil, and three blank FDMS filter, were used, when either the SPFC-SBET or the SPFC-UBM was applied. In addition, a method blank was performed by running the extractant only through the complete procedure. A spike recovery test was also performed by running the extractant spiked at 10020 μg $L^{-1}$ for Fe and 250 μg $L^{-1}$ for other PTE, through the complete procedure. The washing process for filter holders was performed as described in Section 5.2.1.3.

#### 5.3.1.4. Batch models

As was described in Section 5.2.1.4.

#### 5.3.1.5. Digestion of residues and mass balance

As was described in Section 5.2.1.5.

#### 5.3.1.6. Real $PM_{10}$ samples

In this study, five real $PM_{10}$ samples, collected on FDMS filters and sampled by TEOM FDMS instruments, were collected from five air quality monitoring stations by staff of Glasgow City Council, Scotland, UK. These stations are located in Glasgow at Byres Road, Broomhill Road, Nithsdale Road, High Street, and Burgher Street. The samples from Nithsdale Road (exposed from 23$^{rd}$ September 2015 to 7$^{th}$ October 2015) and High Street (no exposure dates available) were used for applying the SPFC-UBM. The samples from Byres Road (exposed from 1$^{st}$ October to 15$^{th}$ October 2015) and Broomhill Road (no exposure dates available) were used for applying the SPFC-SBET, while the sample from Burgher Street (no exposure dates available) was used for the SPDC-SBET.

#### 5.3.1.7. Analyte quantification

Extracts and digests obtained from the batch, the SPFC dynamic extraction models, and microwave digestion were analysed by ICP-MS as described in Section 3.6. The IDL and PDL, shown in Table 5.14, were calculated using Equations 2.16 and 2.17.

**Table 5.14. Instrumental (IDL) and procedural (PDL) detection limits for the single-pass dynamic model with fraction collection of the simplified bioaccessibility extraction test (SPFC-SBET) and the stomach phase of the unified bioaccessibility method (SPFC-UBM) by ICP-MS**

| Isotopes | SPFC-SBET | | SPFC-UBM | |
|---|---|---|---|---|
| | IDL ($\mu g\ L^{-1}$) | PDL ($mg\ kg^{-1}$) | IDL ($\mu g\ L^{-1}$) | PDL ($mg\ kg^{-1}$) |
| $^{75}As$ | 0.012 | 0.001 | 0.012 | 0.0005 |
| $^{111}Cd$ | 0.008 | 0.0004 | 0.011 | 0.0004 |
| $^{52}Cr$ | 0.022 | 0.001 | 0.010 | 0.0004 |
| $^{65}Cu$ | 0.337 | 0.017 | 0.293 | 0.011 |
| $^{56}Fe$ | 0.669 | 0.033 | 8.31 | 0.312 |
| $^{55}Mn$ | 0.037 | 0.002 | 0.037 | 0.001 |
| $^{60}Ni$ | 0.005 | 0.0003 | 0.107 | 0.004 |
| $^{208}Pb$ | 0.091 | 0.005 | 0.028 | 0.001 |
| $^{66}Zn$ | 0.094 | 0.005 | 0.507 | 0.019 |

#### 5.3.1.8. Quality control and reference material

As was described in Section 5.2.1.7.

### 5.3.2. Results and discussion

#### 5.3.2.1. Effect of loaded FDMS filters on the flow rate of extractant

As the porosity of filters could create back pressure and affect the flow rate of an extractant flowed continuously by a peristaltic pump,[152] and since the porosity of FDMS filters is not known,[111] the effect of loaded FDMS filters on the stability of the flow rate of an extractant was investigated. This was accomplished by testing three flow rates: 1.0, 1.5, and 2.0 mL $min^{-1}$. Three loaded FDMS filters prepared using BGS RM 102 Ironstone Soil were used for each flow rate. The analytical procedure for the SPFC-SBET as described in Section 5.3.1.3 was followed. The volume of subfractions was measured using a 10 mL measuring cylinder. The actual flow rate was calculated by dividing the volume of a subfraction by the time used to collect it (i.e. 5 min). Results obtained demonstrated that loaded FDMS filters did not affect the flow rate of the extractant (see Fig. 5.20). The values of the flow rates

obtained were 1.00 ± 0.02, 1.50 ± 0.01, and 2.00 ± 0.02 mL $min^{-1}$, corresponding well to the theoretical values set using the pump controls. To avoid leakage and reduce the flow resistance of the filter holder containing a loaded filter that could occur with high flow rates, 1.0 mL $min^{-1}$ was chosen for subsequent work. It also meant that results obtained by applying the SPFC-SBET could be meaningfully compared with those achieved by applying the SPDC-SBET, as 1.0 mL $min^{-1}$ is also a suitable flow rate for ICP-MS.

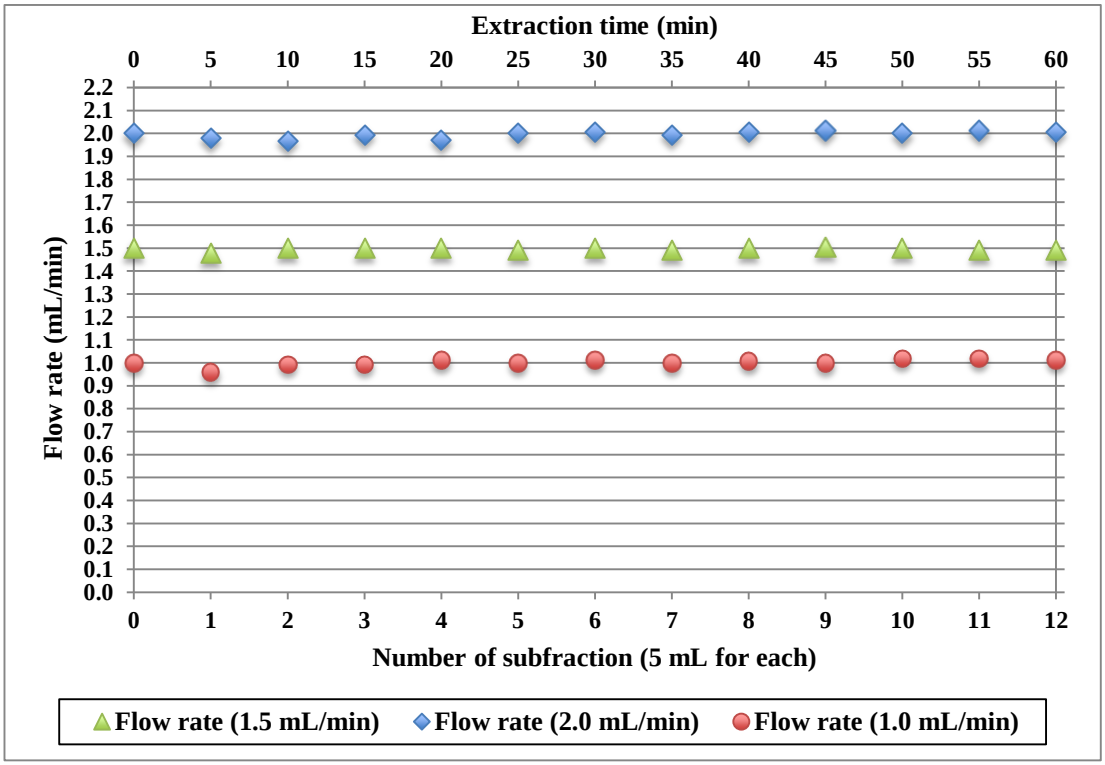


**Figure 5.20. Effect of loaded FDMS filters (mean, n=3) using BGS RM 102 Ironstone Soil on the flow rate of glycine (0.4 M, pH 1.5) delivered by a peristaltic pump**

### 5.3.2.2. Bioaccessible PTE concentration in blank FDMS filters

The SPFC-SBET and the SPFC-UBM were applied to blank FDMS filters. Three blank FDMS filters were used for each method, and results obtained are shown in Tables 5.15 and 5.16. As expected, the bioaccessible concentration was very low for all PTE tested, except for Zn, where it was relatively high. This is likely because the fact that Zn is used as a binder for FDMS filters. The mass balance was generally acceptable according to the Student's t-test (see Tables 5.15 and 5.16).

**Table 5.15. Concentrations of potentially toxic elements (PTE) in the bioaccessible and residual fractions, together with pseudototal content and mass balance in blank FDMS filters using the single-pass dynamic model of the simplified bioaccessibility extraction test (SBET) with fraction collection (SPFC-SBET)**

| PTE | Models | Bioaccessible fraction (µg filter$^{-1}$) Mean (n=3) ± SD | Residual fraction (µg filter$^{-1}$) Mean (n=3) ± SD | Sum ± $SD_C$ (µg filter$^{-1}$) | Pseudototal (µg filter$^{-1}$) Mean (n=3) ± SD | % Mass balance ± $SD_C$ | Student's t-test at 0.05 significance level | |
|---|---|---|---|---|---|---|---|---|
| | | | | | | | $t_{calculated}$ | $t_{critical}$ |
| **As** | **Batch** | < RB | 0.318 ± 0.039 | 0.318 ± 0.039 | 0.251 ± 0.027 | 127 ± 21 | 2.44 | 2.78 |
| | **SPFC** | < RB | 0.330 ± 0.030 | 0.330 ± 0.030 | 0.281 ± 0.047 | 118 ± 22 | 1.54 | 2.78 |
| **Cd** | **Batch** | < IDL | < RB | NC | < RB | NC | NC | NC |
| | **SPFC** | < IDL | < RB | NC | < RB | NC | NC | NC |
| **Cr** | **Batch** | 0.001 ± 0.0003 | 2.80 ± 0.03 | 2.81 ± 0.03 | 2.72 ± 0.11 | 103 ± 4 | 1.05 | 3.18 |
| | **SPFC** | 0.002 ± 0.001 | 2.77 ± 0.16 | 2.77 ± 0.16 | 2.88 ± 0.25 | 96.4 ± 10.0 | 0.59 | 2.78 |
| **Cu** | **Batch** | < IDL | < RB | NC | < RB | NC | NC | NC |
| | **SPFC** | 0.003 ± 0.002 | 0.256 ± 0.081 | 0.259 ± 0.081 | < RB | NC | NC | NC |
| **Fe** | **Batch** | 0.422 ± 0.148 | 83.0 ± 6.1 | 83.4 ± 6.1 | 60.5 ± 2.3 | 138 ± 11 | **6.31** | 3.18 |
| | **SPFC** | 0.026 ± 0.003 | 67.0 ± 4.8 | 67.0 ± 4.8 | 59.6 ± 3.7 | 112 ± 11 | 2.11 | 2.78 |
| **Mn** | **Batch** | 0.076 ± 0.039 | 1.42 ± 0.44 | 1.49 ± 0.45 | 0.932 ± 0.114 | 160 ± 52 | 2.24 | 3.18 |
| | **SPFC** | < RB | 1.26 ± 0.12 | 1.26 ± 0.12 | 0.869 ± 0.139 | 145 ± 27 | **3.73** | 2.78 |
| **Ni** | **Batch** | 0.002 ± 0.0005 | 0.053 ± 0.018 | 0.054 ± 0.018 | 0.084 ± 0.007 | 64.5 ± 22.3 | 2.76 | 3.18 |
| | **SPFC** | < RB | < IDL | NC | < IDL | NC | NC | NC |
| **Pb** | **Batch** | < RB | 0.530 ± 0.048 | 0.530 ± 0.048 | 0.456 ± 0.027 | 116 ± 13 | 2.31 | 2.78 |
| | **SPFC** | < IDL | 0.543 ± 0.056 | 0.543 ± 0.056 | 0.471 ± 0.025 | 115 ± 13 | 2.04 | 2.78 |
| **Zn** | **Batch** | 2.07 ± 0.10 | 1010 ± 28 | 1010 ± 28 | 867 ± 154 | 117 ± 21 | 1.26 | 3.18 |
| | **SPFC** | 2.20 ± 0.47 | 939 ± 105 | 941 ± 105 | 604 ± 315 | 156 ± 83 | 1.76 | 2.78 |

n= number of replicates; $SD_C$: combined standard deviation; Sum = (Bioaccessible fraction + Residual fraction); % Mass balance = $\frac{\text{Sum}}{\text{pseudototal}} \times 100$; < IDL: less than instrumental detection limit; < RB: less than reagent blank; NC: not calculated

**Table 5.16. Concentrations of potentially toxic elements (PTE) in the bioaccessible and residual fractions, together with pseudototal content and mass balance in blank FDMS filters using the single-pass dynamic model of the stomach phase of the unified bioaccessibility method (UBM) with fraction collection (SPFC-UBM)**

| PTE | Models | Bioaccessible fraction (μg filter$^{-1}$) Mean (n=3) ± SD | Residual fraction (μg filter$^{-1}$) Mean (n=3) ± SD | Sum ± $SD_C$ (μg filter$^{-1}$) | Pseudototal (μg filter$^{-1}$) Mean (n=3) ± SD | % Mass balance ± $SD_C$ | Student's t-test at 0.05 significance level | |
|---|---|---|---|---|---|---|---|---|
| | | | | | | | $t_{calculated}$ | $t_{calculated}$ |
| **As** | **Batch** | < RB | 0.288 ± 0.025 | 0.288 ± 0.025 | 0.276 ± 0.016 | 104 ± 11 | 0.69 | 2.78 |
| | **SPFC** | < IDL | 0.341 ± 0.012 | 0.341 ± 0.012 | 0.336 ± 0.011 | 101 ± 5 | 0.50 | 2.78 |
| **Cd** | **Batch** | < RB | < RB | NC | < RB | NC | NC | NC |
| | **SPFC** | < IDL | < RB | NC | < RB | NC | NC | NC |
| **Cr** | **Batch** | < IDL | 2.58 ± 0.07 | 2.58 ± 0.07 | 2.59 ± 0.05 | 99.6 ± 3.3 | 0.21 | 2.78 |
| | **SPFC** | < IDL | 2.74 ± 0.08 | 2.74 ± 0.08 | 2.63 ± 0.02 | 104 ± 3 | 2.13 | 2.78 |
| **Cu** | **Batch** | 0.061 ± 0.047 | < RB | 0.061 ± 0.047 | < RB | NC | NC | NC |
| | **SPFC** | < IDL | 0.182 ± 0.022 | 0.182 ± 0.022 | 0.172 ± 0.017 | 106 ± 17 | 0.64 | 2.78 |
| **Fe** | **Batch** | < IDL | 64.6 ± 4.1 | 64.6 ± 4.1 | 60.1 ± 2.2 | 107 ± 8 | 1.67 | 2.78 |
| | **SPFC** | < IDL | 86.0 ± 1.9 | 86.0 ± 1.9 | 63.2 ± 1.1 | 136 ± 4 | **17.8** | 2.78 |
| **Mn** | **Batch** | 0.060 ± 0.040 | 1.02 ± 0.09 | 1.08 ± 0.10 | 1.08 ± 0.01 | 100 ± 9 | 0.06 | 12.7 |
| | **SPFC** | < IDL | 1.05 ± 0.04 | 1.05 ± 0.04 | 1.10 ± 0.02 | 95.5 ± 4.0 | 1.85 | 2.78 |
| **Ni** | **Batch** | < IDL | 0.208 ± 0.006 | 0.208 ± 0.006 | 0.241 ± 0.006 | 86.4 ± 3.2 | **6.88** | 2.78 |
| | **SPFC** | < IDL | 0.310 ± 0.004 | 0.310 ± 0.004 | 0.318 ± 0.011 | 98.0 ± 4.0 | 1.11 | 2.78 |
| **Pb** | **Batch** | < IDL | 0.474 ± 0.006 | 0.474 ± 0.006 | 0.473 ± 0.007 | 100 ± 2 | 0.25 | 2.78 |
| | **SPFC** | < IDL | 0.544 ± 0.016 | 0.544 ± 0.016 | 0.523 ± 0.002 | 104 ± 3 | 2.27 | 4.30 |
| **Zn** | **Batch** | 3.10 ± 1.03 | 985 ± 6 | 988 ± 6 | 898 ± 79 | 110 ± 10 | 1.54 | 3.18 |
| | **SPFC** | 0.972 ± 0.385 | 970 ± 34 | 971 ± 34 | 919 ± 38 | 106 ± 6 | 1.77 | 2.78 |

n= number of replicates; $SD_C$: combined standard deviation; $\text{Sum} = (\text{Bioaccessible fraction} + \text{Residual fraction})$; $\%\ \text{Mass balance} = \frac{\text{Sum}}{\text{pseudototal}} \times 100$; < IDL: less than instrumental detection limit; < RB: less than reagent blank; NC: not calculated

#### 5.3.2.3. Single-pass dynamic model of the SBET with fraction collection (SPFC-SBET)

The extractograms of PTE in the simulated $PM_{10}$ samples, prepared using BGS RM 102 Ironstone Soil and NIST SRM 2711A Montana II Soil, extracted by the SPFC-SBET, are presented in the Figures 5.21-5.38 (and tabulated in Appendices D1-D4). The largest bioaccessible concentration was observed in the first 5 mL leached (i.e. subfraction 1) for all PTE determined, except for Cr in BGS RM 102 Ironstone Soil, where it was in subfraction 4. As BGS RM 102 and NIST SRM 2711A were prepared from naturally elevated in PTE and anthropogenically contaminated soils, respectively, this rapid mobilisation suggests that these elements were adsorbed on surfaces of soil components and they were not strongly bound. For Cr in BGS RM 102, the slow mobilisation may be because of the nature of Cr species such as $CrO_4^{2-}$ and $CrO_3^{3-}$. These ions tend to be adsorbed on anion exchange sites of soils such as iron oxides, which are likely to be present in higher levels in the BGS RM 102 as it is a ferritic brown earth soil. This interpretation is in agreement with the results obtained in this work, where the Cr leaching profile was similar to some extent to Fe, which might suggest that Cr is mainly associated with Fe oxides in this soil.

Although 10 mL of the SBET's reagent was used for the batch model, the volume used for obtaining batch-equivalent concentrations using the SPFC-SBET ranged from 25 mL (i.e. the volume required for five subfractions) for As in BGS RM 102 to 55 mL (i.e. the volume required for eleven subfractions) for Fe in NIST SRM 2711A. This was probably due to the effect of contact time between the reagent and samples, where it was one hour for 10 mL for the batch model, while for the SPFC-SBET, it was only 10 min for 10 mL (i.e. the volume required for two subfractions). In general, bioaccessible concentrations achieved using the batch model were higher than those obtained by the SPFC-SBET. That was not expected as 60 mL of fresh SBET's reagent was used for one hour when the SPFC-SBET was applied compared with 10 mL used for the batch model. This was likely because the batch model of the SBET is more prone to contamination than the SPFC-SBET. The pH of extracts for each subfraction obtained was less than 2 (see Fig. 5.39), as required in the SBET procedure.

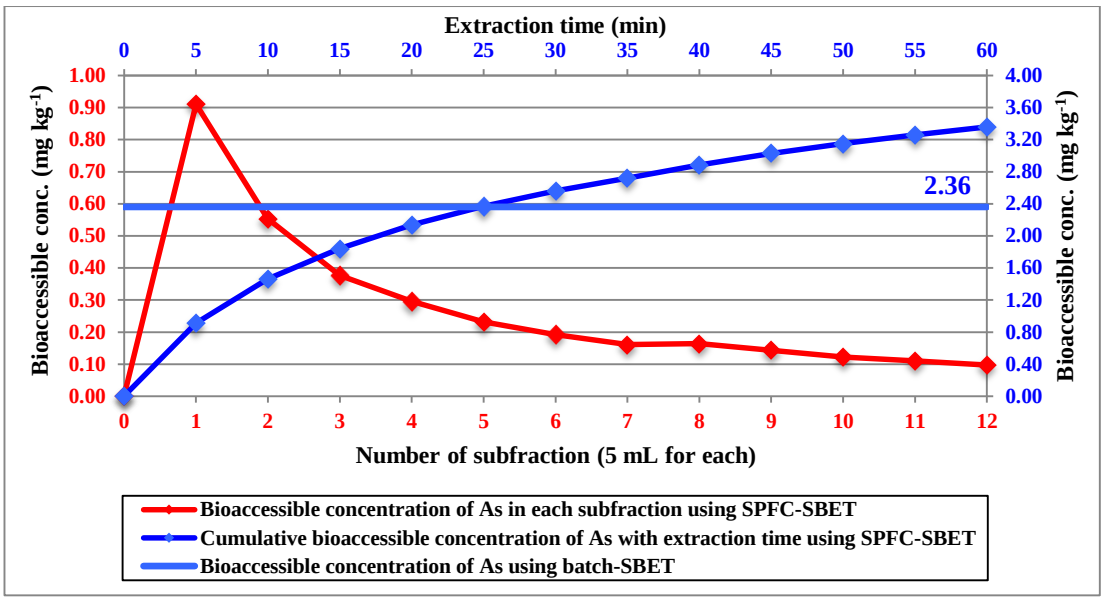


**Figure 5.21. Bioaccessible concentration of As in subfractions obtained by extraction of the simulated $PM_{10}$ samples (BGS RM 102 Ironstone Soil on FDMS filter) using the single-pass dynamic model of the simplified bioaccessibility extraction test (SBET) with fraction collection (SPFC-SBET)**

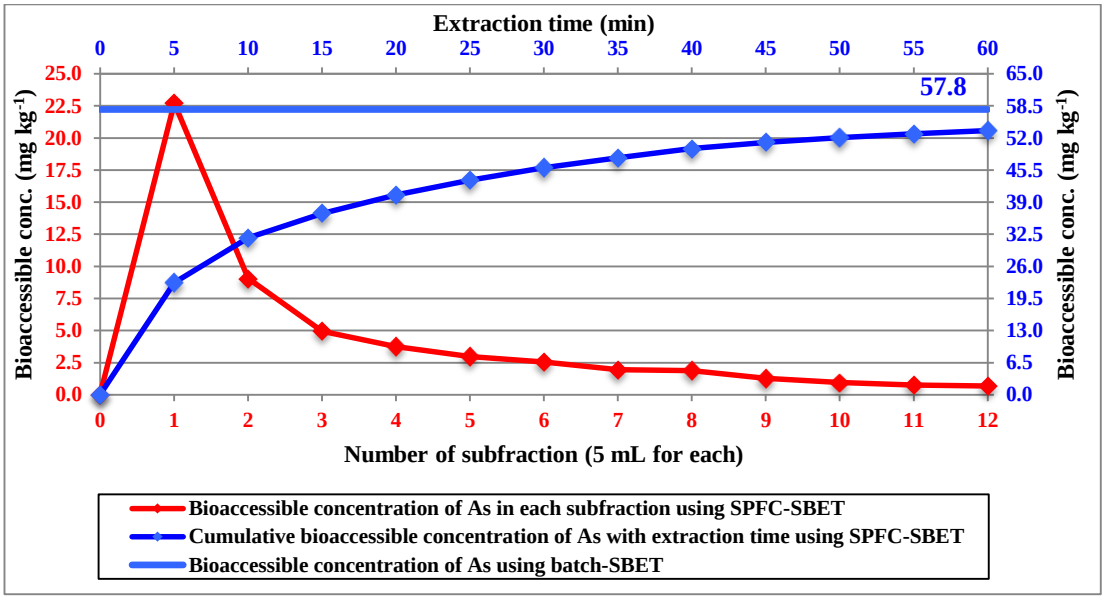


**Figure 5.22. Bioaccessible concentration of As in subfractions obtained by extraction of the simulated $PM_{10}$ samples (NIST SRM 2711A Montana II Soil on FDMS filter) using the single-pass dynamic model of the simplified bioaccessibility extraction test (SBET) with fraction collection (SPFC-SBET)**

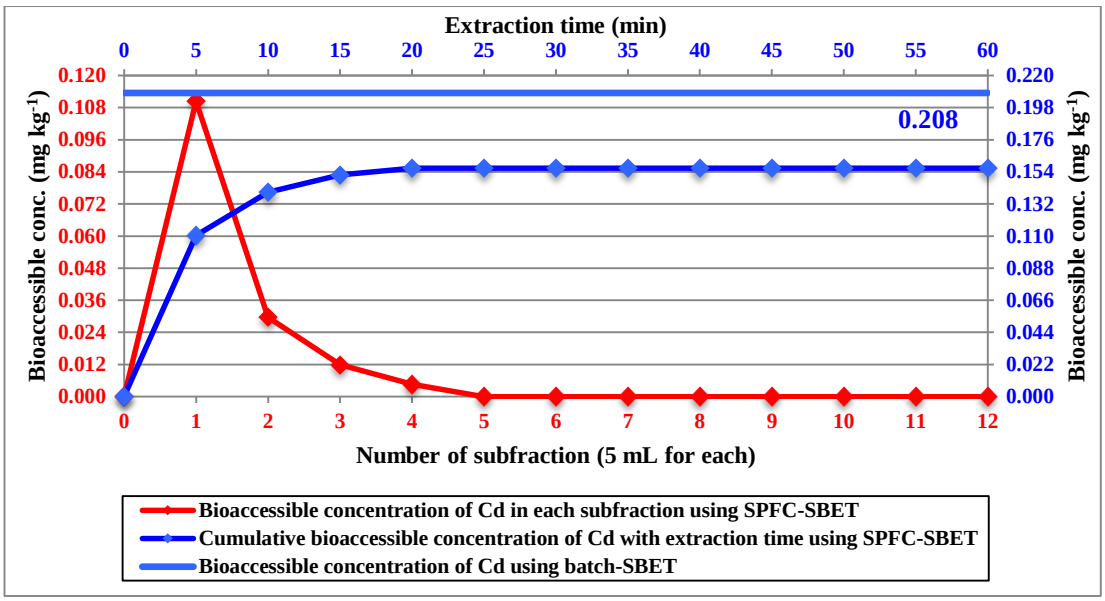


**Figure 5.23. Bioaccessible concentration of Cd in subfractions obtained by extraction of the simulated $PM_{10}$ samples (BGS RM 102 Ironstone Soil on FDMS filter) using the single-pass dynamic model of the simplified bioaccessibility extraction test (SBET) with fraction collection (SPFC-SBET)**

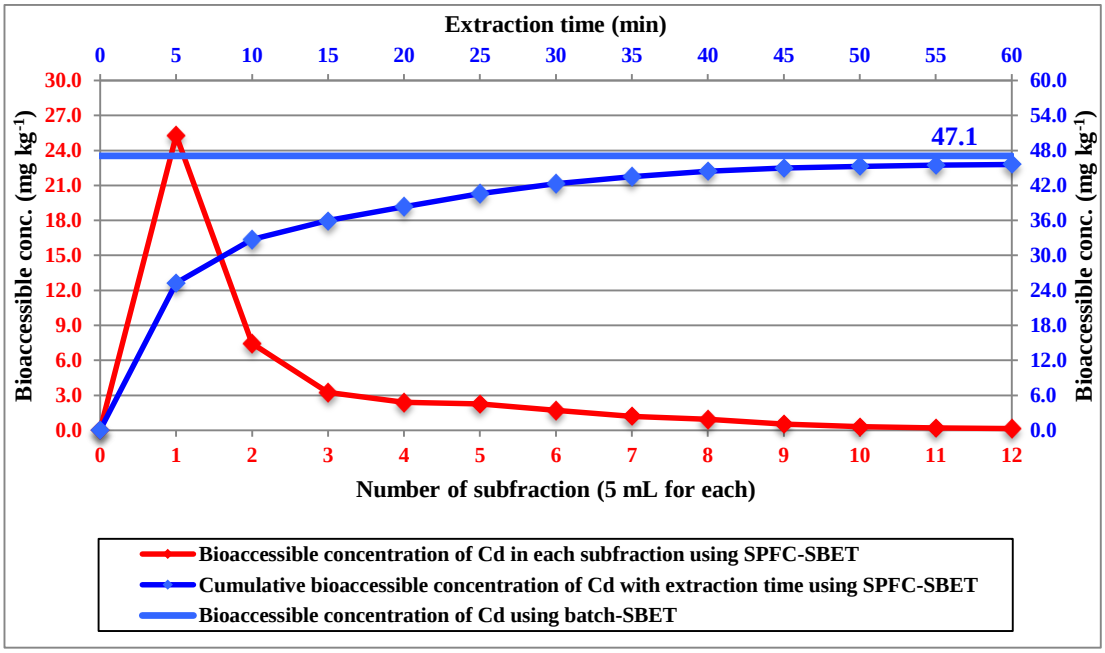


**Figure 5.24. Bioaccessible concentration of Cd in subfractions obtained by extraction of the simulated $PM_{10}$ samples (NIST SRM 2711A Montana II Soil on FDMS filter) using the single-pass dynamic model of the simplified bioaccessibility extraction test (SBET) with fraction collection (SPFC-SBET)**

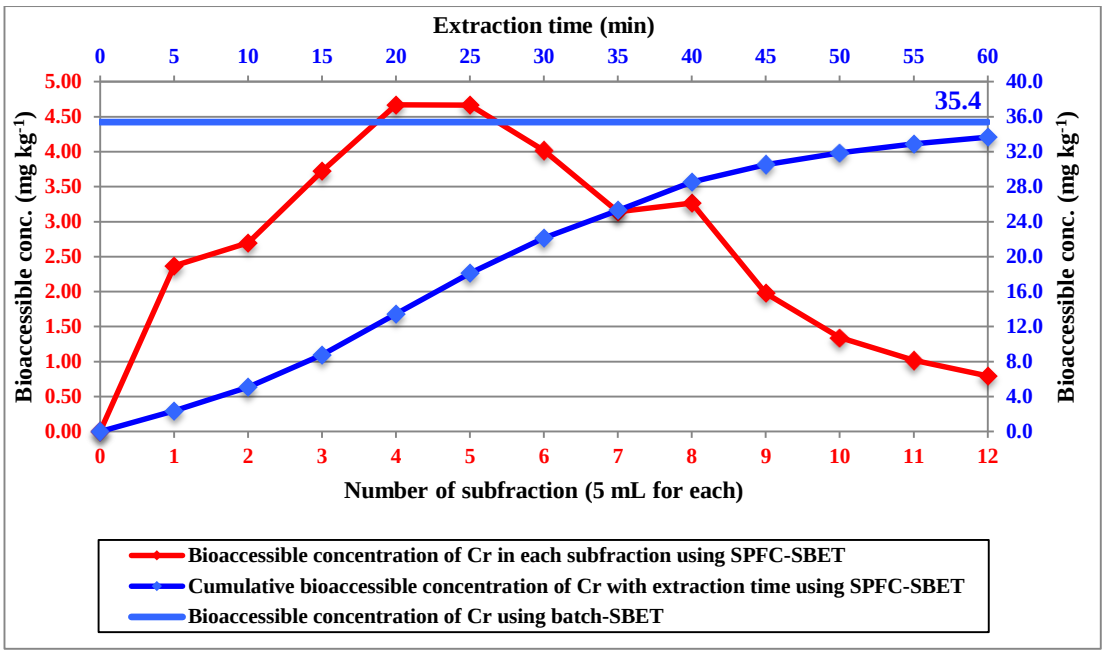


**Figure 5.25. Bioaccessible concentration of Cr in subfractions obtained by extraction of the simulated $PM_{10}$ samples (BGS RM 102 Ironstone Soil on FDMS filter) using the single-pass dynamic model of the simplified bioaccessibility extraction test (SBET) with fraction collection (SPFC-SBET)**

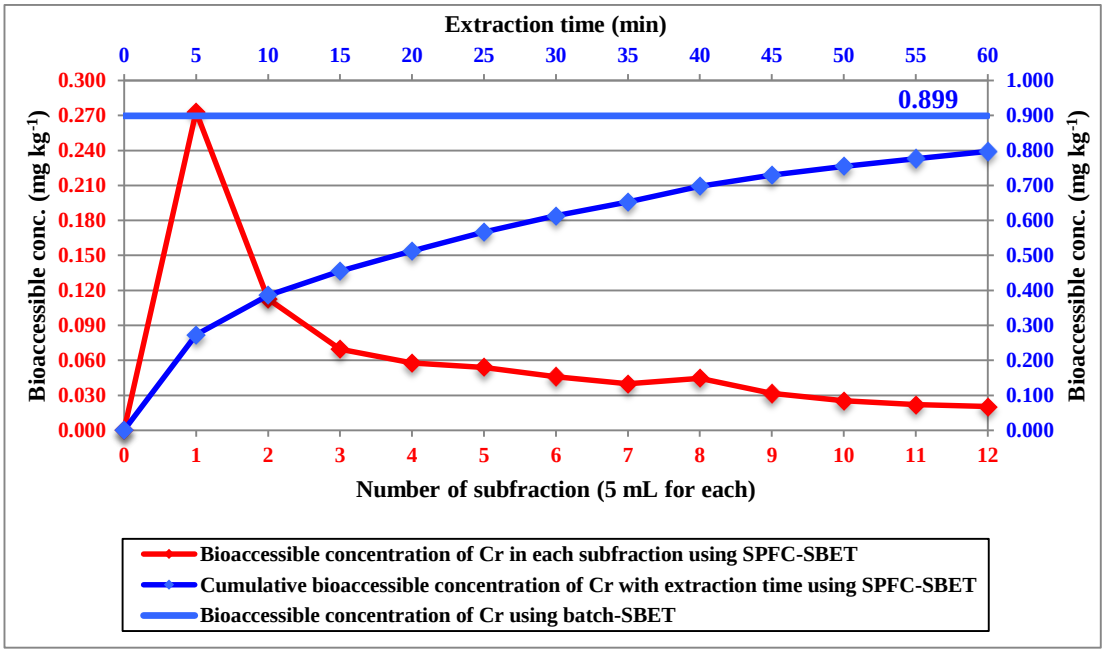


**Figure 5.26. Bioaccessible concentration of Cr in subfractions obtained by extraction of the simulated $PM_{10}$ samples (NIST SRM 2711A Montana II Soil on FDMS filter) using the single-pass dynamic model of the simplified bioaccessibility extraction test (SBET) with fraction collection (SPFC-SBET)**

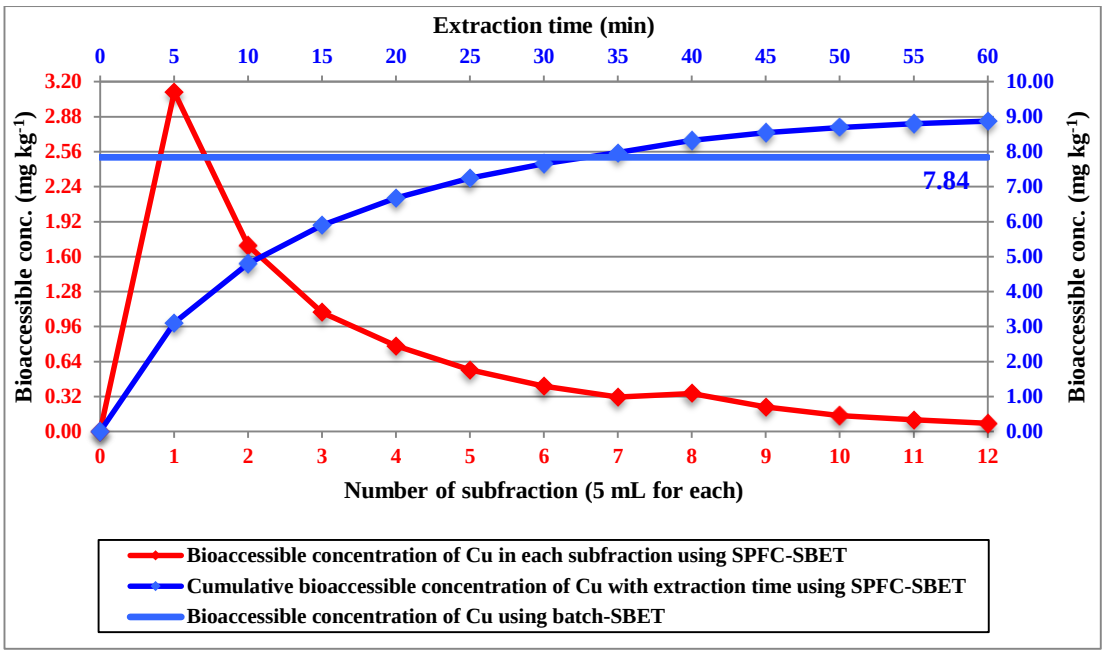


**Figure 5.27. Bioaccessible concentration of Cu in subfractions obtained by extraction of the simulated $PM_{10}$ samples (BGS RM 102 Ironstone Soil on FDMS filter) using the single-pass dynamic model of the simplified bioaccessibility extraction test (SBET) with fraction collection (SPFC-SBET)**

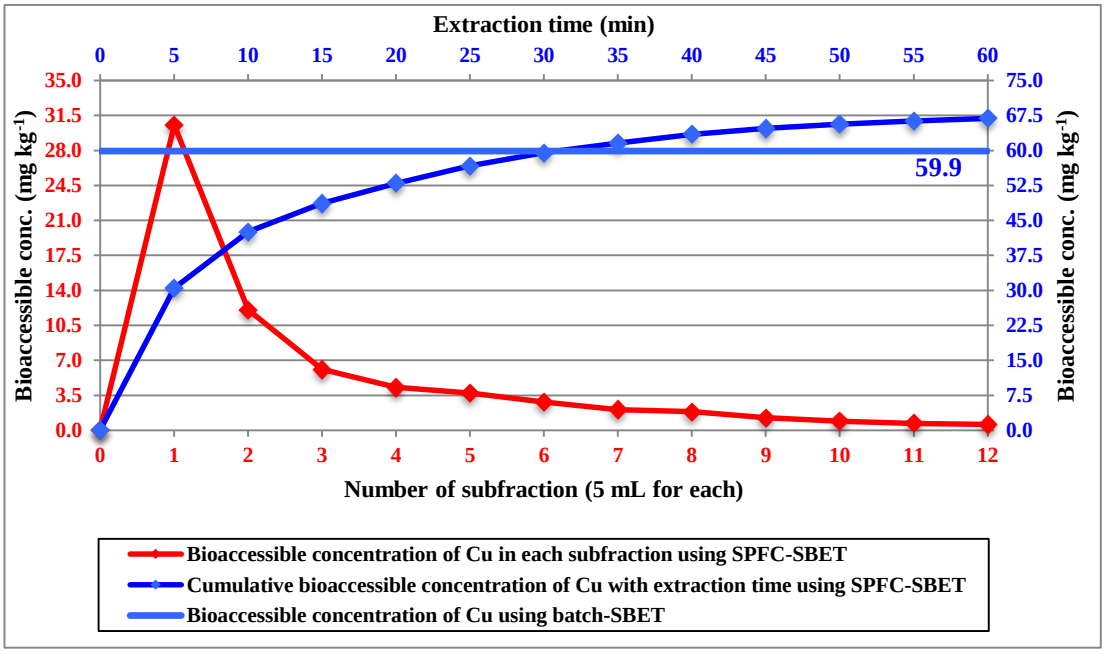


**Figure 5.28. Bioaccessible concentration of Cu in subfractions obtained by extraction of the simulated $PM_{10}$ samples (NIST SRM 2711A Montana II Soil on FDMS filter) using the single-pass dynamic model of the simplified bioaccessibility extraction test (SBET) with fraction collection (SPFC-SBET)**

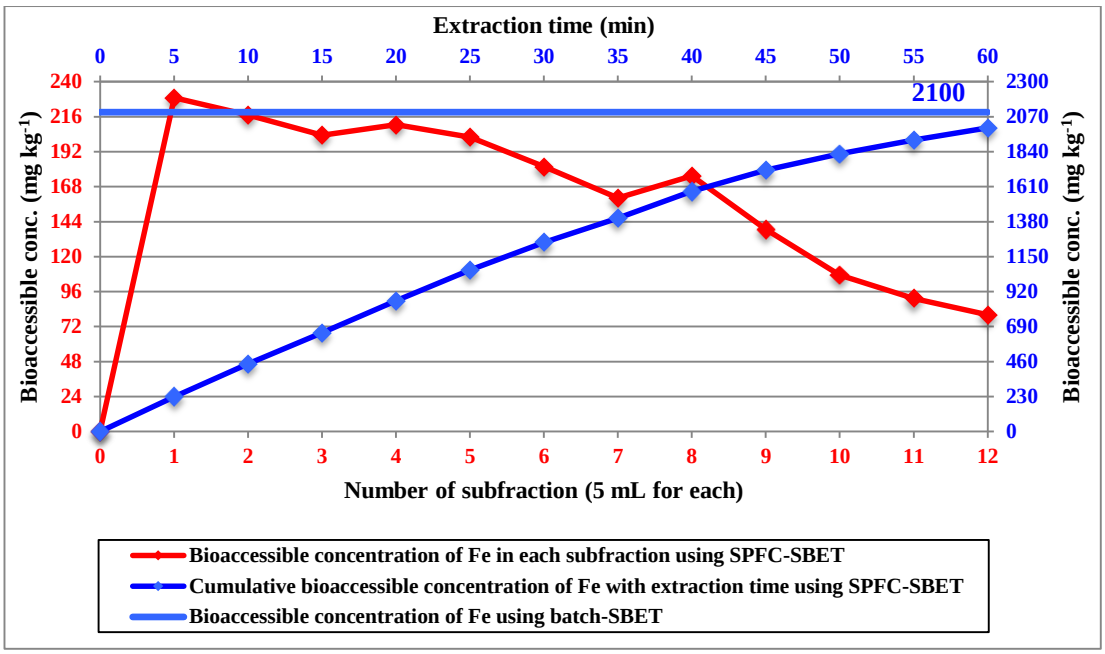


**Figure 5.29. Bioaccessible concentration of Fe in subfractions obtained by extraction of the simulated $PM_{10}$ samples (BGS RM 102 Ironstone Soil on FDMS filter) using the single-pass dynamic model of the simplified bioaccessibility extraction test (SBET) with fraction collection (SPFC-SBET)**

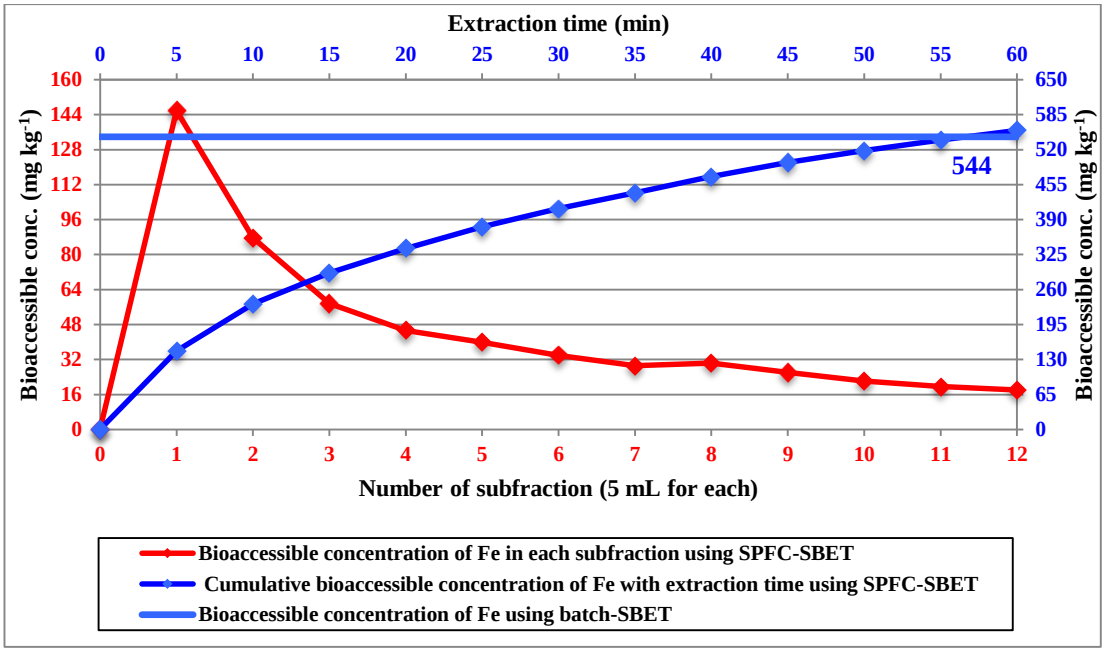


**Figure 5.30. Bioaccessible concentration of Fe in subfractions obtained by extraction of the simulated $PM_{10}$ samples (NIST SRM 2711A Montana II Soil on FDMS filter) using the single-pass dynamic model of the simplified bioaccessibility extraction test (SBET) with fraction collection (SPFC-SBET)**

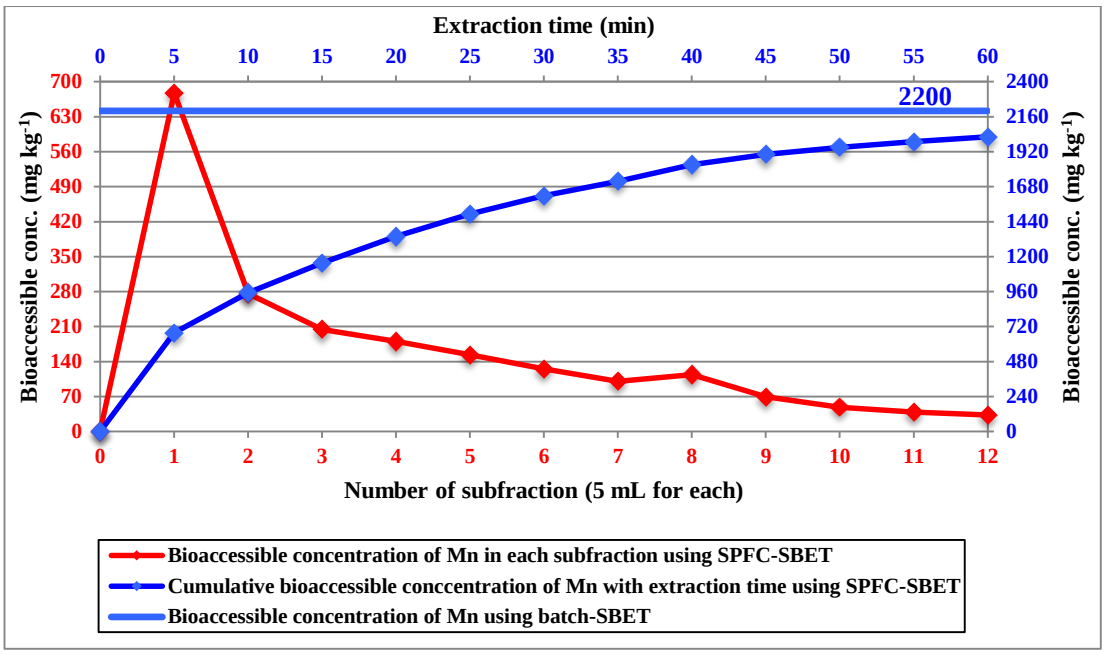


**Figure 5.31. Bioaccessible concentration of Mn in subfractions obtained by extraction of the simulated $PM_{10}$ samples (BGS RM 102 Ironstone Soil on FDMS filter) using the single-pass dynamic model of the simplified bioaccessibility extraction test (SBET) with fraction collection (SPFC-SBET)**

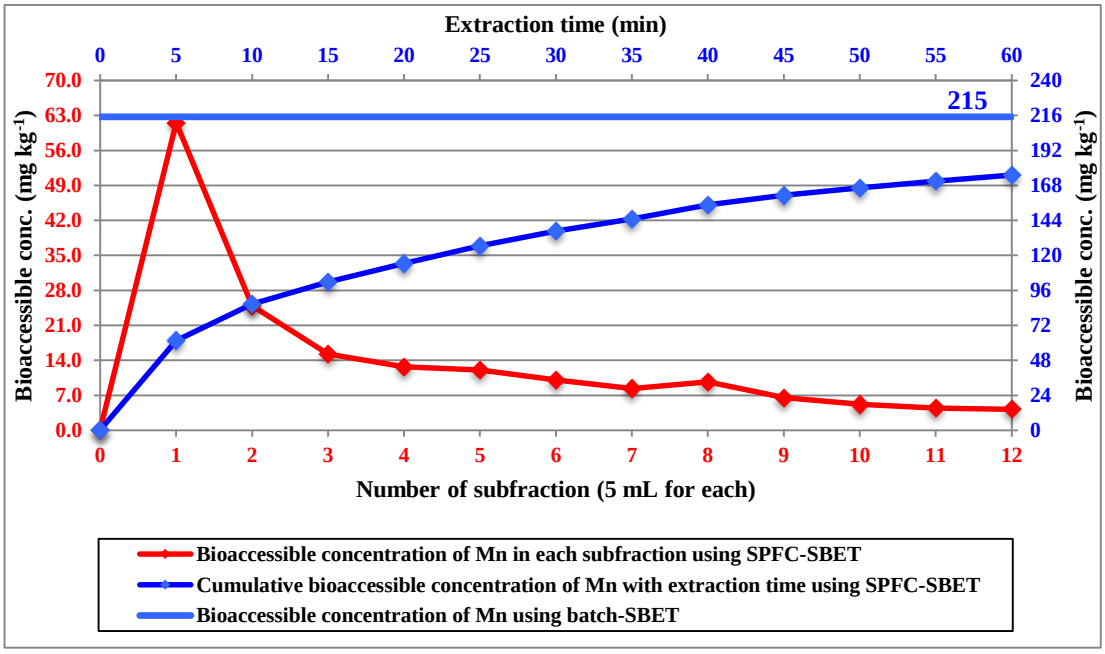


**Figure 5.32. Bioaccessible concentration of Mn in subfractions obtained by extraction of the simulated $PM_{10}$ samples (NIST SRM 2711A Montana II Soil on FDMS filter) using the single-pass dynamic model of the simplified bioaccessibility extraction test (SBET) with fraction collection (SPFC-SBET)**

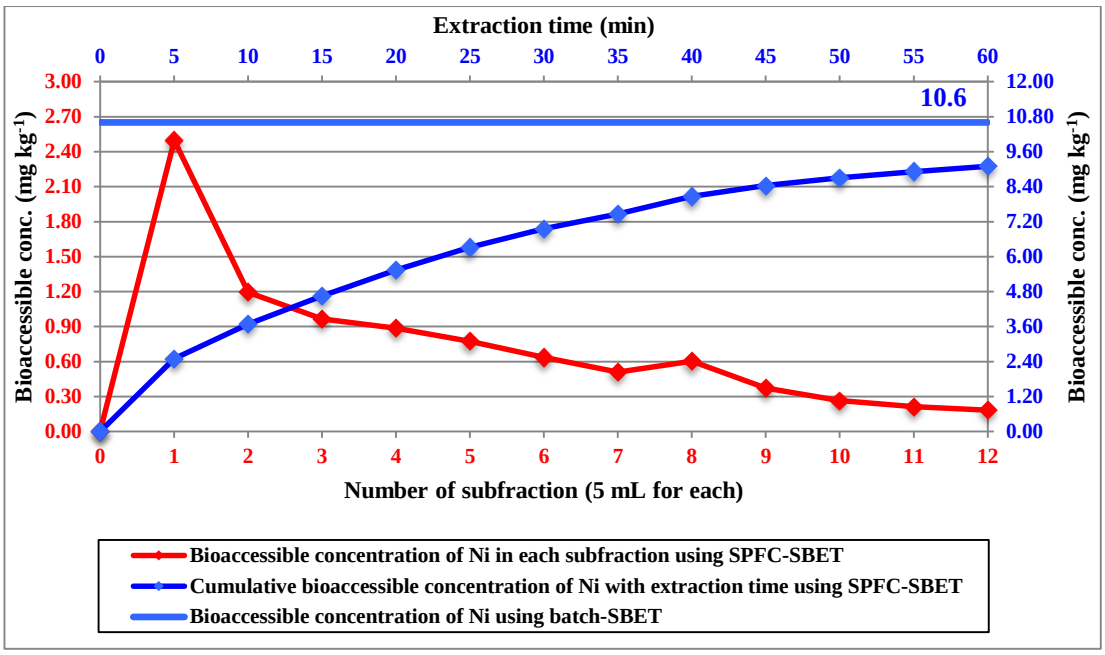


**Figure 5.33. Bioaccessible concentration of Ni in subfractions obtained by extraction of the simulated $PM_{10}$ samples (BGS RM 102 Ironstone Soil on FDMS filter) using the single-pass dynamic model of the simplified bioaccessibility extraction test (SBET) with fraction collection (SPFC-SBET)**

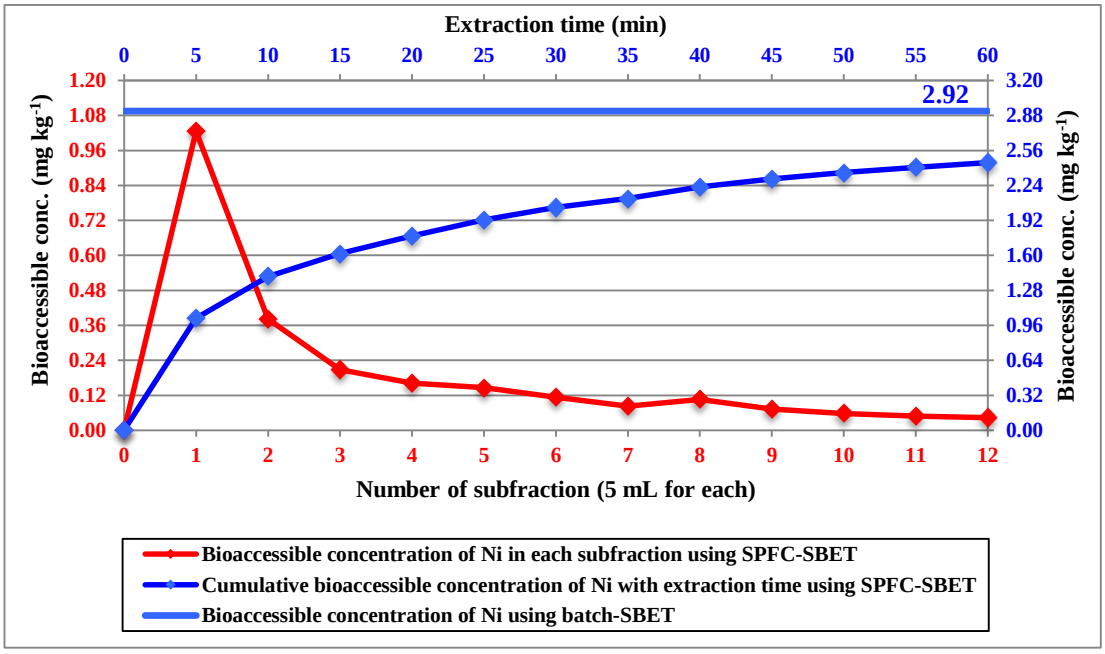


**Figure 5.34. Bioaccessible concentration of Ni in subfractions obtained by extraction of the simulated $PM_{10}$ samples (NIST SRM 2711A Montana II Soil on FDMS filter) using the single-pass dynamic model of the simplified bioaccessibility extraction test (SBET) with fraction collection (SPFC-SBET)**

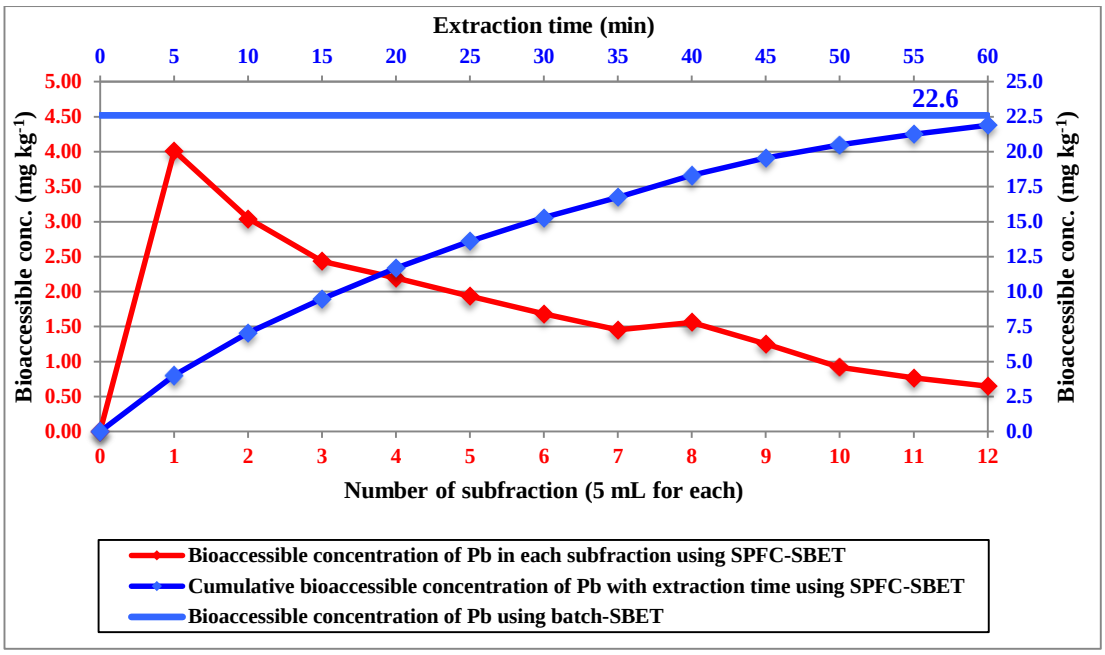


**Figure 5.35. Bioaccessible concentration of Pb in subfractions obtained by extraction of the simulated $PM_{10}$ samples (BGS RM 102 Ironstone Soil on FDMS filter) using the single-pass dynamic model of the simplified bioaccessibility extraction test (SBET) with fraction collection (SPFC-SBET)**

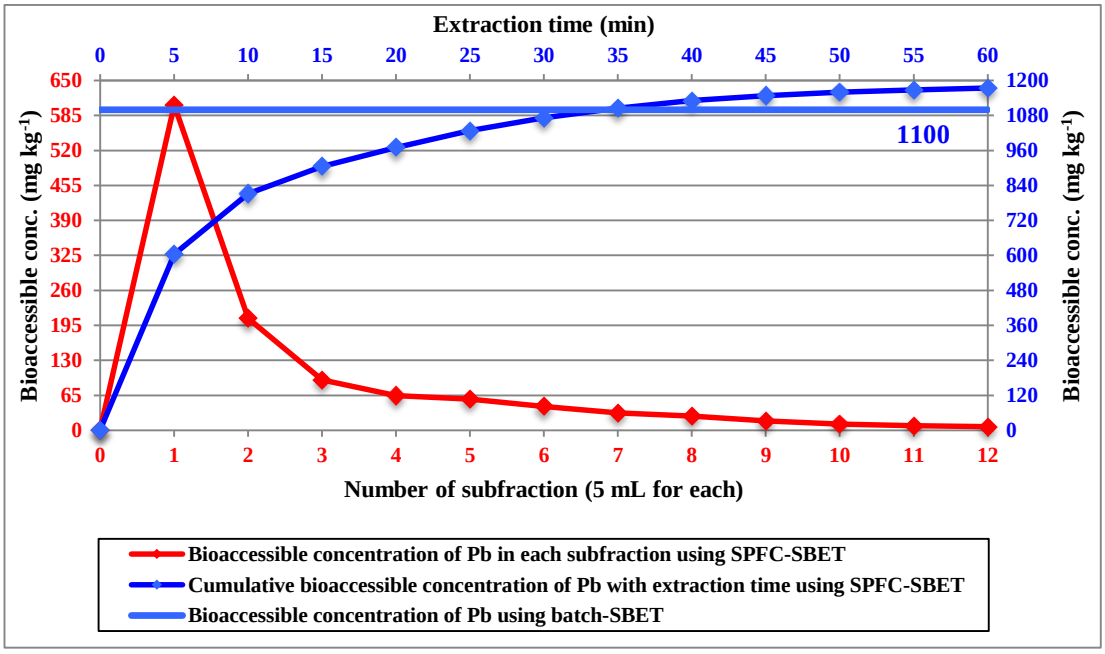


**Figure 5.36. Bioaccessible concentration of Pb in subfractions obtained by extraction of the simulated $PM_{10}$ samples (NIST SRM 2711A Montana II Soil on FDMS filter) using the single-pass dynamic model of the simplified bioaccessibility extraction test (SBET) with fraction collection (SPFC-SBET)**

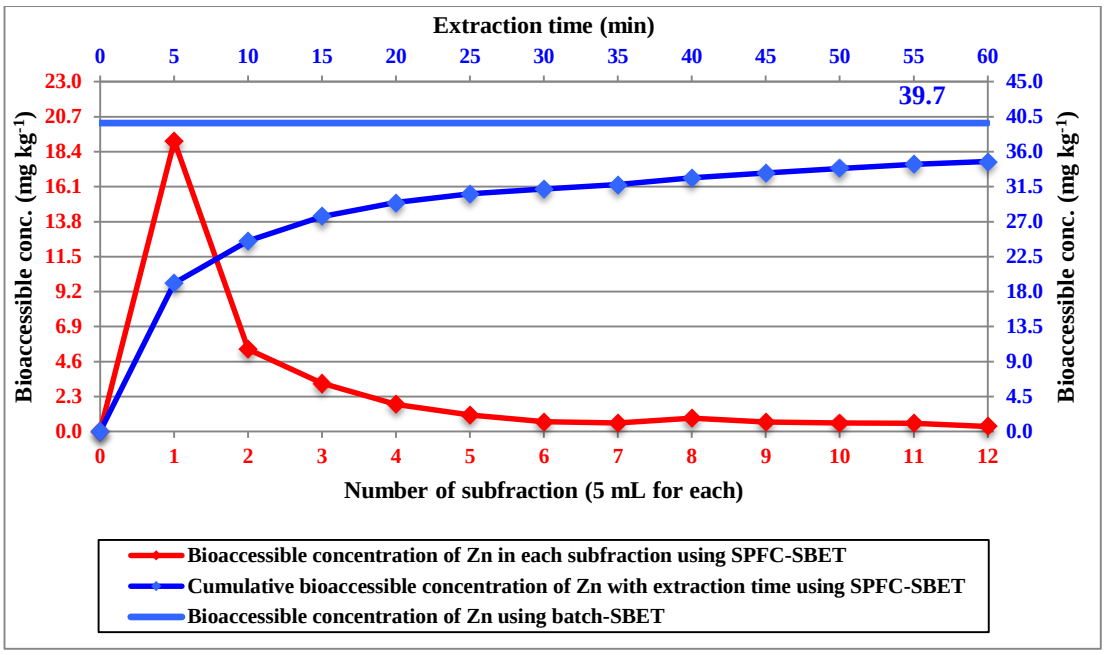


**Figure 5.37. Bioaccessible concentration of Zn in subfractions obtained by extraction of the simulated $PM_{10}$ samples (BGS RM 102 Ironstone Soil on FDMS filter) using the single-pass dynamic model of the simplified bioaccessibility extraction test (SBET) with fraction collection (SPFC-SBET)**

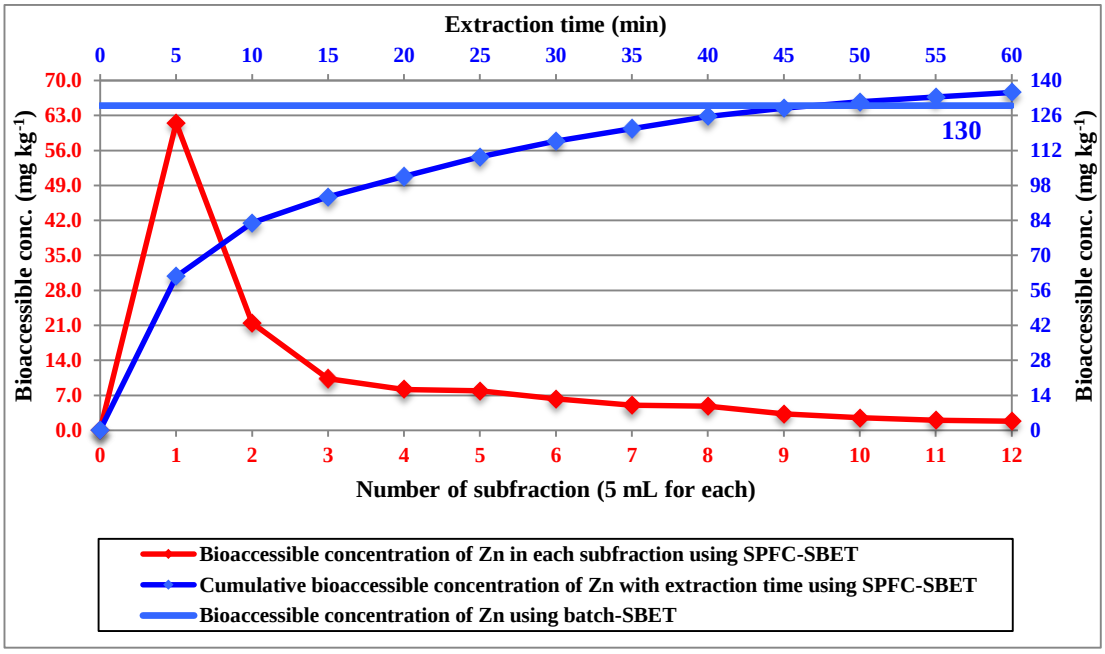


**Figure 5.38. Bioaccessible concentration of Zn in subfractions obtained by extraction of the simulated $PM_{10}$ samples (NIST SRM 2711A Montana II Soil on FDMS filter) using the single-pass dynamic model of the simplified bioaccessibility extraction test (SBET) with fraction collection (SPFC-SBET)**

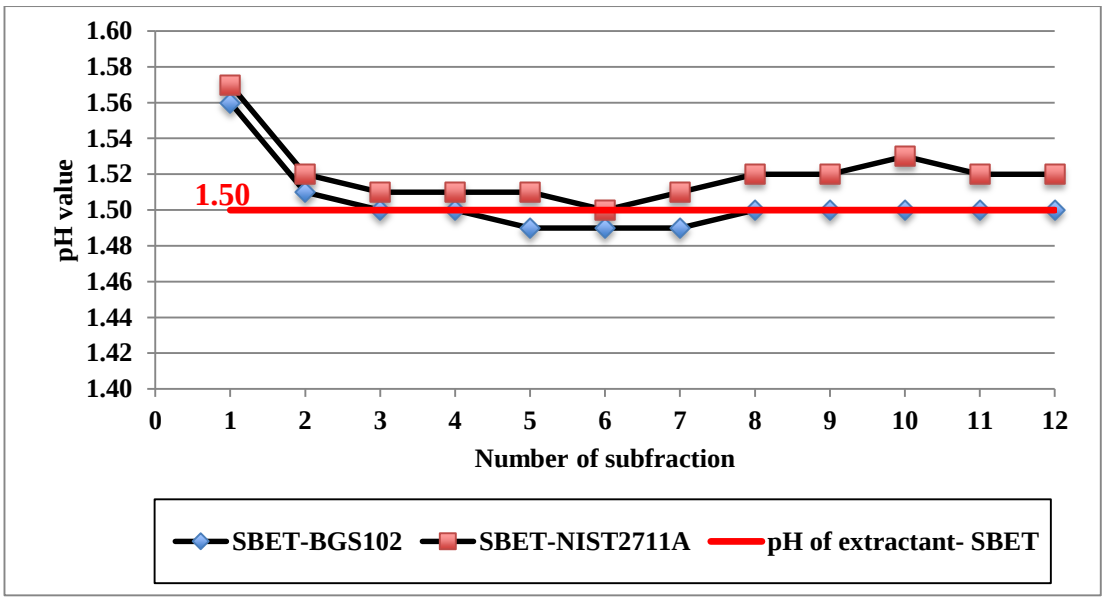


**Figure 5.39. Values of pH for each subfraction obtained by applying the the single-pass dynamic model of the simplified bioaccessibility extraction test (SBET) with fraction collection (SPFC-SBET) using BGS RM 102 Ironstone Soil and NIST SRM 2711A Montana II Soil**

#### 5.3.2.4. Single-pass dynamic model of the stomach phase of the UBM with fraction collection (SPFC-UBM)

Figures 5.40-5.57 show the extractograms of PTE in the simulated $PM_{10}$ samples, prepared using BGS RM 102 Ironstone Soil and NIST SRM 2711A Montana II Soil, extracted by the SPFC-UBM (see Appendices D5-D8). For all PTE tested in BGS RM 102 Ironstone Soil and NIST SRM 2711A (except for Cr, Fe, and Pb in BGS RM 102 Ironstone Soil and Fe in NIST SRM 2711A), the maximum extractability was observed in the first subfraction (i.e. in the first 3.75 mL of leachate). This trend was similar to the SPFC-SBET, however, both Fe and Pb were released in a different fashion. This may be because of the difference of subfraction volume adopted for each method. The reagent volume required for achieving the batch-equivalent concentrations when the SPFC-UBM was applied, was from 11.25 mL (i.e. the volume required for three subfractions) for Cu and Pb in NIST SRM 2711A to 56.25 mL (i.e. the volume required for fifteen subfractions) for Ni in BGS RM 102.

The difference in leaching profile for Fe and Pb might indicate that Pb is not associated with Fe. Similar to the SBET in terms of possibility of contamination, the bioaccessible concentration for some PTE tested (Cd and Cu in BGS102 and Cr, Fe, and Ni in NIST SRM 2711A) was high for the batch model compared with that obtained by the SPFC-UBM. The pH of leachates in 16 subfractions (see Fig. 5.58) was within the criteria specified for the UBM (i.e. less than 1.5). The bioaccessible concentrations of PTE obtained by the SPFC-UBM were generally high compared with those obtained by SPFC-SBET. As mentioned in Section 4.3.2, this is likely because the difference in pH value adopted for each method, and presence of mucin in the reagent of the stomach phase of the UBM may also increase the bioaccessibility of PTE.

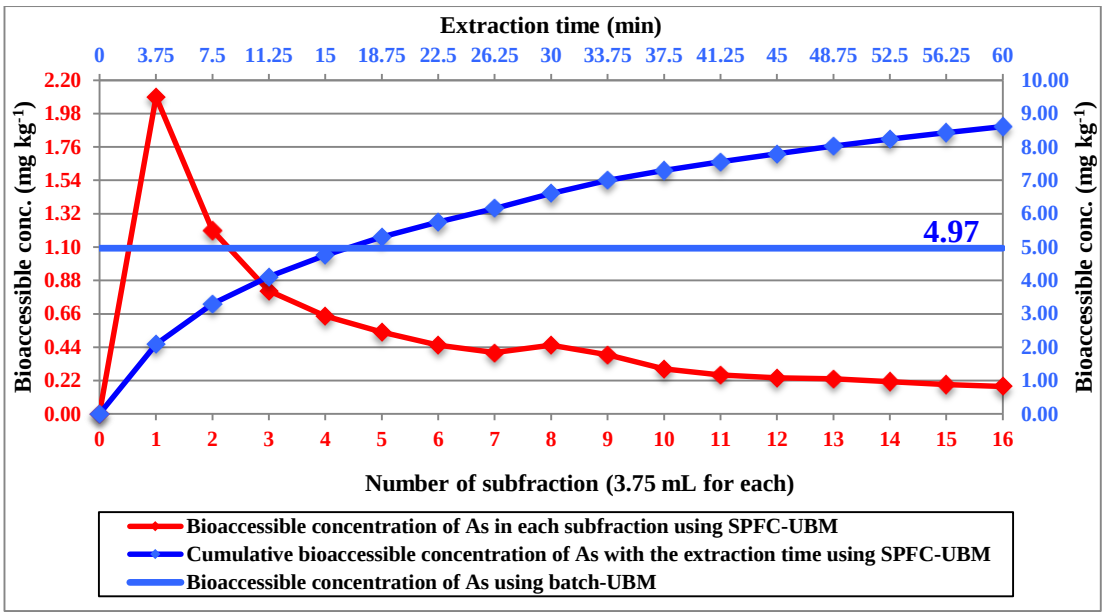


**Figure 5.40. Bioaccessible concentration of As in subfractions obtained by extraction of the simulated $PM_{10}$ samples (BGS RM 102 Ironstone Soil on FDMS filter) using the single-pass dynamic model of the stomach phase of the unified bioaccessibility method (UBM) with fraction collection (SPFC-UBM)**

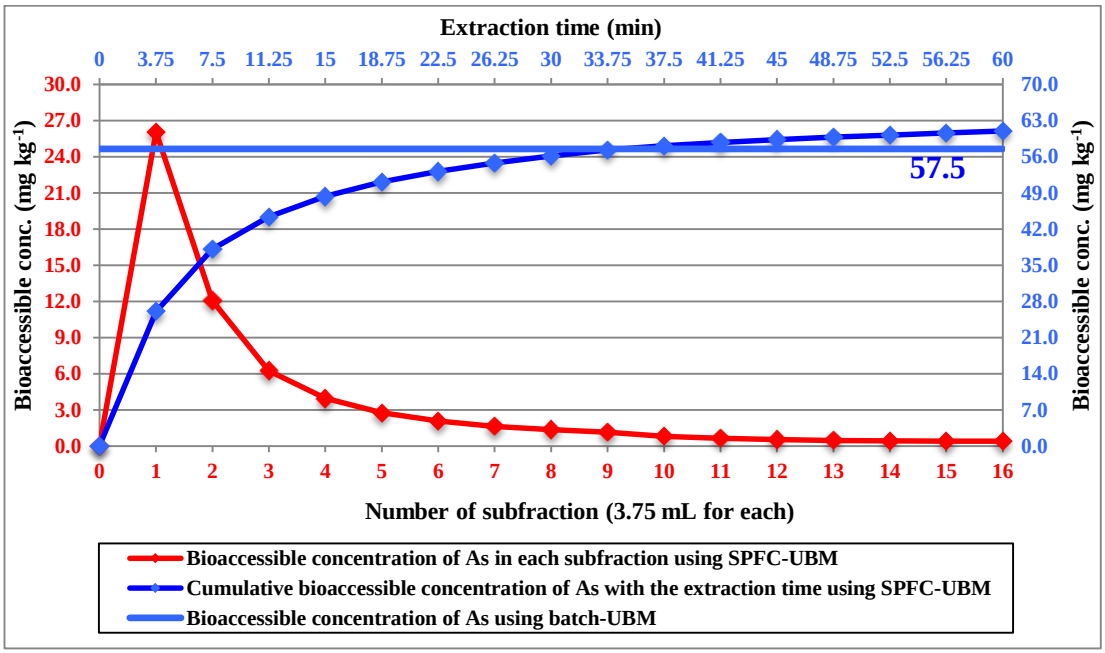


**Figure 5.41. Bioaccessible concentration of As in subfractions obtained by extraction of the simulated $PM_{10}$ samples (NIST SRM 2711A Montana II Soil on FDMS filter) using the single-pass dynamic model of the stomach phase of the unified bioaccessibility method (UBM) with fraction collection (SPFC-UBM)**

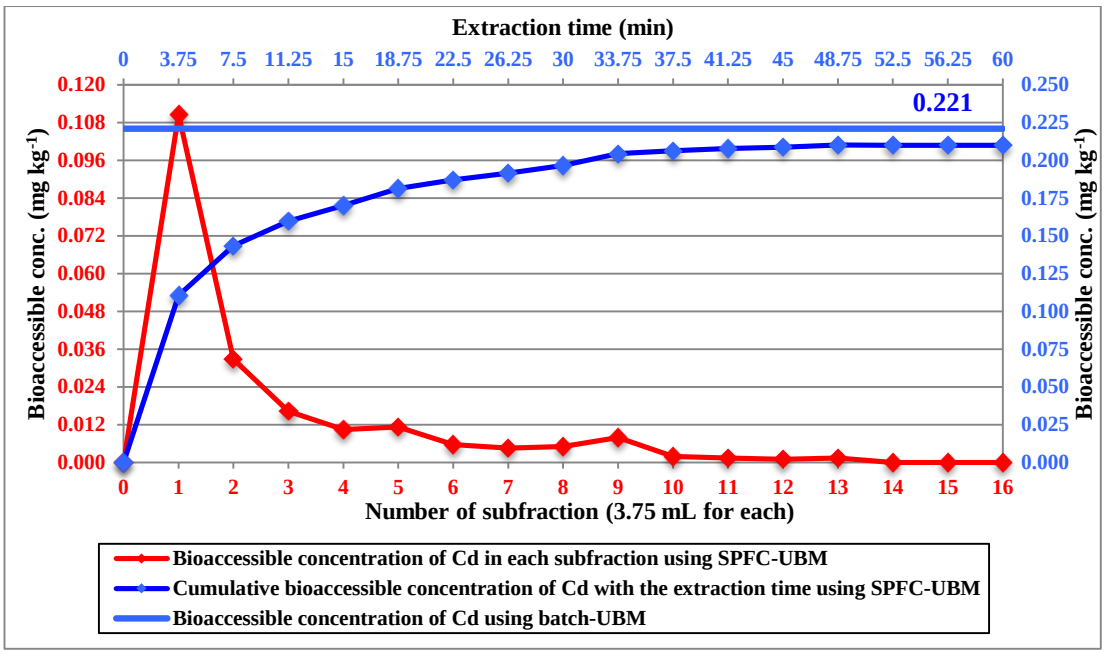


**Figure 5.42. Bioaccessible concentration of Cd in subfractions obtained by extraction of the simulated $PM_{10}$ samples (BGS RM 102 Ironstone Soil on FDMS filter) using the single-pass dynamic model of the stomach phase of the unified bioaccessibility method (UBM) with fraction collection (SPFC-UBM)**

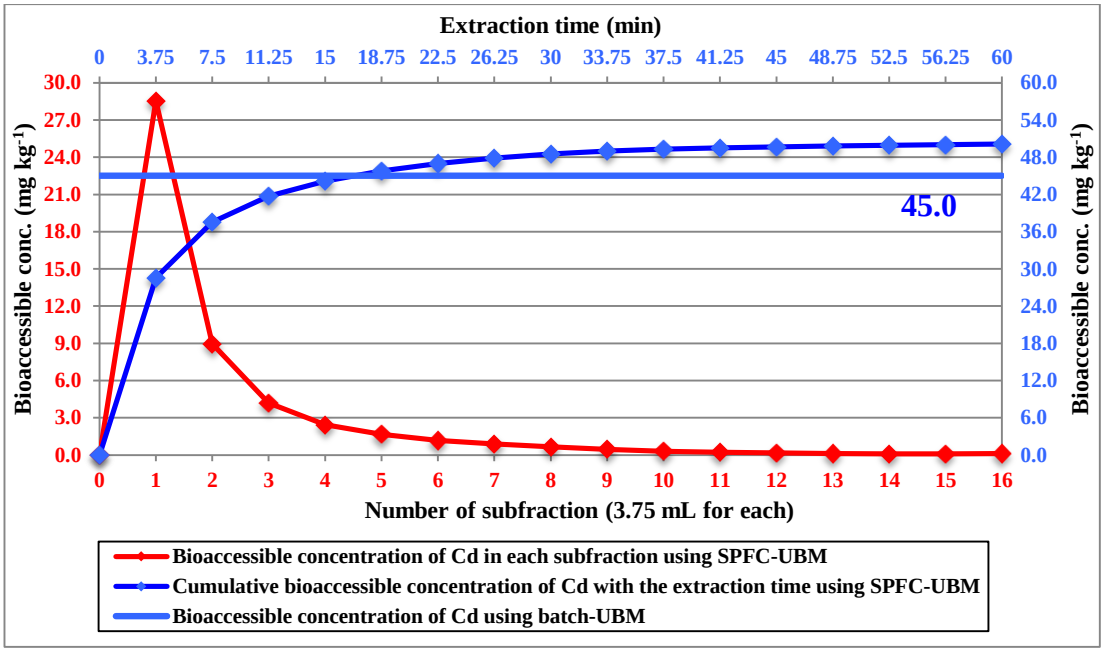


**Figure 5.43. Bioaccessible concentration of Cd in subfractions obtained by extraction of the simulated $PM_{10}$ samples (NIST SRM 2711A Montana II Soil on FDMS filter) using the single-pass dynamic model of the stomach phase of the unified bioaccessibility method (UBM) with fraction collection (SPFC-UBM)**

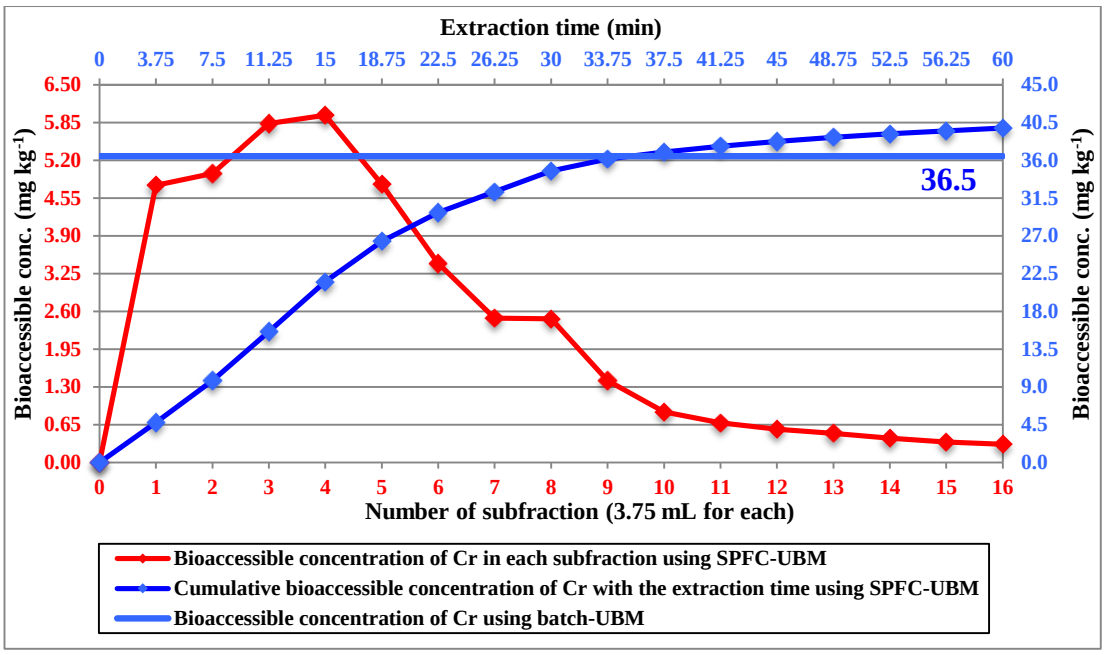


**Figure 5.44. Bioaccessible concentration of Cr in subfractions obtained by extraction of the simulated $PM_{10}$ samples (BGS RM 102 Ironstone Soil on FDMS filter) using the single-pass dynamic model of the stomach phase of the unified bioaccessibility method (UBM) with fraction collection (SPFC-UBM)**

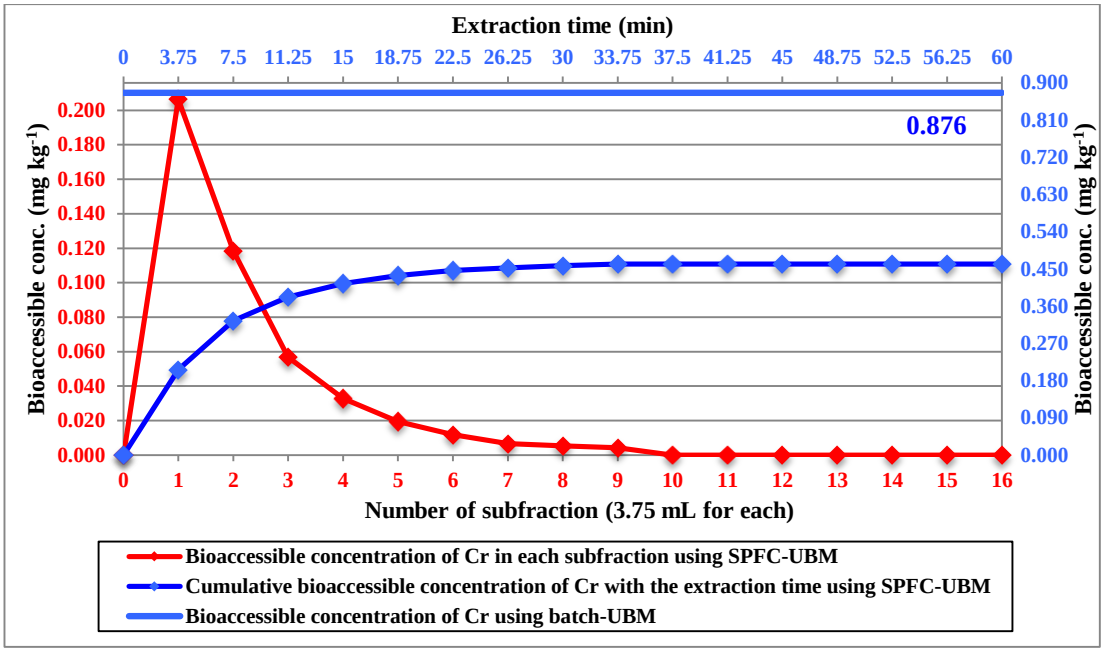


**Figure 5.45. Bioaccessible concentration of Cr in subfractions obtained by extraction of the simulated $PM_{10}$ samples (NIST SRM 2711A Montana II Soil on FDMS filter) using the single-pass dynamic model of the stomach phase of the unified bioaccessibility method (UBM) with fraction collection (SPFC-UBM)**

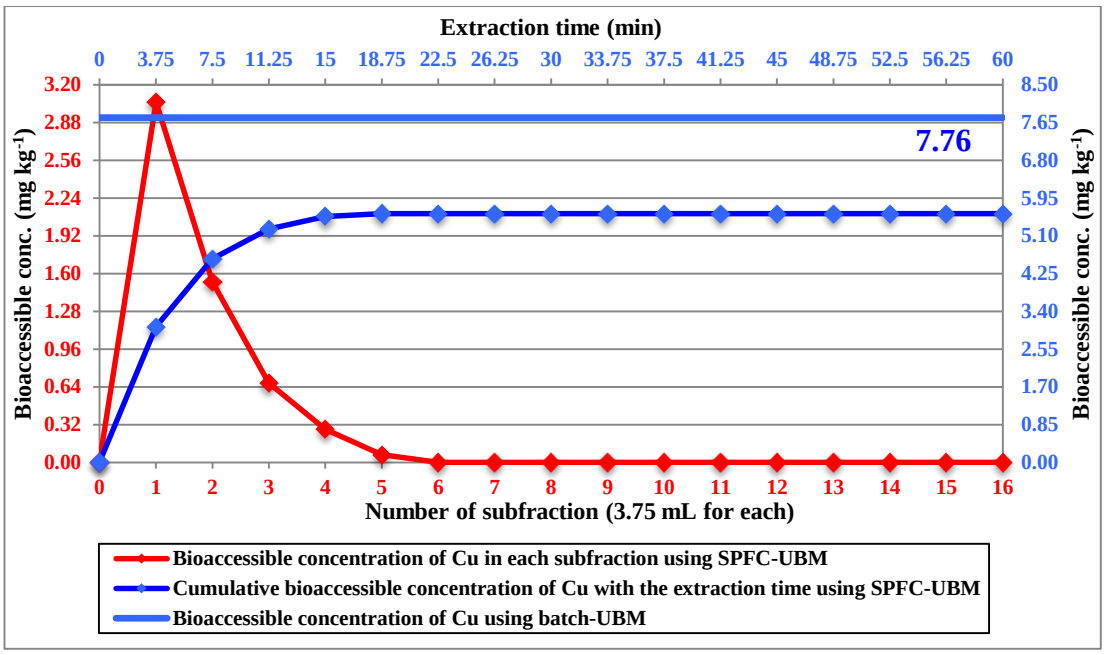


**Figure 5.46. Bioaccessible concentration of Cu in subfractions obtained by extraction of the simulated $PM_{10}$ samples (BGS RM 102 Ironstone Soil on FDMS filter) using the single-pass dynamic model of the stomach phase of the unified bioaccessibility method (UBM) with fraction collection (SPFC-UBM)**

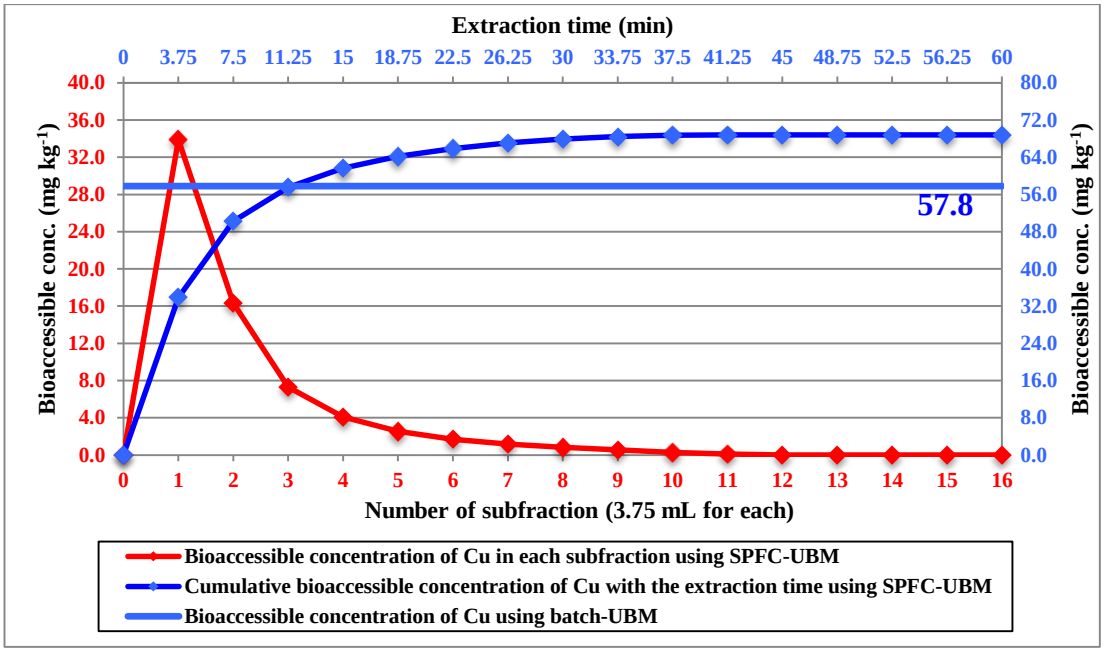


**Figure 5.47. Bioaccessible concentration of Cu in subfractions obtained by extraction of the simulated $PM_{10}$ samples (NIST SRM 2711A Montana II Soil on FDMS filter) using the single-pass dynamic model of the stomach phase of the unified bioaccessibility method (UBM) with fraction collection (SPFC-UBM)**

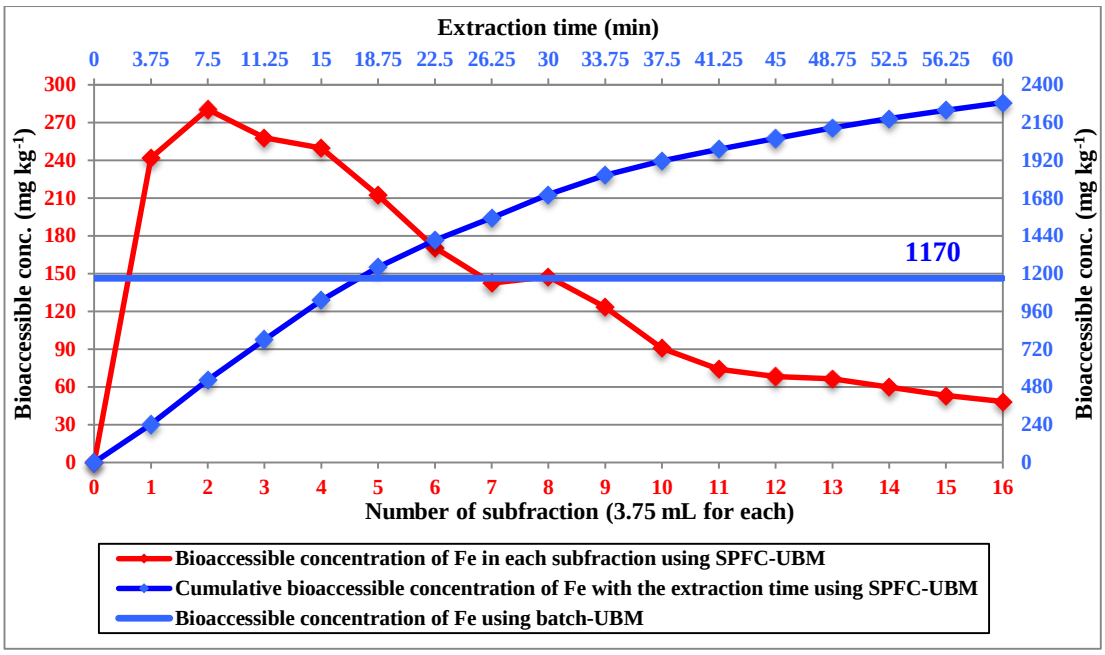


**Figure 5.48. Bioaccessible concentration of Fe in subfractions obtained by extraction of the simulated $PM_{10}$ samples (BGS RM 102 Ironstone Soil on FDMS filter) using the single-pass dynamic model of the stomach phase of the unified bioaccessibility method (UBM) with fraction collection (SPFC-UBM)**

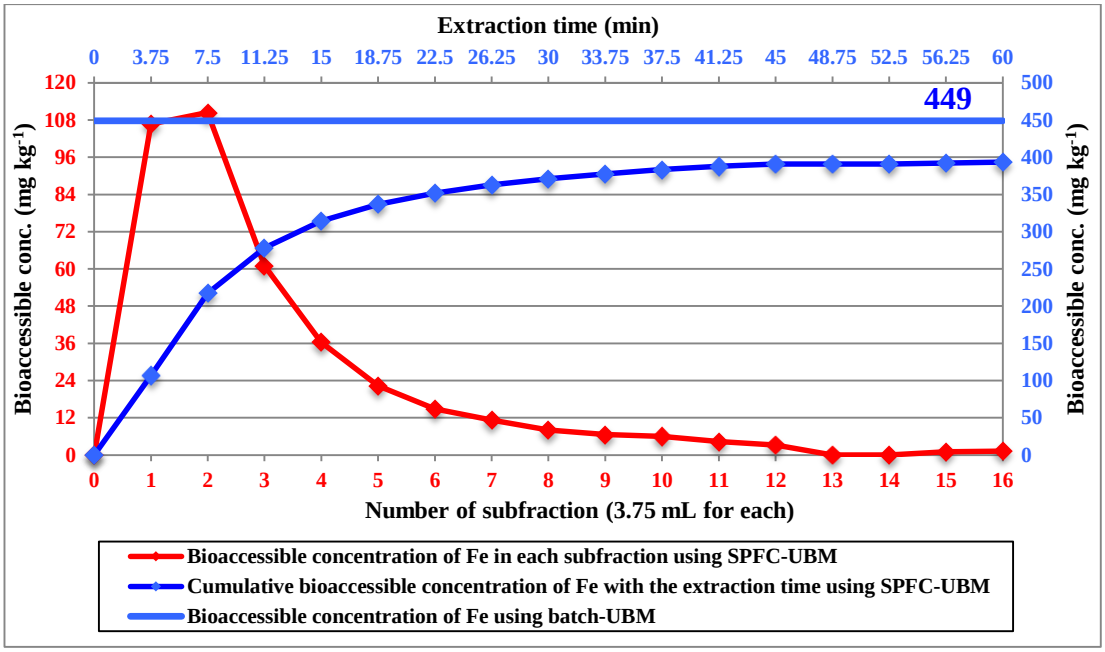


**Figure 5.49. Bioaccessible concentration of Fe in subfractions obtained by extraction of the simulated $PM_{10}$ samples (NIST SRM 2711A Montana II Soil on FDMS filter) using the single-pass dynamic model of the stomach phase of the unified bioaccessibility method (UBM) with fraction collection (SPFC-UBM)**

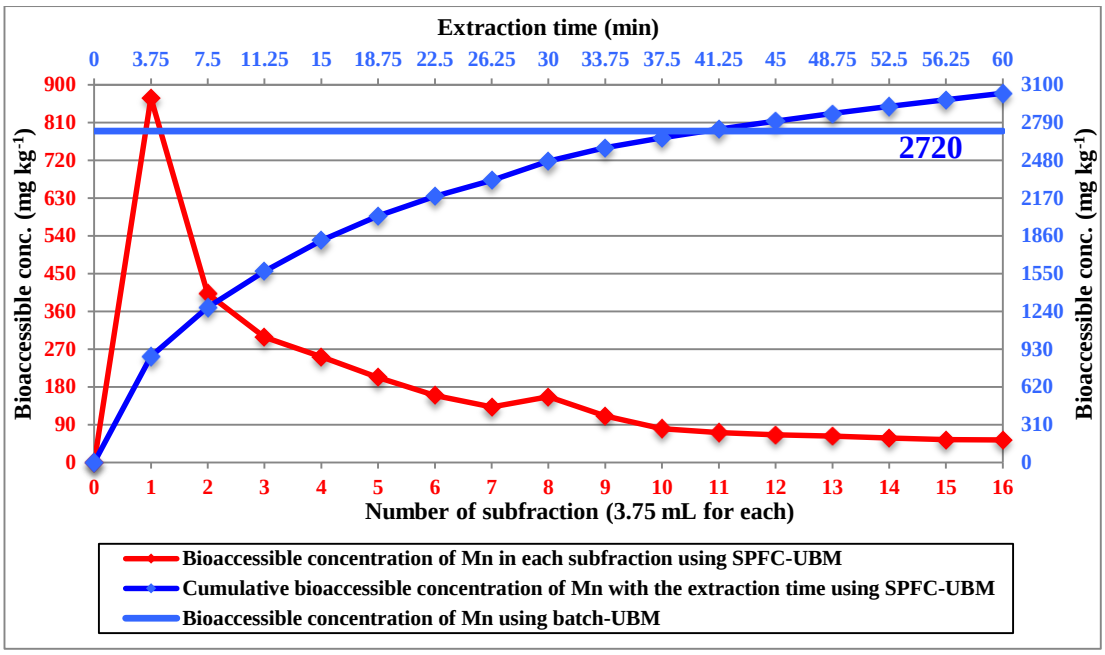


**Figure 5.50. Bioaccessible concentration of Mn in subfractions obtained by extraction of the simulated $PM_{10}$ samples (BGS RM 102 Ironstone Soil on FDMS filter) using the single-pass dynamic model of the stomach phase of the unified bioaccessibility method (UBM) with fraction collection (SPFC-UBM)**

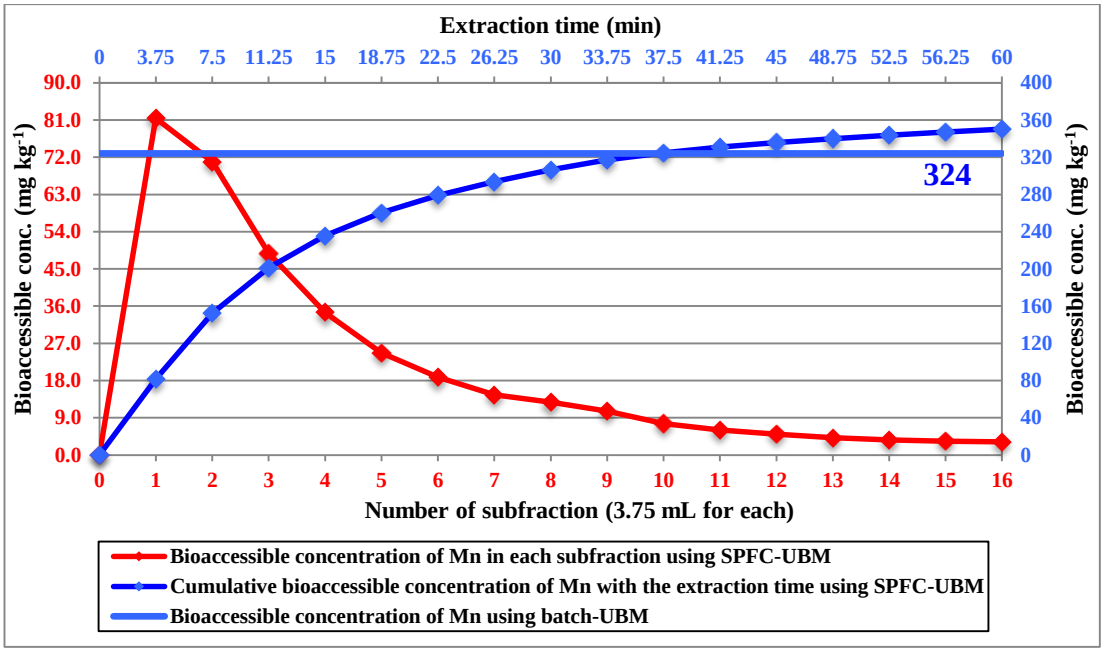


**Figure 5.51. Bioaccessible concentration of Mn in subfractions obtained by extraction of the simulated $PM_{10}$ samples (NIST SRM 2711A Montana II Soil on FDMS filter) using the single-pass dynamic model of the stomach phase of the unified bioaccessibility method (UBM) with fraction collection (SPFC-UBM)**

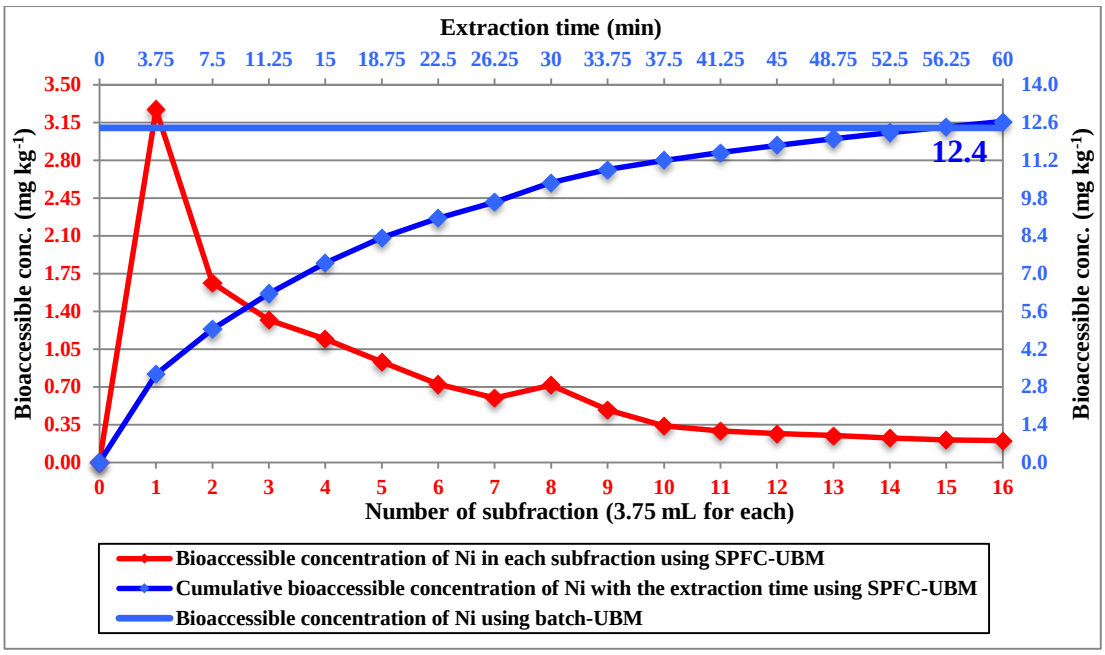


**Figure 5.52. Bioaccessible concentration of Ni in subfractions obtained by extraction of the simulated $PM_{10}$ samples (BGS RM 102 Ironstone Soil on FDMS filter) using the single-pass dynamic model of the stomach phase of the unified bioaccessibility method (UBM) with fraction collection (SPFC-UBM)**

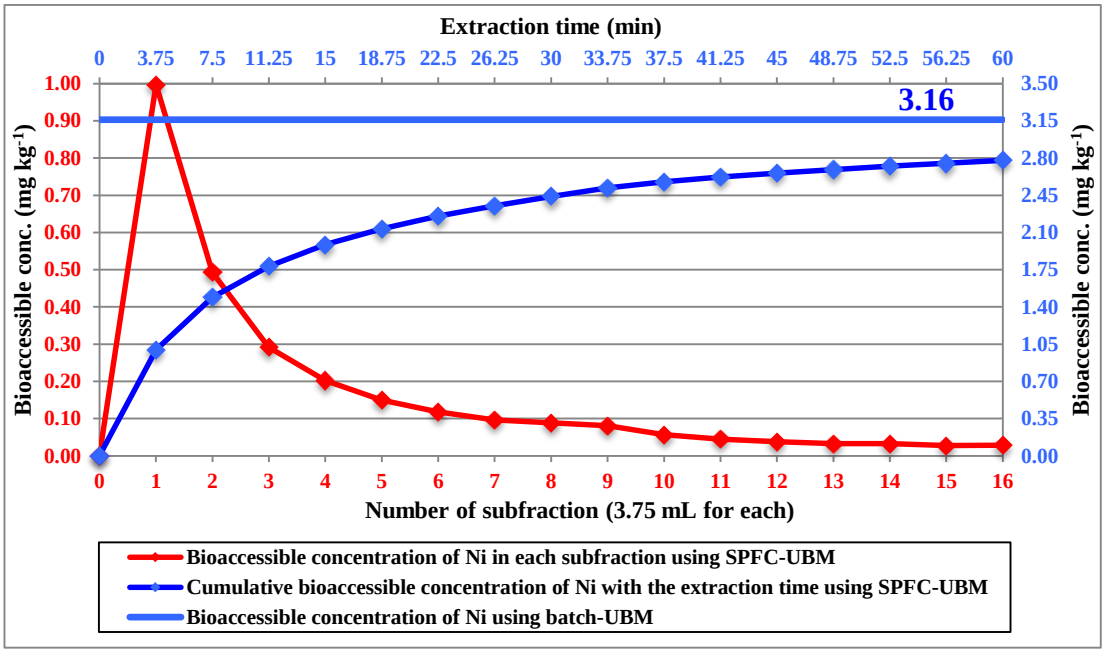


**Figure 5.53. Bioaccessible concentration of Ni in subfractions obtained by extraction of the simulated $PM_{10}$ samples (NIST SRM 2711A Montana II Soil on FDMS filter) using the single-pass dynamic model of the stomach phase of the unified bioaccessibility method (UBM) with fraction collection (SPFC-UBM)**

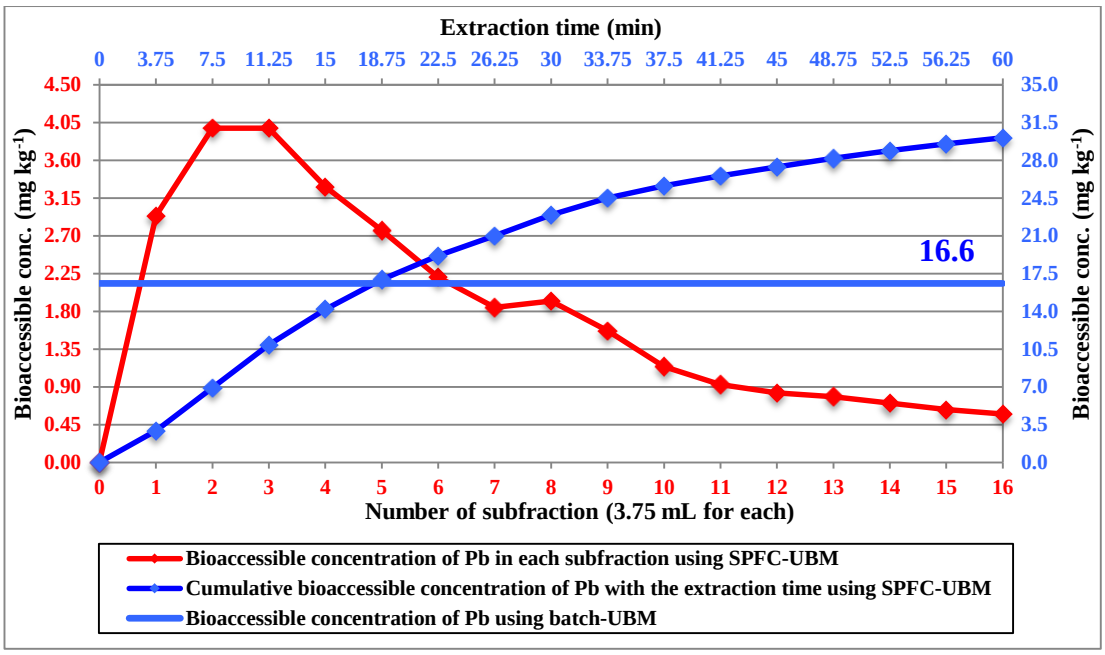


**Figure 5.54. Bioaccessible concentration of Pb in subfractions obtained by extraction of the simulated $PM_{10}$ samples (BGS RM 102 Ironstone Soil on FDMS filter) using the single-pass dynamic model of the stomach phase of the unified bioaccessibility method (UBM) with fraction collection (SPFC-UBM)**

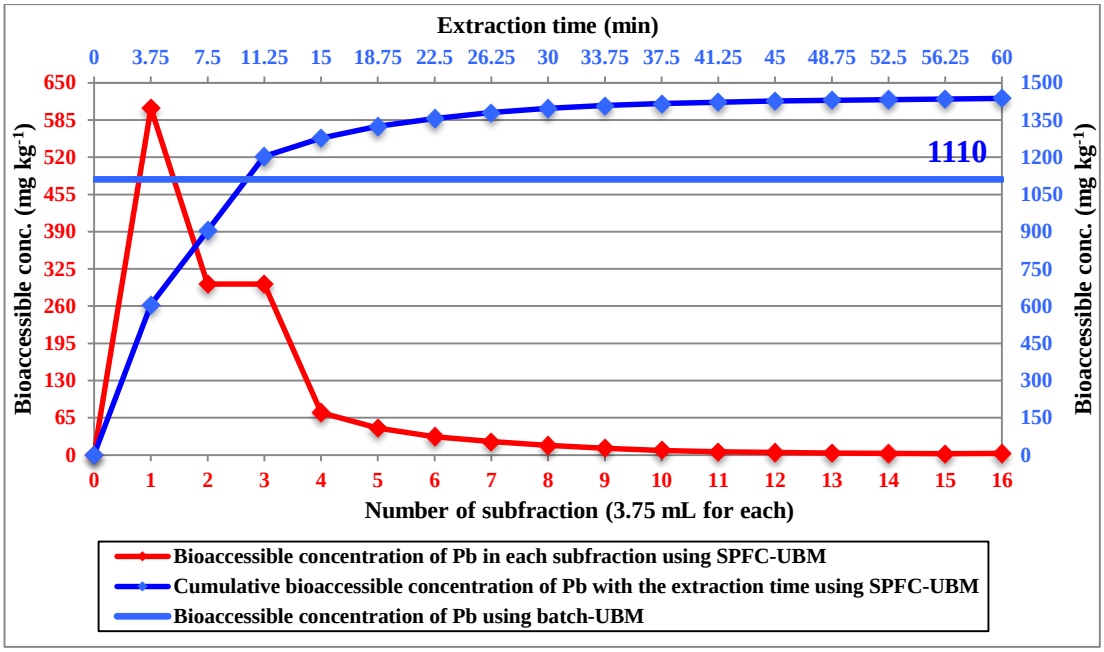


**Figure 5.55. Bioaccessible concentration of Pb in subfractions obtained by extraction of the simulated $PM_{10}$ samples (NIST SRM 2711A Montana II Soil on FDMS filter) using the single-pass dynamic model of the stomach phase of the unified bioaccessibility method (UBM) with fraction collection (SPFC-UBM)**

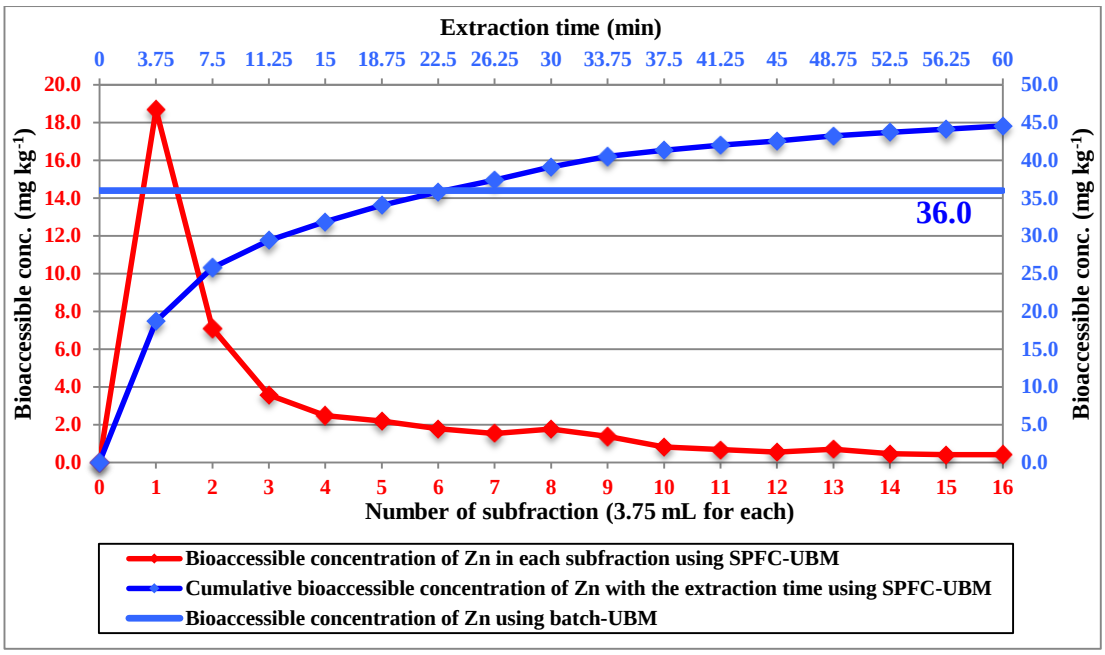


**Figure 5.56. Bioaccessible concentration of Zn in subfractions obtained by extraction of the simulated $PM_{10}$ samples (BGS RM 102 Ironstone Soil on FDMS filter) using the single-pass dynamic model of the stomach phase of the unified bioaccessibility method (UBM) with fraction collection (SPFC-UBM)**

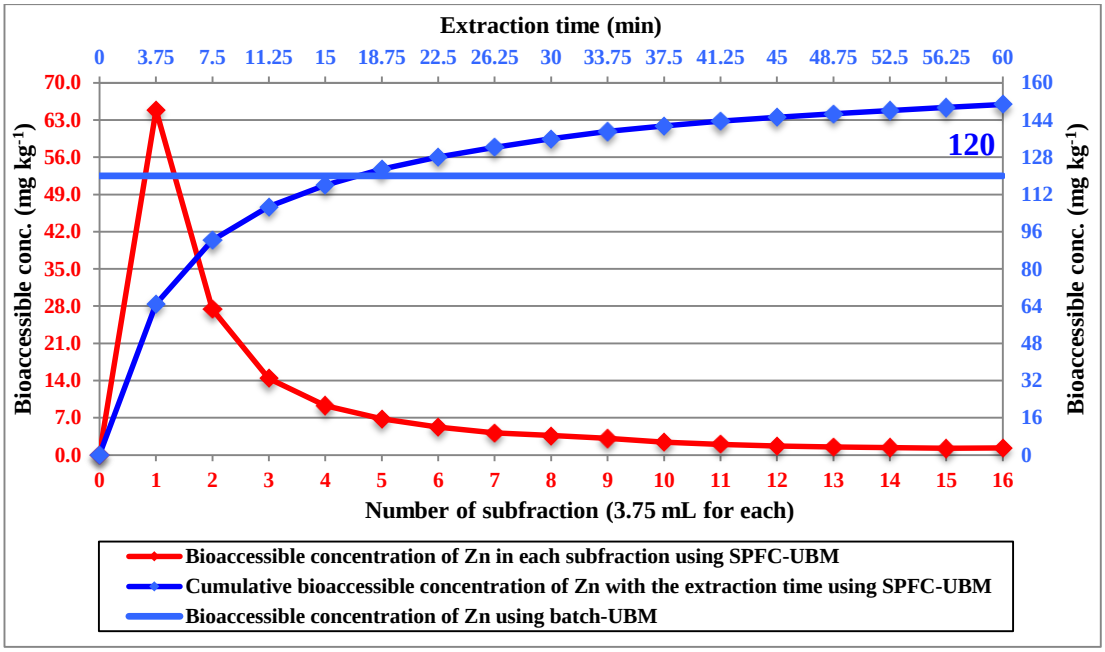


**Figure 5.57. Bioaccessible concentration of Zn in subfractions obtained by extraction of the simulated $PM_{10}$ samples (NIST SRM 2711A Montana II Soil on FDMS filter) using the single-pass dynamic model of the stomach phase of the unified bioaccessibility method (UBM) with fraction collection (SPFC-UBM)**

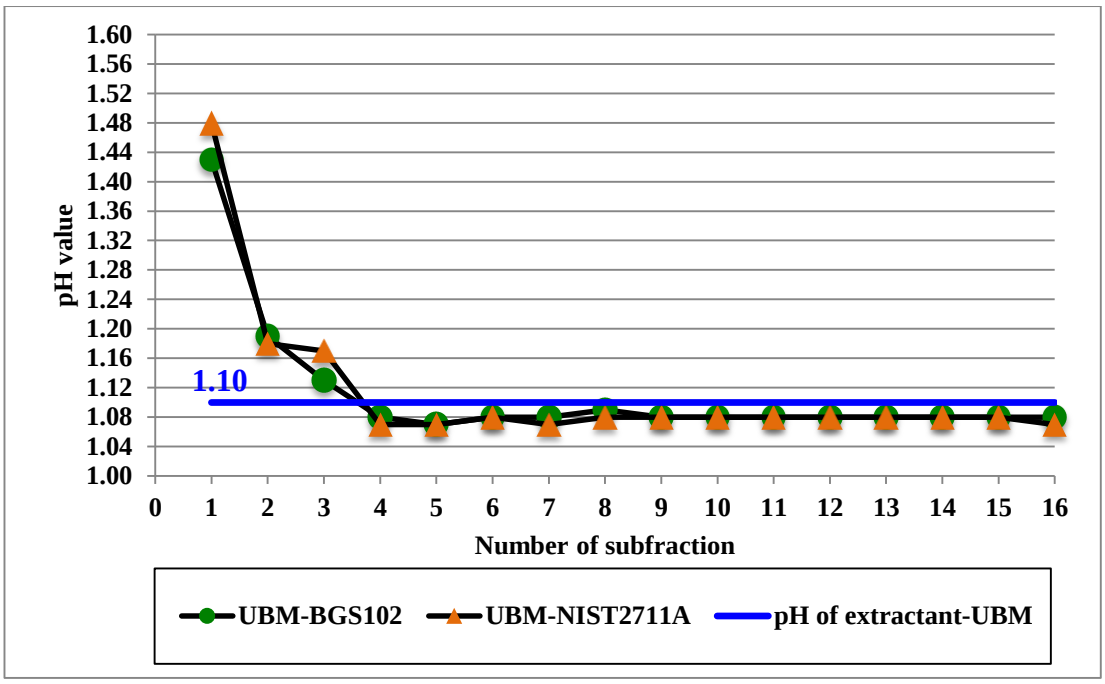


**Figure 5.58. Values of pH for each subfraction obtained by applying the single-pass dynamic model of the stomach phase of the unified bioaccessibility method (UBM) with fraction collection (SPFC-UBM) using BGS RM 102 Ironstone Soil and NIST SRM 2711A Montana II Soil**

### 5.3.2.5. Mass balance

Tables 5.17-5.20 show the bioaccessible and residual fractions of PTE as well as the sum of fractions with respect to the pseudototal PTE content (i.e. mass balance). These fractions were extracted from simulated $PM_{10}$ samples prepared using BGS RM 102 Ironstone Soil and NIST SRM 2711A Montana II Soil, by the batch models, SPFC-SBET, and the SPFC-UBM. Values of Z-score shown in Tables 5.17-5.20 were calculated using Equations 2.28 and 2.30. According to these values, mass balance was verified, where in general, the sum of fractions was in agreement with the measured pseudototal PTE concentration for both batch and the SPFC models. For the batch model of the SBET, 73% of Z-scores were acceptable, 20% satisfactory, and 7% not satisfactory, while for batch model of the stomach phase of the UBM, 53% were acceptable, 27% satisfactory, and 20% not satisfactory. For the SPFC-SBET, 100% of Z-scores were acceptable, while for the SPFC-UBM, 88% were acceptable and 12% satisfactory. For Zn, Z-score was not calculated, as the pseudototal content of blank FDMS filters was variable (see Tables 5.15 and 5.16).

**Table 5.17. Concentrations of potentially toxic elements (PTE) in the bioaccessible and residual fractions, together with pseudototal content and mass balance in simulated $PM_{10}$ samples (BGS RM 102 Ironstone Soil on FDMS filters) using the single-pass dynamic model of the simplified bioaccessibility extraction test (SBET) with fraction collection (SPFC-SBET)**

| PTE | Models | Bioaccessible fraction (mg $kg^{-1}$) Mean (n=3) ± U (% RSD) | Residual fraction (mg $kg^{-1}$) Mean (n=3) ± U | Sum ± $U_C$ (mg $kg^{-1}$) | Pseudototal (mg $kg^{-1}$) Mean (n=3) ± U | % Mass balance ± $U_C$ | %Spike recovery | Z-Score |
|---|---|---|---|---|---|---|---|---|
| **As** | **Batch** | 2.36 ± 0.27 **(0.314)** | 82.9 ± 9.6 | 85.3 ± 9.6 | 98.1 ± 11.3 | 86.9 ± 14.0 | 100 | -1.8 |
| | **SPFC** | 3.20 ± 0.37 **(14.5)** | 90.6 ± 10.5 | 93.8 ± 10.5 | 100 ± 12 | 93.4 ± 15.0 | 102 | -0.9 |
| **Cd** | **Batch** | 0.208 ± 0.024 **(1.27)** | < RB | NC | < RB | NC | 100 | NC |
| | **SPFC** | 0.147 ± 0.017 **(13.4)** | 0.155 ± 0.018 | 0.302 ± 0.025 | 0.304 ± 0.035 | 99.4 ± 14.1 | 102 | -0.1 |
| **Cr** | **Batch** | 35.4 ± 4.1 **(2.74)** | 140 ± 16 | 176 ± 17 | 188 ± 22 | 93.6 ± 14.0 | 101 | -0.9 |
| | **SPFC** | 32.9 ± 3.8 **(7.82)** | 143 ± 17 | 176 ± 17 | 196 ± 23 | 90.0 ± 13.5 | 100 | -1.4 |
| **Cu** | **Batch** | 7.84 ± 0.91 **(0.514)** | 12.8 ± 1.5 | 20.6 ± 1.7 | 27.5 ± 3.2 | 75.0 ± 10.7 | 104 | -3.5 |
| | **SPFC** | 8.36 ± 0.97 **(16.0)** | 16.7 ± 1.9 | 25.1 ± 2.2 | 23.8 ± 2.7 | 105 ± 15 | 101 | 0.8 |
| **Fe** | **Batch** | 2100 ± 242 **(0.073)** | 115000 ± 13300 | 117000 ± 13300 | 135000 ± 15600 | 86.4 ± 14.0 | 103 | -1.9 |
| | **SPFC** | 1930 ± 223 **(9.95)** | 127000 ± 14700 | 129000 ± 14700 | 139000 ± 16000 | 92.9 ± 15.1 | 100 | -1.0 |
| **Mn** | **Batch** | 2200 ± 254 **(1.45)** | 3950 ± 456 | 6150 ± 522 | 6410 ± 740 | 96.0 ± 13.8 | 104 | -0.6 |
| | **SPFC** | 1950 ± 225 **(6.71)** | 4260 ± 492 | 6210 ± 541 | 6530 ± 755 | 95.0 ± 13.7 | 100 | -0.7 |
| **Ni** | **Batch** | 10.6 ± 1.2 **(2.77)** | 58.4 ± 6.7 | 69.0 ± 6.9 | 72.7 ± 8.4 | 95.0 ± 14.5 | 103 | -0.7 |
| | **SPFC** | 8.75 ± 1.01 **(7.69)** | 60.4 ± 7.0 | 69.1 ± 7.0 | 74.0 ± 8.5 | 93.5 ± 14.4 | 101 | -0.9 |
| **Pb** | **Batch** | 22.6 ± 2.6 **(3.42)** | 47.9 ± 5.5 | 70.5 ± 6.1 | 74.9 ± 8.6 | 94.2 ± 13.6 | 101 | -0.8 |
| | **SPFC** | 21.0 ± 2.4 **(9.36)** | 54.0 ± 6.2 | 75.1 ± 6.7 | 77.3 ± 8.9 | 97.1 ± 14.2 | 100 | -0.4 |
| **Zn** | **Batch** | 39.7 ± 4.6 **(8.17)** | < FB | NC | < FB | NC | 87 | NC |
| | **SPFC** | 32.2 ± 3.7 **(6.54)** | < FB | NC | < FB | NC | 102 | NC |

$U = \frac{(K \times \text{Mean} \times \%RSD)}{100 \times \sqrt{n}}$ , K = 2, % RSD = 10, n= number of replicates; $Z - \text{Score} = \frac{(\text{Sum} - \text{Pseudototal})}{SD_R/\sqrt{n}}$, $SD_R = \frac{\text{Mean of pseudototal} \times 10}{100}$, n= number of independent replicates; $U_C$: combined uncertainty; Sum = (Bioaccessible fraction + Residual fraction); % Mass balance = $\frac{\text{Sum}}{\text{pseudototal}} \times 100$; < RB: less than reagent blank; < FB: less than filter blank; NC: not calculated

**Table 5.18. Concentrations of potentially toxic elements (PTE) in the bioaccessible and residual fractions, together with pseudototal content and mass balance in simulated $PM_{10}$ samples (NIST SRM 2711A Montana II Soil on FDMS filters) using the single-pass dynamic model of the simplified bioaccessibility extraction test (SBET) with fraction collection (SPFC-SBET)**

| PTE | Models | Bioaccessible fraction (mg $kg^{-1}$) Mean (n=3) ± U (% RSD) | Residual fraction (mg $kg^{-1}$) Mean (n=3) ± U | Sum ± $U_C$ (mg $kg^{-1}$) | Pseudototal (mg $kg^{-1}$) Mean (n=3) ± U | % Mass balance ± $U_C$ | Z-Score |
|---|---|---|---|---|---|---|---|
| **As** | **Batch** | 57.8 ± 6.7 **(1.26)** | 37.7 ± 4.4 | 95.4 ± 8.0 | 94.7 ± 10.9 | 101 ± 14 | 0.1 |
| | **SPFC** | 54.1 ± 6.2 **(3.45)** | 40.0 ± 4.6 | 94.1 ± 7.8 | 94.9 ± 11.0 | 99.1 ± 14.1 | -0.1 |
| **Cd** | **Batch** | 47.1 ± 5.4 **(2.32)** | 5.18 ± 0.60 | 52.2 ± 5.5 | 49.3 ± 5.7 | 106 ± 17 | 0.8 |
| | **SPFC** | 46.2 ± 5.3 **(4.33)** | 5.16 ± 0.60 | 51.4 ± 5.4 | 50.2 ± 5.8 | 102 ± 16 | 0.3 |
| **Cr** | **Batch** | 0.899 ± 0.104 **(2.57)** | 24.9 ± 2.9 | 25.8 ± 2.9 | 32.1 ± 3.7 | 80.3 ± 12.9 | -2.8 |
| | **SPFC** | 0.803 ± 0.093 **(5.01)** | 29.6 ± 3.4 | 30.4 ± 3.4 | 30.9 ± 3.6 | 98.6 ± 15.9 | -0.2 |
| **Cu** | **Batch** | 59.9 ± 6.9 **(2.69)** | 59.4 ± 6.9 | 119 ± 10 | 130 ± 15 | 91.7 ± 13.0 | -1.2 |
| | **SPFC** | 67.4 ± 7.8 **(3.51)** | 59.1 ± 6.8 | 127 ± 10 | 130 ± 15 | 97.4 ± 13.8 | -0.4 |
| **Fe** | **Batch** | 544 ± 63 **(2.67)** | 19400 ± 2240 | 19900 ± 2240 | 24500 ± 2830 | 81.3 ± 13.1 | -2.6 |
| | **SPFC** | 554 ± 64 **(0.661)** | 23400 ± 2700 | 24000 ± 2700 | 24300 ± 2810 | 98.7 ± 15.9 | -0.2 |
| **Mn** | **Batch** | 215 ± 25 **(1.97)** | 281 ± 32 | 496 ± 41 | 573 ± 66 | 86.7 ± 12.3 | -1.9 |
| | **SPFC** | 176 ± 20 **(4.11)** | 389 ± 45 | 565 ± 49 | 574 ± 66 | 98.4 ± 14.2 | -0.2 |
| **Ni** | **Batch** | 2.92 ± 0.34 **(2.34)** | 12.5 ± 1.4 | 15.4 ± 1.5 | 18.4 ± 2.1 | 83.9 ± 12.6 | -2.3 |
| | **SPFC** | 2.48 ± 0.29 **(5.62)** | 15.3 ± 1.8 | 17.8 ± 1.8 | 18.0 ± 2.1 | 98.9 ± 15.2 | -0.2 |
| **Pb** | **Batch** | 1100 ± 127 **(2.75)** | 265 ± 31 | 1360 ± 131 | 1310 ± 151 | 104 ± 16 | 0.5 |
| | **SPFC** | 1180 ± 136 **(3.56)** | 164 ± 19 | 1340 ± 138 | 1320 ± 152 | 102 ± 16 | 0.2 |
| **Zn** | **Batch** | 130 ± 15 **(3.53)** | < FB | NC | < FB | NC | NC |
| | **SPFC** | 137 ± 16 **(4.28)** | < FB | NC | < FB | NC | NC |

$U = \frac{(K\times \text{Mean} \times \%RSD)}{100 \times \sqrt{n}}$ , K = 2, % RSD = 10, n= number of replicates; $Z-\text{Score} = \frac{(\text{Sum}-\text{Pseudototal})}{SD_R/\sqrt{n}}$, $SD_R = \frac{\text{Mean of pseudototal} \times 10}{100}$, n= number of independent replicates; $U_C$: combined uncertainty; $\text{Sum} = (\text{Bioaccessible fraction} + \text{Residual fraction})$; $\%\ \text{Mass balance} = \frac{\text{Sum}}{\text{pseudototal}} \times 100$; < FB: less than filter blank; < RB: less than reagent blank; NC: not calculated

**Table 5.19. Concentrations of potentially toxic elements (PTE) in the bioaccessible and residual fractions, together with pseudototal content and mass balance in simulated $PM_{10}$ samples (BGS RM 102 Ironstone Soil on FDMS filters) using the single-pass dynamic model of the stomach phase of the unified bioaccessibility method (UBM) with fraction collection (SPFC-UBM)**

| PTE | Models | Bioaccessible fraction (mg $kg^{-1}$) Mean (n=3) ± U (% RSD) | Residual fraction (mg $kg^{-1}$) Mean (n=3) ± U | Sum ± $U_C$ (mg $kg^{-1}$) | Pseudototal (mg $kg^{-1}$) Mean (n=3) ± U | % Mass balance ± $U_C$ | %Spike recovery | Z-Score |
|---|---|---|---|---|---|---|---|---|
| **As** | **Batch** | 4.97 ± 0.57 **(0.945)** | 76.0 ± 8.8 | 81.0 ± 8.8 | 104 ± 12 | 77.6 ± 12.3 | 98 | -3.2 |
| | **SPFC** | 8.49 ± 0.98 **(0.956)** | 89.7 ± 10.4 | 98.2 ± 10.4 | 99.5 ± 11.5 | 98.7 ± 15.5 | 95 | -0.2 |
| **Cd** | **Batch** | 0.221 ± 0.026 **(1.28)** | < RB | NC | < RB | NC | 99 | NC |
| | **SPFC** | 0.209 ± 0.024 **(12.5)** | 0.105 ± 0.012 | 0.314 ± 0.027 | 0.332 ± 0.038 | 94.7 ± 13.6 | 93 | -0.7 |
| **Cr** | **Batch** | 36.5 ± 4.2 **(0.383)** | 118 ± 14 | 155 ± 14 | 187 ± 22 | 82.8 ± 12.2 | 97 | -2.4 |
| | **SPFC** | 39.4 ± 4.5 **(0.179)** | 139 ± 16 | 178 ± 17 | 188 ± 22 | 94.9 ± 14.1 | 96 | -0.7 |
| **Cu** | **Batch** | 7.76 ± 0.90 **(6.48)** | 16.1 ± 1.9 | 23.9 ± 2.1 | 24.8 ± 2.9 | 96.1 ± 13.9 | 94 | -0.5 |
| | **SPFC** | 5.60 ± 0.65 **(14.3)** | 14.9 ± 1.7 | 20.5 ± 1.8 | 23.2 ± 2.7 | 88.3 ± 12.9 | 95 | -1.7 |
| **Fe** | **Batch** | 1170 ± 135 **(2.00)** | 105000 ± 12100 | 106000 ± 12100 | 137000 ± 15800 | 77.4 ± 12.6 | 87 | -3.2 |
| | **SPFC** | 2250 ± 260 **(0.563)** | 128000 ± 14800 | 130000 ± 14800 | 130000 ± 15000 | 99.9 ± 16.2 | 91 | 0.0 |
| **Mn** | **Batch** | 2720 ± 314 **(0.571)** | 3490 ± 403 | 6210 ± 511 | 6600 ± 762 | 94.2 ± 13.4 | 101 | -0.8 |
| | **SPFC** | 2990 ± 345 **(1.68)** | 3500 ± 404 | 6490 ± 532 | 6270 ± 724 | 104 ± 15 | 95 | 0.5 |
| **Ni** | **Batch** | 12.4 ± 1.4 **(0.378)** | 51.3 ± 5.9 | 63.7 ± 6.1 | 75.5 ± 8.7 | 84.4 ± 12.7 | 98 | -2.2 |
| | **SPFC** | 12.5 ± 1.4 **(1.91)** | 60.0 ± 6.9 | 72.5 ± 7.1 | 71.3 ± 8.2 | 102 ± 15 | 96 | 0.2 |
| **Pb** | **Batch** | 16.6 ± 1.9 **(1.44)** | 53.1 ± 6.1 | 69.7 ± 6.4 | 78.0 ± 9.0 | 89.3 ± 13.2 | 100 | -1.5 |
| | **SPFC** | 29.6 ± 3.4 **(1.15)** | 42.0 ± 4.8 | 71.6 ± 5.9 | 74.9 ± 8.7 | 95.6 ± 13.6 | 97 | -0.6 |
| **Zn** | **Batch** | 36.0 ± 4.2 **(1.44)** | < FB | NC | < FB | NC | 112 | NC |
| | **SPFC** | 44.0 ± 5.1 **(1.15)** | < FB | NC | < FB | NC | 90 | NC |

$U = \frac{(K \times \text{Mean} \times \%RSD)}{100 \times \sqrt{n}}$ , K = 2, % RSD = 10, n= number of replicates; $Z - \text{Score} = \frac{(\text{Sum} - \text{Pseudototal})}{SD_R/\sqrt{n}}$, $SD_R = \frac{\text{Mean of pseudototal} \times 10}{100}$, n= number of independent replicates; $U_C$: combined uncertainty; Sum = (Bioaccessible fraction + Residual fraction); % Mass balance = $\frac{\text{Sum}}{\text{pseudototal}} \times 100$; < FB: less than filter blank; < RB: less than reagent blank; NC: not calculated

**Table 5.20. Concentrations of potentially toxic elements (PTE) in the bioaccessible and residual fractions, together with pseudototal content and mass balance in simulated $PM_{10}$ samples (NIST SRM 2711A Montana II Soil on FDMS filters) using the single-pass dynamic model of the stomach phase of the unified bioaccessibility method (UBM) with fraction collection (SPFC-UBM)**

| PTE | Models | Bioaccessible fraction (mg $kg^{-1}$) Mean (n=3) ± U (% RSD) | Residual fraction (mg $kg^{-1}$) Mean (n=3) ± U | Sum ± $U_C$ (mg $kg^{-1}$) | Pseudototal (mg $kg^{-1}$) Mean (n=3) ± U | % Mass balance ± $U_C$ | Z-Score |
|---|---|---|---|---|---|---|---|
| **As** | **Batch** | 57.5 ± 6.6 **(1.40)** | 37.0 ± 4.3 | 94.6 ± 7.9 | 96.8 ± 11.2 | 97.7 ± 13.9 | -0.3 |
| | **SPFC** | 61.0 ± 7.0 **(5.26)** | 37.4 ± 4.3 | 98.3 ± 8.3 | 92.1 ± 10.6 | 107 ± 15 | 1.0 |
| **Cd** | **Batch** | 45.0 ± 5.2 **(0.284)** | 6.84 ± 0.79 | 51.9 ± 5.3 | 49.1 ± 5.7 | 106 ± 16 | 0.8 |
| | **SPFC** | 50.1 ± 5.8 **(4.49)** | 4.58 ± 0.53 | 54.7 ± 5.8 | 47.7 ± 5.5 | 115 ± 18 | 2.1 |
| **Cr** | **Batch** | 0.876 ± 0.101 **(0.393)** | 21.9 ± 2.5 | 22.7 ± 2.5 | 31.5 ± 3.6 | 72.1 ± 11.6 | -3.9 |
| | **SPFC** | 0.462 ± 0.053 **(7.79)** | 28.5 ± 3.3 | 29.0 ± 3.3 | 29.6 ± 3.4 | 97.7 ± 15.8 | -0.3 |
| **Cu** | **Batch** | 57.8 ± 6.7 **(0.946)** | 68.2 ± 7.9 | 126 ± 10 | 134 ± 16 | 93.7 ± 13.3 | -0.9 |
| | **SPFC** | 68.8 ± 7.9 **(6.74)** | 33.2 ± 3.8 | 102 ± 9 | 102 ± 12 | 100 ± 14 | 0.0 |
| **Fe** | **Batch** | 449 ± 52 **(1.84)** | 18600 ± 2150 | 19100 ± 2150 | 24400 ± 2810 | 78.4 ± 12.6 | -3.0 |
| | **SPFC** | 396 ± 46 **(10.3)** | 22300 ± 2580 | 22700 ± 2580 | 22800 ± 2640 | 99.5 ± 16.1 | -0.1 |
| **Mn** | **Batch** | 324 ± 37 **(0.263)** | 199 ± 23 | 523 ± 44 | 579 ± 67 | 90.4 ± 12.9 | -1.4 |
| | **SPFC** | 350 ± 40 **(5.83)** | 225 ± 26 | 575 ± 48 | 542 ± 63 | 106 ± 15 | 0.9 |
| **Ni** | **Batch** | 3.16 ± 0.37 **(1.30)** | 13.0 ± 1.5 | 16.1 ± 1.5 | 19.1 ± 2.2 | 84.6 ± 12.7 | -2.2 |
| | **SPFC** | 2.78 ± 0.32 **(5.52)** | 15.0 ± 1.7 | 17.8 ± 1.8 | 17.7 ± 2.0 | 100 ± 15 | 0.1 |
| **Pb** | **Batch** | 1110 ± 128 **(1.05)** | 316 ± 36 | 1430 ± 133 | 1310 ± 151 | 109 ± 16 | 1.3 |
| | **SPFC** | 1410 ± 166 **(0.420)** | 114 ± 13 | 1524 ± 166 | 1270 ± 147 | 120 ± 19 | 2.8 |
| **Zn** | **Batch** | 120 ± 14 **(5.26)** | < FB | NC | < FB | NC | NC |
| | **SPFC** | 151 ± 17 **(2.03)** | < FB | NC | < FB | NC | NC |

$U = \frac{(K\times \text{Mean} \times \%RSD)}{100 \times \sqrt{n}}$ , K = 2, % RSD = 10, n= number of replicates; $Z - \text{Score} = \frac{(\text{Sum}-\text{Pseudototal})}{SD_R/\sqrt{n}}$, $SD_R = \frac{\text{Mean of pseudototal} \times 10}{100}$, n= number of independent replicates; $U_C$: combined uncertainty; $\text{Sum} = (\text{Bioaccessible fraction} + \text{Residual fraction})$; $\%\ \text{Mass balance} = \frac{\text{Sum}}{\text{pseudototal}} \times 100$; < FB: less than filter blank; < RB: less than reagent blank; NC: not calculated

#### 5.3.2.6. Quality control

The RSD was used to ascertain the precision of the models of the SBET and the stomach phase of the UBM. All of the RSD's values were less than 10% for the batch models of the SBET and the stomach phase of the UBM. For the SPFC-SBET and SPFC-UBM, 83% of RSD's values were less than 10% (see Tables 5.17-5.20). However, the remaining 17% of RSD's values for the SPFC-SBET and for the SPFC-UBM ranged from 13.4 to 16.0% and from 10.3 to 14.3%, respectively.

In addition to validation of the mass balance as described in Section 5.3.2.5, a spike recovery test for a known amount of PTE spiked into the methods' extractants was also performed. For the batch model of the SBET, spike recoveries were 100 ± 4% (except for Zn, where it was 87%), whilst for the SPFC-SBET, they were 100 ± 2%. For the spiked extractant of stomach phase of the UBM, recoveries were 100 ± 6% (except for Fe and Zn, which were 87 and 112%, respectively) for the batch model, and 100 ± 10% for the SPFC-UBM (see Tables 5.17 and 5.19).

Although the recommended value of Pb in NIST SRM 2711A and the guidance values of As, Cd, and Pb in BGS RM 102 were established for the batch models of the SBET and the stomach phase of the UBM, respectively, these values were also used to verify the accuracy of the dynamic models. Recoveries of these values are shown in Table 5.21. For the SPFC-SBET, the recovery was in a good agreement with the recommended Pb value (106 ± 6%), however, for the SPFC-UBM, only the Cd bioaccessible value was within the guidance value.

Accuracy of *aqua regia* microwave digestion was ascertained using BCR CRM 143R Sewage Sludge Amended Soil and the recoveries obtained were calculated with respect to certified values as illustrated in Table 5.22. All were in agreement with the certified values, where they were within 100 ± 7%.

**Table 5.21. Recoveries of recommended or guidance values for the bioaccessible concentration of potentially toxic elements (PTE) in simulated $PM_{10}$ samples prepared using BGS RM 102 Ironstone Soil and NIST SRM 2711A Montana II Soil extracted by applying the single-pass dynamic model with fraction collection of the simplified bioaccessibility extraction test (SPFC-SBET) and the stomach phase of the unified bioaccessibility method (SPFC-UBM)**

| PTE | Bioaccessible fraction Mean ± SD ($mg.kg^{-1}$) | Recommended or guidance values Mean ± SD ($mg.kg^{-1}$) | % Recovery of recommended or guidance (for stomach phase) values |
|---|---|---|---|
| | **SPFC-SBET** | | |
| **Pb in NIST2711A** | 1180 ± 42 | 1110 ± 49 | 106 ± 6 |
| | **SPFC-UBM** | | |
| **As in BGS102** | 8.49 ± 0.08 | 4.52 ± 1.28 | 188 ± 53 |
| **Cd in BGS102** | 0.209 ± 0.026 | 0.281 ± 0.170 | 74 ± 46 |
| **Pb in BGS102** | 29.6 ± 0.3 | 13 ± 6 | 227 ± 105 |

SD: standard deviation

**Table 5.22. Comparison between found and certified values for BCR CRM 143R Sewage Sludge Amended Soil subjected to microwave assisted *aqua regia* digestion in parallel to residual material from the single-pass dynamic model with fraction collection of the simplified bioaccessibility extraction test (SPFC-SBET) and the stomach phase of the unified bioaccessibility method (SPFC-UBM)**

| PTE | Cd | Cr | Mn | Ni | Pb | Zn |
|---|---|---|---|---|---|---|
| **Certified pseudototal values (Mean ± SD)** | 72.0 ± 1.8 | 426 ± 12 | 858 ± 11 | 296 ± 4 | 174 ± 5 | 1063 ± 16 |
| **Measured pseudototal PTE content for the SPFC-SBET** | | | | | | |
| **Measured values (Mean ± SD)** | 70.0 ± 1.0 | 460 ± 5 | 892 ± 11 | 294 ± 8 | 173 ± 3 | 1030 ± 5 |
| **% Recovery** | 97.2 ± 2.8 | 108 ± 3 | 104 ± 2 | 99.4 ± 2.9 | 99.5 ± 3.4 | 96.8 ± 1.5 |
| **Measured pseudototal PTE content for the SPFC-UBM** | | | | | | |
| **Measured values (Mean ± SD)** | 67.0 ± 0.3 | 438 ± 21 | 849 ± 1 | 283 ± 2 | 170 ± 4 | 990 ± 2 |
| **% Recovery** | 93.1 ± 2.4 | 103 ± 6 | 98.9 ± 1.3 | 95.6 ± 1.5 | 97.6 ± 3.7 | 93.1 ± 1.4 |

SD: standard deviation

### 5.3.2.7. Analysis of real samples

To verify the applicability of use of this dynamic model to determine the bioaccessible concentration of PTE in real $PM_{10}$ samples, two real $PM_{10}$ samples for each method were analysed. As the aim of this work was not to assess inter-element associations or sources of air pollution in a certain area, the SPFC-SBET and the SPFC-UBM were conducted by continuously pumping 60 mL of the extractants at 1.0 mL $min^{-1}$ flow rate through real samples of $PM_{10}$. The leachate was then collected in one fraction (60 mL) instead of subfractions. The extracts were stored in polyethylene bottles at 4 °C prior to analysis by ICP-MS as described in Section 3.6. Table 5.23 shows the bioaccessible PTE concentration in real $PM_{10}$ samples. The results showed high bioaccessible concentration for Cu, Fe, Pb, and Zn. This was in agreement with results obtained by a study[106] conducted in an industrial city (Nanjing) in China, where the SBET was used to measure the bioaccessible concentration of PTE in total suspended particulates (TSP) and $PM_{2.5}$ collected on filters.

**Table 5.23. Bioaccessible concentration of potentially toxic elements (PTE) in real $PM_{10}$ samples obtained by applying the single-pass dynamic model with fraction collection of the simplified bioaccessibility extraction test (SPFC-SBET) and the stomach phase of the unified bioaccessibility method (SPFC-UBM)**

| PTE | SPFC-SBET (µg $filter^{-1}$) | | SPFC-SBET (ng $m^{-3}$) | | SPFC-UBM (µg $filter^{-1}$) | | SPFC-UBM (ng $m^{-3}$) | |
|---|---|---|---|---|---|---|---|---|
| | Byres Road | Broom Hill | Byres Road | Broom Hill | Nithsdale Road | High Street | Nithsdale Road | High Street |
| **As** | 0.037 | 0.038 | 0.617 | **NA** | 0.043 | 0.016 | 0.705 | **NA** |
| **Cd** | 0.013 | 0.009 | 0.213 | **NA** | < RB | 0.009 | < RB | **NA** |
| **Cr** | 0.010 | 0.015 | 0.158 | **NA** | < RB | < DL | < RB | **NA** |
| **Cu** | 0.673 | 0.828 | 11.1 | **NA** | 0.973 | 0.845 | 16.1 | **NA** |
| **Fe** | 1.14 | 1.891 | 18.8 | **NA** | < IDL | < IDL | < IDL | **NA** |
| **Mn** | 0.182 | 0.203 | 3.01 | **NA** | 0.158 | 0.146 | 2.62 | **NA** |
| **Ni** | 0.056 | 0.047 | 0.929 | **NA** | 0.028 | 0.007 | 0.464 | **NA** |
| **Pb** | 0.763 | 0.606 | 12.6 | **NA** | 0.486 | 0.409 | 8.03 | **NA** |
| **Zn** | 3.46 | 0.876 | 57.3 | **NA** | 3.64 | 11.2 | 60.1 | **NA** |

< RB: less than reagent blank; < IDL: less than instrumental detection limit; NA: no exposure dates available

## 5.4. Experiment 3: Single-pass dynamic extraction model with direct coupling to ICP-MS (SPDC)

For the purpose of the on-line analysis by ICP-MS, the non-equilibrium-based continuous dynamic extraction model for the SBET, described in the Section 5.3, was developed to be used for on-line determination of the PTE in inhaled and subsequently ingested $PM_{10}$ under biological condition using a new tandem system.

### 5.4.1. Experimental

#### 5.4.1.1. Apparatus and reagents

As was described in Section 5.2.1.1.

#### 5.4.1.2 Simulation of $PM_{10}$ samples

As was described in Section 5.2.1.2.

#### 5.4.1.3. Analytical procedure

The system used for the SPDC is shown in Fig 5.59. In addition to the constituents of the system described in Section 5.3.1.3, two 50 mL centrifuge tubes were added. The first tube was used for the solution of an internal standard and the second was for the residual extracts accumulated inside the chamber of ICP-MS. All four channels of the peristaltic pump were used. Three channels were used to deliver the solution of internal standard and the extractant as well as the rinse solution (2% $HNO_3$), whereas the fourth one was used to remove the residual extracts from the chamber of ICP-MS. The outlet of the filter holder was connected to a T-connector, which was connected to the nebulizer of ICP-MS. The 0.51 mm extension tubing was used for connecting the inlet and outlet of the pump to the parts of system.

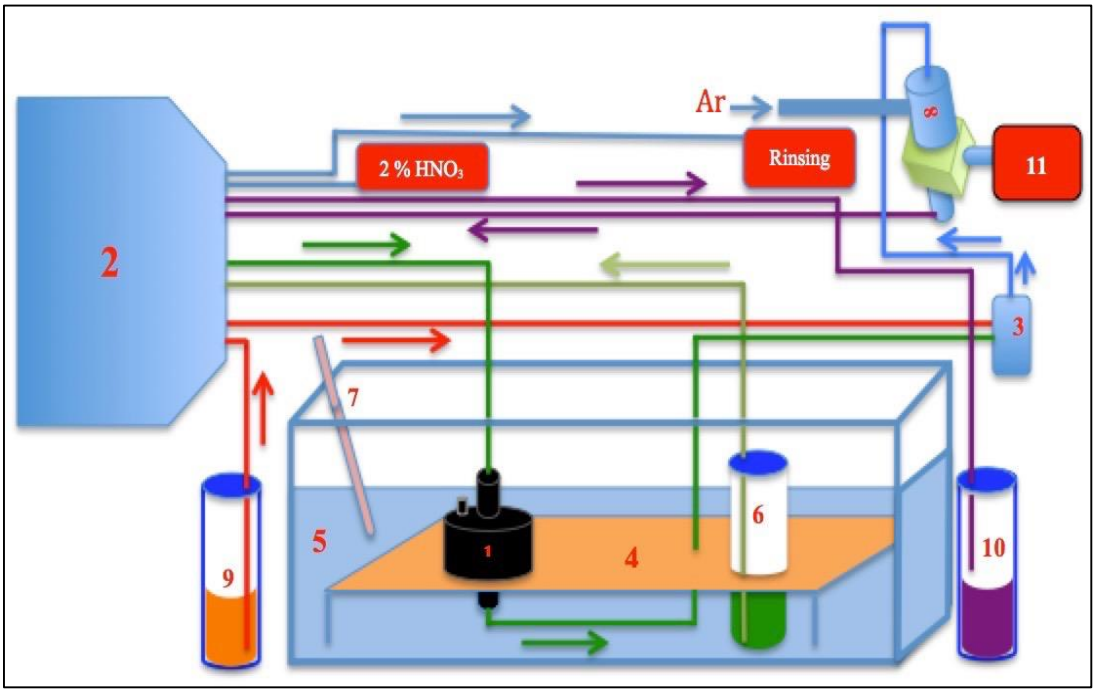


(1) Polycarbonate filter holder (2) Peristaltic pump (3) T-connecter (4) Plastic rack (5) Water bath (6) Extractant tube (7) Thermometer (8) Nebuliser (9) Internal standard tube (10) residual tube (11) Torch-ICP-MS

**Figure 5.59. Schematic diagram of the single-pass dynamic extraction device with direct coupling to ICP-MS**

This dynamic model was applied to the SBET only as the control of pH for the stomach phase of the UBM is problematic. Filter holders containing simulated $PM_{10}$ samples was prepared as described in Section 5.2.1.3. A 50 mL aliquot of the 0.4 M glycine (37 °C, pH 1.5 ± 0.05) was transferred to the extractant tube by means of a micropipette. The flow rate of the second channel (extractant channel) was set at 1.5 mL $min^{-1}$ for 5 min and other channels were on disabled mode. The vent cap of the filter holder was opened. The pump was then run for 5 min, and the vent cap was then closed. The flow rate of the extractant channel was then changed to 1 mL $min^{-1}$. The plastic rack contained the filter holder and the extractant tube was then placed into the pre-thermostated water bath at 37 °C.

The flow rate of the first channel (internal standard channel) was then set at 0.1 mL $min^{-1}$, with the other three channels on disabled mode, and the pump was run until the internal standard entered the T- connector. The flow rate of the third channel (extracts residual channel) was then set at 1.1 mL $min^{-1}$. The pump was then run (except the fourth channel, that was set on disabled mode) until the solution of

the extract mixed with the internal standard reached the nebuliser. The pump was then run for 1 hour, simultaneously with the method of analysis described in Section 5.4.1.6. The last 10 mL of the 0.4 M glycine was added to the extractant tube during the extraction.

Three simulated PM10 samples prepared using NIST SRM 2711A Montana II Soil, and three blank FDMS filter, were used. In addition, a method blank was performed by running the extractant only through the complete procedure. A spike recovery test was also performed by running the extractant, spiked at 10020 μg $L^{-1}$ for Fe and 250 μg $L^{-1}$ for other PTE, through the complete procedure. Filter holders was washed by pumping 2% $HNO_3$ at a flow rate of 1 mL $min^{-1}$ for 3 min using the fourth channel of the pump. The third channel was used during the washing process, while the other two channels were on disabled mode.

#### 5.4.1.4. Batch model

As was described in Section 5.2.1.4.

#### 5.4.1.5. Digestion of residues and mass balance

As was described in Section 5.2.1.5.

#### 5.4.1.6. Analyte quantification

Extracts and digests obtained from the batch extraction model and microwave digestion were analysed by ICP-MS as described in Section 3.6.

Time resolved analysis mode (TRA) was used when the SPDC-SBET was conducted. This mode is one of the modes of the Agilent 7700x ICP-MS instrument software. In the TRA mode, a time chart is produced between the intensity of a transient signal and time during an analysis. The parameters of TRA mode and the operation condition for ICP-MS were as shown in Table 5.24.

**Table 5.24.** Operation conditions of ICP-MS and parameters of the TRA

| **ICP-MS conditions** | |
|---|---|
| Power (watt) | 1550 |
| Quadrupole bias (v) | -15 |
| Octopole bias (v) | -18 |
| Nebulizer gas flow (L $min^{-1}$) | 1.05 |
| Plasma gas flow (L $min^{-1}$) | 15 |
| Auxiliary gas flow (L $min^{-1}$) | 0.9 |
| Collision cell gas (L $min^{-1}$) | He (4.5) He (4.5) for all masses determined, except for $^{111}Cd$ and $^{208}Pb$, no gas mode was chosen |
| Sample uptake rate (mL $min^{-1}$) | 1 |
| **TRA Parameters** | |
| Number of peaks | 1 |
| Number of points per peak | 1 |
| Signals monitored for quantification | $^{75}As$, $^{111}Cd$, $^{52}Cr$, $^{63}Cu$, $^{56}Fe$, $^{55}Mn$, $^{60}Ni$, $^{208}Pb$, and $^{66}Zn$ |
| Signals monitored for internal standard | $^{209}Bi$, $^{115}In$, $^{72}Ge$, $^{175}Lu$, and $^{45}Sc$ |
| Integration time (sec) | (0.1) For all masses determined, except $^{75}As$, $^{111}Cd$, $^{52}Cr$, and $^{60}Ni$, was (1.0) |
| Sampling period (sec) | 5.029 |
| Number of repetitions for data acquisition | 1 |
| Acquisition time per sampling period (sec) | 5.029 |
| Total acquisition time of analysis (sec) | 3600 |
| Real time plot (time chart) (sec) | 3600 |
| Type of running a sample analysis | Running a sample manually using acquired data run |

***Calibration of ICP-MS using TRA mode***

The ICP-MS was calibrated using the same mode used for samples analysis (i.e. TRA mode). Parameters of the TRA mode was similar to these described in Table 5.24, except the total acquisition time of analysis was 120 sec. The system (Fig 5.59) and the procedure described in Section 5.4.1.3 were used for calibration of the ICP-MS with minor modifications. These modifications involved: removing the filter holder from the system; connecting the outlet of the second channel (extractant channel) of the pump directly to the T-connector; and connecting the inlet of the second channel to the standard solution tubes. The T-connector was then connected to the standard solutions or calibration blank using the second channel. The pump was run for 4 min, whereas the method of analysis was only run in the last two minutes. The system was washed with 2% $HNO_3$ for 2 min using the fourth channel of the pump before and between the analyses of standard solutions and the calibration blank.

For quality control of analysis, two of the calibration standards were re-analysed, one between the analysis and one at the end of the sample run to check for instrumental drift. This was conducted similarly to the procedure used for analysis of the standard solutions.

***Handling of data***

As only the signal for PTE (in counts per second) was obtained from the software of the ICP-MS using the TRA mode, the raw data obtained from the analysis was handled off-line using Microsoft Excel 2011. To obtain calibration curves, the steps below were followed:

1. The ratio between the signal for the PTE tested (in counts per second) and signal for the internal standard (also in the counts per second) was calculated for the calibration blank and the four standards.
2. Mean of these ratios was calculated for each PTE for each calibrant.
3. Calibration curves were then plotted.
4. From the calibration curves, the R-squared and linear equations were obtained.

5. The IDL and PDL, shown in Table 5.25, were calculated using Equations 2.16 and 2.17.
6. As the signal for PTE was measured every 5 second, and to compare with the results obtained from the SPFC-SBET, where the bioaccessible PTE concentration was determined every 5 minutes, the sum of the bioaccessible concentration for 60, 120, 180, 240, 300, 360, 420, 480, 540, 600, 660, and 720 measurements (i.e. at 5 min intervals) was calculated for each sample. The mean of the bioaccessible concentration for each interval was then calculated for the three samples analysed.

For samples, after calculating the ratios between analyte signal and signal of the internal standards (both in counts per second), these ratios were substituted in the equations of calibration curves to obtain the concentrations of PTE in μg $L^{-1}$. These concentrations were converted to mg $kg^{-1}$ using the Equation 3.1.

**Table 5.25. Instrumental (IDL) and procedural (PDL) detection limits for the single-pass dynamic model of the simplified bioaccessibility extraction test (SBET) with direct coupling to ICP-MS (SPDC-SBET)**

| Isotopes | SPDC-SBET | |
|---|---|---|
| | IDL (μg $L^{-1}$) | PDL (μg $kg^{-1}$) |
| $^{75}As$ | 0.284 | 0.236 |
| $^{111}Cd$ | 0.003 | 0.002 |
| $^{52}Cr$ | 2.19 | 1.82 |
| $^{65}Cu$ | 0.091 | 0.076 |
| $^{56}Fe$ | 5.50 | 4.57 |
| $^{55}Mn$ | 0.016 | 0.013 |
| $^{60}Ni$ | 0.064 | 0.053 |
| $^{208}Pb$ | 0.015 | 0.012 |
| $^{66}Zn$ | 1.04 | 0.863 |

#### 5.4.1.7. Real $PM_{10}$ samples

As was described in Section 5.3.1.6.

#### 5.4.1.8. Quality control and reference material

As was described in Section 5.2.1.7.

### 5.4.2. Results and discussion

#### 5.4.2.1. Concentration of PTE in blank FDMS filters

Table 5.26 shows the bioaccessible PTE concentration in blank FDMS filters extracted using the SPDC-SBET as well as their residual fractions and pseudototal content of non-extracted filters. For all PTE tested, the bioaccessible concentration was below the IDLs, except for Zn, where it was detectable as it is used as a binder for FDMS filters.

**Table 5.26. Concentrations of potentially toxic elements (PTE) in the bioaccessible and residual fractions, together with pseudototal content and mass balance in blank FDMS filters using the single-pass dynamic model of the simplified bioaccessibility extraction test (SBET) with direct coupling to ICP-MS (SPDC-SBET)**

| PTE | Models | Bioaccessible fraction (µg filter$^{-1}$) Mean (n=3) ± SD | Residual fraction (µg filter$^{-1}$) Mean (n=3) ± SD | Sum ± $SD_C$ (µg filter$^{-1}$) | Pseudototal (µg filter$^{-1}$) Mean (n=3) ± SD | % Mass balance ± $SD_C$ | Student's t-test at 0.05 significance level | |
|---|---|---|---|---|---|---|---|---|
| | | | | | | | $t_{calculated}$ | $t_{critical}$ |
| **As** | **Batch** | < RB | 0.318 ± 0.039 | 0.318 ± 0.039 | 0.251 ± 0.027 | 127 ± 21 | 2.44 | 2.78 |
| | **SPDC** | < IDL | 0.185 ± 0.029 | 0.185 ± 0.029 | 0.324 ± 0.034 | 57.1 ± 10.8 | **5.34** | 2.78 |
| **Cd** | **Batch** | < IDL | < RB | NC | < RB | NC | NC | NC |
| | **SPDC** | < IDL | < RB | NC | < RB | NC | NC | NC |
| **Cr** | **Batch** | 0.001 ± 0.0003 | 2.80 ± 0.03 | 2.81 ± 0.03 | 2.72 ± 0.11 | 103 ± 4 | 1.05 | 3.18 |
| | **SPDC** | < IDL | 2.10 ± 0.25 | 2.10 ± 0.25 | 2.63 ± 0.18 | 79.8 ± 10.9 | **3.01** | 2.78 |
| **Cu** | **Batch** | < IDL | < RB | NC | < RB | NC | NC | NC |
| | **SPDC** | < IDL | < RB | < RB | < RB | NC | NC | NC |
| **Fe** | **Batch** | 0.422 ± 0.148 | 83.0 ± 6.1 | 83.4 ± 6.1 | 60.5 ± 2.3 | 138 ± 11 | **6.31** | 3.18 |
| | **SPDC** | < IDL | 47.9 ± 33.4 | 47.9 ± 33.4 | 62.8 ± 4.6 | 76.3 ± 53.5 | 0.76 | 2.78 |
| **Mn** | **Batch** | 0.076 ± 0.039 | 1.42 ± 0.44 | 1.49 ± 0.45 | 0.932 ± 0.114 | 160 ± 52 | 2.24 | 3.18 |
| | **SPDC** | < IDL | 1.06 ± 0.19 | 1.06 ± 0.19 | 1.19 ± 0.15 | 89.1 ± 19.6 | 0.93 | 2.78 |
| **Ni** | **Batch** | 0.002 ± 0.0005 | 0.053 ± 0.018 | 0.054 ± 0.018 | 0.084 ± 0.007 | 64.5 ± 22.3 | 2.76 | 3.18 |
| | **SPDC** | < IDL | 0.178 ± 0.025 | 0.178 ± 0.025 | 0.280 ± 0.040 | 63.6 ± 12.8 | **3.73** | 2.78 |
| **Pb** | **Batch** | < RB | 0.530 ± 0.048 | 0.530 ± 0.048 | 0.456 ± 0.027 | 116 ± 13 | 2.31 | 2.78 |
| | **SPDC** | < IDL | 0.401 ± 0.064 | 0.401 ± 0.064 | 0.430 ± 0.038 | 93.3 ± 17 | 0.67 | 2.78 |
| **Zn** | **Batch** | 2.07 ± 0.10 | 1010 ± 28 | 1010 ± 28 | 867 ± 154 | 117 ± 21 | 1.26 | 3.18 |
| | **SPDC** | 3.35 ± 0.39 | 876 ± 128 | 879 ± 128 | 945 ± 108 | 93.0 ± 17.2 | 0.63 | 3.18 |

n= number of replicates; $SD_C$: combined standard deviation; Sum = (Bioaccessible fraction + Residual fraction); % Mass balance = $\frac{\text{Sum}}{\text{pseudototal}} \times 100$; < IDL: less than instrumental detection limit; < RB: less than reagent blank; NC: not calculated

### 5.4.2.2. Single-pass dynamic model of the SBET with direct coupling to ICP-MS (SPDC-SBET)

The leaching profiles for PTE in simulated $PM_{10}$ samples, prepared using NIST SRM 2711A Montana II Soil, extracted by the SPDC-SBET are depicted in Figures 5.60-5.67 (and also tabulated in Appendix E1). Data obtained from the SPFC-SBET (discussed in Section 5.3.2.3) are also plotted for comparison. For all PTE tested, the maximum of the bioaccessible concentration was observed in the first 5 minutes of the total leaching time (60 min), except for Cr, where it was below the IDL (see Appendices E2-E9). This was in agreement with the time when the maximum of the bioaccessible PTE concentration was leached using the SPFC-SBET, which was released in the first 5 minutes (i.e. the time for each subfraction). As is shown in Figures 5.60-5.67, and according to the Student's t-test at 95% confidence level (see Table 5.27), there was no significant difference between the bioaccessible concentration of PTE obtained by extraction of the simulated $PM_{10}$ samples (NIST SRM 2711A Montana II Soil on FDMS filter) using the SPFC-SBET and the SPDC-SBET.

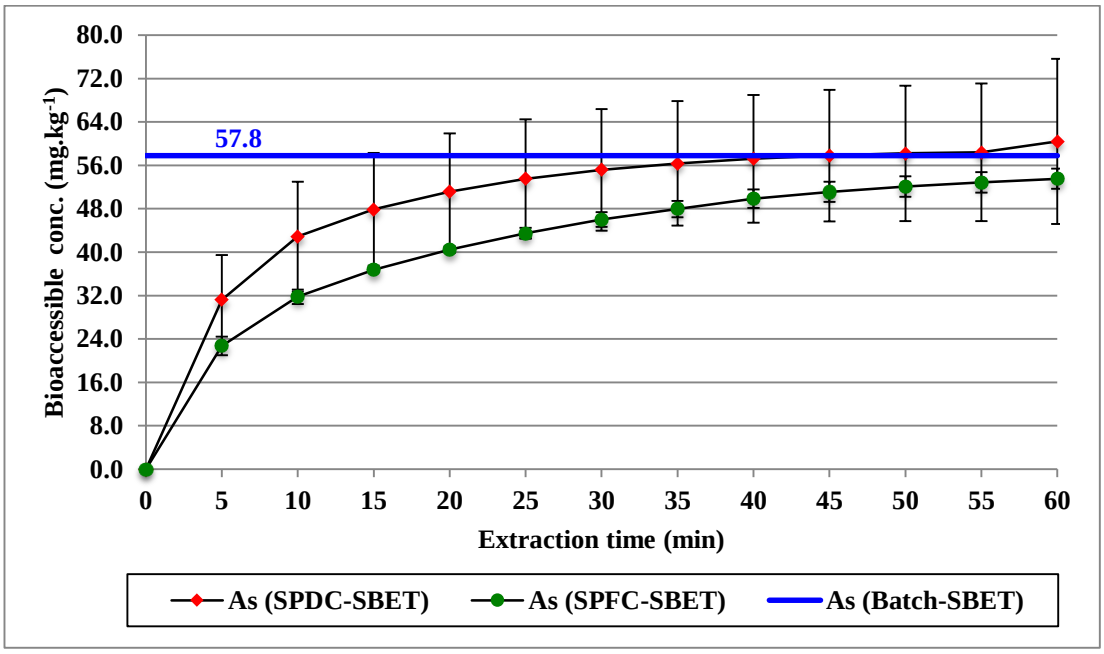


**Figure 5.60. Cumulative bioaccessible concentration of As obtained by extraction of the simulated $PM_{10}$ samples (NIST SRM 2711A Montana II Soil on FDMS filter) using the single-pass dynamic model of the simplified bioaccessibility extraction test (SBET) with fraction collection (SPFC-SBET) and with direct coupling to ICP-MS (SPDC-SBET); error bars represent one standard deviations (n=3)**

**Table 5.27. T-test at 0.05 significance level between the mean (n=3) of the cumulative bioaccessible concentration (mg $kg^{-1}$) of potentially toxic elements obtained by extraction of the simulated $PM_{10}$ samples (NIST SRM 2711A Montana II Soil on FDMS filter) using the single-pass dynamic model of the simplified bioaccessibility extraction test (SBET) with fraction collection (SPFC-SBET) and with direct coupling to ICP-MS (SPDC-SBET) (n=3)**

| Time (min) | As | Cd | Cr | Cu | Fe | Mn | Ni | Pb | Zn |
|---|---|---|---|---|---|---|---|---|---|
| **5** | 1.74[a] | 1.29[a] | < IDL | 0.727[a] | 1.02[a] | 0.801[a] | 0.904[a] | 1.00[a] | 0.359[a] |
| **10** | 1.88 | 1.36 | < IDL | 0.686 | 0.897[a] | 0.670 | 0.832[a] | 1.11[a] | 0.082 |
| **15** | 1.86 | 1.29 | < IDL | 0.601 | 1.22[a] | 0.478 | 1.16[a] | 1.09 | 0.192 |
| **20** | 1.72 | 1.18 | < IDL | 0.489 | 1.55[a] | 0.274 | 1.18[a] | 0.905 | 0.431 |
| **25** | 1.59 | 1.04 | < IDL | 0.340 | 1.99 | 0.045[a] | 1.21[a] | 0.618[a] | 0.646 |
| **30** | 1.41 | 0.920 | < IDL | 0.206 | 2.38 | 0.142[a] | 1.21[a] | 0.360[a] | 0.800 |
| **35** | 1.26 | 0.831 | < IDL | 0.109 | 2.71 | 0.273[a] | 1.16[a] | 0.178[a] | 0.911 |
| **40** | 1.07 | 0.756 | < IDL | 0.001 | 3.18 | 0.545[a] | 1.25[a] | 0.013[a] | 1.03 |
| **45** | 0.942 | 0.718 | < IDL | 0.063 | 3.52 | 0.643[a] | 1.26[a] | 0.074[a] | 1.08 |
| **50** | 0.843 | 0.699 | < IDL | 0.100 | 3.79 | 0.687[a] | 1.25[a] | 0.116[a] | 1.11 |
| **55** | 0.751 | 0.687 | < IDL | 0.138 | 4.17 | 0.747[a] | 1.27[a] | 0.146[a] | 1.14 |
| **60** | 0.779 | 0.692 | < IDL | 0.064 | 2.41 | 0.360[a] | 1.32[a] | 0.028[a] | 0.796 |

[a] means that F-test was passed, a degree of freedom (ν) = 4, and $t_{critical}$ = 2.78; < IDL: less instrumental detection limit; SD: standard deviation; ν = 2, $t_{critical}$ = 4.30, and F-test was failed unless otherwise indicated

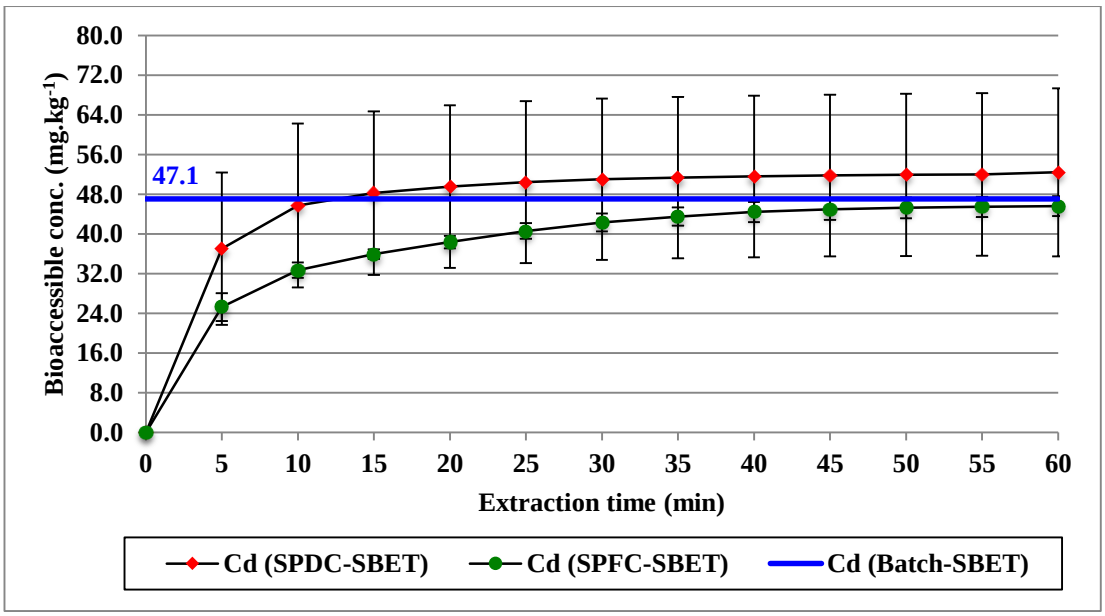


**Figure 5.61. Cumulative bioaccessible concentration of Cd obtained by extraction of the simulated $PM_{10}$ samples (NIST SRM 2711A Montana II Soil on FDMS filter) using the single-pass dynamic model of the simplified bioaccessibility extraction test (SBET) with fraction collection (SPFC-SBET) and with direct coupling to ICP-MS (SPDC-SBET); error bars represent one standard deviations (n=3)**

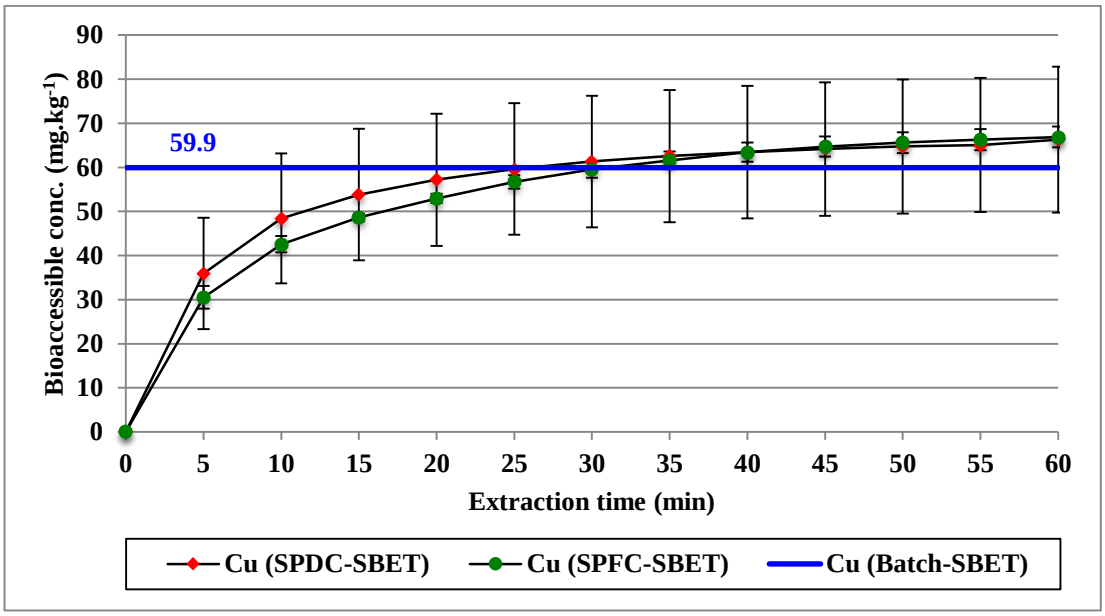


**Figure 5.62. Cumulative bioaccessible concentration of Cu obtained by extraction of the simulated $PM_{10}$ samples (NIST SRM 2711A Montana II Soil on FDMS filter) using the single-pass dynamic model of the simplified bioaccessibility extraction test (SBET) with fraction collection (SPFC-SBET) and with direct coupling to ICP-MS (SPDC-SBET); error bars represent one standard deviations (n=3)**

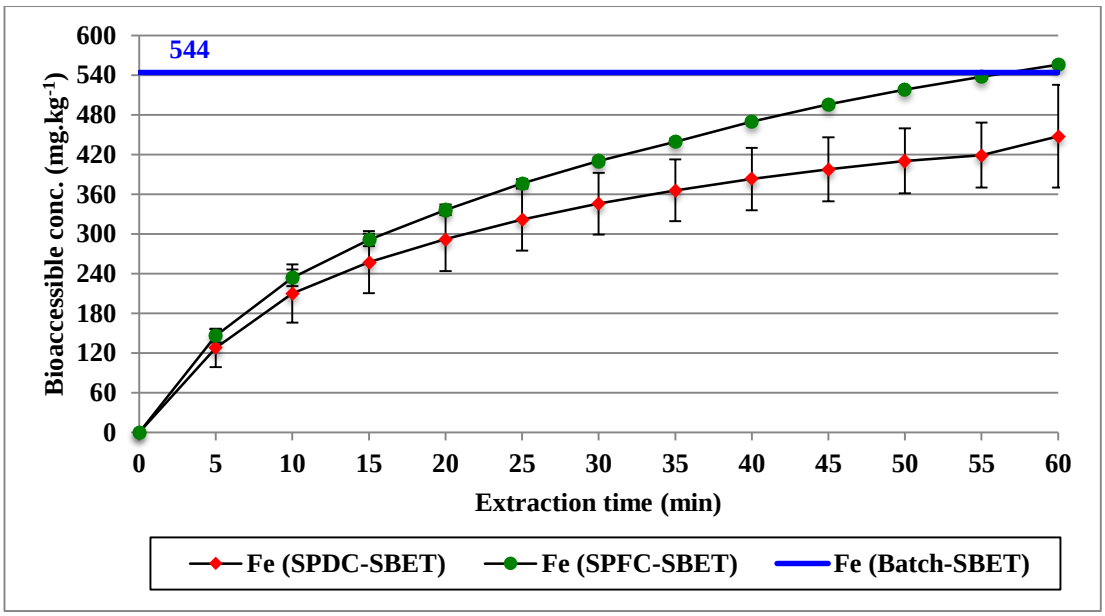


**Figure 5.63. Cumulative bioaccessible concentration of Fe obtained by extraction of the simulated $PM_{10}$ samples (NIST SRM 2711A Montana II Soil on FDMS filter) using the single-pass dynamic model of the simplified bioaccessibility extraction test (SBET) with fraction collection (SPFC-SBET) and with direct coupling to ICP-MS (SPDC-SBET); error bars represent one standard deviations (n=3)**

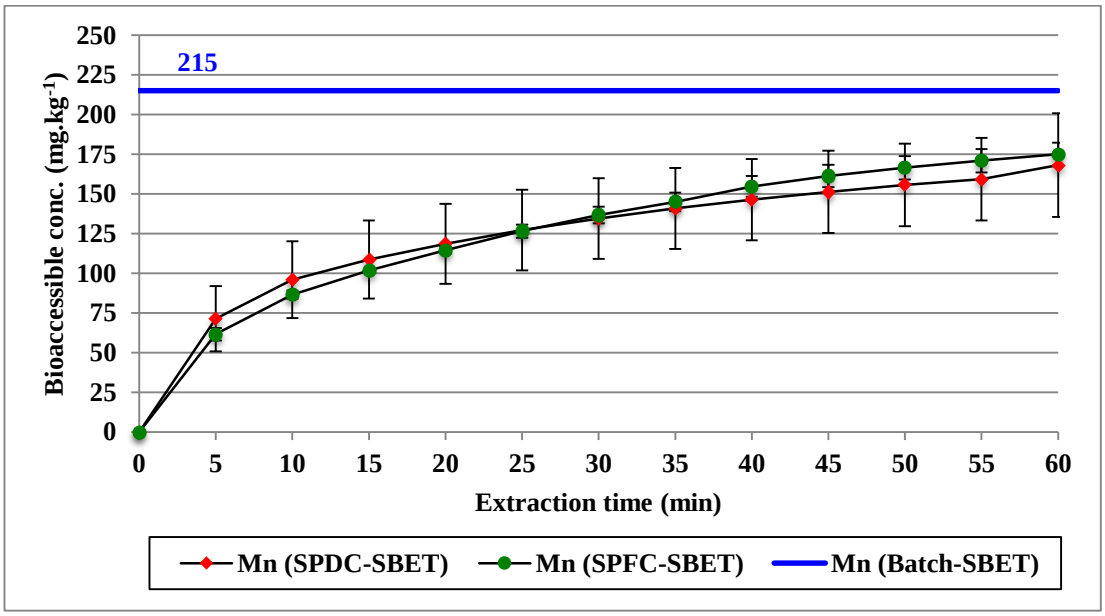


**Figure 5.64. Cumulative bioaccessible concentration of Mn obtained by extraction of the simulated $PM_{10}$ samples (NIST SRM 2711A Montana II Soil on FDMS filter) using the single-pass dynamic model of the simplified bioaccessibility extraction test (SBET) with fraction collection (SPFC-SBET) and with direct coupling to ICP-MS (SPDC-SBET); error bars represent one standard deviations (n=3)**

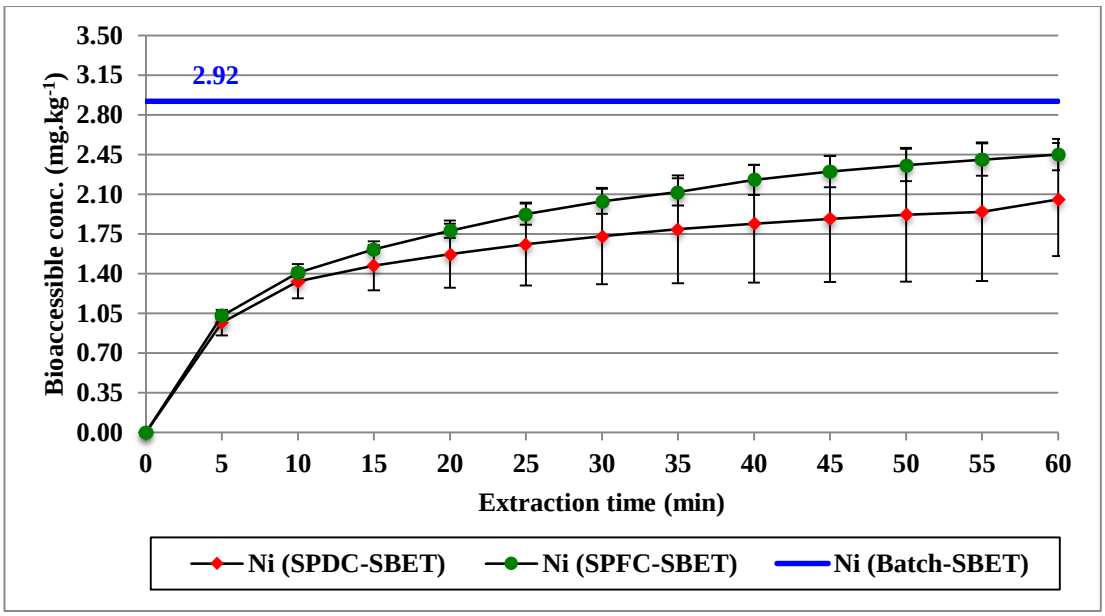


**Figure 5.65. Cumulative bioaccessible concentration of Ni obtained by extraction of the simulated $PM_{10}$ samples (NIST SRM 2711A Montana II Soil on FDMS filter) using the single-pass dynamic model of the simplified bioaccessibility extraction test (SBET) with fraction collection (SPFC-SBET) and with direct coupling to ICP-MS (SPDC-SBET); error bars represent one standard deviations (n=3)**

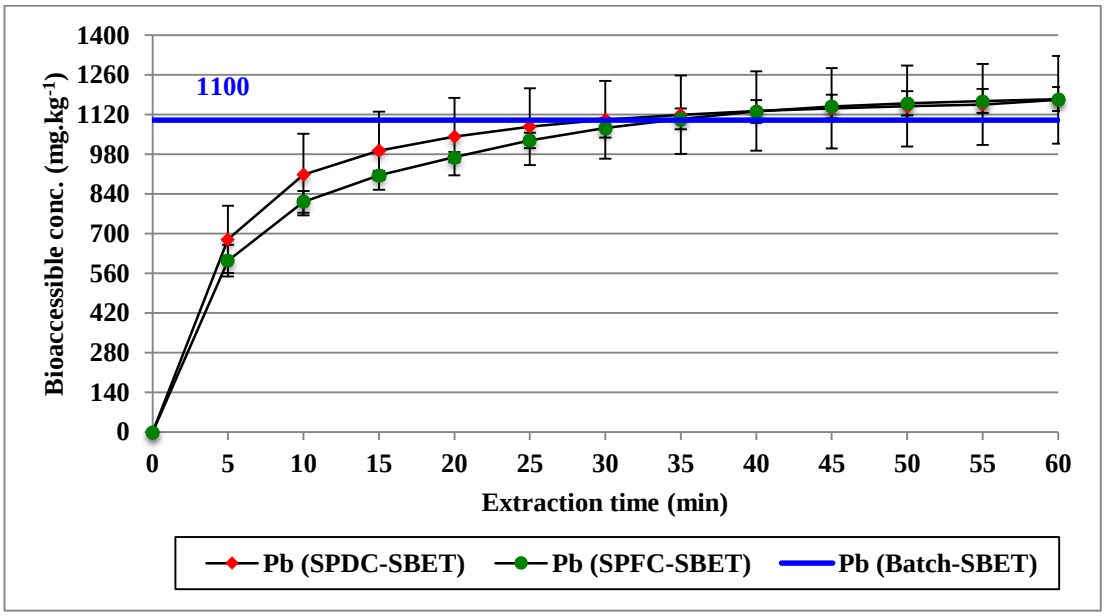


**Figure 5.66. Cumulative bioaccessible concentration of Pb obtained by extraction of the simulated $PM_{10}$ samples (NIST SRM 2711A Montana II Soil on FDMS filter) using the single-pass dynamic model of the simplified bioaccessibility extraction test (SBET) with fraction collection (SPFC-SBET) and with direct coupling to ICP-MS (SPDC-SBET); error bars represent one standard deviations (n=3)**

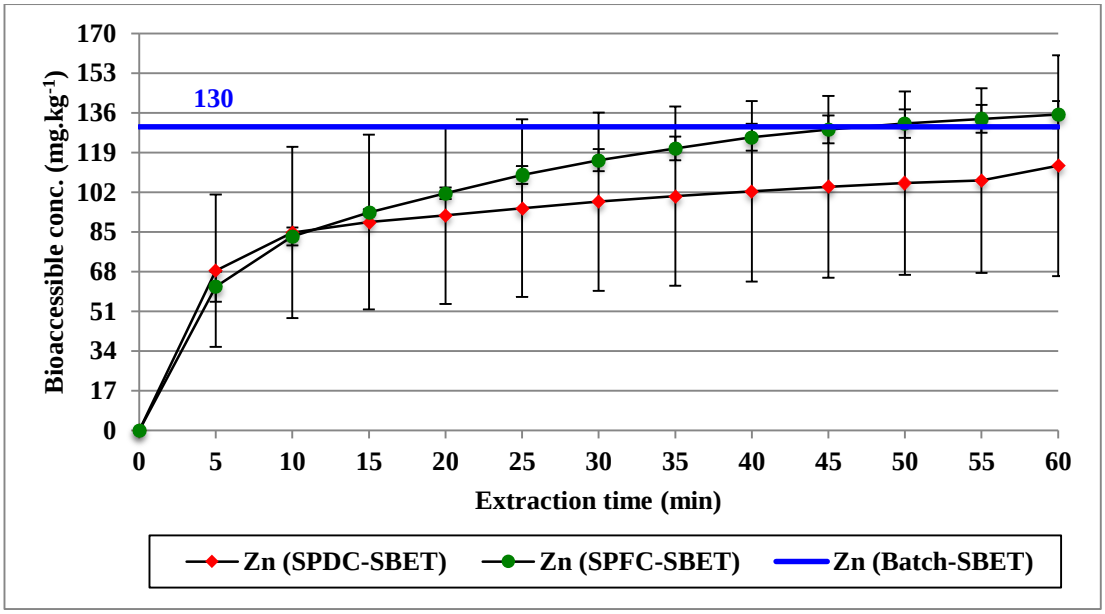


**Figure 5.67. Cumulative bioaccessible concentration of Zn obtained by extraction of the simulated $PM_{10}$ samples (NIST SRM 2711A Montana II Soil on FDMS filter) using the single-pass dynamic model of the simplified bioaccessibility extraction test (SBET) with fraction collection (SPFC-SBET) and with direct coupling to ICP-MS (SPDC-SBET); error bars represent one standard deviations (n=3)**

### 5.4.2.3. Mass balance

The bioaccessible and residual fractions of PTE as well as the sum of fractions with respect to the pseudototal PTE content (i.e. mass balance), released from simulated $PM_{10}$ samples using NIST SRM 2711A Montana II Soil, extracted by the batch model and the SPDC-SBET are summarised in Table 5.28. Values of Z-score shown in Table 5.28 were calculated using Equations 2.28 and 2.30. According to these values, mass balances were verified, where the sum of fraction agreed with the measured pseudototal PTE concentration for the batch model and the SPDC-SBET. For the batch model, 62% of Z-scores were acceptable, and 38% satisfactory, whilst for the SPDC-SBET, 86% of Z-scores were acceptable and 14% were satisfactory. For Zn, Z-score was not calculated, as the pseudototal content of the blank FDMS filters was variable (see Table 5.26).

#### 5.4.2.4. Quality control

The precision of the models of the SBET was ascertained using the RSD. All RSD's values were less than 10% for the batch models of the SBET, while for the SPDC-SBET, the repeatability represented by RSD was not as good as the batch model, with RSD values from 13.2 for Pb to 41.7% for Zn (see Table 5.28). In addition to the validation of mass balance as described in Section 5.4.2.3, a spike recovery test for known amount of PTE spiked with the methods' extractants were also performed to ascertain the trueness of the models. For the batch model of the SBET, spike recoveries were 100 ± 4% (except for Zn, it was 87%), whilst for the SPDC-SBET, they were 100 ± 9%.

Recommended value of the bioaccessible Pb fraction (1110 ± 49 $mg.kg^{-1}$) in NIST SRM 2711A was used to assess the accuracy of the SPDC-SBET. A recovery for the bioaccessible Pb fraction (1170 ± 155 $mg.kg^{-1}$) obtained by applying this model was 105 ± 15%. The performance of the microwave digestion was ascertained by using BCR CRM 143R Sewage Sludge Amended Soil (see Table 5.29). The recoveries with respect to certified PTE values were within 100 ± 7%, indicating that the accuracy of samples digestion was acceptable.

**Table 5.28. Concentrations of potentially toxic elements (PTE) in the bioaccessible and residual fractions, together with pseudototal content and mass balance in simulated $PM_{10}$ samples (NIST SRM 2711A Montana II Soil on FDMS filters) using the single-pass dynamic model of the simplified bioaccessibility extraction test (SBET) with direct coupling to ICP-MS (SPDC-SBET)**

| PTE | Models | Bioaccessible fraction (mg $kg^{-1}$) Mean (n=3) ± U (% RSD) | Residual fraction (mg $kg^{-1}$) Mean (n=3) ± U | Sum ± $U_C$ (mg $kg^{-1}$) | Pseudototal (mg $kg^{-1}$) Mean (n=3) ± U | % Mass balance ± $U_C$ | %Spike recovery | Z-Score |
|---|---|---|---|---|---|---|---|---|
| **As** | **Batch** | 57.8 ± 6.7 **(1.26)** | 37.7 ± 4.4 | 95.4 ± 8.0 | 94.7 ± 10.9 | 101 ± 14 | 100 | 0.1 |
| | **SPDC** | 60.4 ± 7.0 **(25.3)** | 29.8 ± 3.4 | 90.1 ± 7.8 | 96.1 ± 11.1 | 93.8 ± 13.5 | 105 | -0.9 |
| **Cd** | **Batch** | 47.1 ± 5.4 **(2.32)** | 5.18 ± 0.60 | 52.2 ± 5.5 | 49.3 ± 5.7 | 106 ± 17 | 100 | 0.8 |
| | **SPDC** | 52.4 ± 6.1 **(32.3)** | 3.78 ± 0.44 | 56.2 ± 6.1 | 50.1 ± 5.8 | 112 ± 18 | 91 | 1.7 |
| **Cr** | **Batch** | 0.899 ± 0.104 **(2.57)** | 24.9 ± 2.9 | 25.8 ± 2.9 | 32.1 ± 3.7 | 80.3 ± 12.9 | 101 | -2.8 |
| | **SPDC** | < IDL | 28.4 ± 3.3 | NC | 29.7 ± 3.4 | NC | 100 | NC |
| **Cu** | **Batch** | 59.9 ± 6.9 **(2.69)** | 59.4 ± 6.9 | 119 ± 10 | 130 ± 15 | 91.7 ± 13.0 | 104 | -1.2 |
| | **SPDC** | 66.3 ± 7.7 **(25.0)** | 52.1 ± 6.0 | 118 ± 10 | 127 ± 15 | 93.3 ± 13.2 | 101 | -0.9 |
| **Fe** | **Batch** | 544 ± 63 **(2.67)** | 19400 ± 2240 | 19900 ± 2240 | 24500 ± 2830 | 81.3 ± 13.1 | 103 | -2.6 |
| | **SPDC** | 448 ± 52 **(17.3)** | 19900 ± 2300 | 20400 ± 2300 | 24000 ± 2770 | 85.0 ± 13.7 | 102 | -2.1 |
| **Mn** | **Batch** | 215 ± 25 **(1.97)** | 281 ± 32 | 496 ± 41 | 573 ± 66 | 86.7 ± 12.3 | 104 | -1.9 |
| | **SPDC** | 168 ± 19 **(19.4)** | 352 ± 41 | 520 ± 45 | 571 ± 66 | 91.1 ± 13.1 | 101 | -1.3 |
| **Ni** | **Batch** | 2.92 ± 0.34 **(2.34)** | 12.5 ± 1.4 | 15.4 ± 1.5 | 18.4 ± 2.1 | 83.9 ± 12.6 | 103 | -2.3 |
| | **SPDC** | 2.05 ± 0.24 **(24.3)** | 13.8 ± 1.6 | 15.9 ± 1.6 | 18.1 ± 2.1 | 87.6 ± 13.5 | 107 | -1.7 |
| **Pb** | **Batch** | 1100 ± 127 **(2.75)** | 265 ± 31 | 1360 ± 131 | 1310 ± 151 | 104 ± 16 | 101 | 0.5 |
| | **SPDC** | 1170 ± 135 **(13.2)** | 147 ± 17 | 1320 ± 136 | 1320 ± 152 | 100 ± 15 | 97 | 0.0 |
| **Zn** | **Batch** | 130 ± 15 **(3.53)** | < FB | NC | < FB | NC | 87 | NC |
| | **SPDC** | 113 ± 13 **(41.7)** | < FB | NC | < FB | NC | 108 | NC |

$U = \frac{(K \times \text{Mean} \times \%RSD)}{100 \times \sqrt{n}}$ , K = 2, % RSD = 10, n= number of replicates; $Z - \text{Score} = \frac{(\text{Sum} - \text{Pseudototal})}{SD_R/\sqrt{n}}$, $SD_R = \frac{\text{Mean of pseudototal} \times 10}{100}$, n= number of independent replicates; $U_C$: combined uncertainty; $\text{Sum} = (\text{Bioaccessible fraction} + \text{Residual fraction})$; $\%\ \text{Mass balance} = \frac{\text{Sum}}{\text{pseudototal}} \times 100$; < IDL: less than instrumental detection limit; < FB: less than filter blank; NC: not calculated

**Table 5.29. Comparison between found and certified values for BCR CRM 143R Sewage Sludge Amended Soil subjected to microwave assisted *aqua regia* digestion in parallel to residual material from the single-pass dynamic model of the simplified bioaccessibility extraction test (SBET) with direct coupling to ICP-MS (SPDC-SBET)**

| PTE | Cd | Cr | Mn | Ni | Pb | Zn |
|---|---|---|---|---|---|---|
| **Certified values (Mean ± SD)** | 72.0 ± 1.8 | 426 ± 12 | 858 ± 11 | 296 ± 4 | 174 ± 5 | 1063 ± 16 |
| **Measured values for batch model (Mean ± SD)** | 68.8 ± 1.1 | 454 ± 15 | 886 ± 16 | 294 ± 3 | 173 ± 5 | 1050 ± 11 |
| **% Recovery** | 95.5 ± 2.8 | 107 ± 5 | 103 ± 2 | 99.5 ± 1.7 | 99.3 ± 4.2 | 98.5 ± 1.8 |

SD: standard deviation

### 5.4.2.5. Analysis of real $PM_{10}$ samples

For a real $PM_{10}$ sample (obtained from Burgher Street), the SPDC-SBET was conducted as described in Section 5.4.1.3. Table 5.30 and Figures 5.68-5.69 show the bioaccessible PTE concentration measured in the real $PM_{10}$ sample. Higher bioaccessible concentration was observed for Cu, Fe, Pb, and Zn, whereas the bioaccessible concentration for the rest of the PTE measured was low. Similar to the NIST CRM 2711A, the highest amount of PTE in the real $PM_{10}$ sample was extracted in the first 5 min.

**Table 5.30. Bioaccessible concentration of potentially toxic elements (PTE) in the real $PM_{10}$ sample obtained by applying the single-pass dynamic model of the simplified bioaccessibility extraction test (SBET) with direct coupling to ICP-MS (SPDC-SBET)**

| PTE | As | Cd | Cr | Cu | Fe | Mn | Ni | Pb | Zn |
|---|---|---|---|---|---|---|---|---|---|
| **SBET (μg filter$^{-1}$)** | 0.036 | 0.005 | 0.003 | 1.02 | 4.63 | 0.069 | 0.056 | 0.928 | 2.93 |

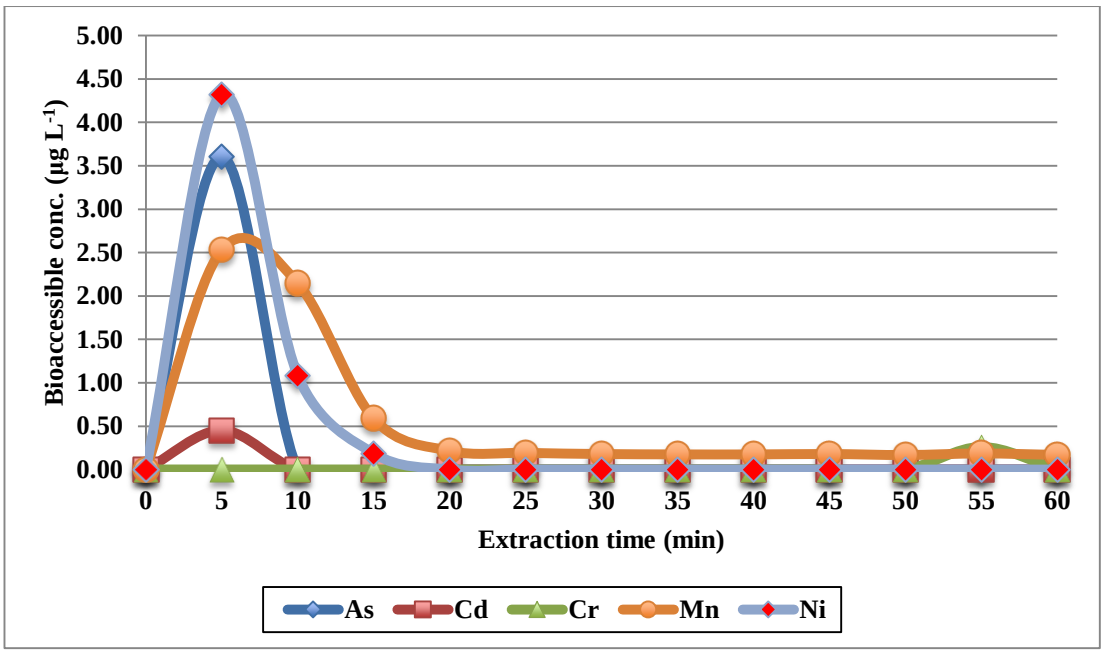


**Figure 5.68. Bioaccessible concentration of potentially toxic elements (PTE) in a real $PM_{10}$ sample obtained by applying the single-pass dynamic model of the simplified bioaccessibility extraction test (SBET) with direct coupling to ICP-MS (SPDC-SBET)**

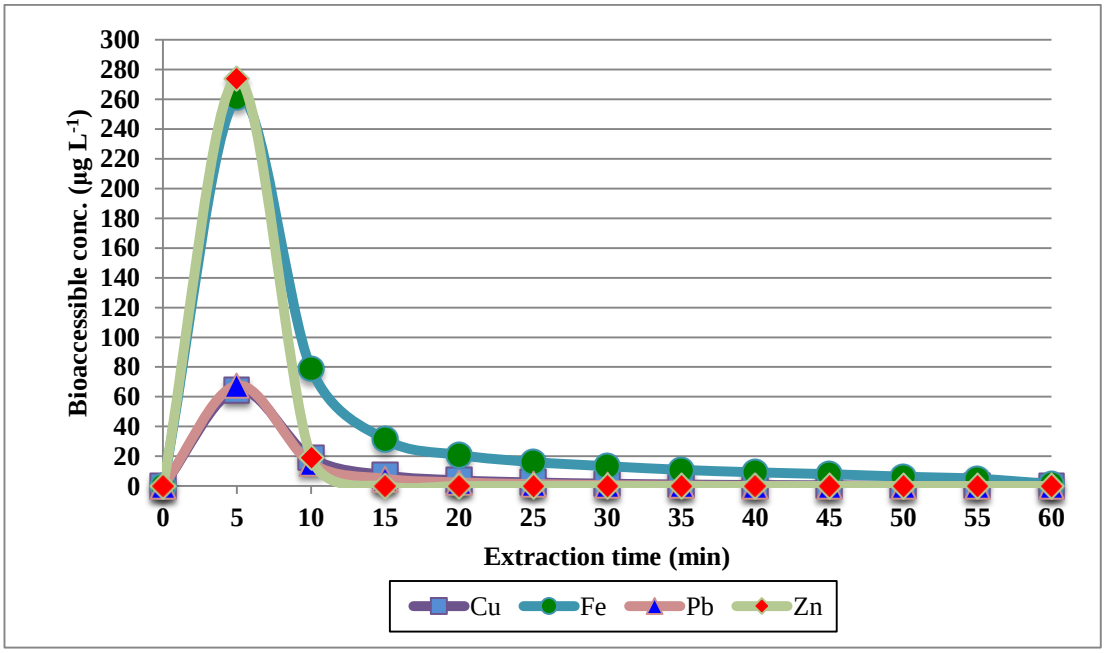


**Figure 5.69. Bioaccessible concentration of potentially toxic elements (PTE) in a real $PM_{10}$ sample obtained by applying the single-pass dynamic model of the simplified bioaccessibility extraction test (SBET) with direct coupling to ICP-MS (SPDC-SBET)**

## 5.5. Conclusion

In this work, along with the batch models, three dynamic models for the SBET and two dynamic models for the stomach phase of the UBM, to measure the bioaccessible PTE concentration in simulated $PM_{10}$ samples as well as in real $PM_{10}$ samples, were presented. The simulated samples were prepared by smearing blank FDMS filters with 100 mg BGS RM 102 Ironstone Soil and NIST SRM 2711A Montana II Soil. A polycarbonate holder filter was used as an extraction cell for these models. The successfully applied dynamic models were: the CL-SBET, the SPFC-SBET, the SPDC-SBET, the CL-UBM, and the SPFC-UBM. Extracts obtained by applying these dynamic models were analysed off-line by ICP-MS, except SPDC-SBET, where the analytes were determined on-line by coupling the extraction system with ICP-MS.

Bioaccessible PTE concentration obtained from these dynamic models and those achieved using modified versions of the batch models of the SBET and the stomach phase of the UBM have been compared. For the CL models, three flow rates for delivery of extractants were investigated, and 1.0 mL $min^{-1}$ flow rate was considered the optimum one. Recoveries of the bioaccessible PTE concentration obtained from the CL-SBET were in most cases within 100 ± 10% with respect to those obtained from the batch model, and it was 97.3 ± 5.3% with respect to the recommended bioaccessible Pb value in NIST SRM 2711A Montana II Soil. For the CL-UBM, recoveries with respect to batch values were mostly within 100 ± 20%, and they were within the guidance bioaccessible values for As, Cd, and Pb in BGS RM 102 Ironstone Soil. The Z-scores for the CL-SBET were acceptable for all PTE tested, except for Cr in NIST SRM 2711A Montana II Soil, where it was satisfactory, whereas for the CL-UBM, all PTE tested had an acceptable Z-score. In general, the lowest values of Z-score were for the CL models compared with those obtained for the batch models. There was no significant difference between the bioaccessible PTE concentration obtained by applying the CL-SBET or the CL-UBM and the available recommended or guidance values.

Before conducting the SPFC models, the effect of loaded FDMS filters on the stability of extractant flow rate was investigated. Three flow rates (1.0, 1.5, and 2.0

mL $min^{-1}$) were studied, and the first one was chosen as no effect was observed for all flow rates tested and it was suitable for direct introduction to the ICP-MS. For these models, fresh portions of the reagents of the methods (the SBET and the stomach phase of the UBM) were pumping continuously for 1 hour through the loaded filters. Extracts obtained were collected as subfractions (12 subfractions, 5 mL each, for the SPFC-SBET and 16 subfractions, 3.75 mL each, for the SPFC-UBM). Results obtained from the SPFC-SBET and SPFC-UBM models, indicated that the first subfraction contained the maximum bioaccessible concentration for the most of PTE determined. Results also detected that, possibly as a result of contamination, some of PTE had been extracted in high amount when the batch models were applied compared with the bioaccessible concentration obtained by applying the SPFC models. Recoveries (mass balance) with respect to the pseudototal content of PTE were generally within 100 ± 10%, and the mass balances obtained had in general acceptable Z-scores ($-2 < Z < +2$).

The single-pass model of the SBET was also coupled with the ICP-MS (SPDC-SBET) and the amount of bioaccessible PTE extracted continuously was measured every 5 seconds using the time resolved analysis mode of acquisition. Results obtained were compared with those obtained from the SPFC-SBET. No significant difference was observed between the extractabilities of PTE achieved using the SPFC-SBET and those obtained by coupling with ICP-MS (SPDC-SBET). The precision of the SPDC-SBET represented by RSD was not as good as the SPFC-SBET, except for Pb, it was 13.2%. However, the SPDC-SBET was a good dynamic model for Pb as the mass balance (100 ± 15%), Z-score (0.0), and recovery of the bioaccessible Pb concentration with respect to recommended value (105%) were better than those for the SPFC-SBET, which they were (102 ± 16%), (0.2), and (106%), respectively. Mass balance recoveries with respect to pseudototal content were within 100 ± 15%, and the acceptable Z-scores obtained verified these balances. Although low sample throughput and long-time analysis for each sample were the disadvantages of the SPFC models, all dynamic models of the SBET and the stomach phase of the UBM including the CL models were successfully applied to measure the bioaccessible PTE concentration in simulated and real $PM_{10}$ samples, with less contamination.

# 6 A novel sequential bioaccessibility testing method for potentially toxic elements in inhaled particulate matter transported into the gastrointestinal tract by mucociliary clearance

## 6.1. Introduction

The respiratory system consists of two functional regions: the conducting airways (i.e. nose, pharynx, larynx, trachea, bronchi, and bronchioles) and the respiratory region (i.e. lungs).[72, 180, 181] Airways surface liquid (ASL) lines the conducting regions,[19, 182] and consists of two layers: a mucus layer and a sol layer. Inhaled particles are trapped by the mucus layer, which is kept at a distance from the epithelium by the sol layer.[72, 183] These layers are separated by a layer of surfactant, and the depth of the sol layer is a little less than the length of cilia that move in the sol layer.[184]

Since the viscosity and elasticity of the mucus layer are higher than the sol layer due to its high content of oligomerized glycoproteins, the mucus only is transported by the tips of the cilia.[184-186] The mucus is cleared out of the deeper airways and nasal cavity by movement of cilia, then it is transported into the gastrointestinal tract through the pharynx.[72, 183] The watery contents of mucus layer are reabsorbed during its movement over the conducting airways. As a result, mucus is not accumulated.[184, 185] Principally, molecular weight, solubility, electrical charge, and pH value determine the absorption kinetic of inhaled substances.[19]

Based on the fact that PM 2.5-10 are transported to the gastrointestinal tract by mucociliary clearance,[19, 73, 74] and there is absorption inside the conducting region of the respiratory system when those particles are transported through it,[19, 73, 184, 185] two compartments should be involved sequentially for assessing the bioaccessibility of PTE. The first compartment should represent the conducting region of the respiratory system (i.e. from bronchial to pharynx). The second should represent the gastrointestinal tract.

For the second compartment, oral bioaccessibility extraction tests can be applied to assess the bioaccessible concentration of PTE in $PM_{10}$. The SBET[91] and the UBM[83]

have been employed for determining the bioaccessible concentration of PTE in PM in a few studies.[105, 106, 137, 144, 187] In some of these, the $PM_{10}$ originated from urban soil samples[105, 137] or from urban street dust,[144] while in others, filter-based samples were used.[106, 187] Falta *et al.*[75] and Puls *et al.*[188] applied a synthetic gastric fluid to determine the bioaccessible concentration of PTE in $PM_{10}$ loaded on cellulose ester filters. Huang *et al.*[100, 189] have employed the PBET to evaluate the oral bioaccessibility of elements in $PM_{2.5}$ collected on 3M$^{TM}$ membranes fixed on the inside of domestic air-conditioning unit dust filters. Another study[106] used SBET for measuring the bioaccessibility and human health risks of As, Cd, Co, Cr, Cu, Mn, Ni, Pb, and Zn in TSP and $PM_{2.5}$ collected on Whatman quartz microfiber filters in Nanjing, China. Limitations of the above studies were mentioned in Chapter 4 of this thesis. However, the work described in Chapter 4 revealed that the SBET and the UBMSG with minor procedural modifications were applicable to measure the bioaccessible concentration of PTE in $PM_{10}$ loaded on FDMS filters.[187]

As the route that obtains the maximum of bioaccessible concentration that can be expected was recommended by the International Organization for Standardization,[95] and since the inhalable $PM_{10}$ enter the respiratory tract through the nose, in this work, the UBMSG included gastric fluid only (UBMG), without addition of the saliva fluid.

For the first compartment, the original version of Gamble solution[190] and its modified versions[191-197] have been used in many studies to estimate the inhaled bioaccessible concentration of PTE in $PM_{10}$ originated from coal-derived fly ash,[198] mine waste,[194, 199] urban surface soils,[197] and smelters dust[200] or in $PM_{10}$ collected on filters (quartz fiber filters,[201, 202] Teflon filters,[203] and cellulose nitrate filters[204]). A more recent study[197] has been conducted to develop an *in vitro* simulated epithelial lung fluid (i.e. ASL) for assessing the inhalation bioaccessibility of Pb in $PM_{10}$ originated from urban surface soils, tailings and smelter wastes from Mitrovica, Kosovo. However, the fluid represented the sum of the two layers of ASL, whereas $PM_{10}$ adhere only to the mucus layer of ASL. The aim of this study was to establish a new sequential extraction method for determining the bioaccessible concentration of PTE in $PM_{10}$ transported to the gastrointestinal tract by mucociliary clearance,

involving:

**Step 1.** a novel extractant representing the mucus layer of ASL to assess bioaccessibility during transport and

**Step 2.** a modified SBET or UBMG to assess bioaccessibility on arrival in the stomach.

## 6.2. Experimental

### 6.2.1. Apparatus and Reagents

Blank Pallflex TX40 FDMS filters, as described in Section 3.3.1, were used. All chemicals were of analytical grade. The apparatus and reagents that used for the SBET and the stomach phase of the UBM were as described in Sections 3.4.1-3.4.2 and 3.5.1-3.5.2 respectively. Sodium bicarbonate was supplied by VWR International, Lutterworth, UK. Lysozyme, glutathione, $MgCl_2.6H_2O$, and dipalmitoyl phosphatidyl choline (DPPC) were obtained from Sigma Aldrich (Gillingham, Dorset, UK).

### 6.2.2. Simulation of $PM_{10}$ samples

Simulated $PM_{10}$ samples were prepared as described in Section 3.2. To investigate whether the FDMS filters affect the solubility of PTE in $PM_{10}$ or not, samples of 100 mg BGS RM 102 Ironstone Soil alone and blank FDMS filters were also involved in this experiment.

### 6.2.3. Constituents of artificial mucus fluid (AMF)

Table 6.1 shows the compositions of AMF. Mucus is a heterogeneous complex watery mixture of, proteins and glycoproteins, lipids and salts.[73, 185, 205] The percentage weight of water in mucus varies from 95 % [72, 185] to 97 %.[183] The second most abundant components in terms of mass are proteins such as glycoproteins or mucins, and some serum proteins e.g. albumin.[73, 183, 185, 205] Mucins are responsible for the viscoelastic properties of mucus.[205] Mucus is composed of 0.5-1 % free protein and either a similar proportion or 2 % of mucin.[72, 180, 185] Due to the low solubility of mucin in water, and to reduce the TDS in the extracts that might affect the ICP-MS analysis, the lower value of mucin concentration (0.5 %) (i.e. 5 g $L^{-1}$) was chosen in this study. The concentration of albumin in ASL is 480-730 mg $L^{-1}$,[180]

and the middle of this range (610 mg $L^{-1}$) was chosen for this study. The third important component of mucus is inorganic salts [183, 205] that constitute ~1 % by weight of mucus.[72, 185]

**Table 6.1. The composition of artificial mucus fluid (AMF)**

| **Reagent** | **Weight of reagent (mg) made up to 100 mL with deionised water** |
|---|---|
| Inorganic reagent | |
| KCl | 224 |
| $NaH_2PO_4$ | 24 |
| $Na_2SO_4$ | 14 |
| NaCl | 620 |
| $CaCl_2.2H_2O$ | 74 |
| $NaHCO_3$ | 504 |
| $MgCl_2.6H_2O$ | 42 |
| Organic reagent | |
| Glutathione | 26.4 |
| Additional reagents | |
| Mucin | 1000 |
| Albumin | 122 |
| DPPC | 220 |
| Lysozyme | 100 |

The concentration of the main ions present, $Na^+$, $Cl^-$ and $K^+$, in ASL is 1838-1953, 2658-2836, and 586 mg $L^{-1}$ respectively,[180] and their concentration in ASL is approximately 45 % less for $Na^+$ and $Cl^-$ and 600 % more for $K^+$ than plasma.[185] In this study, the concentrations of KCl, NaCl, and $NaHCO_3$ were calculated based on the above concentrations of $Na^+$, $Cl^-$ and $K^+$, whilst other salts i.e. $NaH_2PO_4$, $NaSO_4$, $CaCl_2.2H_2O$, and $MgCl_2.6H_2O$ were at similar levels to the concentrations mentioned in the original Gamble solution widely used to determine the inhaled bioaccessible fraction.[190] In addition to the water, proteins and inorganic salts, lipids are another of the principle components of mucus.[73, 183, 185, 205] Mucus is composed of 1 % lipids,[72] and its role is to reduce the surface tension between the layers of ASL.[72, 73] Most of the mucus lipids are phospholipids, and the most abundant of these is phosphatidylcholine[180] that constitutes 11 % of the total lipids (i.e. 0.11 % by weight of mucus ).[206] Therefore, in this study 1.10 g $L^{-1}$ of dipalmitoyl phosphatidylcholine (DPPC) was used. Besides mucins, secretory cells release a variety of antimicrobial molecules e.g., lysozyme[183, 185] that destroys bacteria in respiratory mucus.[205] The

concentration of lysozyme in ASL is 0.1-1 mg $mL^{-1}$.[180] For this study, the middle of the range (0.5 mg $mL^{-1}$) was chosen. Glutathione is also present in ASL at a concentration of 132 mg $L^{-1}$,[180] which was chosen for this work.

### 6.2.4. Experimental parameters

#### 6.2.4.1. Sample size and exposure dose

A moderate seasonal inhalation dose of 100 mg ($PM_{10}$) was calculated for adults according to the equation reported in a study conducted by Sexton *et al*. (Seasonal $PM_{10}$ inhalation = $PM_{limit}$ x $V_{resp}$ x EF),[207] where the inhalation rate ($V_{resp}$) is 20 $m^3$ $day^{-1}$ according to the U.S. EPA,[208] and $PM_{limit}$ is the exposure limit of $PM_{10}$ (40 μg $m^{-3}$) according to the European Environment Agency[209] and EF is the exposure frequency for 125 days. So the sample size of 100 mg was used for this study.

#### 6.2.4.2. Time of extraction

Human studies using the tablet inhalation technique[210] demonstrated that all deposited particles > 6 μm were removed from the airways by mucociliary clearance within 24 hours. However, 49 ± 9 % of particles were cleared by mucociliary clearance with a mean half time of 3.0 ± 1.6 hours in healthy circumstances.[210] Based on the fact that the length of pharynx, larynx, trachea, right and left bronchus is 13, 10.4, 12, 2.5, and 5 cm respectively,[211] and since the minimum and maximum of velocity of mucociliary clearance are 0.4 and 2 cm $min^{-1}$ respectively (with an average 1 cm $min^{-1}$),[72, 180, 185] the time of extraction for this study was set at 1 hour.

#### 6.2.4.3. Volume of fluid

The maximum volume of ASL produced daily ranged between 100 mL [180] and > 125 mL.[212] Schans[184] pointed out that the volume of mucus reaching the trachea daily is 20 mL and King[73] reported that 10 mL reaches the larynx. Another study mentioned that 30 mL of mucus is transported daily into the gastrointestinal tract.[183] In this study, 120 mL per day (5 mL per hour) was chosen for the volume of mucus produced daily, and 30 mL per day (*ca.* 1.5 mL per hour) for the volume of mucus that is transported to the gastrointestinal tract. As a result, when the SBET or UBMG

was conducted sequentially after extraction by the AMF, 3.5 mL was taken for analysis from the supernatant produced after centrifuging the 5 mL suspension and the remainder (1.5 mL) was mixed well with the reagents of the SBET or UBMG methods then was decanted into the 150 mL wide mouth bottle.

#### 6.2.4.4. pH fluid and the temperature of extraction

Normal ASL is slightly acidic, and its mean pH is 6.78.[180, 182] The i*n vivo* studies of ASL pH showed that the value is 6.6 in the airways of normal humans and 7.1 in the trachea of normal mice.[182] However, in human, a mucus pH of 7 is observed,[213] and the value is between 6.9 and 9.0 in tracheal mucus.[214] The pH of the mucus fluid for this study was set at 7.00 ± 0.20. Based on the temperature of the basal human body (37 °C), the temperature of extraction was adjusted to 37 ± 2 °C.

### 6.2.5. Preparation of AMF

To prepare 200 mL of the AMF, the inorganic and organic reagents listed in Table 6.1 were each dissolved in 100 mL deionized water in separate 100 mL volumetric flasks. The prepared reagents were added subsequently to a 500 mL HDPE bottle containing the additional reagents. To obtain the desired pH of 7.00 ± 0.20, 200 μL of 37 % HCl was added. The bottle was put on a magnetic stirrer for 3 hours. Then the pH was adjusted at (7.0 ± 0.2) by using 37 % HCl or 1M NaOH.

### 6.2.6. Sequential bioaccessibility extraction procedure

Six simulated $PM_{10}$ samples, six BGS RM 102 Ironstone Soil samples, and six blank FDMS filters were placed in 150 mL wide mouth bottles. A 5 mL aliquot of AMF adjusted to a pH of 7.00 ± 0.20 at 37 ± 2 °C was added to each of the samples. The pH of each suspension was checked and when necessary adjusted to the desired value (7.00 ± 0.20) by using various solutions of HCl (25, 50, and 100% v/v) and 1 M NaOH. The bottles were then shaken for 1 hour at 100 rpm by using an end-over-end rotator inside a pre-heated incubator at 37 ± 2 °C. The suspensions obtained were decanted into 15 mL centrifuge tubes and the original bottles were kept closed and labeled. The suspensions were centrifuged at 4500 g for 10 minutes. A 3.5 mL aliquot of the supernatant was pipetted out, and 2.5 mL of this was diluted with 2%

$HNO_3$ in a 10 mL volumetric flask for analysis. As the solid to liquid ratio reported in the original procedure of the SBET is 1 g soil to 100 mL of 0.4 M glycine, and since samples of 100 mg were used in this work, 10 mL of 0.4 M glycine was added to half of the centrifuge tubes containing the remaining supernatant and mixed thoroughly, then transferred to the original labeled bottles for completion of the procedure of the SBET (with minor procedural modification as presented in Chapter 4 and Ref[187]). To the other half of the centrifuge tubes containing the remaining supernatant, a 2.25 mL aliquot of the extractant used in the UBMG was added and mix thoroughly then transferred to the original labeled bottles for completion of the procedure of the UBMG (with minor procedural modification as presented in in Chapter 4 and Ref[187]).

### 6.2.7. Chemical analysis

Extracts obtained were analysed by ICP-MS as described in Section 3.6. The IDL and PDL, shown in Table 6.2, were calculated using Equations 2.16 and 2.17.

**Table 6.2. Instrumental (IDL) and procedural (PDL) detection limits for the artificial mucus fluid (AMF) only, AMF extraction followed by the simplified bioaccessibility extraction test (SBET2), and AMF extraction followed by the stomach phase (gastric fluid only) of the unified bioaccessibility method (UBMG)**

| Isotopes | AMF only | | SBET2 | | UBMG | |
|---|---|---|---|---|---|---|
| | IDL ($\mu g\ L^{-1}$) | PDL ($mg\ kg^{-1}$) | IDL ($\mu g\ L^{-1}$) | PDL ($mg\ kg^{-1}$) | IDL ($\mu g\ L^{-1}$) | PDL ($mg\ kg^{-1}$) |
| $^{75}As$ | 0.328 | 0.016 | 0.017 | 0.002 | 0.011 | 0.0004 |
| $^{111}Cd$ | 0.360 | 0.018 | 0.010 | 0.001 | 0.007 | 0.0003 |
| $^{52}Cr$ | 0.464 | 0.023 | 0.565 | 0.065 | 0.120 | 0.005 |
| $^{65}Cu$ | 0.297 | 0.015 | 0.144 | 0.017 | 0.175 | 0.007 |
| $^{56}Fe$ | 17.4 | 0.870 | 20.7 | 2.38 | 28.5 | 1.07 |
| $^{55}Mn$ | 0.317 | 0.016 | 0.093 | 0.011 | 0.112 | 0.004 |
| $^{60}Ni$ | 0.285 | 0.014 | 0.079 | 0.009 | 0.105 | 0.004 |
| $^{208}Pb$ | 0.359 | 0.018 | 0.005 | 0.001 | 0.006 | 0.0002 |
| $^{66}Zn$ | 0.837 | 0.042 | 0.178 | 0.020 | 0.472 | 0.018 |

### 6.2.8. Quality control

For quality control purposes, triplicate samples (except for AMF where six replicates were used) were processed. For accuracy, reagents were spiked to known concentration of PTE (250 μg $L^{-1}$ for all PTE tested except for Fe, where the concentration was 10020 μg $L^{-1}$), and the reagent spike sample was run through the complete procedure. The percentage spike recovery was calculated by using Equation 4.1.

## 6.3. Results and discussion

### 6.3.1. Bioaccessible concentration of PTE in blank FDMS filters

The bioaccessible concentration of PTE in blank FDMS filters is presented in Table 6.3. The bioaccessible concentration was very low for all PTE tested except for Zn. This is likely due to the fact that Zn is used as a binder in the production of the FDMS filters.[187] All subsequent results were corrected for filter blanks for all PTE tested.

**Table 6.3. Bioaccessible concentration of potentially toxic elements (PTE) in the blank FDMS filters using artificial mucus fluid (AMF) only, and the AMF followed by the simplified bioaccessibility extraction test (SBET2) or the stomach phase (gastric fluid only) of the unified bioaccessibility method (UBMG)**

| PTE | AMF (n = 6) | | SBET2 (n = 3) | | UBMG (n = 3) | |
|---|---|---|---|---|---|---|
| | µg $L^{-1}$ Mean ± SD | µg per filter Mean ± SD | µg $L^{-1}$ Mean ± SD | µg per filter Mean ± SD | µg $L^{-1}$ Mean ± SD | µg per filter Mean ± SD |
| **As** | < IDL | < IDL | < IDL | < IDL | 0.705 ± 0.116 | 0.003 ± 0.0004 |
| **Cd** | < IDL | < IDL | < IDL | < IDL | 0.201 ± 0.057 | 0.0008 ± 0.0002 |
| **Cr** | < IDL | < IDL | < IDL | < IDL | < IDL | < IDL |
| **Cu** | 3.63 ± 1.15 | 0.018 ± 0.006 | 0.495 ± 0.376 | 0.006 ± 0.004 | 22.4 ± 2.2 | 0.084 ± 0.008 |
| **Fe** | < IDL | < IDL | < IDL | < IDL | < IDL | < IDL |
| **Mn** | < IDL | < IDL | 4.75 ± 1.89 | 0.055 ± 0.022 | 43.7 ± 6.0 | 0.164 ± 0.023 |
| **Ni** | < IDL | < IDL | 0.035 ± 0.026 | 0.0004 ± 0.0003 | 3.59 ± 2.02 | 0.013 ± 0.008 |
| **Pb** | < IDL | < IDL | 0.383 ± 0.205 | 0.004 ± 0.002 | 3.81 ± 0.02 | 0.014 ± 0.0001 |
| **Zn** | 96.0 ± 47.7 | 0.480 ± 0.238 | 537 ± 82 | 6.18 ± 0.95 | 2190 ± 215 | 8.19 ± 0.81 |

SD: standard deviation; < IDL indicates a value less than the instrumental detection limit; n: number of replicates

### 6.3.2. Sequential bioaccessibility extraction

Results obtained from extraction of the simulated $PM_{10}$ samples and from soil alone samples by using the AMF only (see Table 6.4) demonstrated that only As, Cu, Mn, Ni were detectable. Other PTE concentrations were less than IDL, and that may be because the range of pH that solubilises PTE is different for different analytes.[215]

**Table 6.4. Bioaccessible concentration of potentially toxic elements (PTE) in the simulated $PM_{10}$ samples (soil on FDMS filters) and in soil alone using artificial mucus fluid (AMF) only (n=6)**

| Sample Name | | As (mg kg$^{-1}$) | Cu (mg kg$^{-1}$) | Mn (mg kg$^{-1}$) | Ni (mg kg$^{-1}$) |
|---|---|---|---|---|---|
| **Soil alone** | S1 | 0.742 | 1.87 | 6.41 | < IDL |
| | S2 | 0.805 | 2.17 | 6.21 | < IDL |
| | S3 | 0.792 | 1.85 | 6.92 | 0.178 |
| | S4 | 0.821 | 2.00 | 7.95 | 0.230 |
| | S5 | 0.791 | 1.90 | 7.27 | 0.210 |
| | S6 | 0.761 | 1.84 | 8.18 | 0.211 |
| | Mean | 0.785 | 1.94 | 7.16 | 0.207 |
| | SD | 0.029 | 0.13 | 0.80 | 0.022 |
| | %RSD | 3.68 | 6.58 | 11.2 | 10.6 |
| **Soil on FDMS filter** | SF1 | 0.818 | 1.99 | 7.52 | 0.210 |
| | SF2 | 0.859 | 2.03 | 9.96 | 0.205 |
| | SF3 | 0.821 | 1.83 | 9.81 | 0.187 |
| | SF4 | 0.839 | 1.91 | 10.6 | 0.232 |
| | SF5 | 0.836 | 1.92 | 10.9 | 0.273 |
| | SF6 | 0.798 | 1.72 | 9.78 | 0.432 |
| | Mean | 0.828 | 1.90 | 9.76 | 0.222 |
| | SD | 0.021 | 0.11 | 1.19 | 0.033 |
| | %RSD | 2.52 | 5.84 | 12.2 | 14.9 |
| **%RPD** | | 5.00 | 2.00 | 31.0 | 7.00 |
| **Spike Recovery** | | 92.3 | 90.4 | 92.6 | 97.1 |

SD: standard deviation; n: number of replicates; RSD: Relative standard deviation; < indicates a value less than the instrumental detection limit; RPD: Relative percent difference = $\{|x_1 - x_2|/((x_1+x_2)/2)\}\times 100$ where $x_1$: values in soil alone and $x_2$: values in soil loaded on FDMS filter

In general, values of bioaccessible concentration of detectable PTE were low. The statistical results obtained (t-test at 0.05 significance level) (see Appendices F1 and F2) and the calculation of the RPD showed that there was no significant difference between the bioaccessible concentration of PTE in soils alone and in soil on FDMS filters, except for Mn. This may be because the use of such small mass of sample (100 mg) could present variability due to small-scale heterogeneity. As the reagents of the AMF included phosphate salts (e.g. $NaH_2PO_4$), the formation of insoluble precipitates (chemical immobilization) of phosphate salts could reduce the solubility

of elements, except for As and Cr where the solubility could be increased. This due to the formation of metal phosphate complexes for most elements, while for As and Cr, the effect is due to ion exchange between $PO_4^{3-}$ present in solution and oxyanions ($AsO_3^{3-}$, $AsO_4^{3-}$, and $CrO_4^{2-}$) present at the edge of soil particles.[216] The fact that Cr was not extractable by the AMF may be due to the presence of inorganic and organic compounds (e.g. glutathione) that can decrease the solubility of Cr by reducing $Cr^{VI}$ to $Cr^{III}$, which is less mobile.[217] For Mn and Ni, single and chelating agents that are contained in the AMF (such as DPPC and glutathione) can increase the solubility.[218]

When applying the SBET and the UBMG on simulated $PM_{10}$ samples that had previously been extracted by the AMF, the highest values of bioaccessible concentration of all PTE tested were observed when applying the UBMG (see Table 6.5) except for Fe. Differences may be because of the different pH values used in each method, whereas for Fe, it may be due to the formation of insoluble precipitates.[216] The RPD values between the bioaccessible concentration of PTE in soils alone and in soils on FDMS filters were < 10 % for the majority of PTE tested (see Tables 6.4 and 6.5) indicating that the presence of the filter did not affect the extraction efficiency, so long as blank correction was performed.

**Table 6.5. Bioaccessible concentrations of potentially toxic elements (PTE) in in the simulated $PM_{10}$ samples (BGS RM 102 Ironstone Soil on FDMS filters) and in soil alone using artificial mucus fluid (AMF) followed by the simplified bioaccessibility extraction test (SBET2) or the stomach phase (gastric fluid only) of the unified bioaccessibility method (UBMG)**

| | Sample Name | | | | | | | | %Spike Recovery | | %RPD | |
|---|---|---|---|---|---|---|---|---|---|---|---|---|
| | Soil alone | | | | Soil on FDMS filters | | | | | | | |
| | SBET2 | | UBMG | | SBET2 | | UBMG | | | | | |
| PTE | Mean ± SD (mg $kg^{-1}$) (n=3) | %RSD | Mean ± SD (mg $kg^{-1}$) (n=3) | %RSD | Mean ± SD (mg $kg^{-1}$) (n=3) | %RSD | Mean ± SD (mg $kg^{-1}$) (n=3) | %RSD | SBET2 | UBMG | SBET2 | UBMG |
| **As** | 3.09 ± 0.09 | 2.85 | 3.54 ± 0.08 | 2.22 | 2.98 ± 0.07 | 2.37 | 3.38 ± 0.07 | 2.18 | 94.4 | 95.6 | 3.56 | 4.59 |
| **Cd** | 0.149 ± 0.005 | 3.42 | 0.224 ± 0.013 | 5.71 | 0.145 ± 0.003 | 2.33 | 0.219 ± 0.021 | 9.40 | 90.9 | 97.2 | 2.10 | 2.17 |
| **Cr** | 30.8 ± 0.8 | 2.50 | 39.3 ± 1.4 | 3.43 | 30.5 ± 0.2 | 0.784 | 33.9 ± 2.1 | 6.07 | 88.0 | 97.3 | 1.11 | 14.6 |
| **Cu** | 6.02 ± 0.09 | 1.41 | 7.47 ± 0.45 | 6.05 | 6.36 ± 0.08 | 1.28 | 7.11 ± 0.80 | 11.3 | 90.5 | 96.8 | 5.48 | 4.91 |
| **Fe** | 1040 ± 13 | 1.25 | 903 ± 55 | 6.13 | 1030 ± 14 | 1.39 | 842 ± 26 | 3.11 | 72.6 | 70.7 | 0.321 | 6.94 |
| **Mn** | 1840 ± 29 | 1.58 | 2710 ± 113 | 4.16 | 1800 ± 26 | 1.45 | 2600 ± 144 | 5.57 | 89.2 | 108 | 2.35 | 4.40 |
| **Ni** | 7.97 ± 0.07 | 0.933 | 11.4 ± 0.5 | 3.99 | 7.79 ± 0.15 | 1.94 | 10.4 ± 0.3 | 3.11 | 90.1 | 94.1 | 2.34 | 9.60 |
| **Pb** | 18.4 ± 0.3 | 1.59 | 23.1 ± 1.1 | 4.71 | 17.8 ± 0.3 | 1.79 | 21.6 ± 1.1 | 4.91 | 85.0 | 101 | 3.15 | 6.77 |
| **Zn** | 28.9 ± 0.7 | 2.49 | 40.3 ± 2.5 | 6.26 | 21.9 ± 2.9 | 13.3 | 30.9 ± 1.8 | 5.73 | 86.2 | 107 | 27.5 | 26.5 |

SD: standard deviation; n: number of replicates; RSD: Relative standard deviation; RPD: Relative percent difference = $\{|x_1 - x_2|/((x_1+x_2)/2)\}\times 100$ where $x_1$: values in soil alone and $x_2$: values in soil loaded on FDMS filter

### 6.3.3. Comparison between the sequential and single extraction

Figures 6.1-6.9 show the ratio of the sum of the bioaccessible concentrations of PTE in simulated $PM_{10}$ samples extracted by AMF alone and by AMF sequentially with the SBET (SBET2) or with the UBMG (*i.e.* AMF + SBET2 or AMF + UBMG) to the PTE bioaccessible concentration by using the SBET (*i.e.* SBET1) or the UBMSG procedures alone obtained in previous work described in Chapter 4 (see Table 6.6), expressed as a percentage (see Appendices F3 and F4). The statistical results obtained (t-test at 0.05 significance level), indicated that, for the SBET, there was a significant difference between the SBET1 and the AMF+SBET2 for As, Cd, Cr, Cu, Pb, and Zn in soils loaded on FDMS filters. For the UBMSG, a significant difference was calculated between UBMSG alone and AMF + UBMG for As, Cu, Fe, Ni, and Pb in soils loaded on FDMS filters.

**Table 6.6. Bioaccessible concentrations of potentially toxic elements (PTE) in the simulated $PM_{10}$ samples (BGS RM 102 Ironstone Soil on FDMS filters) using the simplified bioaccessibility extraction test (SBET) (*i.e.* SBET1) and the stomach phase of the unified bioaccessibility method (UBMSG)**[187]

| PTE | Soil on FDMS filters | |
|---|---|---|
| | **SBET1** | **UBMSG** |
| | **Mean ± SD (mg $kg^{-1}$)(n=3)** | **Mean ± SD (mg $kg^{-1}$)(n=3)** |
| **As** | 1.66 ± 0.07 | 4.41 ± 0.07 |
| **Cd** | 0.188 ± 0.007 | 0.217 ± 0.006 |
| **Cr** | 23.3 ± 1.1 | 35.0 ± 0.4 |
| **Cu** | 6.62 ± 0.29 | 7.01 ± 0.18 |
| **Fe** | 1070 ± 22 | 1290 ± 45 |
| **Mn** | 1760 ± 43 | 2780 ± 55 |
| **Ni** | 7.93 ± 0.20 | 12.2 ± 0.2 |
| **Pb** | 13.4 ± 0.3 | 18.4 ± 1.4 |
| **Zn** | 34.8 ± 8.4 | 35.6 ± 3.8 |

SD: standard deviation; n: number of replicates

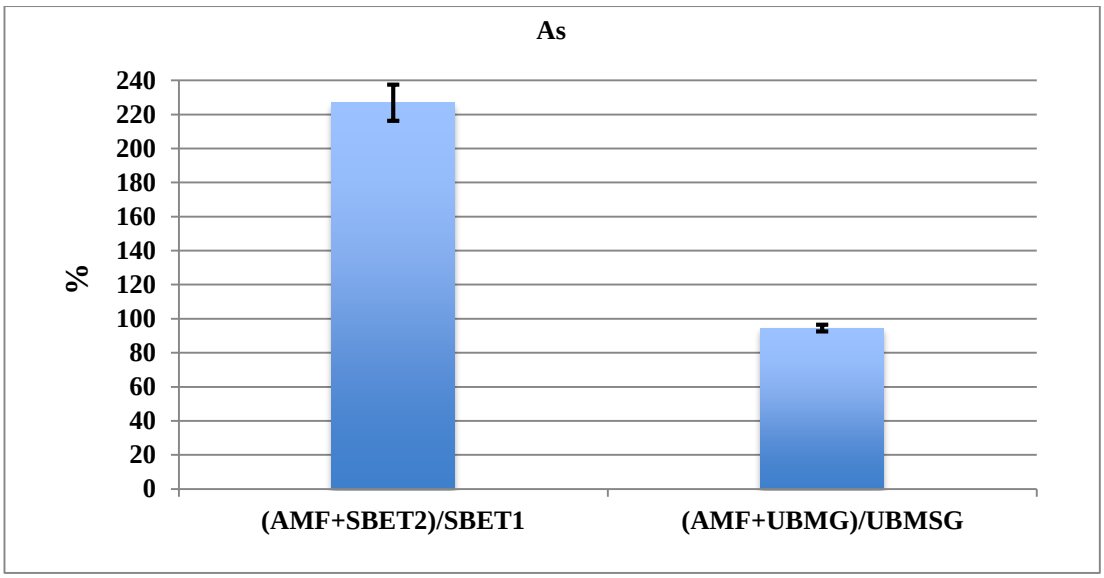


**Figure 6.1. The ratio of the sum of the bioaccessible concentrations of As in simulated $PM_{10}$ samples (soil on FDMS filters) extracted by artificial mucus fluid (AMF) alone and by AMF sequentially with the simplified bioaccessibility extraction test (SBET2) or with the stomach phase (gastric fluid only) of the unified bioaccessibility method (UBMG) to the PTE bioaccessible concentration by using the SBET (*i.e.* SBET1) or the UBMSG procedures alone**

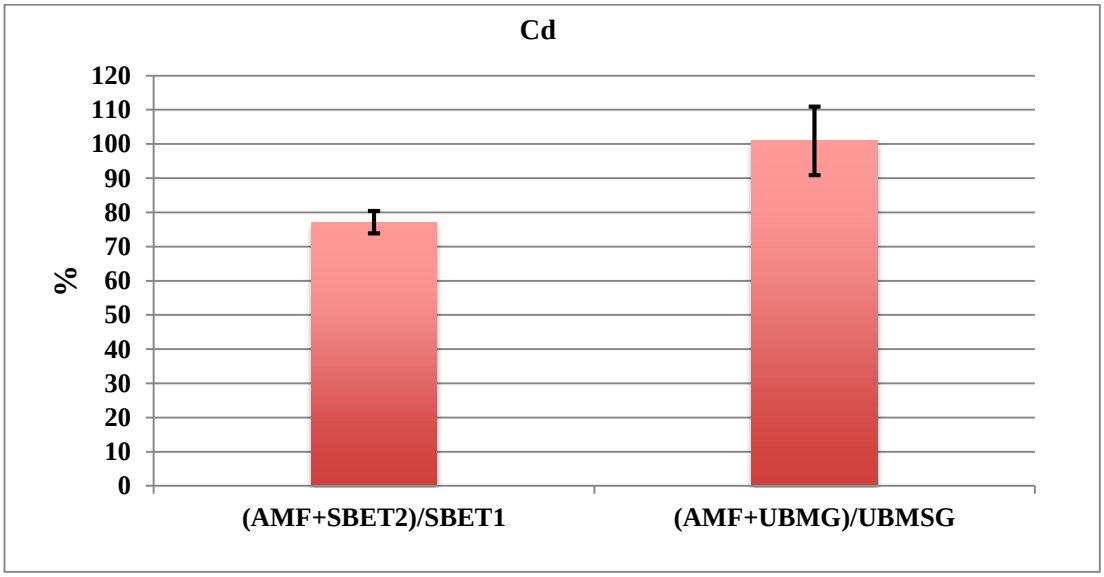


**Figure 6.2. The ratio of the sum of the bioaccessible concentrations of Cd in simulated $PM_{10}$ samples (soil on FDMS filters) extracted by artificial mucus fluid (AMF) alone and by AMF sequentially with the simplified bioaccessibility extraction test (SBET2) or with the stomach phase (gastric fluid only) of the unified bioaccessibility method (UBMG) to the PTE bioaccessible concentration by using the SBET (*i.e.* SBET1) or the UBMSG procedures alone**

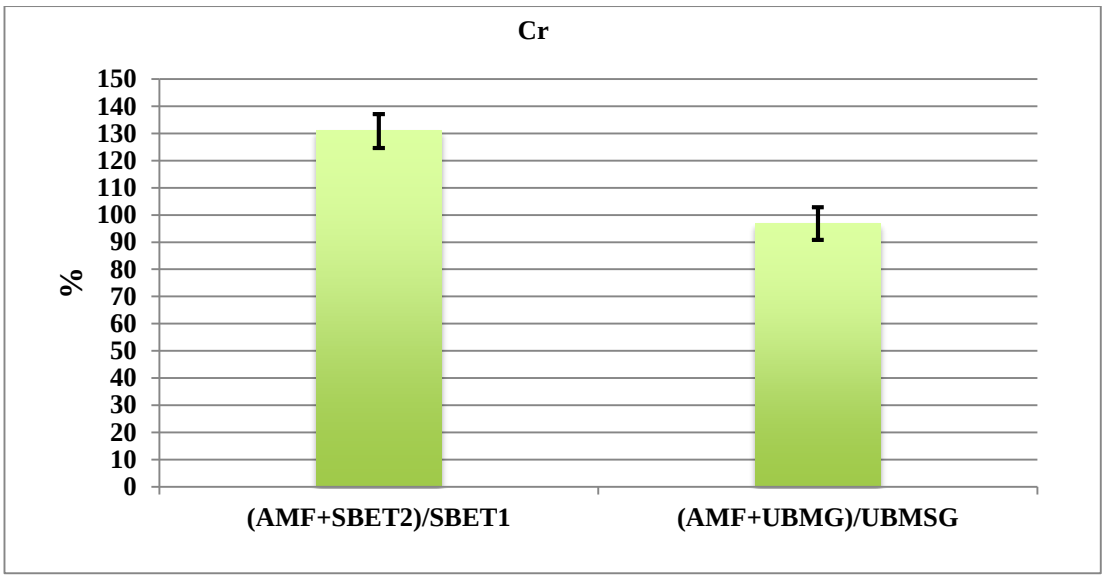


**Figure 6.3. The ratio of the sum of the bioaccessible concentrations of Cr in simulated $PM_{10}$ samples (soil on FDMS filters) extracted by artificial mucus fluid (AMF) alone and by AMF sequentially with the simplified bioaccessibility extraction test (SBET2) or with the stomach phase (gastric fluid only) of the unified bioaccessibility method (UBMG) to the PTE bioaccessible concentration by using the SBET (*i.e.* SBET1) or the UBMSG procedures alone**

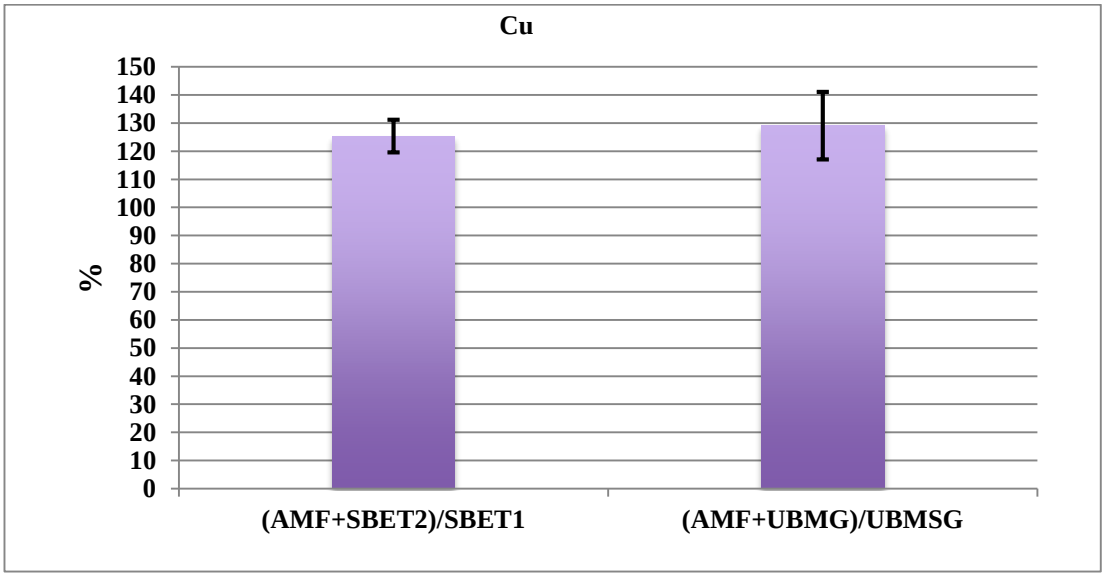


**Figure 6.4. The ratio of the sum of the bioaccessible concentrations of Cu in simulated $PM_{10}$ samples (soil on FDMS filters) extracted by artificial mucus fluid (AMF) alone and by AMF sequentially with the simplified bioaccessibility extraction test (SBET2) or with the stomach phase (gastric fluid only) of the unified bioaccessibility method (UBMG) to the PTE bioaccessible concentration by using the SBET (*i.e.* SBET1) or the UBMSG procedures alone**

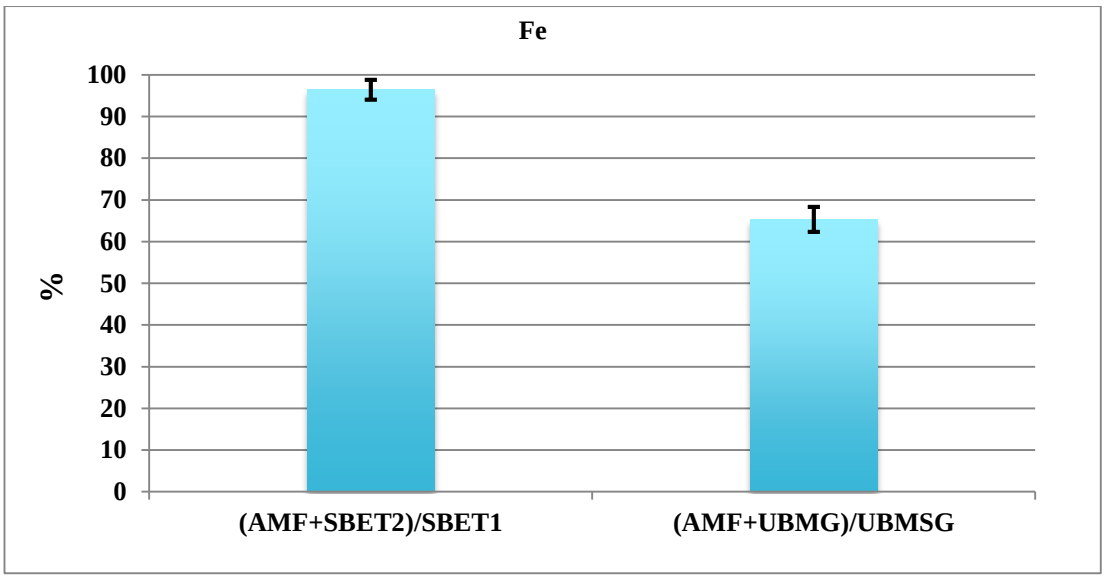


**Figure 6.5. The ratio of the sum of the bioaccessible concentrations of Fe in simulated $PM_{10}$ samples (soil on FDMS filters) extracted by artificial mucus fluid (AMF) alone and by AMF sequentially with the simplified bioaccessibility extraction test (SBET2) or with the stomach phase (gastric fluid only) of the unified bioaccessibility method (UBMG) to the PTE bioaccessible concentration by using the SBET (*i.e.* SBET1) or the UBMSG procedures alone**

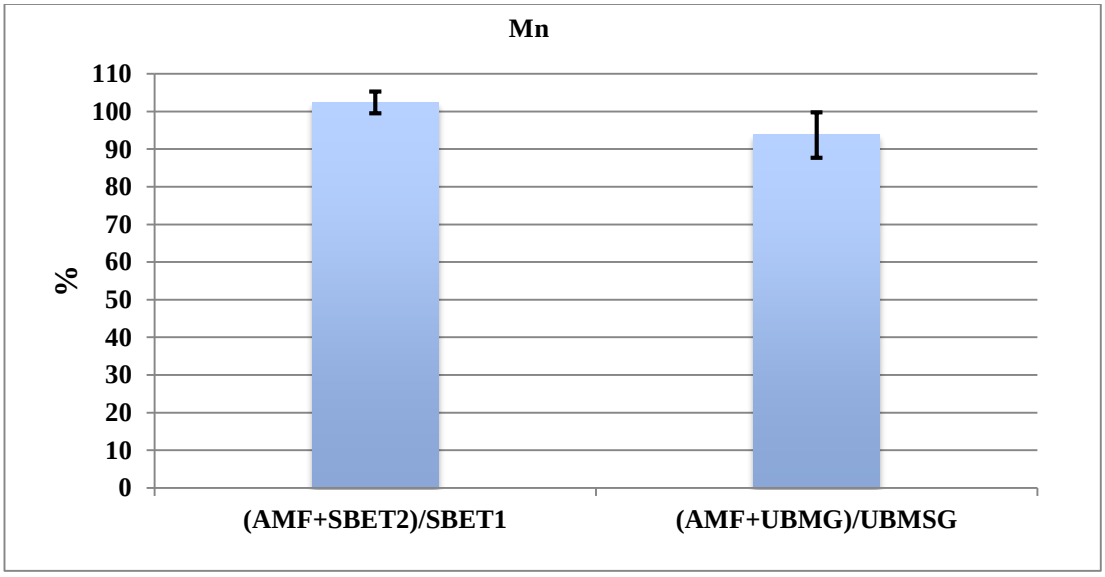


**Figure 6.6. The ratio of the sum of the bioaccessible concentrations of Mn in simulated $PM_{10}$ samples (soil on FDMS filters) extracted by artificial mucus fluid (AMF) alone and by AMF sequentially with the simplified bioaccessibility extraction test (SBET2) or with the stomach phase (gastric fluid only) of the unified bioaccessibility method (UBMG) to the PTE bioaccessible concentration by using the SBET (*i.e.* SBET1) or the UBMSG procedures alone**

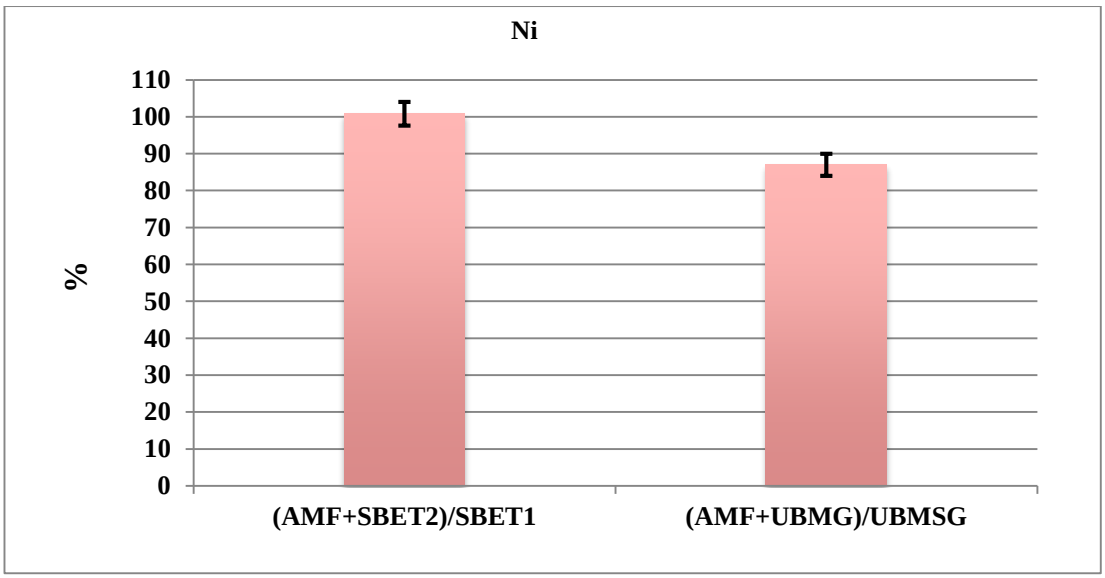


**Figure 6.7. The ratio of the sum of the bioaccessible concentrations of Ni in simulated $PM_{10}$ samples (soil on FDMS filters) extracted by artificial mucus fluid (AMF) alone and by AMF sequentially with the simplified bioaccessibility extraction test (SBET2) or with the stomach phase (gastric fluid only) of the unified bioaccessibility method (UBMG) to the PTE bioaccessible concentration by using the SBET (*i.e.* SBET1) or the UBMSG procedures alone**

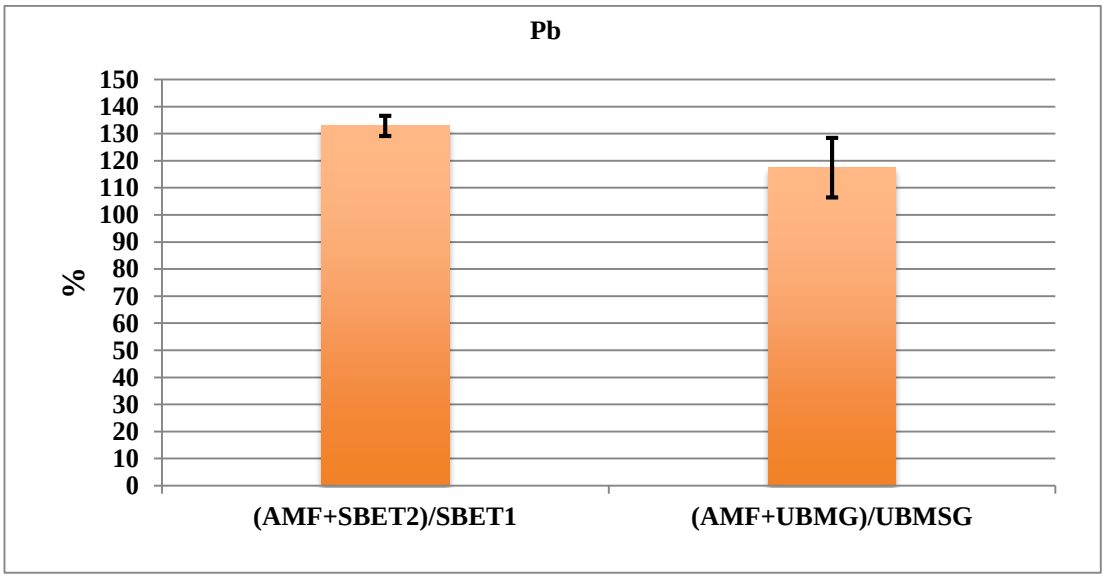


**Figure 6.8. The ratio of the sum of the bioaccessible concentrations of Pb in simulated $PM_{10}$ samples (soil on FDMS filters) extracted by artificial mucus fluid (AMF) alone and by AMF sequentially with the simplified bioaccessibility extraction test (SBET2) or with the stomach phase (gastric fluid only) of the unified bioaccessibility method (UBMG) to the PTE bioaccessible concentration by using the SBET (*i.e.* SBET1) or the UBMSG procedures alone**

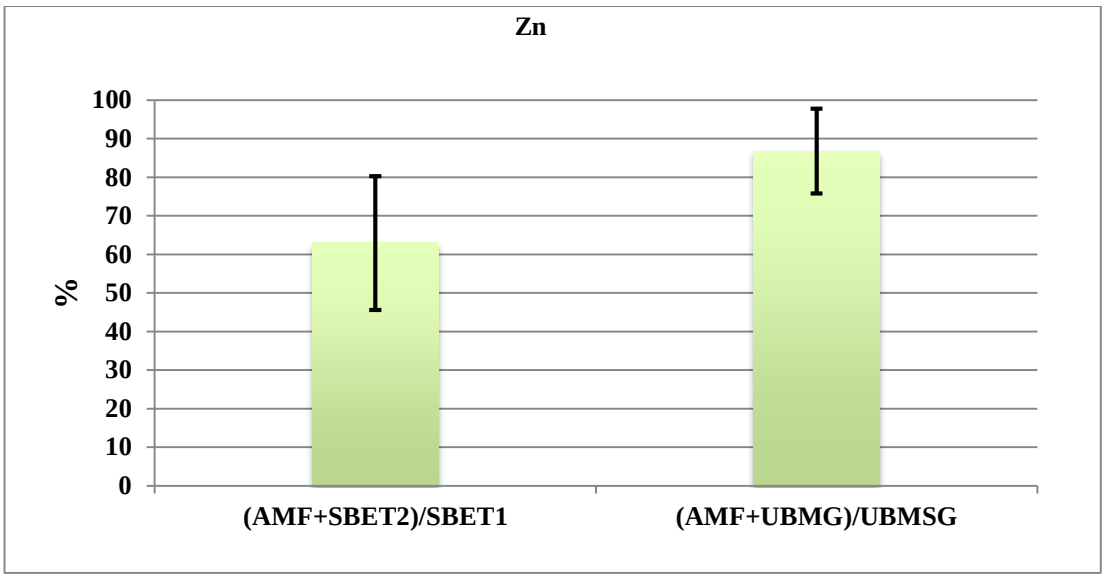


**Figure 6.9. The ratio of the sum of the bioaccessible concentrations of Zn in simulated $PM_{10}$ samples (soil on FDMS filters) extracted by artificial mucus fluid (AMF) alone and by AMF sequentially with the simplified bioaccessibility extraction test (SBET2) or with the stomach phase (gastric fluid only) of the unified bioaccessibility method (UBMG) to the PTE bioaccessible concentration by using the SBET (*i.e.* SBET1) or the UBMSG procedures alone**

Based on the values in Figures 6.1-6.9 and the significant differences obtained from the t-test, the PTE could be grouped into three categories for each method. The first group was PTE that showed no significant difference between single and sequential extraction; the second group was PTE that showed significant difference and the values of bioaccessible concentration of PTE were larger in the sequential extraction, whilst the last group was PTE that showed significant difference and the values of bioaccessible concentration of PTE were lower in the sequential extraction.

For the SBET, the first group comprised Fe, Mn, and Ni; the second included As (+127 %), Cr (+31 %), Cu (+25 %), and Pb (+33 %); and Cd (-23 %) and Zn (-37.1 %) were involved in the third group. In contrast, for the UBMSG, the first group included Cd, Cr, and Mn; the second group comprised Cu (+29 %) and Pb (+17 %); and the last one involved As (-6 %), Fe (-35 %), Ni (-13 %), and Zn (-13.2 %). From the results obtained, Cu, Mn, Pb, and Zn showed the same behavior in both the SBET and UBMSG, where Mn and Zn were involved in the first and third groups, respectively, while Cu and Pb were included in the second group.

The difference in solubility of PTE in different reagents used in this work could be because of the factors that affect the binding between soil and PTE. The first factor is the size and the charge of the PTE (a higher-charge smaller-size ion is generally more strongly bond and thus less mobile).[218] The second factor is pH value (at low pH values, the solubility of PTE is increased due to the competition from $H^+$ for binding sites on soil).[219] The third factor is the displacement of elements from exchange sites by other ions (e.g. the presence of $PO_4^{3-}$ leads to an increase in the solubility of As).[218] Difference may also occur because of metal complexation by organic acids. This can increase or decrease the solubility of PTE depending on the solubility of the organic ligand.[220, 221] For Cu and Pb, which are strongly bond by organic acids,[222] this factor may explain the increase in their concentration in the AMF+SBET2 and AMF+UBMG as the reagents of these sequential procedures contain a larger number of organic acids than those in the SBET1 or UBMSG.

### 6.3.4. Quality control

The results obtained show that the spike recoveries of PTE (Tables 6.4 and 6.5) in all extraction procedures conducted in this work were between 85 and 114 % except for Fe, where it was 72.6 and 70.7 % for SBET2 and UBMG, respectively, when these were conducted sequentially after the extraction by the AMF. This may be due to the formation of insoluble precipitates.[216] For the precision expressed as RSD, approximately 87 % of the RSD values were < 10 %, and 13 % of the values were between 10 and < 15 % (see Tables 6.4 and 6.5).

## 6.4. Conclusion

In this chapter, a new sequential extraction was developed to measure the bioaccessible PTE fraction in $PM_{10}$ that is inhaled and subsequently transported to the gastrointestinal tract by mucociliary clearance. A new artificial mucus fluid (AMF) was applied for determining the inhaled bioaccessible fraction then, sequentially, the SBET and the UBMG were used to determine the ingested bioaccessible fraction. The FDMS filters smeared with BGS RM 102 Ironstone Soil were used as samples to represent $PM_{10}$ collected onto filters. Effect of the presence of filters on the extraction was also assessed. Analysis of the blank FDMS filters

revealed that bioaccessible concentration of all PTE tested was low, except for Zn. The extractability of PTE in $PM_{10}$ was not affected significantly in the presence of the filters. The extractable fraction via the inhalation route was for As (0.785 and 0.828), Cu (1.94 and 1.90), Mn (7.16 and 9.76), and Ni (0.207 and 0.222) mg $kg^{-1}$ in soil alone and in soil loaded onto FDMS filters respectively, whilst concentrations of other PTE tested were less than detection limits. The PTE tested were extractable via the ingestion route either in sequence with AMF or by the SBET or UBM (stomach phase) alone. The comparison of the results from the sequential extraction route and the ingestion route alone demonstrated that, following the sequential route, meant that the assessment of the bioaccessible concentration was not underestimated for As, Cr, Cu, and Pb, nor overestimated for Cd, Fe, Ni and Zn. This was as a result of the difference between the two routes in terms of the constituents of reagents used, which affect the extractability of PTE differentially. Therefore, following the sequential extraction route has given a bioaccessible PTE concentration that is more close to a potential amount of PTE in $PM_{10}$ that might be extracted in the real digestion process.

# 7 Conclusions and further work

## 7.1. Conclusions

This project involved three parts, aiming to optimize, adapt (Chapter 4), and further develop (Chapter 5 and 6) two widely used bioaccessibility tests, the SBET and the UBM, to measure the bioaccessible concentration of PTE in inhaled PM less than 10 μm in diameter ($PM_{10}$) collected onto TX40 filters by the FDMS.

The first step of this project was optimisation of the methods for determining the bioaccessible PTE concentration in $PM_{10}$. Results obtained demonstrated the following.

1. The acrodisc® syringe filters should be washed immediately before use with 80 mL of the same reagent used for extraction to reduce the concentration of Cu and Zn in the procedural blank of the SBET, resulting in improved reproducibility;
2. Very low levels of bioaccessible PTE in blank FDMS filters were extracted by the reagents of the two oral bioaccessibility tests, except for Zn;
3. Filter blanks should be investigated whenever analytical methods are developed; and
4. The miniaturised versions developed of the SBET and the stomach phase of the UBM are appropriate for application to real samples of inhalable airborne $PM_{10}$ collected using the normal sampling devices for routine air quality monitoring.

In the second part of this project, five dynamic models (CL-SBET, CL-UBM, SPFC-SBET, SPFC-UBM, and SPDC-SBET) were established. The results obtained showed the following.

1. For the CL models, 1.0 mL $min^{-1}$ flow rate was considered the optimum one for delivery of extractants;
2. The closed system of the CL-SBET and the CL-UBM could be a good alternative model to the open system of their batch models, avoiding

problematic sample preparation processes such as filtration and centrifuging, and minimizing contamination;

3. For the SPFC-SBET and SPFC-UBM models, the first subfraction contained the largest bioaccessible concentration for most of the PTE determined;
4. The SPFC-SBET and the SPFC-UBM may represent a better simulator for digestion process than the batch models and were less susceptible for contamination;
5. There was no significance different between the bioaccessible PTE concentration obtained using the SPFC-SBET and those obtained by the SPDC-SBET;
6. The SPFC-SBET was more precise than the SPDC-SBET for all PTE tested, however, for Pb in SBDC-SBET, it was good (13.2% RSD); and
7. On-line determination of PTE either in simulated or real $PM_{10}$ samples using the SPDC-SBET was demonstrated for the first time.

The final part of the project involved a successful application of novel artificial mucus fluid (AMF), both as a single extraction, and as part of a sequential extraction with the SBET or the UBMG. This study demonstrated the following.

1. The bioaccessible concentrations of As, Cr, Cu, and Pb obtained from sequential extraction route were higher than those from the ingestion alone route, in contrast, they were lower for Cd, Fe, Ni and Zn; and
2. For assessing the bioaccessibility of PTE in inhaled $PM_{10}$ that are transported into the gastrointestinal tract by mucociliary clearance, a sequential bioaccessibility extraction test involving the AMF followed by artificial gastric fluid is preferred to a single-step process and should be adopted.

The extraction methods conducted in this work - both the static methods (batch and sequential model) and the dynamic (the CL, SPFC, and SPDC model) – have been successfully used to measure the bioaccessible PTE concentration in $PM_{10}$. However, the method that mimics the routes adopted by $PM_{10}$ in the body, and that are most similar to the dynamic and biological conditions of the gastrointestinal tract and respiratory system, would be the most fit for purpose for assessing the risk.

Because they have been designed and optimised specifically for application to airborne particles supported on FDMS filters, the methods developed in this work can be applied by municipal authorities, not only in the UK but worldwide, who use FDMS systems for routine air quality monitoring. They have the potential to allow new insight to be gained into the bioaccessibility of PTE associated with inhalable particles, and to serve as an important tool to aid environmental and public health protection, especially in urban settings.

### 7.2. Further work

There is clear opportunity for the dynamic models developed in this thesis to be automated, and future work could explore options for connecting several closed loop or single pass manifolds to a single ICP-MS instrument for unattended sample extraction.

Other PTE such as Co, Sn, Ti, V, Zr, etc. may cause effects to human health such as biomolecules oxidative damage or acute lung injury. Therefore measurement of these PTE as well as those studied in this thesis would be worthwhile in future studies. To investigate the effect of PTE in $PM_{10}$ in real-life environments, a case study should be conducted where measurement of bioaccessible PTE was investigated in parallel with epidemiological studies on human health.

In addition, it would be useful to apply lung fluids to $PM_{2.5}$ collected onto FDMS filters using the dynamic system used for the SBET and the stomach phase of the UBM in this thesis, as these particles can reach the deeper part of the respiratory system. As a result, a more holistic assessment of risk could be conducted by determining the bioaccessible PTE in both $PM_{10}$ and $PM_{2.5}$. What is more, in future, other batch sequential extraction methods, for example the three-step BCR soil extraction, could also be applied to $PM_{10}$ using dynamic models similar to those developed in this thesis. As a result, extraction time and difficulties could be decreased.

The residence time of $PM_{10}$ in the upper airways was set at one hour for this study, However, the effect of extraction duration on PTE extractability could be investigated. In addition, different solid to liquid ratios could be examined for the

AMF. It would be useful to apply the AMF to other $CRM_s$ such as NIST SRM 2711A for wider validation of the method. For assessing the influence of extractant and sample composition on bioaccessibility of PTE in the $PM_{10}$ a software modelling approach could be used to calculate equilibria associated with the extraction process. In addition, the speciation of PTE in $PM_{10}$, before and after extraction with AMF, and in the AMF-extracts, might be investigated.

In terms of risk assessment of PTE in airborne PM, it is recommended that organizations responsible for air quality monitoring (e.g. Glasgow City Council) should adopt bioaccessibility tests as well as measuring the amount of PM in the air, to obtain information more relevant to toxicity. As FDMS filters have high amounts of Zn, so it would be helpful for determining PTE if a new trace-elements free filter is used for collecting PM in the FDMS instead.

Generally, for more worldwide benefits from the outcomes of this project, particularly in developing countries, there is a need to have regular air quality monitoring systems and apply the methods developed in this study to these systems.

# References


1. N. J. Pekney and C. I. Davidson, *Analytica Chimica Acta*, 2005, **540**, 269-277.

2. B. J. Finlayson-Pitts and J. N. Pitts, *Science*, 1997, **276**, 1045-1051.

3. J. H. Seinfeld; and S. N. Pandis, *Atmospheric Chemistry and Physics: From Air Pollution to Climate Change*, second edn., John Wiley & Sons, Inc, Hoboken, New Jersey, USA, 2006.

4. A. Valavanidis, K. Fiotakis and T. Vlachogianni, *Journal of environmental science and health. Part C, Environmental carcinogenesis & ecotoxicology reviews*, 2008, **26**, 339-362.

5. Health effects institute (HEI), *Understanding the health effects of components of the particulate matter mix: progress and next steps.*, Health effects institute, 2002.

6. A. E. Aust, J. C. Ball, A. A. Hu, J. S. Lighty, K. R. Smith, A. M. Straccia, J. M. Veranth and W. C. Young, *Particle characteristics responsible for effects on human lung epithelial cells* 1041-5505, 2002.

7. D. Fairley, *Environmental Health Perspectives*, 1990, **89**, 159-168.

8. J. Schwartz, *Environmental Research*, 1994, **64**, 36-52.

9. F. Ajmone-Marsan, M. Biasioli, T. Kralj, H. Grcman, C. M. Davidson, A. S. Hursthouse, L. Madrid and S. Rodrigues, *Environmental pollution*, 2008, **152**, 73-81.

10. A. Churg and M. Brauer, *Ultrastructural Pathology*, 2000, **24**, 353-361.

11. A. Churg and M. Brauer, *American Journal of Respiratory and Critical Care Medicine*, 1997, **155**, 2109-2111.

12. S. Utsunomiya, K. A. Jensen, G. J. Keeler and R. C. Ewing, *Environmental Science & Technology*, 2004, **38**, 2289-2297.

13. W. Birmili, A. G. Allen, F. Bary and R. M. Harrison, *Environmental Science & Technology*, 2006, **40**, 1144-1153.

14. D. L. Costa and K. L. Dreher, *Environmental Health Perspectives*, 1997, **105**, 1053-1060.

15. F. Dominici, R. D. Peng, K. Ebisu, S. L. Zeger, J. M. Samet and M. L. Bell, *Environmental Health Perspectives*, 2007, **115**, 1701-1703.

16. Wiener RW and R. CE, *Indoor aerosols and aerosol exposure. In: Willeke K, Baron PA (eds) Aerosol measurement -principles, techniques and applications.*, Van Nostrand Reinhold, New York, 1993.

17. G. Patrick and C. Stirling, *Environmental Health Perspectives*, 1992, **97**, 47-51.

18. R. M. Molina, L. A. Schaider, T. C. Donaghey, J. P. Shine and J. D. Brain, *Environmental pollution*, 2013, **182**, 217-224.

19. V. S. a. N. C. ND Shah, *Journal of Applied Pharmaceutical Science* 2012, **02**, 33-37.

20. C. A. Pope, R. T. Burnett, M. J. Thun, E. E. Calle, D. Krewski, K. Ito and G. D. Thurston, *JAMA-J. Am. Med. Assoc.*, 2002, **287**, 1132-1141.

21. D. M. Brown, M. R. Wilson, W. MacNee, V. Stone and K. Donaldson, *Toxicology and Applied Pharmacology*, 2001, **175**, 191-199.

22. M. T. Cruz, *Monitoring and source apportionment for particulate matter pollution in six Asian countries*, http://ateneophysicslabs.wordpress.com/2013/08/06/monitoring-and-source-apportionment-for-particulate-matter-pollution-in-six-asian-countries-a-talk-by-melliza-templonuevo-cruz/, Accessed 15.07, 2014.

23. S. Mossetti, S. P. Angius and E. Angelino, *International Journal of Environment and Pollution*, 2005, **24**, 247-259.

24. B. Artinano, P. Salvador, D. G. Alonso, X. Querol and A. Alastuey, *Environmental pollution*, 2003, **125**, 453-465.

25. P. Chandra Mouli, S. Venkata Mohan, V. Balaram, M. Praveen Kumar and S. Jayarama Reddy, *Atmospheric Environment*, 2006, **40**, 136-146.

26. S. Ravanbakhsh, M.-T. Zohreh and D. Fereshteh, *RJC Rasayan J. Chem*, 2008, **1**, 757-765.

27. F. Madrid, M. Biasioli and F. Ajmone-Marsan, *Archives of environmental contamination and toxicology*, 2008, **55**, 21-32.

28. Y. J. Cui, Y. G. Zhu, R. H. Zhai, Y. Z. Huang, Y. Qiu and J. Z. Liang, *Environment International*, 2005, **31**, 784-790.

29. V. Ettler, B. Kribek, V. Majer, I. Knesl and M. Mihaljevic, *Journal of Geochemical Exploration*, 2012, **113**, 68-75.

30. V. Ettler, Z. Johan, B. Kribek, O. Sebek and M. Mihaljevic, *Applied Geochemistry*, 2009, **24**, 1-15.

31. O. Sracek, M. Mihaljevic, B. Kribek, V. Majer and F. Veselovsky, *Journal of African Earth Sciences*, 2010, **57**, 14-30.

32. G. J. Urquhart, University of Strathclyde, 2005.

33. J. Sialelli, G. J. Urquhart, C. M. Davidson and A. S. Hursthouse, *Environmental geochemistry and health*, 2010, **32**, 517-527.

34. H. W. Mielke, C. R. Gonzales, M. K. Smith and P. W. Mielke, *Environmental Research*, 1999, **81**, 117-129.

35. M. Zhai, H. A. B. Kampunzu, M. P. Modisi and O. Totolo, *Environmental Geology*, 2003, **45**, 171-180.

36. L. Madrid, E. Diaz-Barrientos and F. Madrid, *Chemosphere*, 2002, **49**, 1301-1308.

37. C. Walter, A. B. McBratney, R. A. V. Rossel and J. A. Markus, *Environmetrics*, 2005, **16**, 339-355.

38. T. B. Chen, Y. M. Zheng, M. Lei, Z. C. Huang, H. T. Wu, H. Chen, K. K. Fan, K. Yu, X. Wu and Q. Z. Tian, *Chemosphere*, 2005, **60**, 542-551.

39. M. Biasioli, R. Barberis and F. Ajmone-Marsan, *Science of the Total Environment*, 2006, **356**, 154-164.

40. N. S. Duzgoren-Aydin, *Science of the Total Environment*, 2007, **385**, 182-195.

41. H. W. Mielke, J. C. Anderson, K. J. Berry, P. W. Mielke, R. L. Chaney and M. Leech, *American Journal of Public Health*, 1983, **73**, 1366-1369.

42. P. W. Abrahams, *Science of the Total Environment*, 2002, **291**, 1-32.

43. S. D. Siciliano, K. James, G. Zhang, A. N. Schafer and J. D. Peak, *Environmental Science & Technology*, 2009, **43**, 6385-6390.

44. C. P. Nathanail and C. McCaffrey, *Land Contamination & Reclamation*, 2003, **11** 309-313.

45. R. Mohanraj, P. A. Azeez and T. Priscilla, *Archives of environmental contamination and toxicology*, 2004, **47**, 162-167.

46. A. J. Fernández Espinosa, M. T. Rodríguez and F. F. Álvarez, *Atmospheric Environment*, 2004, **38**, 873-886.

47. P. Richter, P. Griño, I. Ahumada and A. Giordano, *Atmospheric Environment*, 2007, **41**, 6729-6738.

48. G. Rauret, *Talanta*, 1998, **46**, 449-455.

49. K. K. Chatterjee, *Uses of metals and metallic minerals*, New age international publishers New Delhi, 2007.

50. Alina Kabata-Pendias and A. B. Mukherjee, *Trace elements from soil to human*, Springer-Verlag Berlin Heidelberg, New York, 2007.

51. A. Kabata-Pendias, *Trace elements in soils and plants*, Third Edition edn., CRC Press LLC, USA, 2001.

52. D. E. Newton, *Chemical Elements*, Second Edition edn., Gale, Cengage Learning, China, 2010.

53. A. Marin, A. Lopez-Gonzalvez and C. Barbas, *Analytica Chimica Acta*, 2001, **442**, 305-318.

54. M. Zhang, Y. Song and X. Cai, *The Science of the total environment*, 2007, **376**, 100-108.

55. E. Agency, *Human health toxicological assessment of contaminants in soil.* Science Report – Final SC050021/SR2, Environment Agency, UK, 2009.

56. L. Ferreira-Baptista and E. De Miguel, *Atmospheric Environment*, 2005, **39**, 4501-4512.

57. W. J. G. M. Peijnenburg and T. Jager, *Ecotoxicology and Environmental Safety*, 2003, **56**, 63-77.

58. A. M. Ure, *Fresenius J. Anal. Chem.*, 1990, **337**, 577-581.

59. C. R. M. Rao, A. Sahuquillo and J. F. L. Sanchez, *Water Air Soil Pollut.*, 2008, **189**, 291-333.

60. I. L. Marr, P. Kluge, L. Main, V. Margerin and C. Lescop, *Mikrochim. Acta*, 1995, **119**, 219-232.

61. D. Harvey, *Modern analytical chemistry*, McGraw-Hall Companies, Inc., USA, 2000.

62. S. W. Casteel, C. P. Weis, G. M. Henningsen and W. J. Brattin, *Environmental Health Perspectives*, 2006, **114**, 1162-1171.

63. J. Wragg and M. R. Cave, *In-vitro Methods for the Measurement of the Oral Bioaccessibility of Selected Metals and Metalloids in Soils: A Critical Review* P5-062/TR/01, Environment Agency, UK, 2003.

64. M. V. Ruby, R. Schoof, W. Brattin, M. Goldade, G. Post, M. Harnois, D. E. Mosby, S. W. Casteel, W. Berti, M. Carpenter, D. Edwards, D. Cragin and W. Chappell, *Environmental Science & Technology*, 1999, **33**, 3697-3705.

65. A. G. Oomen, A. Hack, M. Minekus, E. Zeijdner, C. Cornelis, G. Schoeters, W. Verstraete, T. Van de Wiele, J. Wragg, C. J. M. Rompelberg, A. Sips and J. H. Van Wijnen, *Environmental Science & Technology*, 2002, **36**, 3326-3334.

66. B. K. Kramer and P. B. Ryan, Hazardous Waste Research, Department of Chemistry, Emory University, Atlanta, 2000.

67. S. C. Hamel, B. Buckley and P. J. Lioy, *Environmental Science & Technology*, 1998, **32**, 358-362.

68. A. L. Morrison and B. L. Gulson, *Science of the Total Environment*, 2007, **382**, 30-42.

69. H. Roussel, C. Waterlot, A. Pelfrene, C. Pruvot, M. Mazzuca and F. Douay, *Archives of environmental contamination and toxicology*, 2010, **58**, 945-954.

70. M. V. Ruby, A. Davis, R. Schoof, S. Eberle and C. M. Sellstone, *Environmental Science & Technology*, 1996, **30**, 422-430.

71. C. Dabin;, A. Guigonnet-Sergent;, E. Algros; and A. M. Charissou, *Bioavailability and bioaccessibility of pollutants in contaminated soils* STUDY No. 10-0671/1A, State Of Present Knowledge And Research Avenues, 2012.

72. A. Tronde, Dissertation, Uppsala University, 2002.

73. M. King, in *Physiologic basis of respiratory disease* BC Decker Inc, USA, Editon edn., 2005, pp. 409-416.

74. R. Tarran, *Proceedings of the American Thoracic Society*, 2004, **1**, 42-46.

75. T. Falta, A. Limbeck, G. Koellensperger and S. Hann, *Analytical and bioanalytical chemistry*, 2008, **390**, 1149-1157.

76. A. G. Oomen, C. J. M. Rompelberg, M. A. Bruil, C. J. G. Dobbe, D. Pereboom and A. Sips, *Archives of environmental contamination and toxicology*, 2003, **44**, 281-287.

77. G. Schoeters, *J. Toxicol. Env. Health-Pt b-Crit. Rev.*, 2010, **13**, 232-241.

78. J. Wragg and M. Cave, *Analytica Chimica Acta*, 2012, **722**, 43-54.

79. M. V. Ruby, A. Davis, T. E. Link, R. Schoof, R. L. Chaney, G. B. Freeman and P. Bergstrom, *Environmental Science & Technology*, 1993, **27**, 2870-2877.

80. J. W. a. M. R. Cave, *In-vitro Methods for the Measurement of the Oral Bioaccessibility of Selected Metals and Metalloids in Soils: A Critical Review*

P5-062/TR/01, Environment Agency, Rio House, Waterside Drive, Aztec West, Almondsbury, Bristol, BS32 4UD., 2003a.

81. N. T. Basta, R. Gradwohl, K. L. Snethen and J. L. Schroder, *J. Environ. Qual.*, 2001, **30**, 1222-1230.

82. J. Y. Kim, K. W. Kim, J. U. Lee, J. S. Lee and J. Cook, *Environmental geochemistry and health*, 2002, **24**, 215-227.

83. J. Wragg, M. Cave, N. Basta, E. Brandon, S. Casteel, S. Denys, C. Gron, A. Oomen, K. Reimer, K. Tack and T. Van de Wiele, *Science of the Total Environment*, 2011, **409**, 4016-4030.

84. A. L. Juhasz, J. Weber, E. Smith, R. Naidu, M. Rees, A. Rofe, T. Kuchel and L. Sansom, *Environmental Science & Technology*, 2009, **43**, 9487-9494.

85. M. C. Navarro, C. Perez-Sirvent, M. J. Martinez-Sanchez, J. Vidal and J. Marimon, *Chemosphere*, 2006, **63**, 484-489.

86. K. D. Bradham, K. G. Scheckel, C. M. Nelson, P. E. Seales, G. E. Lee, M. F. Hughes, B. W. Miller, A. Yeow, T. Gilmore, S. M. Serda, S. Harper and D. J. Thomas, *Environmental Health Perspectives*, 2011, **119**, 1629-1634.

87. J. Moreda-Piñeiro, A. Moreda-Piñeiro, V. Romarís-Hortas, C. Moscoso-Pérez, P. López-Mahía, S. Muniategui-Lorenzo, P. Bermejo-Barrera and D. Prada-Rodríguez, *TrAC Trends in Analytical Chemistry*, 2011, **30**, 324-345.

88. USEPA, *Guidance for Evaluating the Oral Bioavailability of Metals in Soils for Use in Human Health Risk Assessment*, USA, 2007.

89. M. Intawongse and J. R. Dean, *Trac-Trends in Analytical Chemistry*, 2006, **25**, 876-886.

90. E. A. Medlin, University of Colorado at Boulder, 1997.

91. USEPA, *Standard Operating Procedure for an In Vitro Bioaccessibility Assay for Lead in Soil* 9200.2-86, Environmental Protection Agency, USA, 2012.

92. M. C. J Wragg, H Taylor, N Basta, E Brandon, S Casteel, C Gron, A Oomen, T Van de Wiele, *Inter-laboratory Trial of a Unified Bioaccessibility Procedure* Open report OR/07/027, British Geological Survey, Nottingham, 2009.

93. S. Denys, J. Caboche, K. Tack, G. Rychen, J. Wragg, M. Cave, C. Jondreville and C. Feidt, *Environmental Science & Technology*, 2012, **46**, 6252-6260.

94. BARGE and INERIS, *UBM procedure for the measurement of inorganic contaminant bioaccessibility from solid matrices*, http://www.bgs.ac.uk/barge/docs/BARGE_UBM_DEC_2010.pdf, 2014.

95. M. Rosende, L. M. Magalhaes, M. A. Segundo and M. Miro, *Analytica Chimica Acta*, 2014, **842**, 1-10.

96. A. Broadway, M. R. Cave, J. Wragg, F. M. Fordyce, R. J. F. Bewley, M. C. Graham, B. T. Ngwenya and J. G. Farmer, *Science of the Total Environment*, 2010, **409**, 267-277.

97. A. Barsby, J. M. McKinley, U. Ofterdinger, M. Young, M. R. Cave and J. Wragg, *Science of the Total Environment*, 2012, **433**, 398-417.

98. A. Robache, F. Mathé, J.-C. Galloo and R. Guillermo, *The Analyst*, 2000, **125**, 1855-1859.

99. H. Yongming, D. Peixuan, C. Junji and E. S. Posmentier, *The Science of the total environment*, 2006, **355**, 176-186.

100. M. Huang, W. Wang, C. Y. Chan, K. C. Cheung, Y. B. Man, X. Wang and M. H. Wong, *The Science of the total environment*, 2014, **479-480**, 117-124.

101. F. Rueda-Holgado, M. R. Palomo-Marin, L. Calvo-Blazquez, F. Cereceda-Balic and E. Pinilla-Gil, *Talanta*, 2014, **125**, 125-130.

102. B. S. Sagagi, PhD thesis, University of Strathclyde, 2013.

103. D. W. Layton and P. I. Beamer, *Environmental Science & Technology*, 2009, **43**, 8199-8205.

104. D. Voutsa and C. Samara, *Atmospheric Environment*, 2002, **36**, 3583-3590.

105. F. Madrid, M. Biasioli and F. Ajmone-Marsan, *Archives of environmental contamination and toxicology*, 2008, **55**, 21-32.

106. X. Hu, Y. Zhang, Z. Ding, T. Wang, H. Lian, Y. Sun and J. Wu, *Atmospheric Environment*, 2012, **57**, 146-152.

107. P. Lawson and S. Tellis, Personal Communication, Air Monitors Ltd, UK, 2015.

108. O. Butler, Personal Communication, Health and Safety Laboratory, UK, 2015.

109. T. F. Scientific, *Operating guide for TEOM-FDMS 1405-F ambient particulate monitor*, http://www.thermoscientific.com/content/dam/tfs/ATG/EPD/EPD Documents/Product Manuals & Specifications/Air Quality Instruments and Systems/Particulate/EPM-manual-1405F.pdf, 2014.

110. D. L. Vaughn and A. E. Ray, *Standard Operating Procedure for the Continuous Measurement of Particulate Matter*,

http://www.epa.gov/ttnamti1/files/ambient/pm25/sop_project/8500C_FDMS_SOP_Draft.pdf, 2014.

111. PALL Lif Sciences, *Filtration products for air monitoring and sampling*, http://www.pall.com/pdfs/Laboratory/08.1868_Air_Monitoring_SS.pdf, 2014.

112. C. S. Eskilsson and E. Bjorklund, *J. Chromatogr. A*, 2000, **902**, 227-250.

113. F. E. Smith and E. A. Arsenault, *Talanta*, 1996, **43**, 1207-1268.

114. P. Quevauviller, J.-L. Imbert and M. Ollé, *Microchimica Acta*, 1993, **112**, 147-154.

115. J. Nieuwenhuize, C. H. Poleyvos, A. H. Vandenakker and W. Vandelft, *Analyst*, 1991, **116**, 347-351.

116. C. Bettiol, L. Stievano, M. Bertelle, F. Delfino and E. Argese, *Applied Geochemistry*, 2008, **23**, 1140-1151.

117. J. R. Dean, *Methods for environmental trace analysis*, John Wiley & Sons Ltd., England, UK, 2003.

118. N. E. Leadbeater, *Microwave heating as a tool for sustainable chemistry*, CRC Press, Taylor and Francis Group, LLC, USA, 2011.

119. R. S. Z. Mester, *Sample preparation for trace element analysis*, Elsevier B. V. , The Netherlands, 2003.

120. P. A. Mello, J. S. Barin and R. A. Guarnieri, in *Microwave-Assisted Sample Preparation for Trace Element Analysis*, ed. É. M. d. M. Flores, Elsevier, Amsterdam, Editon edn., 2014, pp. 59-75.

121. J. R. Dean, *Practical iductively coupled plasma spectroscopy*, John Wiley & Sons, Ltd, England, UK, 2005.

122. V. Sandroni and C. M. M. Smith, *Analytica Chimica Acta*, 2002, **468**, 335-344.

123. F. Vanhaecke, M. Resano and L. Moens, *Analytical and bioanalytical chemistry*, 2002, **374**, 188-195.

124. D. Beauchemin, *Analytical Chemistry*, 2010, **82**, 4786-4810.

125. E. M. S. F. James W. Robinson, & George M. Frame II, *Undergraduate instrumental analysis*, Taylor & Francis e-Library, New York, 2005.

126. D. C. Harris, *Quantitative chemical analysis*, W. H. Freeman and Company New York, 2007.

127. R. Thomas, *Practical guide to ICP-MS*, Marcel Dekker, Inc., New York, USA, 2004.

128. *High throughtput analysis of rock digests using the 7700x ICP-MS with HMI and ISIS-DS*, http://www.agilent.com/cs/library/articlereprints/public/5990_6783EN.pdf, Accessed March, 2016.

129. P. Patnaik, *Handbook of environmental analysis*, second edition edn., CRC Press / Taylor & Francis Group, USA, 2010.

130. S. Bell, *A beginner's guide to uncertainty of measurement*, http://www.npl.co.uk/publications/a-beginners-guide-to-uncertainty-in-measurement, Accessed 7th March, 2016.

131. J. N. Miller and J. C. Miller, *Statistics and chemometrics for analytical chemistry*, Sixth edition edn., Pearson Education Limited, UK, 2010.

132. S. Mitra, *Sample preparation techniques in analytical chemistry*, John Wiley & Sons, Inc., New Jersey, 2003.

133. D. Kealey and P. J. Haines, *Analytical chemistry*, Taylor & Francis e-Library, UK, 2005.

134. S. B. Green and N. J. Salkind, *Using SPSS for Windows and Macintosh : analyzing and understanding data*, 5th edition edn., Pearson Education International, London, UK, 2008.

135. G. W. Heiman, *Basic statistics for the behavioral sciences*, Wadsworth, Cenage Learning, USA, 2011.

136. L. Jorhem, J. Engman and T. Schroder, *Fresenius J. Anal. Chem.*, 2001, **370**, 178-182.

137. N. Cruz, S. M. Rodrigues, D. Tavares, R. J. Monteiro, L. Carvalho, T. Trindade, A. C. Duarte, E. Pereira and P. F. Romkens, *Chemosphere*, 2015, **135**, 304-311.

138. J. G. Farmer, A. Broadway, M. R. Cave, J. Wragg, F. M. Fordyce, M. C. Graham, B. T. Ngwenya and R. J. Bewley, *The Science of the total environment*, 2011, **409**, 4958-4965.

139. A. L. Juhasz, E. Smith, J. Weber, M. Rees, T. Kuchel, A. Rofe, L. Sansom and R. Naidu, *J. Environ. Sci. Health Part A-Toxic/Hazard. Subst. Environ. Eng.*, 2013, **48**, 604-611.

140. S. Das, J. S. Jean and S. Kar, *Ecotoxicol Environ Saf*, 2013, **92**, 252-257.

141. S. M. Rodrigues, N. Cruz, C. Coelho, B. Henriques, L. Carvalho, A. C. Duarte, E. Pereira and P. F. Romkens, *Environmental pollution*, 2013, **183**, 234-242.

142. J. Li, Y. Wei, L. Zhao, J. Zhang, Y. Shangguan, F. Li and H. Hou, *Ecotoxicol Environ Saf*, 2014, **110**, 308-315.

143. S.-W. Lee, B.-T. Lee, J.-Y. Kim, K.-W. Kim and J.-S. Lee, *Environmental Monitoring and Assessment*, 2006, **119**, 233-244.

144. B. B. Yu, Y. Wang and Q. X. Zhou, *PLoS One*, 2014, **9**, 9.

145. A. L. Juhasz, E. Smith, J. Weber, M. Rees, A. Rofe, T. Kuchel, L. Sansom and R. Naidu, *Chemosphere*, 2007, **69**, 69-78.

146. S. Tellis, Personal Communication, Air Monitors Ltd, UK, 2015.

147. A. Leufroy, L. Noel, D. Beauchemin and T. Guerin, *Analytical and bioanalytical chemistry*, 2012, **402**, 2849-2859.

148. M. Minekus, P. Marteau, R. Havenaar and J. H. J. Huisintveld, *ATLA-Altern. Lab. Anim.*, 1995, **23**, 197-209.

149. M. Y. Chu and D. Beauchemin, *J. Anal. At. Spectrom.*, 2004, **19**, 1213-1216.

150. S. Torres-Escribano, S. Denis, S. Blanquet-Diot, M. Calatayud, L. Barrios, D. Velez, M. Alric and R. Montoro, *The Science of the total environment*, 2011, **409**, 604-611.

151. M. Culen, A. Rezacova, J. Jampilek and J. Dohnal, *Journal of pharmaceutical sciences*, 2013, **102**, 2995-3017.

152. J. Shiowatana, N. Tantidanai, S. Nookabkaew and D. Nacapricha, *Environment International*, 2001, **26**, 381-387.

153. J. Buanuam, J. Shiowatana and P. Pongsakul, *Journal of environmental monitoring : JEM*, 2005, **7**, 778-784.

154. W. Boonjob, M. Miro and V. Cerda, *Analytical Chemistry*, 2008, **80**, 7319-7326.

155. N. Kaewkhomdee, C. Kalambaheti, S. Predapitakkun, A. Siripinyanond and J. Shiowatana, *Analytical and bioanalytical chemistry*, 2006, **386**, 363-369.

156. W. Boonjob, M. Zevenhoven, P. Ek, M. Hupa, A. Ivaska and M. Miró, *J. Anal. At. Spectrom.*, 2012, **27**, 841.

157. P. S. Fedotov, W. J. Fitz, R. Wennrich, P. Morgenstern and W. W. Wenzel, *Analytica Chimica Acta*, 2005, **538**, 93-98.

158. O. N. Katasonova, P. S. Fedotov, V. K. Karandashev and B. Y. Spivakov, *Journal of Analytical Chemistry*, 2005, **60**, 684-690.

159. P. S. Fedotov, E. Y. Savonina, R. Wennrich and B. Y. Spivakov, *Analyst*, 2006, **131**, 509-515.

160. P. S. Fedotov, E. Y. Savonina, R. Wennrich and D. V. Ladonin, *Geoderma*, 2007, **142**, 58-68.

161. M. Rosende, E. Y. Savonina, P. S. Fedotov, M. Miro, V. Cerda and R. Wennrich, *Talanta*, 2009, **79**, 1081-1088.

162. E. Y. Savonina, P. S. Fedotov and T. G. Laperdina, *Journal of Analytical Chemistry*, 2011, **66**, 119-124.

163. E. Y. Savonina, P. S. Fedotov and R. Wennrich, *Talanta*, 2012, **88**, 369-374.

164. J. Buanuam, K. Tiptanasup, J. Shiowatana, M. Miro and E. Harald Hansen, *Journal of environmental monitoring : JEM*, 2006, **8**, 1248-1254.

165. J. Buanuam and R. Wennrich, *Journal of hazardous materials*, 2010, **184**, 849-854.

166. J. Buanuam and R. Wennrich, *Journal of environmental monitoring : JEM*, 2011, **13**, 1672-1677.

167. J. X. Qiao and X. L. Hou, *Journal of environmental radioactivity*, 2010, **101**, 244-249.

168. M. Schreiber, M. Otto, P. S. Fedotov and R. Wennrich, *Chemosphere*, 2005, **61**, 107-115.

169. X. Long, M. Miro and E. H. Hansen, *Analyst*, 2006, **131**, 132-140.

170. M. Rosende, M. Miro, M. A. Segundo, J. L. Lima and V. Cerda, *Analytical and bioanalytical chemistry*, 2011, **400**, 2217-2227.

171. P. S. Fedotov, M. S. Ermolin, A. I. Ivaneev, N. N. Fedyunina, V. K. Karandashev and Y. G. Tatsy, *Chemosphere*, 2016, **146**, 371-378.

172. V. Dufailly, T. Guérin, L. Noël, J.-M. Frémy and D. Beauchemin, *J. Anal. At. Spectrom.*, 2008, **23**, 1263.

173. N. S. Horner and D. Beauchemin, *Anal Chim Acta*, 2012, **717**, 1-6.

174. A. Leufroy, L. Noel, D. Beauchemin and T. Guerin, *Food Chem*, 2012, **135**, 623-633.

175. R. P. Lamsal and D. Beauchemin, *Analytica Chimica Acta*, 2015, **867**, 9-17.

176. A. Mukhtar and A. Limbeck, *J. Anal. At. Spectrom.*, 2010, **25**, 1056.

177. A. Limbeck, C. Wagner, B. Lendl and A. Mukhtar, *Anal Chim Acta*, 2012, **750**, 111-119.

178. M. Rosende and M. Miró, *TrAC Trends in Analytical Chemistry*, 2013, **45**, 67-78.

179. B. L. Larner, A. J. Seen and A. T. Townsend, *Analytica Chimica Acta*, 2006, **556**, 444-449.

180. M. Wilson, *Microbial Inhabitants of Humans: Their ecology and role in health and disease*, The press syndicate of the University of Cambridge, UK, 2005.

181. N. P. Chaturvedi and H. Solanki, *Int J App Pharm*, 2013, **5**, 7-10.

182. A. W. Ng, A. Bidani and T. A. Heming, *Lung*, 2004, **182**, 297-317.

183. J. V. Fahy and B. F. Dickey, *N Engl J Med*, 2010, **363**, 2233-2247.

184. C. P. v. d. Schans, *Respiratory care*, 2007, **52**, 1150 –1156.

185. R. G. E. Houtmeyers, G. Gayan-Ramirez, M. Decramer, *Eur Respir J* 1999, **13**, 1177-1188.

186. E. H.-U. Helena Eixarch, Christoph Beisswenger and Udo Bock, *Journal of Epithelial Biology & Pharmacology*, 2010, **3**, 1-14.

187. J. A. H. Alpofead, C. M. Davidson and D. Littlejohn, *Analytical Methods*, 2016, **8**, 5466-5474.

188. C. Puls, A. Limbeck and S. Hann, *Atmospheric Environment*, 2012, **55**, 213-219.

189. M. J. Huang, X. W. Chen, Y. G. Zhao, C. Y. Chan, W. Wang, X. M. Wang and M. H. Wong, *Environmental pollution*, 2014, **188**, 37-44.

190. O. R. Moss, *Health Phys.*, 1979, **36**, 447-448.

191. M. Takaya, Y. Shinohara, F. Serita, M. Ono-Ogasawara, N. Otaki, T. Toya, A. Takata, K. Yoshida and N. Kohyama, *Ind. Health*, 2006, **44**, 639-644.

192. A. E. Taunton, M. E. Gunter, G. K. Druschel and S. A. Wood, *Am. Miner.*, 2010, **95**, 1624-1635.

193. W. Stopford, J. Turner, D. Cappellini and T. Brock, *Journal of Environmental Monitoring*, 2003, **5**, 675.

194. J. Wragg and B. Klinck, *J. Environ. Sci. Health Part A-Toxic/Hazard. Subst. Environ. Eng.*, 2007, **42**, 1223-1231.

195. J. E. Gray, G. S. Plumlee, S. A. Morman, P. L. Higueras, J. G. Crock, H. A. Lowers and M. L. Witten, *Environmental Science & Technology*, 2010, **44**, 4782-4788.

196. C. Julien, P. Esperanza, M. Bruno and L. Y. Alleman, *Journal of Environmental Monitoring*, 2011, **13**, 621-630.

197. N. Boisa, N. Elom, J. R. Dean, M. E. Deary, G. Bird and J. A. Entwistle, *Environment International*, 2014, **70**, 132-142.

198. J. Twining, P. McGlinn, E. Loi, K. Smith and R. Giere, *Environmental Science & Technology*, 2005, **39**, 7749-7756.

199. L. A. Schaider, D. B. Senn, D. J. Brabander, K. D. McCarthy and J. P. Shine, *Environmental Science & Technology*, 2007, **41**, 4164-4171.

200. V. Ettler, M. Vitkova, M. Mihaljevic, O. Sebek, M. Klementova, F. Veselovsky, P. Vybiral and B. Kribek, *Environmental geochemistry and health*, 2014, **36**, 919-933.

201. K. P. Kim, C. Y. Wu, B. K. Birky and W. E. Bolch, *Radiat. Prot. Dosim.*, 2007, **123**, 41-55.

202. L. I. D. da Silva, L. Yokoyama, L. B. Maia, M. I. C. Monteiro, F. V. M. Pontes, M. C. Cameiro and A. A. Neto, *Microchem J.*, 2015, **118**, 266-271.

203. J. J. Niu, P. E. Rasmussen, N. M. Hassan and R. Vincent, *Water Air Soil Pollut.*, 2010, **213**, 211-225.

204. C. L. S. Wiseman and F. Zereini, *Atmospheric Environment*, 2014, **89**, 282-289.

205. W. D. Kim, *European Respiratory Journal*, 1997, **10**, 1914-1917.

206. R. W. Lewis, *Lipids*, 1971, **6**, 859-861.

207. K. Sexton, M. A. Callahan and E. F. Bryan, *Environmental Health Perspectives*, 1995, **103**, 13-29.

208. USEPA, *Risk assessment guidance for superfund volume i: human health evaluation manual: Supplemental guidance "standard default exposure factors" Interim final.* OSWER DIRECTIVE: 9285.6-03, EPA, 1991.

209. European Environment Agency, *Particulate matter (PM10) 2009 - Annual limit value for the protection of human health*, http://www.eea.europa.eu/data-and-maps/figures/particulate-matter-pm10-annual-limit-value-for-the-protection-of-human-health-3, 2015.

210. W. Moller, K. Haussinger, L. Ziegler-Heitbrock and J. Heyder, *Respiratory research*, 2006, **7**, 10.

211. S. K. Singh, *Human Respiratory viral infection.* , CRC PressTaylor & Francis Group, USA, 2014.

212. G. A. Thibodeau; and K. T. Patton, T*he human body in health & disease*, Fourth edn., Elsevier, USA, 2005.

213. M. E. K. Nam Soo Joo, Jin V Wu, Yamil Saenz, Sujatha Jayaraman, Alan S Verkman, Jeffrey J Wine, J*OP. J. Pancreas (Online)*, 2001, 2**,** 280-284.

214. C. Clary-Meinesz, J. Mouroux, J. Cosson, P. Huitorel and B. Blaive, E*uropean Respiratory Journal*, 1998, 1**1,** 330-333.

215. N. J. Barrow and B. R. Whelan, E*ur. J. Soil Sci.*, 1998, 4**9,** 683-692.

216. J. C. Seaman, J. S. Arey and P. M. Bertsch, J. *Environ. Qual.*, 2001, 3**0,** 460-469.

217. P. M. Jardine, S. E. Fendorf, M. A. Mayes, I. L. Larsen, S. C. Brooks and W. B. Bailey, E*nvironmental Science & Technology*, 1999, 3**3,** 2939-2944.

218. R. Naidu, K. S. Sajwan and M. N. V. Prasad, T*race elements in the environment: biogeochemistry, biotechnology, and bioremediation*, CRC/Taylor and Francis, Boca Raton, 2006.

219. R. Naidu, N. S. Bolan, R. S. Kookana and K. G. Tiller, E*ur. J. Soil Sci.*, 1994, 4**5,** 419-429.

220. L. P. Weng, E. J. M. Temminghoff, S. Lofts, E. Tipping and W. H. Van Riemsdijk, E*nvironmental Science & Technology*, 2002, 3**6,** 4804-4810.

221. G. Barancikova and J. Makovnikova, P*lant Soil Environ.*, 2003, 4**9,** 565-571.

222. H. Kerndorff and M. Schnitzer, G*eochim. Cosmochim. Acta*, 1980, 4**4,** 1701-1708.

**Appendix A. The bioaccessible concentrations of potentially toxic elements (PTE) in BGS RM 102 Ironstone Soil (1) alone and (2) when smeared on FDMS filters to simulated $PM_{10}$ samples, as obtained with the miniaturised simplified bioaccessibility extraction test (SBET) and stomach phase of the unified bioaccessibility method (UBM)**

| PTE | SBET (n=3) | | | | UBM (stomach phase) (n=3) | | | | % Spike Recovery | |
|---|---|---|---|---|---|---|---|---|---|---|
| | Soil alone | | Soil on FDMS filters | | Soil alone | | Soil on FDMS filters | | SBET | UBM (stomach phase) |
| | Mean ± SD (mg $kg^{-1}$) | RSD (%) | Mean ± SD (mg $kg^{-1}$) | %RSD | Mean ± SD (mg $kg^{-1}$) | %RSD | Mean ± SD (mg $kg^{-1}$) | %RSD | | |
| **As** | 1.67 ± 0.03 | 1.47 | 1.66 ± 0.07 | 4.06 | 4.40 ± 0.04 | 0.838 | 4.41 ± 0.07 | 1.50 | 91.5 | 103 |
| **Cd** | 0.184 + 0.003 | 1.58 | 0.188 ± 0.007 | 3.68 | 0.224 ± 0.002 | 1.05 | 0.217 ± 0.006 | 2.57 | 88.2 | 101 |
| **Cr** | 21.7 ± 0.3 | 1.46 | 23.3 ± 1.1 | 4.72 | 35.9 ± 1.2 | 3.43 | 35.0 ± 0.4 | 1.23 | 91.4 | 102 |
| **Cu** | 6.64 ± 0.30 | 4.52 | 6.62 ± 0.29 | 4.41 | 7.29 ± 0.16 | 2.17 | 7.01 ± 0.18 | 2.52 | 93.8 | 100 |
| **Fe** | 993 ± 2 | 0.175 | 1070 ± 22 | 2.09 | 1230 ± 54 | 4.37 | 1290 ± 45 | 3.48 | 95.2 | 93.5 |
| **Mn** | 1690 ± 23 | 1.38 | 1760 ± 43 | 2.45 | 2810 ± 49 | 1.74 | 2780 ± 55 | 1.97 | 94.0 | 93.6 |
| **Ni** | 7.60 ± 0.09 | 1.12 | 7.93 ± 0.20 | 2.56 | 13.7 ± 2.0 | 14.9 | 12.2 ± 0.2 | 1.97 | 93.5 | 100 |
| **Pb** | 12.8 ± 0.04 | 0.346 | 13.4 ± 0.3 | 2.36 | 17.3 ± 0.8 | 4.64 | 18.4 ± 1.4 | 7.43 | 86.8 | 104 |
| **Zn** | 23.0 ± 1.2 | 5.21 | 34.8 ± 8.4 | 24.0 | 34.6 ± 1.2 | 3.43 | 35.6 ± 3.8 | 10.8 | 94.9 | 114 |

SD: one standard deviation; n: number of replicates

**Appendix B. One way ANOVA for optimization of extractant flow rate for the closed-loop dynamic model of the simplified bioaccessibility extraction test (SBET) by comparing the bioaccessible PTE concentration (Xcontrol) obtained by using its batch model with those obtained using its closed-loop dynamic model at three flow rates, X1, X2, and X3 (0.166, 1.0, and 10.0 mL $min^{-1}$, respectively**

ONEWAY Bioaccessible_As_SBET BY group
/STATISTICS HOMOGENEITY
/POSTHOC=TUKEY ALPHA(0.05)

**Oneway**

**Test of Homogeneity of Variances**

Bioaccessible_As_SBET

| Levene Statistic | df1 | df2 | Sig. |
|---|---|---|---|
| .384 | 3 | 8 | .767 |

**ANOVA**

Bioaccessible_As_SBET

| | Sum of Squares | df | Mean Square | F | Sig. |
|---|---|---|---|---|---|
| Between Groups | .208 | 3 | .069 | 10.715 | .004 |
| Within Groups | .052 | 8 | .006 | | |
| Total | .259 | 11 | | | |

**Post Hoc Tests**

**Multiple Comparisons**

Dependent Variable: Bioaccessible_As_SBET

Tukey HSD

| (I) group | (J) group | Mean Difference (I-J) | Std. Error | Sig. | 95% Confidence Interval | |
|---|---|---|---|---|---|---|
| | | | | | Lower Bound | Upper Bound |
| Xcontrol | X1 | -.11333 | .06562 | .371 | -.3235 | .0968 |
| | X2 | -.04000 | .06562 | .926 | -.2501 | .1701 |
| | X3 | -.34000* | .06562 | .004 | -.5501 | -.1299 |
| X1 | Xcontrol | .11333 | .06562 | .371 | -.0968 | .3235 |
| | X2 | .07333 | .06562 | .690 | -.1368 | .2835 |
| | X3 | -.22667* | .06562 | .035 | -.4368 | -.0165 |
| X2 | Xcontrol | .04000 | .06562 | .926 | -.1701 | .2501 |
| | X1 | -.07333 | .06562 | .690 | -.2835 | .1368 |
| | X3 | -.30000* | .06562 | .008 | -.5101 | -.0899 |
| X3 | Xcontrol | .34000* | .06562 | .004 | .1299 | .5501 |
| | X1 | .22667* | .06562 | .035 | .0165 | .4368 |
| | X2 | .30000* | .06562 | .008 | .0899 | .5101 |

*. The mean difference is significant at the 0.05 level

## Appendix B. Continued…

ONEWAY Bioaccessible_Cd_SBET BY group
/STATISTICS HOMOGENEITY
/POSTHOC=TUKEY ALPHA(0.05)

**Oneway**

**Test of Homogeneity of Variances**

Bioaccessible_Cd_SBET

| Levene Statistic | df1 | df2 | Sig. |
|---|---|---|---|
| .215 | 3 | 8 | .883 |

**ANOVA**

Bioaccessible_Cd_SBET

| | Sum of Squares | df | Mean Square | F | Sig. |
|---|---|---|---|---|---|
| Between Groups | .002 | 3 | .001 | 11.547 | .003 |
| Within Groups | .000 | 8 | .000 | | |
| Total | .003 | 11 | | | |

**Post Hoc Tests**

**Multiple Comparisons**

Dependent Variable: Bioaccessible_Cd_SBET

Tukey HSD

| (I) group | (J) group | Mean Difference (I-J) | Std. Error | Sig. | 95% Confidence Interval | |
|---|---|---|---|---|---|---|
| | | | | | Lower Bound | Upper Bound |
| Xcontrol | X1 | -.037333* | .006360 | .002 | -.05770 | -.01697 |
| | X2 | -.016333 | .006360 | .122 | -.03670 | .00403 |
| | X3 | -.018000 | .006360 | .085 | -.03837 | .00237 |
| X1 | Xcontrol | .037333* | .006360 | .002 | .01697 | .05770 |
| | X2 | .021000* | .006360 | .043 | .00063 | .04137 |
| | X3 | .019333 | .006360 | .063 | -.00103 | .03970 |
| X2 | Xcontrol | .016333 | .006360 | .122 | -.00403 | .03670 |
| | X1 | -.021000* | .006360 | .043 | -.04137 | -.00063 |
| | X3 | -.001667 | .006360 | .993 | -.02203 | .01870 |
| X3 | Xcontrol | .018000 | .006360 | .085 | -.00237 | .03837 |
| | X1 | -.019333 | .006360 | .063 | -.03970 | .00103 |
| | X2 | .001667 | .006360 | .993 | -.01870 | .02203 |

*. The mean difference is significant at the 0.05 level

## Appendix B. Continued…

ONEWAY Bioaccessible_Cr_SBET BY group
/STATISTICS HOMOGENEITY
/POSTHOC=TUKEY ALPHA(0.05)

**Oneway**

**Test of Homogeneity of Variances**

Bioaccessible_Cr_SBET

| Levene Statistic | df1 | df2 | Sig. |
|---|---|---|---|
| 1.360 | 3 | 8 | .323 |

**ANOVA**

Bioaccessible_Cr_SBET

| | Sum of Squares | df | Mean Square | F | Sig. |
|---|---|---|---|---|---|
| Between Groups | 3.256 | 3 | 1.085 | .667 | .595 |
| Within Groups | 13.013 | 8 | 1.627 | | |
| Total | 16.269 | 11 | | | |

**Post Hoc Tests**

**Multiple Comparisons**

Dependent Variable: Bioaccessible_Cr_SBET

Tukey HSD

| (I) group | (J) group | Mean Difference (I-J) | Std. Error | Sig. | 95% Confidence Interval | |
|---|---|---|---|---|---|---|
| | | | | | Lower Bound | Upper Bound |
| Xcontrol | X1 | -.96667 | 1.04137 | .791 | -4.3015 | 2.3682 |
| | X2 | -1.06667 | 1.04137 | .741 | -4.4015 | 2.2682 |
| | X3 | -1.40000 | 1.04137 | .563 | -4.7348 | 1.9348 |
| X1 | Xcontrol | .96667 | 1.04137 | .791 | -2.3682 | 4.3015 |
| | X2 | -.10000 | 1.04137 | 1.000 | -3.4348 | 3.2348 |
| | X3 | -.43333 | 1.04137 | .974 | -3.7682 | 2.9015 |
| X2 | Xcontrol | 1.06667 | 1.04137 | .741 | -2.2682 | 4.4015 |
| | X1 | .10000 | 1.04137 | 1.000 | -3.2348 | 3.4348 |
| | X3 | -.33333 | 1.04137 | .988 | -3.6682 | 3.0015 |
| X3 | Xcontrol | 1.40000 | 1.04137 | .563 | -1.9348 | 4.7348 |
| | X1 | .43333 | 1.04137 | .974 | -2.9015 | 3.7682 |
| | X2 | .33333 | 1.04137 | .988 | -3.0015 | 3.6682 |

## Appendix B. Continued…

ONEWAY Bioaccessible_Cu_SBET BY group
/STATISTICS HOMOGENEITY
/POSTHOC=TUKEY ALPHA(0.05)

**Oneway**

**Test of Homogeneity of Variances**

Bioaccessible_Cu_SBET

| Levene Statistic | df1 | df2 | Sig. |
|---|---|---|---|
| 2.539 | 3 | 8 | .130 |

**ANOVA**

Bioaccessible_Cu_SBET

| | Sum of Squares | df | Mean Square | F | Sig. |
|---|---|---|---|---|---|
| Between Groups | 4.266 | 3 | 1.422 | 3.842 | .057 |
| Within Groups | 2.960 | 8 | .370 | | |
| Total | 7.226 | 11 | | | |

**Post Hoc Tests**

**Multiple Comparisons**

Dependent Variable: Bioaccessible_Cu_SBET

Tukey HSD

| (I) group | (J) group | Mean Difference (I-J) | Std. Error | Sig. | 95% Confidence Interval | |
|---|---|---|---|---|---|---|
| | | | | | Lower Bound | Upper Bound |
| Xcontrol | X1 | -1.53000 | .49669 | .059 | -3.1206 | .0606 |
| | X2 | -.17000 | .49669 | .985 | -1.7606 | 1.4206 |
| | X3 | -.42333 | .49669 | .829 | -2.0139 | 1.1673 |
| X1 | Xcontrol | 1.53000 | .49669 | .059 | -.0606 | 3.1206 |
| | X2 | 1.36000 | .49669 | .096 | -.2306 | 2.9506 |
| | X3 | 1.10667 | .49669 | .195 | -.4839 | 2.6973 |
| X2 | Xcontrol | .17000 | .49669 | .985 | -1.4206 | 1.7606 |
| | X1 | -1.36000 | .49669 | .096 | -2.9506 | .2306 |
| | X3 | -.25333 | .49669 | .954 | -1.8439 | 1.3373 |
| X3 | Xcontrol | .42333 | .49669 | .829 | -1.1673 | 2.0139 |
| | X1 | -1.10667 | .49669 | .195 | -2.6973 | .4839 |
| | X2 | .25333 | .49669 | .954 | -1.3373 | 1.8439 |

## Appendix B. Continued…

ONEWAY Bioaccessible_Fe_SBET BY group
/STATISTICS HOMOGENEITY
/POSTHOC=TUKEY ALPHA(0.05)

**Oneway**

**Test of Homogeneity of Variances**

Bioaccessible_Fe_SBET

| Levene Statistic | df1 | df2 | Sig. |
|---|---|---|---|
| 3.781 | 3 | 8 | .059 |

**ANOVA**

Bioaccessible_Fe_SBET

| | Sum of Squares | df | Mean Square | F | Sig. |
|---|---|---|---|---|---|
| Between Groups | 14101.667 | 3 | 4700.556 | .995 | .443 |
| Within Groups | 37776.000 | 8 | 4722.000 | | |
| Total | 51877.667 | 11 | | | |

**Post Hoc Tests**

**Multiple Comparisons**

Dependent Variable: Bioaccessible_Fe_SBET

Tukey HSD

| (I) group | (J) group | Mean Difference (I-J) | Std. Error | Sig. | 95% Confidence Interval | |
|---|---|---|---|---|---|---|
| | | | | | Lower Bound | Upper Bound |
| Xcontrol | X1 | 50.33333 | 56.10704 | .807 | -129.3412 | 230.0078 |
| | X2 | -11.00000 | 56.10704 | .997 | -190.6745 | 168.6745 |
| | X3 | -45.33333 | 56.10704 | .849 | -225.0078 | 134.3412 |
| X1 | Xcontrol | -50.33333 | 56.10704 | .807 | -230.0078 | 129.3412 |
| | X2 | -61.33333 | 56.10704 | .703 | -241.0078 | 118.3412 |
| | X3 | -95.66667 | 56.10704 | .381 | -275.3412 | 84.0078 |
| X2 | Xcontrol | 11.00000 | 56.10704 | .997 | -168.6745 | 190.6745 |
| | X1 | 61.33333 | 56.10704 | .703 | -118.3412 | 241.0078 |
| | X3 | -34.33333 | 56.10704 | .925 | -214.0078 | 145.3412 |
| X3 | Xcontrol | 45.33333 | 56.10704 | .849 | -134.3412 | 225.0078 |
| | X1 | 95.66667 | 56.10704 | .381 | -84.0078 | 275.3412 |
| | X2 | 34.33333 | 56.10704 | .925 | -145.3412 | 214.0078 |

## Appendix B. Continued…

ONEWAY Bioaccessible_Mn_SBET BY group
/STATISTICS HOMOGENEITY
/POSTHOC=TUKEY ALPHA(0.05)

**Oneway**

**Test of Homogeneity of Variances**

Bioaccessible_Mn_SBET

| Levene Statistic | df1 | df2 | Sig. |
|---|---|---|---|
| 1.146 | 3 | 8 | .388 |

**ANOVA**

Bioaccessible_Mn_SBET

| | Sum of Squares | df | Mean Square | F | Sig. |
|---|---|---|---|---|---|
| Between Groups | 90881.583 | 3 | 30293.861 | 5.573 | .023 |
| Within Groups | 43483.333 | 8 | 5435.417 | | |
| Total | 134364.917 | 11 | | | |

**Post Hoc Tests**

**Multiple Comparisons**

Dependent Variable: Bioaccessible_Mn_SBET

Tukey HSD

| (I) group | (J) group | Mean Difference (I-J) | Std. Error | Sig. | 95% Confidence Interval | |
|---|---|---|---|---|---|---|
| | | | | | Lower Bound | Upper Bound |
| Xcontrol | X1 | -241.33333* | 60.19644 | .016 | -434.1035 | -48.5632 |
| | X2 | -111.33333 | 60.19644 | .320 | -304.1035 | 81.4368 |
| | X3 | -79.00000 | 60.19644 | .581 | -271.7702 | 113.7702 |
| X1 | Xcontrol | 241.33333* | 60.19644 | .016 | 48.5632 | 434.1035 |
| | X2 | 130.00000 | 60.19644 | .214 | -62.7702 | 322.7702 |
| | X3 | 162.33333 | 60.19644 | .102 | -30.4368 | 355.1035 |
| X2 | Xcontrol | 111.33333 | 60.19644 | .320 | -81.4368 | 304.1035 |
| | X1 | -130.00000 | 60.19644 | .214 | -322.7702 | 62.7702 |
| | X3 | 32.33333 | 60.19644 | .947 | -160.4368 | 225.1035 |
| X3 | Xcontrol | 79.00000 | 60.19644 | .581 | -113.7702 | 271.7702 |
| | X1 | -162.33333 | 60.19644 | .102 | -355.1035 | 30.4368 |
| | X2 | -32.33333 | 60.19644 | .947 | -225.1035 | 160.4368 |

*. The mean difference is significant at the 0.05 level

## Appendix B. Continued…

ONEWAY Bioaccessible_Ni_SBET BY group
/STATISTICS HOMOGENEITY
/POSTHOC=TUKEY ALPHA(0.05)

**Oneway**

**Test of Homogeneity of Variances**

Bioaccessible_Ni_SBET

| Levene Statistic | df1 | df2 | Sig. |
|---|---|---|---|
| 2.285 | 3 | 8 | .156 |

**ANOVA**

Bioaccessible_Ni_SBET

| | Sum of Squares | df | Mean Square | F | Sig. |
|---|---|---|---|---|---|
| Between Groups | 3.886 | 3 | 1.295 | 12.024 | .002 |
| Within Groups | .862 | 8 | .108 | | |
| Total | 4.748 | 11 | | | |

**Post Hoc Tests**

**Multiple Comparisons**

Dependent Variable: Bioaccessible_Ni_SBET

Tukey HSD

| (I) group | (J) group | Mean Difference (I-J) | Std. Error | Sig. | 95% Confidence Interval | |
|---|---|---|---|---|---|---|
| | | | | | Lower Bound | Upper Bound |
| Xcontrol | X1 | -1.34000* | .26800 | .005 | -2.1982 | -.4818 |
| | X2 | -.16000 | .26800 | .930 | -1.0182 | .6982 |
| | X3 | .04667 | .26800 | .998 | -.8116 | .9049 |
| X1 | Xcontrol | 1.34000* | .26800 | .005 | .4818 | 2.1982 |
| | X2 | 1.18000* | .26800 | .010 | .3218 | 2.0382 |
| | X3 | 1.38667* | .26800 | .004 | .5284 | 2.2449 |
| X2 | Xcontrol | .16000 | .26800 | .930 | -.6982 | 1.0182 |
| | X1 | -1.18000* | .26800 | .010 | -2.0382 | -.3218 |
| | X3 | .20667 | .26800 | .865 | -.6516 | 1.0649 |
| X3 | Xcontrol | -.04667 | .26800 | .998 | -.9049 | .8116 |
| | X1 | -1.38667* | .26800 | .004 | -2.2449 | -.5284 |
| | X2 | -.20667 | .26800 | .865 | -1.0649 | .6516 |

*. The mean difference is significant at the 0.05 level

## Appendix B. Continued…

ONEWAY Bioaccessible_Pb_SBET BY group
/STATISTICS HOMOGENEITY
/POSTHOC=TUKEY ALPHA(0.05)

**Oneway**

**Test of Homogeneity of Variances**

Bioaccessible_Pb_SBET

| Levene Statistic | df1 | df2 | Sig. |
|---|---|---|---|
| 1.587 | 3 | 8 | .267 |

**ANOVA**

Bioaccessible_Pb_SBET

| | Sum of Squares | df | Mean Square | F | Sig. |
|---|---|---|---|---|---|
| Between Groups | 5.903 | 3 | 1.968 | 3.046 | .092 |
| Within Groups | 5.167 | 8 | .646 | | |
| Total | 11.069 | 11 | | | |

**Post Hoc Tests**

**Multiple Comparisons**

Dependent Variable: Bioaccessible_Pb_SBET

Tukey HSD

| (I) group | (J) group | Mean Difference (I-J) | Std. Error | Sig. | 95% Confidence Interval | |
|---|---|---|---|---|---|---|
| | | | | | Lower Bound | Upper Bound |
| Xcontrol | X1 | -1.80000 | .65617 | .096 | -3.9013 | .3013 |
| | X2 | -1.30000 | .65617 | .271 | -3.4013 | .8013 |
| | X3 | -1.60000 | .65617 | .146 | -3.7013 | .5013 |
| X1 | Xcontrol | 1.80000 | .65617 | .096 | -.3013 | 3.9013 |
| | X2 | .50000 | .65617 | .869 | -1.6013 | 2.6013 |
| | X3 | .20000 | .65617 | .989 | -1.9013 | 2.3013 |
| X2 | Xcontrol | 1.30000 | .65617 | .271 | -.8013 | 3.4013 |
| | X1 | -.50000 | .65617 | .869 | -2.6013 | 1.6013 |
| | X3 | -.30000 | .65617 | .966 | -2.4013 | 1.8013 |
| X3 | Xcontrol | 1.60000 | .65617 | .146 | -.5013 | 3.7013 |
| | X1 | -.20000 | .65617 | .989 | -2.3013 | 1.9013 |
| | X2 | .30000 | .65617 | .966 | -1.8013 | 2.4013 |

## Appendix B. Continued…

ONEWAY Bioaccessible_Zn_SBET BY group
/STATISTICS HOMOGENEITY WELCH
/POSTHOC=GH ALPHA(0.05)

**Oneway**

**Test of Homogeneity of Variances**

Bioaccessible_Zn_SBET

| Levene Statistic | df1 | df2 | Sig. |
|---|---|---|---|
| 6.191 | 3 | 8 | .018 |

**Robust Tests of Equality of Means**

Bioaccessible_Zn_SBET

| | Statistic[a] | df1 | df2 | Sig. |
|---|---|---|---|---|
| Welch | 4.367 | 3 | 4.209 | .089 |

a. Asymptotically F distributed.

**Post Hoc Tests**

**Multiple Comparisons**

Dependent Variable: Bioaccessible_Zn_SBET

Games-Howell

| (I) group | (J) group | Mean Difference (I-J) | Std. Error | Sig. | 95% Confidence Interval | |
|---|---|---|---|---|---|---|
| | | | | | Lower Bound | Upper Bound |
| Xcontrol | X1 | -12.10000 | 13.28805 | .804 | -83.7202 | 59.5202 |
| | X2 | 12.50000 | 5.50444 | .279 | -13.4229 | 38.4229 |
| | X3 | -2.66667 | 5.70799 | .962 | -28.1521 | 22.8187 |
| X1 | Xcontrol | 12.10000 | 13.28805 | .804 | -59.5202 | 83.7202 |
| | X2 | 24.60000 | 12.66316 | .410 | -55.2961 | 104.4961 |
| | X3 | 9.43333 | 12.75295 | .876 | -68.9185 | 87.7851 |
| X2 | Xcontrol | -12.50000 | 5.50444 | .279 | -38.4229 | 13.4229 |
| | X1 | -24.60000 | 12.66316 | .410 | -104.4961 | 55.2961 |
| | X3 | -15.16667 | 4.04530 | .067 | -31.7952 | 1.4619 |
| X3 | Xcontrol | 2.66667 | 5.70799 | .962 | -22.8187 | 28.1521 |
| | X1 | -9.43333 | 12.75295 | .876 | -87.7851 | 68.9185 |
| | X2 | 15.16667 | 4.04530 | .067 | -1.4619 | 31.7952 |

**Appendix C. One way ANOVA for optimization of extractant flow rate for the closed-loop dynamic model of the stomach phase of the unified bioaccessibility method (UBM) by comparing the bioaccessible PTE concentration (Xcontrol) obtained by using the its batch model with those obtained using its closed-loop dynamic model at three flow rates, X1, X2, and X3 (0.0625, 1.0, and 3.75 mL $min^{-1}$, respectively**

```
ONEWAY Bioaccessible_As_Stomach_phase_of_UBM BY group
/STATISTICS HOMOGENEITY
/POSTHOC=TUKEY ALPHA(0.05).
```

**Oneway**

**Test of Homogeneity of Variances**

Bioaccessible_As_Stomach_phase_of_UBM

| Levene Statistic | df1 | df2 | Sig. |
|---|---|---|---|
| 2.637 | 3 | 8 | .121 |

**ANOVA**

Bioaccessible_As_Stomach_phase_of_UBM

| | Sum of Squares | df | Mean Square | F | Sig. |
|---|---|---|---|---|---|
| Between Groups | .602 | 3 | .201 | 3.730 | .061 |
| Within Groups | .430 | 8 | .054 | | |
| Total | 1.032 | 11 | | | |

**Post Hoc Tests**

**Multiple Comparisons**

Dependent Variable: Bioaccessible_As_Stomach_phase_of_UBM

Tukey HSD

| (I) group | (J) group | Mean Difference (I-J) | Std. Error | Sig. | 95% Confidence Interval | |
|---|---|---|---|---|---|---|
| | | | | | Lower Bound | Upper Bound |
| Xcontrol | X1 | .16667 | .18934 | .815 | -.4397 | .7730 |
| | X2 | .58333 | .18934 | .059 | -.0230 | 1.1897 |
| | X3 | .41333 | .18934 | .207 | -.1930 | 1.0197 |
| X1 | Xcontrol | -.16667 | .18934 | .815 | -.7730 | .4397 |
| | X2 | .41667 | .18934 | .203 | -.1897 | 1.0230 |
| | X3 | .24667 | .18934 | .586 | -.3597 | .8530 |
| X2 | Xcontrol | -.58333 | .18934 | .059 | -1.1897 | .0230 |
| | X1 | -.41667 | .18934 | .203 | -1.0230 | .1897 |
| | X3 | -.17000 | .18934 | .806 | -.7763 | .4363 |
| X3 | Xcontrol | -.41333 | .18934 | .207 | -1.0197 | .1930 |
| | X1 | -.24667 | .18934 | .586 | -.8530 | .3597 |
| | X2 | .17000 | .18934 | .806 | -.4363 | .7763 |

## Appendix C. Continued…

ONEWAY Bioaccessible_Cd_Stomach_phase_of_UBM BY group
/STATISTICS HOMOGENEITY
/POSTHOC=TUKEY ALPHA(0.05).

**Oneway**

**Test of Homogeneity of Variances**

Bioaccessible_Cd_Stomach_phase_of_UBM

| Levene Statistic | df1 | df2 | Sig. |
|---|---|---|---|
| 3.717 | 3 | 8 | .061 |

**ANOVA**

Bioaccessible_Cd_Stomach_phase_of_UBM

| | Sum of Squares | df | Mean Square | F | Sig. |
|---|---|---|---|---|---|
| Between Groups | .013 | 3 | .004 | 18.978 | .001 |
| Within Groups | .002 | 8 | .000 | | |
| Total | .015 | 11 | | | |

**Post Hoc Tests**

**Multiple Comparisons**

Dependent Variable: Bioaccessible_Cd_Stomach_phase_of_UBM

Tukey HSD

| (I) group | (J) group | Mean Difference (I-J) | Std. Error | Sig. | 95% Confidence Interval | |
|---|---|---|---|---|---|---|
| | | | | | Lower Bound | Upper Bound |
| Xcontrol | X1 | .011333 | .012466 | .801 | -.02859 | .05125 |
| | X2 | .063333* | .012466 | .004 | .02341 | .10325 |
| | X3 | .078333* | .012466 | .001 | .03841 | .11825 |
| X1 | Xcontrol | -.011333 | .012466 | .801 | -.05125 | .02859 |
| | X2 | .052000* | .012466 | .013 | .01208 | .09192 |
| | X3 | .067000* | .012466 | .003 | .02708 | .10692 |
| X2 | Xcontrol | -.063333* | .012466 | .004 | -.10325 | -.02341 |
| | X1 | -.052000* | .012466 | .013 | -.09192 | -.01208 |
| | X3 | .015000 | .012466 | .642 | -.02492 | .05492 |
| X3 | Xcontrol | -.078333* | .012466 | .001 | -.11825 | -.03841 |
| | X1 | -.067000* | .012466 | .003 | -.10692 | -.02708 |
| | X2 | -.015000 | .012466 | .642 | -.05492 | .02492 |

*. The mean difference is significant at the 0.05 level

## Appendix C. Continued…

ONEWAY Bioaccessible_Cr_Stomach_phase_of_UBM BY group
/STATISTICS HOMOGENEITY WELCH
/POSTHOC=GH ALPHA(0.05).

**Oneway**

**Test of Homogeneity of Variances**

Bioaccessible_Cr_Stomach_phase_of_UBM

| Levene Statistic | df1 | df2 | Sig. |
|---|---|---|---|
| 8.841 | 3 | 8 | .006 |

**Robust Tests of Equality of Means**

Bioaccessible_Cr_Stomach_phase_of_UBM

| | Statistic[a] | df1 | df2 | Sig. |
|---|---|---|---|---|
| Welch | 189.354 | 3 | 4.061 | .000 |

a. Asymptotically F distributed.

**Post Hoc Tests**

**Multiple Comparisons**

Dependent Variable: Bioaccessible_Cr_Stomach_phase_of_UBM

Games-Howell

| (I) group | (J) group | Mean Difference (I-J) | Std. Error | Sig. | 95% Confidence Interval | |
|---|---|---|---|---|---|---|
| | | | | | Lower Bound | Upper Bound |
| Xcontrol | X1 | 3.60000 | 1.99805 | .458 | -9.8075 | 17.0075 |
| | X2 | 9.06667* | .33333 | .000 | 7.7086 | 10.4247 |
| | X3 | 8.13333* | .91954 | .021 | 2.6019 | 13.6648 |
| X1 | Xcontrol | -3.60000 | 1.99805 | .458 | -17.0075 | 9.8075 |
| | X2 | 5.46667 | 1.99694 | .255 | -7.9654 | 18.8987 |
| | X3 | 4.53333 | 2.17307 | .340 | -6.5811 | 15.6477 |
| X2 | Xcontrol | -9.06667* | .33333 | .000 | -10.4247 | -7.7086 |
| | X1 | -5.46667 | 1.99694 | .255 | -18.8987 | 7.9654 |
| | X3 | -.93333 | .91712 | .758 | -6.5022 | 4.6355 |
| X3 | Xcontrol | -8.13333* | .91954 | .021 | -13.6648 | -2.6019 |
| | X1 | -4.53333 | 2.17307 | .340 | -15.6477 | 6.5811 |
| | X2 | .93333 | .91712 | .758 | -4.6355 | 6.5022 |

*. The mean difference is significant at the 0.05 level

## Appendix C. Continued…

```
ONEWAY Bioaccessible_Cu_Stomach_phase_of_UBM BY group
/STATISTICS HOMOGENEITY
/POSTHOC=TUKEY ALPHA(0.05).
```

**Oneway**

**Test of Homogeneity of Variances**

Bioaccessible_Cu_Stomach_phase_of_UBM

| Levene Statistic | df1 | df2 | Sig. |
|---|---|---|---|
| 1.331 | 3 | 8 | .331 |

**ANOVA**

Bioaccessible_Cu_Stomach_phase_of_UBM

| | Sum of Squares | df | Mean Square | F | Sig. |
|---|---|---|---|---|---|
| Between Groups | 3.309 | 3 | 1.103 | 7.764 | .009 |
| Within Groups | 1.137 | 8 | .142 | | |
| Total | 4.446 | 11 | | | |

**Post Hoc Tests**

**Multiple Comparisons**

Dependent Variable: Bioaccessible_Cu_Stomach_phase_of_UBM

Tukey HSD

| (I) group | (J) group | Mean Difference (I-J) | Std. Error | Sig. | 95% Confidence Interval | |
|---|---|---|---|---|---|---|
| | | | | | Lower Bound | Upper Bound |
| Xcontrol | X1 | 1.35000* | .30776 | .010 | .3644 | 2.3356 |
| | X2 | .54667 | .30776 | .350 | -.4389 | 1.5322 |
| | X3 | 1.12333* | .30776 | .027 | .1378 | 2.1089 |
| X1 | Xcontrol | -1.35000* | .30776 | .010 | -2.3356 | -.3644 |
| | X2 | -.80333 | .30776 | .115 | -1.7889 | .1822 |
| | X3 | -.22667 | .30776 | .880 | -1.2122 | .7589 |
| X2 | Xcontrol | -.54667 | .30776 | .350 | -1.5322 | .4389 |
| | X1 | .80333 | .30776 | .115 | -.1822 | 1.7889 |
| | X3 | .57667 | .30776 | .310 | -.4089 | 1.5622 |
| X3 | Xcontrol | -1.12333* | .30776 | .027 | -2.1089 | -.1378 |
| | X1 | .22667 | .30776 | .880 | -.7589 | 1.2122 |
| | X2 | -.57667 | .30776 | .310 | -1.5622 | .4089 |

*. The mean difference is significant at the 0.05 level

## Appendix C. Continued…

```
ONEWAY Bioaccessible_Fe_Stomach_phase_of_UBM BY group
/STATISTICS HOMOGENEITY
/POSTHOC=TUKEY ALPHA(0.05).
```

**Oneway**

**Test of Homogeneity of Variances**

Bioaccessible_Fe_Stomach_phase_of_UBM

| Levene Statistic | df1 | df2 | Sig. |
|---|---|---|---|
| 1.590 | 3 | 8 | .266 |

**ANOVA**

Bioaccessible_Fe_Stomach_phase_of_UBM

| | Sum of Squares | df | Mean Square | F | Sig. |
|---|---|---|---|---|---|
| Between Groups | 469135.000 | 3 | 156378.333 | 17.697 | .001 |
| Within Groups | 70692.667 | 8 | 8836.583 | | |
| Total | 539827.667 | 11 | | | |

**Post Hoc Tests**

**Multiple Comparisons**

Dependent Variable: Bioaccessible_Fe_Stomach_phase_of_UBM

Tukey HSD

| (I) group | (J) group | Mean Difference (I-J) | Std. Error | Sig. | 95% Confidence Interval | |
|---|---|---|---|---|---|---|
| | | | | | Lower Bound | Upper Bound |
| Xcontrol | X1 | 442.00000* | 76.75321 | .002 | 196.2092 | 687.7908 |
| | X2 | 249.66667* | 76.75321 | .047 | 3.8759 | 495.4575 |
| | X3 | 509.00000* | 76.75321 | .001 | 263.2092 | 754.7908 |
| X1 | Xcontrol | -442.00000* | 76.75321 | .002 | -687.7908 | -196.2092 |
| | X2 | -192.33333 | 76.75321 | .133 | -438.1241 | 53.4575 |
| | X3 | 67.00000 | 76.75321 | .819 | -178.7908 | 312.7908 |
| X2 | Xcontrol | -249.66667* | 76.75321 | .047 | -495.4575 | -3.8759 |
| | X1 | 192.33333 | 76.75321 | .133 | -53.4575 | 438.1241 |
| | X3 | 259.33333* | 76.75321 | .039 | 13.5425 | 505.1241 |
| X3 | Xcontrol | -509.00000* | 76.75321 | .001 | -754.7908 | -263.2092 |
| | X1 | -67.00000 | 76.75321 | .819 | -312.7908 | 178.7908 |
| | X2 | -259.33333* | 76.75321 | .039 | -505.1241 | -13.5425 |

*. The mean difference is significant at the 0.05 level

## Appendix C. Continued…

```
ONEWAY Bioaccessible_Mn_Stomach_phase_of_UBM BY group
/STATISTICS HOMOGENEITY
/POSTHOC=TUKEY ALPHA(0.05).
```

**Oneway**

**Test of Homogeneity of Variances**

Bioaccessible_Mn_Stomach_phase_of_UBM

| Levene Statistic | df1 | df2 | Sig. |
|---|---|---|---|
| 3.680 | 3 | 8 | .062 |

**ANOVA**

Bioaccessible_Mn_Stomach_phase_of_UBM

| | Sum of Squares | df | Mean Square | F | Sig. |
|---|---|---|---|---|---|
| Between Groups | 1741740.333 | 3 | 580580.111 | 22.961 | .000 |
| Within Groups | 202283.333 | 8 | 25285.417 | | |
| Total | 1944023.667 | 11 | | | |

**Post Hoc Tests**

**Multiple Comparisons**

Dependent Variable: Bioaccessible_Mn_Stomach_phase_of_UBM

Tukey HSD

| (I) group | (J) group | Mean Difference (I-J) | Std. Error | Sig. | 95% Confidence Interval | |
|---|---|---|---|---|---|---|
| | | | | | Lower Bound | Upper Bound |
| Xcontrol | X1 | 683.33333* | 129.83430 | .003 | 267.5582 | 1099.1085 |
| | X2 | 940.33333* | 129.83430 | .000 | 524.5582 | 1356.1085 |
| | X3 | 921.00000* | 129.83430 | .000 | 505.2249 | 1336.7751 |
| X1 | Xcontrol | -683.33333* | 129.83430 | .003 | -1099.1085 | -267.5582 |
| | X2 | 257.00000 | 129.83430 | .271 | -158.7751 | 672.7751 |
| | X3 | 237.66667 | 129.83430 | .327 | -178.1085 | 653.4418 |
| X2 | Xcontrol | -940.33333* | 129.83430 | .000 | -1356.1085 | -524.5582 |
| | X1 | -257.00000 | 129.83430 | .271 | -672.7751 | 158.7751 |
| | X3 | -19.33333 | 129.83430 | .999 | -435.1085 | 396.4418 |
| X3 | Xcontrol | -921.00000* | 129.83430 | .000 | -1336.7751 | -505.2249 |
| | X1 | -237.66667 | 129.83430 | .327 | -653.4418 | 178.1085 |
| | X2 | 19.33333 | 129.83430 | .999 | -396.4418 | 435.1085 |

*. The mean difference is significant at the 0.05 level

## Appendix C. Continued…

```
ONEWAY Bioaccessible_Ni_Stomach_phase_of_UBM BY group
  /STATISTICS HOMOGENEITY
  /POSTHOC=TUKEY ALPHA(0.05).
```

**Oneway**

**Test of Homogeneity of Variances**

Bioaccessible_Ni_Stomach_phase_of_UBM

| Levene Statistic | df1 | df2 | Sig. |
|---|---|---|---|
| 3.683 | 3 | 8 | .062 |

**ANOVA**

Bioaccessible_Ni_Stomach_phase_of_UBM

| | Sum of Squares | df | Mean Square | F | Sig. |
|---|---|---|---|---|---|
| Between Groups | 34.273 | 3 | 11.424 | 22.714 | .000 |
| Within Groups | 4.024 | 8 | .503 | | |
| Total | 38.296 | 11 | | | |

**Post Hoc Tests**

**Multiple Comparisons**

Dependent Variable: Bioaccessible_Ni_Stomach_phase_of_UBM

Tukey HSD

| (I) group | (J) group | Mean Difference (I-J) | Std. Error | Sig. | 95% Confidence Interval | |
|---|---|---|---|---|---|---|
| | | | | | Lower Bound | Upper Bound |
| Xcontrol | X1 | 2.66667* | .57906 | .008 | .8123 | 4.5210 |
| | X2 | 4.29667* | .57906 | .000 | 2.4423 | 6.1510 |
| | X3 | 3.96000* | .57906 | .001 | 2.1056 | 5.8144 |
| X1 | Xcontrol | -2.66667* | .57906 | .008 | -4.5210 | -.8123 |
| | X2 | 1.63000 | .57906 | .086 | -.2244 | 3.4844 |
| | X3 | 1.29333 | .57906 | .194 | -.5610 | 3.1477 |
| X2 | Xcontrol | -4.29667* | .57906 | .000 | -6.1510 | -2.4423 |
| | X1 | -1.63000 | .57906 | .086 | -3.4844 | .2244 |
| | X3 | -.33667 | .57906 | .935 | -2.1910 | 1.5177 |
| X3 | Xcontrol | -3.96000* | .57906 | .001 | -5.8144 | -2.1056 |
| | X1 | -1.29333 | .57906 | .194 | -3.1477 | .5610 |
| | X2 | .33667 | .57906 | .935 | -1.5177 | 2.1910 |

*. The mean difference is significant at the 0.05 level

## Appendix C. Continued…

ONEWAY Bioaccessible_Pb_Stomach_phase_of_UBM BY group
/STATISTICS HOMOGENEITY
/POSTHOC=TUKEY ALPHA(0.05).

**Oneway**

**Test of Homogeneity of Variances**

Bioaccessible_Pb_Stomach_phase_of_UBM

| Levene Statistic | df1 | df2 | Sig. |
|---|---|---|---|
| .092 | 3 | 8 | .962 |

**ANOVA**

Bioaccessible_Pb_Stomach_phase_of_UBM

| | Sum of Squares | df | Mean Square | F | Sig. |
|---|---|---|---|---|---|
| Between Groups | 114.761 | 3 | 38.254 | 20.815 | .000 |
| Within Groups | 14.702 | 8 | 1.838 | | |
| Total | 129.463 | 11 | | | |

**Post Hoc Tests**

**Multiple Comparisons**

Dependent Variable: Bioaccessible_Pb_Stomach_phase_of_UBM

Tukey HSD

| (I) group | (J) group | Mean Difference (I-J) | Std. Error | Sig. | 95% Confidence Interval | |
|---|---|---|---|---|---|---|
| | | | | | Lower Bound | Upper Bound |
| Xcontrol | X1 | 6.80000* | 1.10688 | .001 | 3.2554 | 10.3446 |
| | X2 | 5.33333* | 1.10688 | .006 | 1.7887 | 8.8780 |
| | X3 | 8.15000* | 1.10688 | .000 | 4.6054 | 11.6946 |
| X1 | Xcontrol | -6.80000* | 1.10688 | .001 | -10.3446 | -3.2554 |
| | X2 | -1.46667 | 1.10688 | .574 | -5.0113 | 2.0780 |
| | X3 | 1.35000 | 1.10688 | .633 | -2.1946 | 4.8946 |
| X2 | Xcontrol | -5.33333* | 1.10688 | .006 | -8.8780 | -1.7887 |
| | X1 | 1.46667 | 1.10688 | .574 | -2.0780 | 5.0113 |
| | X3 | 2.81667 | 1.10688 | .126 | -.7280 | 6.3613 |
| X3 | Xcontrol | -8.15000* | 1.10688 | .000 | -11.6946 | -4.6054 |
| | X1 | -1.35000 | 1.10688 | .633 | -4.8946 | 2.1946 |
| | X2 | -2.81667 | 1.10688 | .126 | -6.3613 | .7280 |

*. The mean difference is significant at the 0.05 level

## Appendix C. Continued…

```
ONEWAY Bioaccessible_Zn_Stomach_phase_of_UBM BY group
  /STATISTICS HOMOGENEITY
  /POSTHOC=TUKEY ALPHA(0.05).
```

**Oneway**

**Test of Homogeneity of Variances**

Bioaccessible_Zn_Stomach_phase_of_UBM

| Levene Statistic | df1 | df2 | Sig. |
|---|---|---|---|
| 1.784 | 3 | 8 | .228 |

**ANOVA**

Bioaccessible_Zn_Stomach_phase_of_UBM

| | Sum of Squares | df | Mean Square | F | Sig. |
|---|---|---|---|---|---|
| Between Groups | 633.848 | 3 | 211.283 | 4.940 | .032 |
| Within Groups | 342.150 | 8 | 42.769 | | |
| Total | 975.998 | 11 | | | |

**Post Hoc Tests**

**Multiple Comparisons**

Dependent Variable: Bioaccessible_Zn_Stomach_phase_of_UBM

Tukey HSD

| (I) group | (J) group | Mean Difference (I-J) | Std. Error | Sig. | 95% Confidence Interval | |
|---|---|---|---|---|---|---|
| | | | | | Lower Bound | Upper Bound |
| Xcontrol | X1 | 10.73333 | 5.33971 | .261 | -6.3663 | 27.8330 |
| | X2 | 5.16667 | 5.33971 | .771 | -11.9330 | 22.2663 |
| | X3 | 19.61333* | 5.33971 | .026 | 2.5137 | 36.7130 |
| X1 | Xcontrol | -10.73333 | 5.33971 | .261 | -27.8330 | 6.3663 |
| | X2 | -5.56667 | 5.33971 | .731 | -22.6663 | 11.5330 |
| | X3 | 8.88000 | 5.33971 | .400 | -8.2196 | 25.9796 |
| X2 | Xcontrol | -5.16667 | 5.33971 | .771 | -22.2663 | 11.9330 |
| | X1 | 5.56667 | 5.33971 | .731 | -11.5330 | 22.6663 |
| | X3 | 14.44667 | 5.33971 | .101 | -2.6530 | 31.5463 |
| X3 | Xcontrol | -19.61333* | 5.33971 | .026 | -36.7130 | -2.5137 |
| | X1 | -8.88000 | 5.33971 | .400 | -25.9796 | 8.2196 |
| | X2 | -14.44667 | 5.33971 | .101 | -31.5463 | 2.6530 |

*. The mean difference is significant at the 0.05 level

**Appendix D1. Bioaccessible conc. (mg $kg^{-1}$) of potentially toxic elements for each subfraction obtained by extraction of the simulated $PM_{10}$ samples (BGS RM 102 Ironstone Soil on FDMS filter) using the single-pass dynamic model of the simplified bioaccessibility extraction test (SBET) with fraction collection (SPFC-SBET)**

| Subfraction number | As Mean (n=3) ± SD | Cd Mean (n=3) ± SD | Cr Mean (n=3) ± SD | Cu Mean (n=3) ± SD | Fe Mean (n=3) ± SD | Mn Mean (n=3) ± SD | Ni Mean (n=3) ± SD | Pb Mean (n=3) ± SD | Zn Mean (n=3) ± SD |
|---|---|---|---|---|---|---|---|---|---|
| **1** | 0.911 ± 0.079 | 0.110 ± 0.010 | 2.37 ± 0.31 | 3.11 ± 0.35 | 229 ± 36 | 677 ± 68 | 2.50 ± 0.20 | 4.01 ± 0.37 | 19.1 ± 1.3 |
| **2** | 0.553 ± 0.078 | 0.030 ± 0.012 | 2.70 ± 0.11 | 1.70 ± 0.27 | 217 ± 9 | 276 ± 57 | 1.19 ± 0.18 | 3.04 ± 0.27 | 5.41 ± 2.60 |
| **3** | 0.376 ± 0.046 | 0.012 ± 0.005 | 3.72 ± 0.47 | 1.09 ± 0.13 | 203 ± 23 | 204 ± 25 | 0.967 ± 0.089 | 2.43 ± 0.20 | 3.16 ± 1.22 |
| **4** | 0.296 ± 0.031 | 0.005 ± 0.003 | 4.67 ± 0.40 | 0.784 ± 0.076 | 210 ± 18 | 180 ± 15 | 0.887 ± 0.055 | 2.19 ± 0.11 | 1.79 ± 0.70 |
| **5** | 0.232 ± 0.025 | < IDL | 4.67 ± 0.28 | 0.565 ± 0.050 | 202 ± 11 | 154 ± 7 | 0.775 ± 0.026 | 1.93 ± 0.05 | 1.10 ± 0.36 |
| **6** | 0.192 ± 0.014 | < IDL | 4.02 ± 0.12 | 0.415 ± 0.034 | 182 ± 7 | 125 ± 5 | 0.635 ± 0.018 | 1.68 ± 0.03 | 0.646 ± 0.227 |
| **7** | 0.161 ± 0.009 | < IDL | 3.14 ± 0.04 | 0.316 ± 0.025 | 160 ± 3 | 101 ± 5 | 0.510 ± 0.016 | 1.45 ± 0.02 | 0.561 ± 0.190 |
| **8** | 0.164 ± 0.004 | < IDL | 3.27 ± 0.15 | 0.348 ± 0.024 | 175 ± 7 | 114 ± 8 | 0.603 ± 0.025 | 1.56 ± 0.09 | 0.873 ± 0.225 |
| **9** | 0.143 ± 0.005 | < IDL | 1.98 ± 0.13 | 0.226 ± 0.009 | 139 ± 6 | 69.5 ± 4.5 | 0.372 ± 0.014 | 1.25 ± 0.11 | 0.629 ± 0.180 |
| **10** | 0.122 ± 0.006 | < IDL | 1.34 ± 0.14 | 0.147 ± 0.010 | 107 ± 7 | 48.6 ± 4.4 | 0.265 ± 0.017 | 0.921 ± 0.07 | 0.561 ± 0.199 |
| **11** | 0.110 ± 0.005 | < IDL | 1.02 ± 0.09 | 0.106 ± 0.002 | 91.3 ± 4.3 | 38.8 ± 2.1 | 0.213 ± 0.008 | 0.766 ± 0.04 | 0.544 ± 0.310 |
| **12** | 0.098 ± 0.002 | < IDL | 0.796 ± 0.082 | 0.075 ± 0.007 | 80.0 ± 5.1 | 33.1 ± 2.7 | 0.184 ± 0.013 | 0.649 ± 0.05 | 0.342 ± 0.149 |

< IDL: less instrumental detection limit; SD: standard deviation

**Appendix D2. Bioaccessible conc. (mg $kg^{-1}$) of potentially toxic elements accumulated with extraction time obtained by extraction of the simulated $PM_{10}$ samples (BGS RM 102 Ironstone Soil on FDMS filter) using the single-pass dynamic model of the simplified bioaccessibility extraction test (SBET) with fraction collection (SPFC-SBET)**

| Time (min) | As Mean (n=3) ± SD | Cd Mean (n=3) ± SD | Cr Mean (n=3) ± SD | Cu Mean (n=3) ± SD | Fe Mean (n=3) ± SD | Mn Mean (n=3) ± SD | Ni Mean (n=3) ± SD | Pb Mean (n=3) ± SD | Zn Mean (n=3) ± SD |
|---|---|---|---|---|---|---|---|---|---|
| **5** | 0.911 ± 0.079 | 0.110 ± 0.010 | 2.37 ± 0.31 | 3.11 ± 0.35 | 229 ± 36 | 677 ± 68 | 2.50 ± 0.20 | 4.01 ± 0.37 | 19.1 ± 1.3 |
| **10** | 1.46 ± 0.35 | 0.140 ± 0.019 | 5.07 ± 1.67 | 4.81 ± 1.26 | 446 ± 145 | 953 ± 154 | 3.69 ± 0.71 | 7.05 ± 1.87 | 24.5 ± 3.7 |
| **15** | 1.84 ± 0.39 | 0.152 ± 0.019 | 8.79 ± 2.12 | 5.90 ± 1.33 | 650 ± 168 | 1160 ± 156 | 4.66 ± 0.73 | 9.49 ± 2.06 | 27.7 ± 3.3 |
| **20** | 2.14 ± 0.41 | 0.156 ± 0.020 | 13.5 ± 2.5 | 6.68 ± 1.36 | 860 ± 185 | 1340 ± 157 | 5.55 ± 0.75 | 11.7 ± 2.17 | 29.5 ± 3.2 |
| **25** | 2.37 ± 0.43 | < IDL | 18.1 ± 2.8 | 7.24 ± 1.37 | 1060 ± 197 | 1490 ± 156 | 6.32 ± 0.75 | 13.6 ± 2.2 | 30.6 ± 3.2 |
| **30** | 2.56 ± 0.44 | < IDL | 22.1 ± 2.9 | 7.66 ± 1.37 | 1240 ± 204 | 1620 ± 153 | 6.96 ± 0.75 | 15.3 ± 2.3 | 31.2 ± 3.1 |
| **35** | 2.72 ± 0.45 | < IDL | 25.3 ± 2.9 | 7.98 ± 1.37 | 1400 ± 206 | 1720 ± 148 | 7.47 ± 0.73 | 16.8 ± 2.2 | 31.8 ± 3.0 |
| **40** | 2.89 ± 0.46 | < IDL | 28.6 ± 2.8 | 8.32 ± 1.35 | 1580 ± 202 | 1830 ± 140 | 8.07 ± 0.71 | 18.3 ± 2.1 | 32.7 ± 2.8 |
| **45** | 3.03 ± 0.46 | < IDL | 30.5 ± 2.7 | 8.55 ± 1.35 | 1720 ± 199 | 1900 ± 136 | 8.44 ± 0.70 | 19.6 ± 2.1 | 33.3 ± 2.7 |
| **50** | 3.15 ± 0.46 | < IDL | 31.9 ± 2.6 | 8.70 ± 1.34 | 1830 ± 195 | 1950 ± 132 | 8.70 ± 0.68 | 20.5 ± 2.0 | 33.8 ± 2.5 |
| **55** | 3.26 ± 0.47 | < IDL | 32.9 ± 2.6 | 8.80 ± 1.33 | 1920 ± 192 | 1990 ± 131 | 8.92 ± 0.68 | 21.2 ± 2.0 | 34.4 ± 2.3 |
| **60** | 3.36 ± 0.47 | < IDL | 33.7 ± 2.6 | 8.88 ± 1.34 | 2000 ± 192 | 2020 ± 131 | 9.10 ± 0.67 | 21.9 ± 2.0 | 34.7 ± 2.1 |

< IDL: less instrumental detection limit; SD: standard deviation

**Appendix D3. Bioaccessible conc. (mg $kg^{-1}$) of potentially toxic elements for each subfraction obtained by extraction of the simulated $PM_{10}$ samples (NIST SRM 2711A Montana II Soil on FDMS filter) using the single-pass dynamic model of the simplified bioaccessibility extraction test (SBET) with fraction collection (SPFC-SBET)**

| Subfraction number | As Mean (n=3) ± SD | Cd Mean (n=3) ± SD | Cr Mean (n=3) ± SD | Cu Mean (n=3) ± SD | Fe Mean (n=3) ± SD | Mn Mean (n=3) ± SD | Ni Mean (n=3) ± SD | Pb Mean (n=3) ± SD | Zn Mean (n=3) ± SD |
|---|---|---|---|---|---|---|---|---|---|
| **1** | 22.7 ± 1.7 | 25.3 ± 2.8 | 0.273 ± 0.017 | 30.5 ± 2.6 | 146 ± 10 | 61.6 ± 3.9 | 1.03 ± 0.03 | 604 ± 56 | 61.5 ± 6.4 |
| **2** | 9.06 ± 0.75 | 7.44 ± 0.95 | 0.110 ± 0.009 | 12.0 ± 0.8 | 87.7 ± 0.1 | 24.9 ± 2.5 | 0.381 ± 0.05 | 208 ± 22 | 21.5 ± 3.0 |
| **3** | 4.95 ± 0.42 | 3.24 ± 0.58 | 0.070 ± 0.005 | 6.09 ± 0.51 | 57.6 ± 0.4 | 15.3 ± 1.4 | 0.208 ± 0.03 | 93.5 ± 12.4 | 10.4 ± 1.7 |
| **4** | 3.76 ± 0.26 | 2.39 ± 0.38 | 0.058 ± 0.003 | 4.29 ± 0.33 | 45.3 ± 0.2 | 12.7 ± 0.8 | 0.162 ± 0.012 | 64.6 ± 7.2 | 8.17 ± 0.88 |
| **5** | 2.98 ± 0.52 | 2.25 ± 0.74 | 0.054 ± 0.008 | 3.74 ± 0.81 | 39.9 ± 2.3 | 12.1 ± 1.9 | 0.146 ± 0.031 | 57.9 ± 15.2 | 7.87 ± 1.94 |
| **6** | 2.54 ± 0.40 | 1.71 ± 0.46 | 0.046 ± 0.005 | 2.84 ± 0.52 | 33.9 ± 1.5 | 10.1 ± 1.1 | 0.114 ± 0.017 | 44.3 ± 9.3 | 6.33 ± 1.15 |
| **7** | 1.95 ± 0.28 | 1.19 ± 0.44 | 0.040 ± 0.007 | 2.07 ± 0.32 | 29.2 ± 1.2 | 8.35 ± 0.74 | 0.083 ± 0.011 | 32.2 ± 6.7 | 5.00 ± 0.95 |
| **8** | 1.88 ± 0.31 | 0.930 ± 0.390 | 0.045 ± 0.009 | 1.86 ± 0.37 | 30.4 ± 2.0 | 9.72 ± 0.92 | 0.106 ± 0.014 | 26.4 ± 6.9 | 4.85 ± 0.96 |
| **9** | 1.28 ± 0.12 | 0.520 ± 0.111 | 0.032 ± 0.005 | 1.26 ± 0.15 | 26.0 ± 1.3 | 6.54 ± 0.50 | 0.073 ± 0.006 | 17.2 ± 2.5 | 3.30 ± 0.26 |
| **10** | 0.958 ± 0.059 | 0.304 ± 0.019 | 0.025 ± 0.004 | 0.898 ± 0.068 | 22.2 ± 0.9 | 5.19 ± 0.32 | 0.058 ± 0.004 | 11.4 ± 0.7 | 2.50 ± 0.11 |
| **11** | 0.766 ± 0.039 | 0.192 ± 0.047 | 0.022 ± 0.002 | 0.693 ± 0.037 | 19.6 ± 0.4 | 4.46 ± 0.27 | 0.048 ± 0.003 | 8.28 ± 0.80 | 2.02 ± 0.25 |
| **12** | 0.673 ± 0.047 | 0.151 ± 0.066 | 0.020 ± 0.003 | 0.581 ± 0.052 | 18.1 ± 0.4 | 4.20 ± 0.30 | 0.044 ± 0.004 | 6.63 ± 1.29 | 1.81 ± 0.32 |

< IDL: less instrumental detection limit; SD: standard deviation

**Appendix D4. Bioaccessible conc. (mg $kg^{-1}$) of potentially toxic elements accumulated with extraction time obtained by extraction of the simulated $PM_{10}$ samples (NIST SRM 2711A Montana II Soil on FDMS filter) using the single-pass dynamic model of the simplified bioaccessibility extraction test (SBET) with fraction collection (SPFC-SBET)**

| Time (min) | As Mean (n=3) ± SD | Cd Mean (n=3) ± SD | Cr Mean (n=3) ± SD | Cu Mean (n=3) ± SD | Fe Mean (n=3) ± SD | Mn Mean (n=3) ± SD | Ni Mean (n=3) ± SD | Pb Mean (n=3) ± SD | Zn Mean (n=3) ± SD |
|---|---|---|---|---|---|---|---|---|---|
| **5** | 22.7 ± 1.7 | 25.3 ± 2.8 | 0.273 ± 0.017 | 30.5 ± 2.6 | 146 ± 10 | 61.6 ± 3.9 | 1.03 ± 0.03 | 604 ± 56 | 61.5 ± 6.4 |
| **10** | 31.8 ± 1.3 | 32.7 ± 1.6 | 0.386 ± 0.012 | 42.6 ± 1.8 | 234 ± 13 | 86.5 ± 2.7 | 1.41 ± 0.04 | 812 ± 38 | 83.1 ± 3.8 |
| **15** | 36.7 ± 0.4 | 36.0 ± 1.0 | 0.455 ± 0.003 | 48.7 ± 0.9 | 291 ± 9 | 102 ± 0.1 | 1.62 ± 0.04 | 906 ± 16 | 93.4 ± 1.3 |
| **20** | 40.5 ± 0.6 | 38.4 ± 1.3 | 0.513 ± 0.010 | 53.0 ± 1.1 | 337 ± 8 | 114 ± 2 | 1.78 ± 0.06 | 970 ± 18 | 102 ± 2 |
| **25** | 43.5 ± 1.0 | 40.6 ± 1.6 | 0.567 ± 0.018 | 56.7 ± 1.5 | 376 ± 6 | 127 ± 4 | 1.92 ± 0.09 | 1030 ± 27 | 109 ± 4 |
| **30** | 46.0 ± 1.3 | 42.3 ± 1.8 | 0.613 ± 0.022 | 59.5 ± 1.9 | 410 ± 5 | 137 ± 5 | 2.04 ± 0.11 | 1070 ± 34 | 116 ± 5 |
| **35** | 48.0 ± 1.5 | 43.5 ± 1.9 | 0.653 ± 0.025 | 61.6 ± 2.0 | 440 ± 5 | 145 ± 6 | 2.12 ± 0.12 | 1100 ± 36 | 121 ± 5 |
| **40** | 49.8 ± 1.7 | 44.4 ± 2.0 | 0.698 ± 0.030 | 63.5 ± 2.2 | 470 ± 3 | 155 ± 7 | 2.23 ± 0.13 | 1130 ± 40 | 126 ± 6 |
| **45** | 51.1 ± 1.8 | 45.0 ± 2.1 | 0.729 ± 0.034 | 64.7 ± 2.3 | 496 ± 3 | 161 ± 7 | 2.30 ± 0.14 | 1150 ± 42 | 129 ± 6 |
| **50** | 52.1 ± 1.9 | 45.3 ± 2.1 | 0.755 ± 0.037 | 65.6 ± 2.4 | 518 ± 3 | 166 ± 7 | 2.36 ± 0.14 | 1160 ± 43 | 131 ± 6 |
| **55** | 52.8 ± 1.9 | 45.5 ± 2.1 | 0.777 ± 0.039 | 66.3 ± 2.4 | 538 ± 3 | 171 ± 7 | 2.41 ± 0.14 | 1170 ± 43 | 133 ± 6 |
| **60** | 53.5 ± 1.9 | 45.6 ± 2.0 | 0.797 ± 0.040 | 66.9 ± 2.4 | 556 ± 4 | 175 ± 7 | 2.45 ± 0.14 | 1180 ± 42 | 135 ± 6 |

< IDL: less instrumental detection limit; SD: standard deviation

**Appendix D5. Bioaccessible conc. (mg $kg^{-1}$) of potentially toxic elements for each subfraction obtained by extraction of the simulated $PM_{10}$ samples (BGS RM 102 Ironstone Soil on FDMS filter) using the single-pass dynamic model of the stomach phase of the unified bioaccessibility method (UBM) with fraction collection (SPFC-UBM)**

| Subfraction number | As Mean (n=3) ± SD | Cd Mean (n=3) ± SD | Cr Mean (n=3) ± SD | Cu Mean (n=3) ± SD | Fe Mean (n=3) ± SD | Mn Mean (n=3) ± SD | Ni Mean (n=3) ± SD | Pb Mean (n=3) ± SD | Zn Mean (n=3) ± SD |
|---|---|---|---|---|---|---|---|---|---|
| **1** | 2.09 ± 0.12 | 0.111 ± 0.014 | 4.77 ± 0.80 | 3.05 ± 0.35 | 242 ± 38 | 869 ± 31 | 3.27 ± 0.16 | 2.94 ± 0.50 | 18.7 ± 0.9 |
| **2** | 1.21 ± 0.13 | 0.033 ± 0.005 | 4.97 ± 0.67 | 1.53 ± 0.25 | 280 ± 31 | 402 ± 46 | 1.67 ± 0.19 | 3.98 ± 0.45 | 7.10 ± 0.96 |
| **3** | 0.811 ± 0.038 | 0.016 ± 0.002 | 5.83 ± 0.14 | 0.673 ± 0.087 | 258 ± 7 | 298 ± 9 | 1.32 ± 0.05 | 3.98 ± 0.45 | 3.59 ± 0.38 |
| **4** | 0.646 ± 0.025 | 0.010 ± 0.001 | 5.98 ± 0.18 | 0.280 ± 0.056 | 250 ± 10 | 252 ± 8 | 1.14 ± 0.02 | 3.29 ± 0.18 | 2.49 ± 0.11 |
| **5** | 0.541 ± 0.041 | 0.011 ± 0.004 | 4.78 ± 0.34 | 0.066 ± 0.058 | 212 ± 18 | 202 ± 11 | 0.933 ± 0.053 | 2.76 ± 0.28 | 2.19 ± 0.06 |
| **6** | 0.453 ± 0.021 | 0.006 ± 0.001 | 3.43 ± 0.14 | < IDL | 171 ± 9 | 160 ± 5 | 0.724 ± 0.015 | 2.21 ± 0.15 | 1.78 ± 0.11 |
| **7** | 0.405 ± 0.024 | 0.005 ± 0.001 | 2.48 ± 0.14 | < IDL | 142 ± 9 | 132 ± 6 | 0.597 ± 0.021 | 1.85 ± 0.13 | 1.54 ± 0.09 |
| **8** | 0.454 ± 0.023 | 0.005 ± 0.001 | 2.47 ± 0.04 | < IDL | 148 ± 3 | 156 ± 5 | 0.715 ± 0.014 | 1.92 ± 0.06 | 1.77 ± 0.22 |
| **9** | 0.389 ± 0.016 | 0.008 ± 0.006 | 1.41 ± 0.07 | < IDL | 124 ± 3 | 111 ± 3 | 0.487 ± 0.015 | 1.57 ± 0.03 | 1.37 ± 0.14 |
| **10** | 0.296 ± 0.008 | 0.002 ± 0.001 | 0.867 ± 0.029 | < IDL | 90.7 ± 1.8 | 80.6 ± 1.8 | 0.338 ± 0.004 | 1.14 ± 0.03 | 0.830 ± 0.140 |
| **11** | 0.257 ± 0.010 | 0.001 ± 0.001 | 0.680 ± 0.016 | < IDL | 74.2 ± 1.8 | 71.2 ± 1.8 | 0.292 ± 0.001 | 0.928 ± 0.023 | 0.676 ± 0.180 |
| **12** | 0.238 ± 0.001 | 0.001 ± 0.001 | 0.573 ± 0.011 | < IDL | 68.2 ± 5.2 | 65.9 ± 0.4 | 0.266 ± 0.007 | 0.828 ± 0.016 | 0.549 ± 0.144 |
| **13** | 0.231 ± 0.012 | 0.001 ± 0.001 | 0.500 ± 0.009 | < IDL | 66.3 ± 8.4 | 63.0 ± 0.8 | 0.249 ± 0.005 | 0.783 ± 0.060 | 0.698 ± 0.382 |
| **14** | 0.213 ± 0.013 | < IDL | 0.418 ± 0.001 | < IDL | 59.8 ± 8.5 | 58.3 ± 1.0 | 0.227 ± 0.006 | 0.705 ± 0.052 | 0.460 ± 0.152 |
| **15** | 0.194 ± 0.013 | < IDL | 0.352 ± 0.007 | < IDL | 53.2 ± 6.7 | 54.3 ± 1.9 | 0.208 ± 0.008 | 0.628 ± 0.045 | 0.406 ± 0.124 |
| **16** | 0.182 ± 0.007 | < IDL | 0.312 ± 0.025 | < IDL | 48.3 ± 3.8 | 53.2 ± 2.5 | 0.201 ± 0.010 | 0.576 ± 0.017 | 0.411 ± 0.133 |

< IDL: less instrumental detection limit; SD: standard deviation

**Appendix D6. Bioaccessible conc. (mg $kg^{-1}$) of potentially toxic elements accumulated with extraction time obtained by extraction of the simulated $PM_{10}$ samples (BGS RM 102 Ironstone Soil on FDMS filter) using the single-pass dynamic model of the stomach phase of the unified bioaccessibility method (UBM) with fraction collection (SPFC-UBM)**

| Time (min) | As Mean (n=3) ± SD | Cd Mean (n=3) ± SD | Cr Mean (n=3) ± SD | Cu Mean (n=3) ± SD | Fe Mean (n=3) ± SD | Mn Mean (n=3) ± SD | Ni Mean (n=3) ± SD | Pb Mean (n=3) ± SD | Zn Mean (n=3) ± SD |
|---|---|---|---|---|---|---|---|---|---|
| **3.75** | 2.09 ± 0.12 | 0.111 ± 0.014 | 4.77 ± 0.80 | 3.05 ± 0.35 | 242 ± 38 | 869 ± 31 | 3.27 ± 0.16 | 2.94 ± 0.50 | 18.7 ± 0.9 |
| **7.5** | 3.30 ± 0.25 | 0.143 ± 0.016 | 9.74 ± 1.46 | 4.58 ± 0.60 | 522 ± 69 | 1270 ± 72 | 4.94 ± 0.34 | 6.92 ± 0.95 | 25.8 ± 1.7 |
| **11.25** | 4.11 ± 0.27 | 0.160 ± 0.016 | 15.6 ± 1.5 | 5.26 ± 0.69 | 780 ± 69 | 1570 ± 78 | 6.26 ± 0.40 | 10.9 ± 1.4 | 29.4 ± 2.1 |
| **15** | 4.76 ± 0.25 | 0.170 ± 0.016 | 21.6 ± 1.3 | 5.54 ± 0.74 | 1030 ± 59 | 1820 ± 74 | 7.40 ± 0.40 | 14.2 ± 1.2 | 31.9 ± 2.0 |
| **18.75** | 5.30 ± 0.22 | 0.181 ± 0.019 | 26.3 ± 1.0 | 5.60 ± 0.80 | 1240 ± 45 | 2030 ± 72 | 8.33 ± 0.40 | 17.0 ± 1.0 | 34.1 ± 2.0 |
| **22.5** | 5.75 ± 0.20 | 0.187 ± 0.019 | 29.8 ± 0.9 | < IDL | 1410 ± 39 | 2190 ± 72 | 9.06 ± 0.40 | 19.2 ± 1.0 | 35.8 ± 1.9 |
| **26.25** | 6.16 ± 0.19 | 0.192 ± 0.019 | 32.2 ± 0.8 | < IDL | 1560 ± 36 | 2320 ± 72 | 9.65 ± 0.42 | 21.0 ± 0.9 | 37.4 ± 1.9 |
| **30** | 6.61 ± 0.16 | 0.197 ± 0.019 | 34.7 ± 0.8 | < IDL | 1700 ± 34 | 2470 ± 69 | 10.4 ± 0.4 | 22.9 ± 0.9 | 39.1 ± 1.6 |
| **33.75** | 7.00 ± 0.15 | 0.204 ± 0.025 | 36.1 ± 0.8 | < IDL | 1830 ± 36 | 2580 ± 68 | 10.9 ± 0.4 | 24.5 ± 0.9 | 40.5 ± 1.8 |
| **37.5** | 7.30 ± 0.14 | 0.206 ± 0.025 | 37.0 ± 0.8 | < IDL | 1920 ± 36 | 2660 ± 67 | 11.2 ± 0.4 | 25.6 ± 0.9 | 41.3 ± 1.6 |
| **41.25** | 7.55 ± 0.14 | 0.208 ± 0.025 | 37.7 ± 0.8 | < IDL | 1990 ± 34 | 2740 ± 66 | 11.5 ± 0.4 | 26.6 ± 0.9 | 42.0 ± 1.5 |
| **45** | 7.79 ± 0.13 | 0.209 ± 0.025 | 38.3 ± 0.8 | < IDL | 2060 ± 39 | 2800 ± 66 | 11.8 ± 0.4 | 27.4 ± 0.9 | 42.6 ± 1.3 |
| **48.75** | 8.02 ± 0.15 | 0.210 ± 0.025 | 38.8 ± 0.8 | < IDL | 2130 ± 47 | 2860 ± 66 | 12.0 ± 0.4 | 28.2 ± 0.9 | 43.3 ± 1.3 |
| **52.5** | 8.24 ± 0.16 | < IDL | 39.2 ± 0.8 | < IDL | 2190 ±56 | 2920 ± 67 | 12.2 ± 0.4 | 28.9 ± 1.0 | 43.7 ± 1.2 |
| **56.25** | 8.43 ± 0.17 | < IDL | 39.5 ± 0.8 | < IDL | 2240 ± 62 | 2980 ± 67 | 12.4 ± 0.4 | 29.5 ± 1.0 | 44.1 ± 1.1 |
| **60** | 8.61 ± 0.17 | < IDL | 39.8 ± 0.8 | < IDL | 2290 ± 64 | 3030 ± 66 | 12.6 ± 0.4 | 30.1 ± 1.0 | 44.5 ± 1.0 |

< IDL: less instrumental detection limit; SD: standard deviation

**Appendix D7. Bioaccessible conc. (mg $kg^{-1}$) of potentially toxic elements for each subfraction obtained by extraction of the simulated $PM_{10}$ samples (NIST SRM 2711A Montana II Soil on FDMS filter) using the single-pass dynamic model of the stomach phase of the unified bioaccessibility method (UBM) with fraction collection (SPFC-UBM)**

| Subfraction number | As Mean (n=3) ± SD | Cd Mean (n=3) ± SD | Cr Mean (n=3) ± SD | Cu Mean (n=3) ± SD | Fe Mean (n=3) ± SD | Mn Mean (n=3) ± SD | Ni Mean (n=3) ± SD | Pb Mean (n=3) ± SD | Zn Mean (n=3) ± SD |
|---|---|---|---|---|---|---|---|---|---|
| **1** | 26.1 ± 2.5 | 28.5 ± 2.2 | 0.206 ± 0.034 | 33.9 ± 4.7 | 107 ± 21 | 81.5 ± 9.4 | 0.997 ± 0.118 | 606 ± 70 | 64.9 ± 6.4 |
| **2** | 12.1 ± 1.5 | 8.97 ± 1.14 | 0.118 ± 0.020 | 16.3 ± 2.2 | 110 ± 24 | 70.9 ± 11.5 | 0.493 ± 0.063 | 299 ± 35 | 27.4 ± 3.2 |
| **3** | 6.25 ± 0.43 | 4.18 ± 0.47 | 0.057 ± 0.005 | 7.31 ± 0.61 | 61.0 ± 2.6 | 48.8 ± 3.4 | 0.292 ± 0.017 | 299 ± 35 | 14.4 ± 1.4 |
| **4** | 3.96 ± 0.42 | 2.45 ± 0.38 | 0.033 ± 0.006 | 4.08 ± 0.77 | 36.4 ± 5.6 | 34.5 ± 2.1 | 0.203 ± 0.018 | 74.0 ± 13.9 | 9.30 ± 1.69 |
| **5** | 2.76 ± 0.26 | 1.66 ± 0.21 | 0.019 ± 0.004 | 2.54 ± 0.47 | 22.3 ± 5.9 | 24.7 ± 2.4 | 0.150 ± 0.014 | 47.1 ± 7.9 | 6.84 ± 1.15 |
| **6** | 2.07 ± 0.11 | 1.17 ± 0.16 | 0.012 ± 0.003 | 1.69 ± 0.21 | 14.8 ± 1.7 | 18.8 ± 1.1 | 0.118 ± 0.008 | 32.1 ± 4.2 | 5.25 ± 0.70 |
| **7** | 1.63 ± 0.13 | 0.896 ± 0.152 | 0.007 ± 0.002 | 1.19 ± 0.12 | 11.3 ± 1.7 | 14.6 ± 1.0 | 0.097 ± 0.008 | 23.4 ± 1.8 | 4.16 ± 0.53 |
| **8** | 1.37 ± 0.08 | 0.658 ± 0.129 | 0.005 ± 0.001 | 0.823 ± 0.067 | 8.05 ± 1.28 | 12.8 ± 0.8 | 0.089 ± 0.006 | 16.7 ± 1.2 | 3.67 ± 0.12 |
| **9** | 1.14 ± 0.19 | 0.463 ± 0.149 | 0.004 ± 0.004 | 0.567 ± 0.136 | 6.57 ± 1.42 | 10.6 ± 1.1 | 0.081 ± 0.012 | 11.9 ± 2.4 | 3.11 ± 0.49 |
| **10** | 0.813 ± 0.159 | 0.294 ± 0.099 | < IDL | 0.271 ± 0.141 | 5.97 ± 2.14 | 7.63 ± 1.01 | 0.056 ± 0.010 | 7.89 ± 1.71 | 2.44 ± 0.31 |
| **11** | 0.651 ± 0.103 | 0.224 ± 0.075 | < IDL | 0.099 ± 0.104 | 4.31 ± 2.13 | 6.08 ± 0.57 | 0.045 ± 0.008 | 5.80 ± 1.26 | 2.01 ± 0.21 |
| **12** | 0.546 ± 0.080 | 0.166 ± 0.063 | < IDL | < IDL | 3.19 ± 1.19 | 5.05 ± 0.33 | 0.038 ± 0.003 | 4.27 ± 1.11 | 1.67 ± 0.12 |
| **13** | 0.466 ± 0.067 | 0.128 ± 0.053 | < IDL | < IDL | < IDL | 4.19 ± 0.32 | 0.033 ± 0.005 | 3.32 ± 0.94 | 1.54 ± 0.11 |
| **14** | 0.417 ± 0.054 | 0.102 ± 0.039 | < IDL | < IDL | < IDL | 3.67 ± 0.21 | 0.032 ± 0.001 | 2.62 ± 0.58 | 1.41 ± 0.09 |
| **15** | 0.390 ± 0.044 | 0.089 ± 0.031 | < IDL | < IDL | 1.02 ± 0.82 | 3.35 ± 0.17 | 0.027 ± 0.004 | 2.29 ± 0.45 | 1.26 ± 0.15 |
| **16** | 0.394 ± 0.013 | 0.109 ± 0.004 | < IDL | < IDL | 1.27 ± 0.79 | 3.19 ± 0.07 | 0.028 ± 0.002 | 2.78 ± 0.21 | 1.31 ± 0.21 |

< IDL: less instrumental detection limit; SD: standard deviation

**Appendix D8. Bioaccessible conc. (mg $kg^{-1}$) of potentially toxic elements accumulated with extraction time obtained by extraction of the simulated $PM_{10}$ samples (NIST SRM 2711A Montana II Soil on FDMS filter) using the single-pass dynamic model of the stomach phase of the unified bioaccessibility method (UBM) with fraction collection (SPFC-UBM)**

| Time (min) | As Mean (n=3) ± SD | Cd Mean (n=3) ± SD | Cr Mean (n=3) ± SD | Cu Mean (n=3) ± SD | Fe Mean (n=3) ± SD | Mn Mean (n=3) ± SD | Ni Mean (n=3) ± SD | Pb Mean (n=3) ± SD | Zn Mean (n=3) ± SD |
|---|---|---|---|---|---|---|---|---|---|
| **3.75** | 26.1 ± 2.5 | 28.5 ± 2.2 | 0.206 ± .0034 | 33.9 ± 4.7 | 107 ± 21 | 81.5 ± 9.4 | 1.00 ± 0.12 | 606 ± 80 | 64.9 ± 6.4 |
| **7.5** | 38.1 ± 3.1 | 37.5 ± 2.1 | 0.325 ± .0042 | 50.2 ± 5.9 | 217 ± 41 | 152 ± 18 | 1.49 ± 0.14 | 905 ± 96 | 92.3 ± 6.2 |
| **11.25** | 44.4 ± 3.0 | 41.7 ± 2.0 | 0.382 ± 0.040 | 57.5 ± 5.5 | 278 ± 43 | 201 ± 20 | 1.78 ± 0.14 | 1200 ± 120 | 107 ± 5 |
| **15** | 48.3 ± 2.6 | 44.2 ± 1.7 | 0.415 ± 0.036 | 61.6 ± 4.9 | 315 ± 38 | 236 ± 19 | 1.99 ± 0.12 | 1280 ± 108 | 116 ± 4 |
| **18.75** | 51.1 ± 2.4 | 45.8 ± 1.6 | 0.434 ± 0.032 | 64.2 ± 4.5 | 337 ± 32 | 260 ± 17 | 2.14 ± 0.11 | 1320 ± 102 | 123 ± 3 |
| **22.5** | 53.2 ± 2.4 | 47.0 ± 1.6 | 0.446 ± 0.032 | 65.9 ± 4.3 | 352 ± 31 | 279 ± 17 | 2.25 ± 0.11 | 1360 ± 98 | 128 ± 3 |
| **26.25** | 54.8 ± 2.5 | 47.9 ± 1.6 | 0.452 ± 0.033 | 67.0 ± 4.3 | 363 ± 32 | 294 ± 17 | 2.35 ± 0.12 | 1380 ± 98 | 132 ± 3 |
| **30** | 56.2 ± 2.5 | 48.5 ± 1.8 | 0.458 ± 0.032 | 67.9 ± 4.3 | 371 ± 32 | 306 ± 17 | 2.44 ± 0.12 | 1400 ± 99 | 136 ± 3 |
| **33.75** | 57.3 ± 2.7 | 49.0 ± 1.9 | 0.462 ± 0.036 | 68.4 ± 4.4 | 378 ± 32 | 317 ± 18 | 2.52 ± 0.13 | 1410 ± 100 | 139 ± 3 |
| **37.5** | 58.1 ± 2.9 | 49.3 ± 2.0 | < IDL | 68.7 ± 4.5 | 384 ± 43 | 325 ± 19 | 2.58 ± 0.14 | 1420 ± 102 | 141 ± 3 |
| **41.25** | 58.8 ± 3.0 | 49.5 ± 2.1 | < IDL | 68.8 ± 4.6 | 388 ± 36 | 331 ± 20 | 2.62 ± 0.15 | 1420 ± 103 | 143 ± 3 |
| **45** | 59.3 ± 3.0 | 49.7 ± 2.1 | < IDL | < IDL | 391 ± 37 | 336 ± 20 | 2.66 ± 0.15 | 1430 ± 104 | 145 ± 3 |
| **48.75** | 59.8 ± 3.1 | 49.8 ± 2.2 | < IDL | < IDL | < IDL | 340 ± 20 | 2.69 ± 0.15 | 1430 ± 105 | 147 ± 3 |
| **52.5** | 60.2 ± 3.2 | 49.9 ± 2.2 | < IDL | < IDL | < IDL | 344 ± 20 | 2.72 ± 0.15 | 1430 ± 106 | 148 ± 3 |
| **56.25** | 60.6 ± 3.2 | 50.0 ± 2.2 | < IDL | < IDL | < IDL | 347 ± 21 | 2.75 ± 0.15 | 1430 ± 106 | 149 ± 3 |
| **60** | 61.0 ± 3.2 | 50.1 ± 2.3 | < IDL | < IDL | < IDL | 350 ± 20 | 2.78 ± 0.15 | 1440 ± 106 | 151 ± 3 |

< IDL: less instrumental detection limit; SD: standard deviation

**Appendix E1. Bioaccessible conc. (mg $kg^{-1}$) of potentially toxic elements accumulated with extraction time obtained by extraction of the simulated $PM_{10}$ samples (NIST SRM 2711A Montana II Soil on FDMS filter) using the single-pass dynamic model of the simplified bioaccessibility extraction test (SBET) with direct coupling to ICP-MS (SPDC-SBET)**

| Time (min) | As Mean (n=3) ± SD | Cd Mean (n=3) ± SD | Cr Mean (n=3) ± SD | Cu Mean (n=3) ± SD | Fe Mean (n=3) ± SD | Mn Mean (n=3) ± SD | Ni Mean (n=3) ± SD | Pb Mean (n=3) ± SD | Zn Mean (n=3) ± SD |
|---|---|---|---|---|---|---|---|---|---|
| **5** | 31.2 ± 8.3 | 37.0 ± 15.4 | < IDL | 35.9 ± 12.6 | 128 ± 29 | 71.3 ± 20.6 | 0.969 ± 0.113 | 680 ± 119 | 68.4 ± 32.7 |
| **10** | 42.9 ± 10.1 | 45.7 ± 16.5 | < IDL | 48.5 ± 14.7 | 210 ± 44 | 96.0 ± 24.3 | 1.33 ± 0.15 | 908 ± 144 | 84.8 ± 36.7 |
| **15** | 47.9 ± 10.4 | 48.2 ± 16.5 | < IDL | 53.8 ± 14.9 | 257 ± 47 | 109 ± 25 | 1.47 ± 0.22 | 993 ± 138 | 89.3 ± 37.4 |
| **20** | 51.1 ± 10.7 | 49.6 ± 16.4 | < IDL | 57.2 ± 15.0 | 292 ± 48 | 118 ± 25 | 1.57 ± 0.30 | 1040 ± 137 | 92.1 ± 37.9 |
| **25** | 53.5 ± 10.9 | 50.5 ± 16.3 | < IDL | 59.6 ± 14.9 | 322 ± 47 | 127 ± 25 | 1.66 ± 0.37 | 1080 ± 136 | 95.2 ± 38.0 |
| **30** | 55.2 ± 11.2 | 51.0 ± 16.3 | < IDL | 61.3 ± 15.9 | 346 ± 47 | 135 ± 26 | 1.73 ± 0.43 | 1100 ± 137 | 98.0 ± 38.2 |
| **35** | 56.4 ± 11.5 | 51.4 ± 16.3 | < IDL | 62.5 ± 15.0 | 366 ± 47 | 141 ± 26 | 1.79 ± 0.48 | 1120 ± 139 | 100 ± 38 |
| **40** | 57.2 ± 11.8 | 51.6 ± 16.3 | < IDL | 63.4 ± 15.0 | 383 ± 47 | 146 ± 26 | 1.84 ± 0.52 | 1130 ± 140 | 102 ± 39 |
| **45** | 57.8 ± 12.1 | 51.8 ± 16.3 | < IDL | 64.2 ± 15.1 | 398 ± 48 | 151 ± 26 | 1.88 ± 0.56 | 1140 ± 142 | 104 ± 39 |
| **50** | 58.2 ± 12.5 | 51.9 ± 16.3 | < IDL | 64.7 ± 15.2 | 410 ± 49 | 156 ± 26 | 1.92 ± 0.59 | 1150 ± 143 | 106 ± 39 |
| **55** | 58.4 ± 12.7 | 52.0 ± 16.4 | < IDL | 65.1 ± 15.2 | 419 ± 49 | 159 ± 26 | 1.95 ± 0.61 | 1155 ± 143 | 107 ± 40 |
| **60** | 60.4 ± 15.2 | 52.4 ± 16.9 | < IDL | 66.3 ± 16.5 | 448 ± 78 | 168 ± 33 | 2.05 ± 0.50 | 1170 ± 155 | 113 ± 47 |

< IDL: less instrumental detection limit; SD: standard deviation

**Appendix E2. Bioaccessible As concentration (mg $kg^{-1}$) in simulated $PM_{10}$ samples, prepared using NIST SRM 2711A Montana II Soil, obtained by applying the single-pass dynamic model of the simplified bioaccessibility extraction test (SBET) with direct coupling to ICP-MS (SPDC-SBET)**

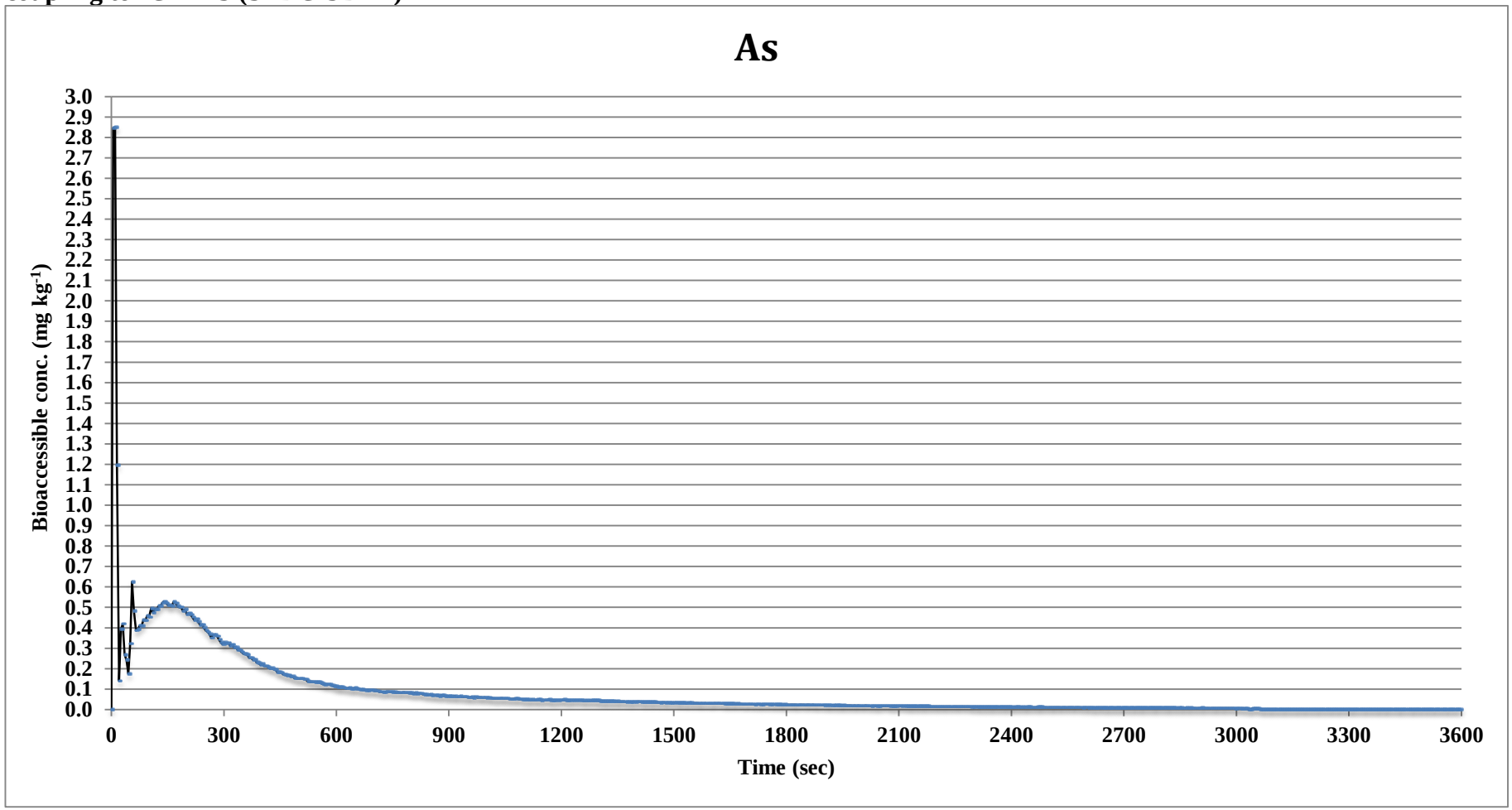

**Appendix E3. Bioaccessible Cd concentration (mg $kg^{-1}$) in simulated $PM_{10}$ samples, prepared using NIST SRM 2711A Montana II Soil, obtained by applying the single-pass dynamic model of the simplified bioaccessibility extraction test (SBET) with direct coupling to ICP-MS (SPDC-SBET)**

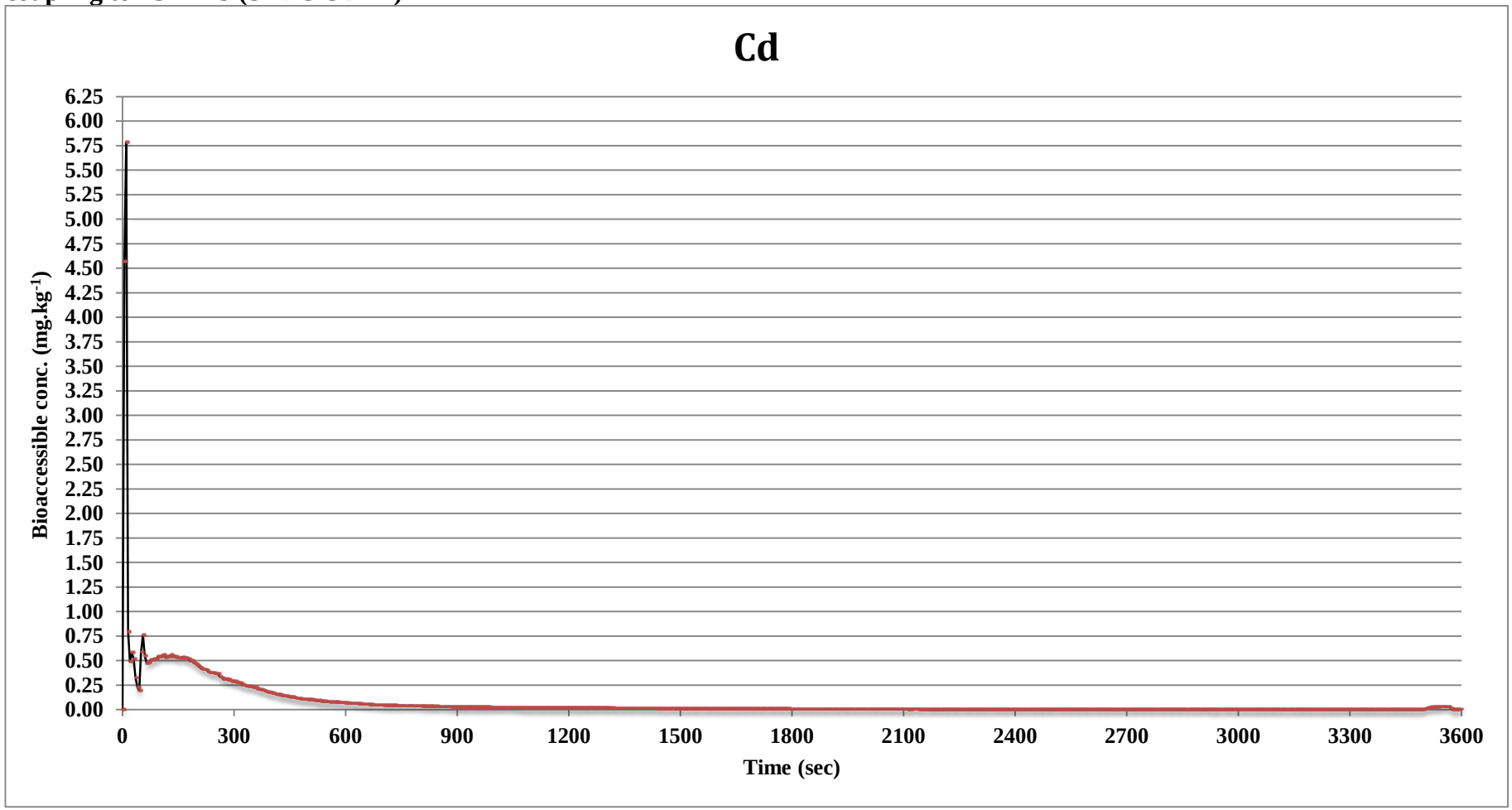

**Appendix E4. Bioaccessible Cu concentration (mg $kg^{-1}$) in simulated $PM_{10}$ samples, prepared using NIST SRM 2711A Montana II Soil, obtained by applying the single-pass dynamic model of the simplified bioaccessibility extraction test (SBET) with direct coupling to ICP-MS (SPDC-SBET)**

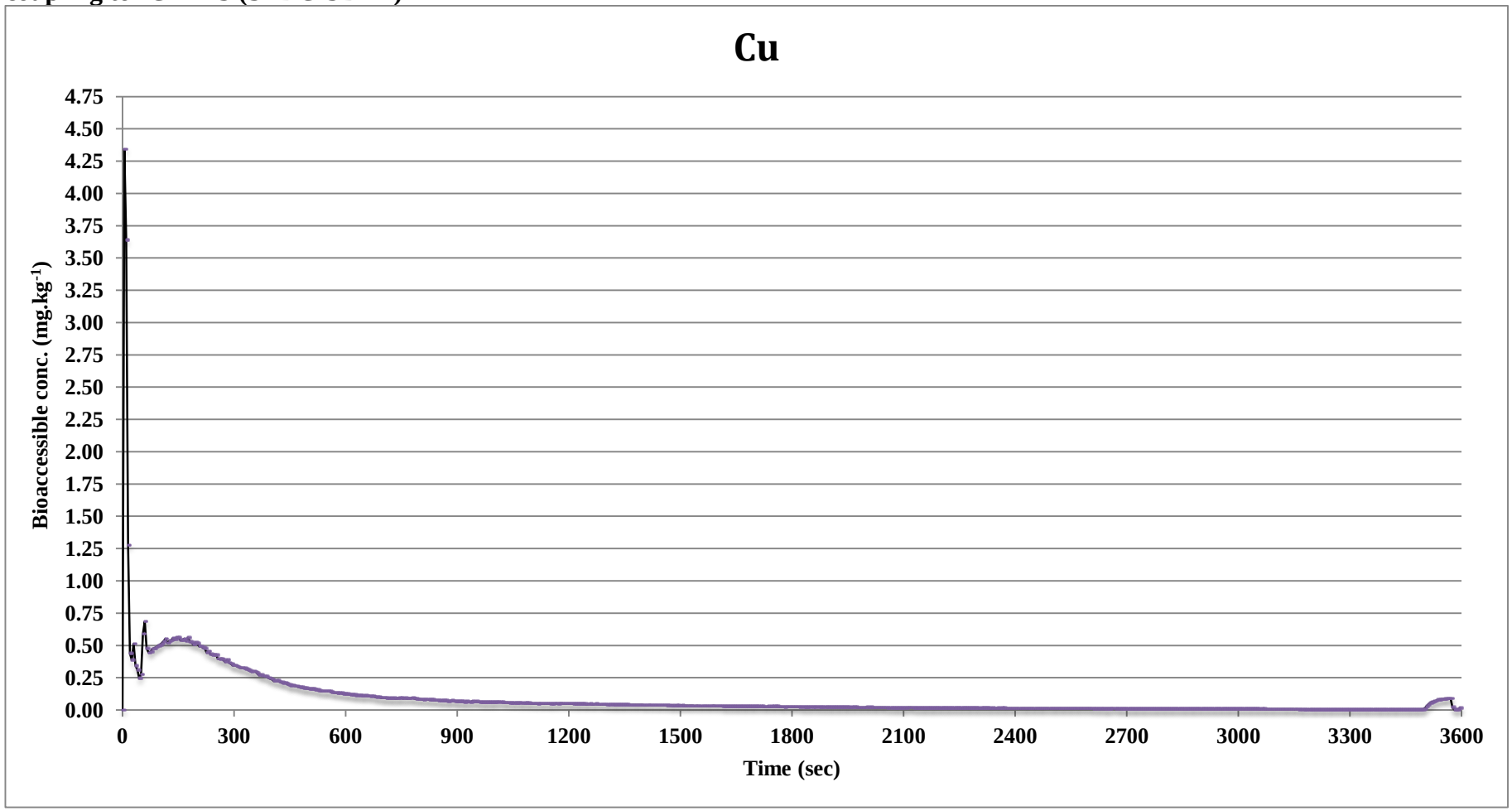

**Appendix E5. Bioaccessible Fe concentration (mg $kg^{-1}$) in simulated $PM_{10}$ samples, prepared using NIST SRM 2711A Montana II Soil, obtained by applying the single-pass dynamic model of the simplified bioaccessibility extraction test (SBET) with direct coupling to ICP-MS (SPDC-SBET)**

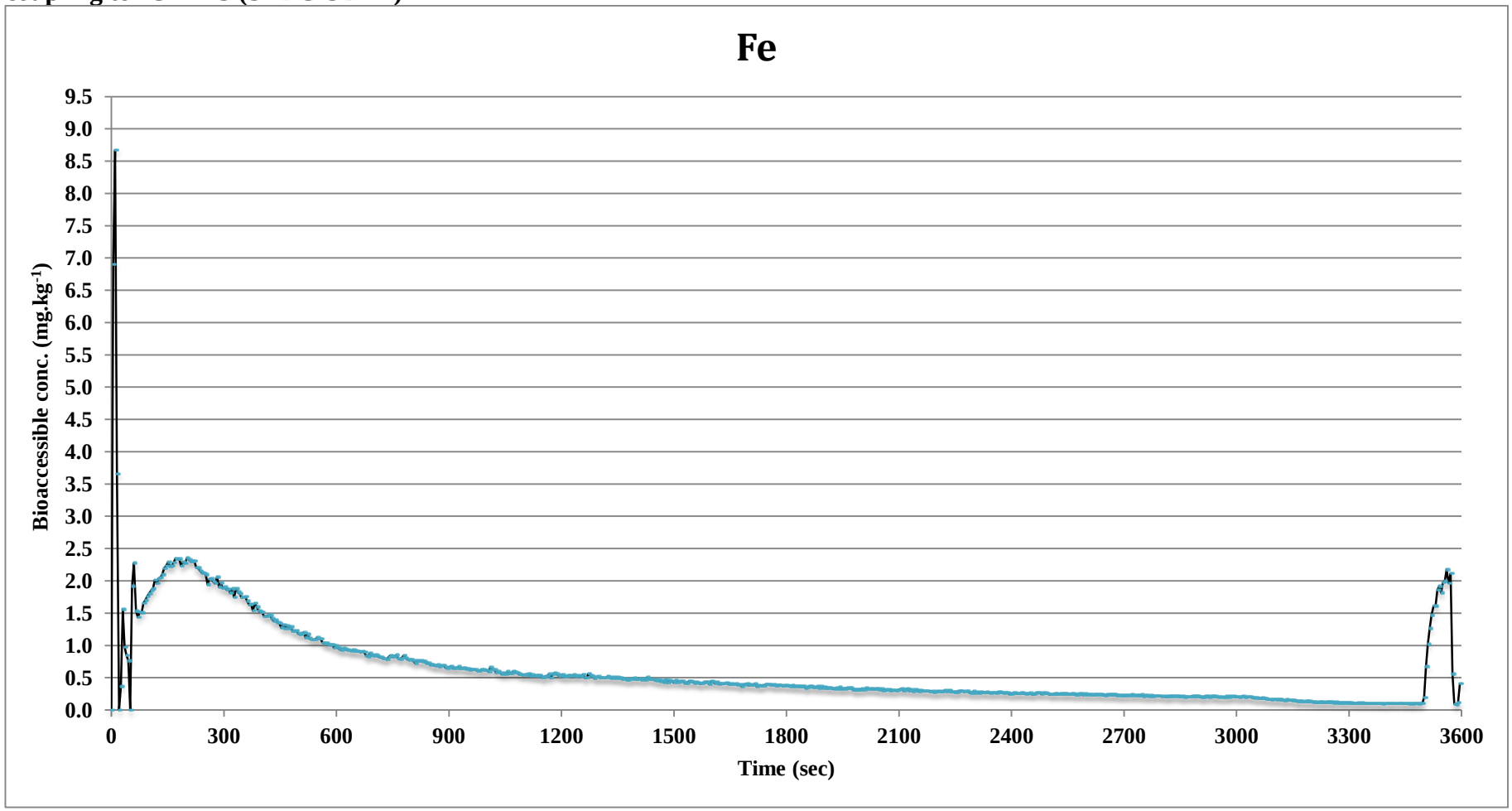

**Appendix E6. Bioaccessible Mn concentration (mg $kg^{-1}$) in simulated $PM_{10}$ samples, prepared using NIST SRM 2711A Montana II Soil, obtained by applying the single-pass dynamic model of the simplified bioaccessibility extraction test (SBET) with direct coupling to ICP-MS (SPDC-SBET)**

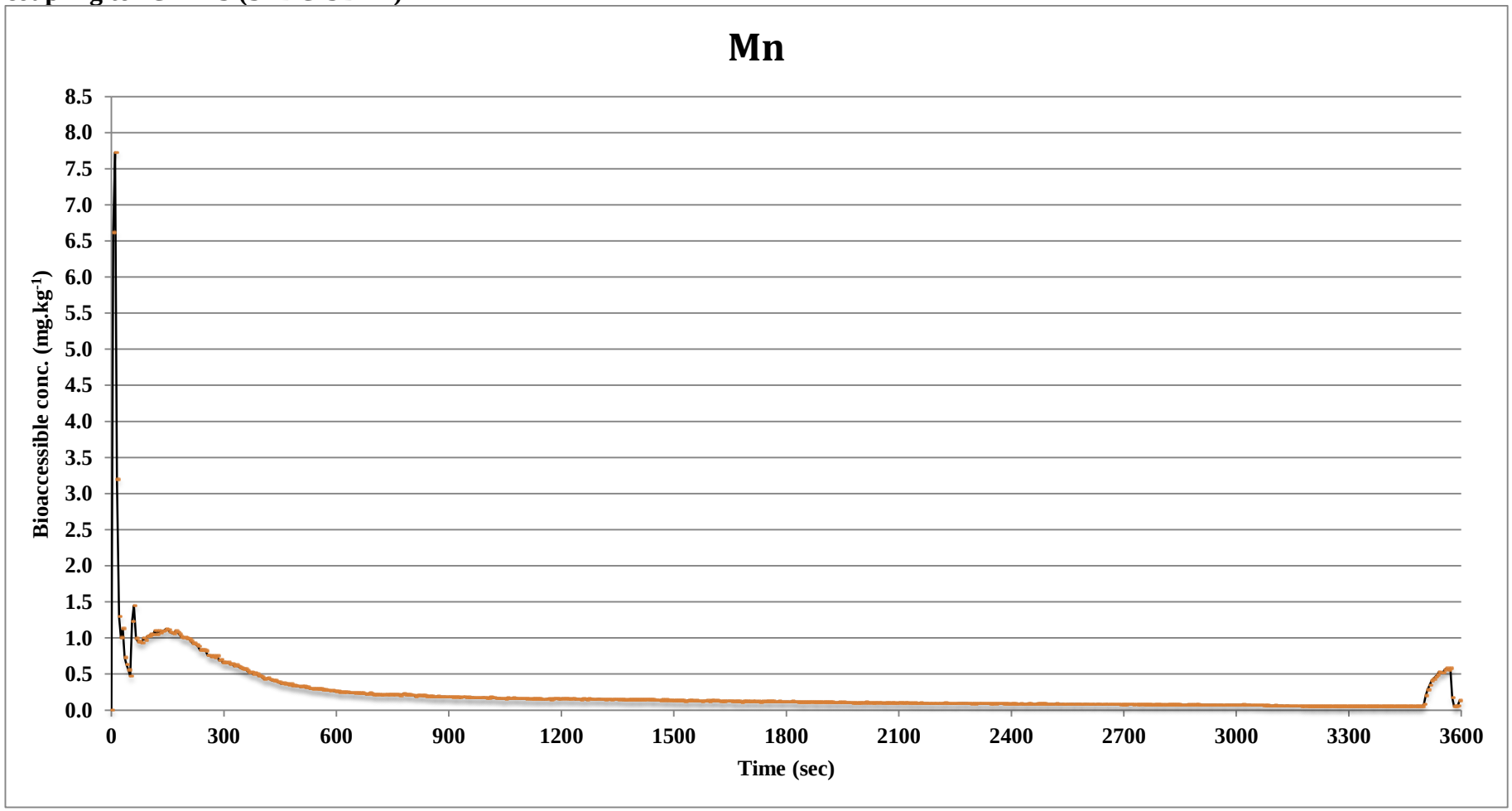

**Appendix E7. Bioaccessible Ni concentration (mg $kg^{-1}$) in simulated $PM_{10}$ samples, prepared using NIST SRM 2711A Montana II Soil, obtained by applying the single-pass dynamic model of the simplified bioaccessibility extraction test (SBET) with direct coupling to ICP-MS (SPDC-SBET)**

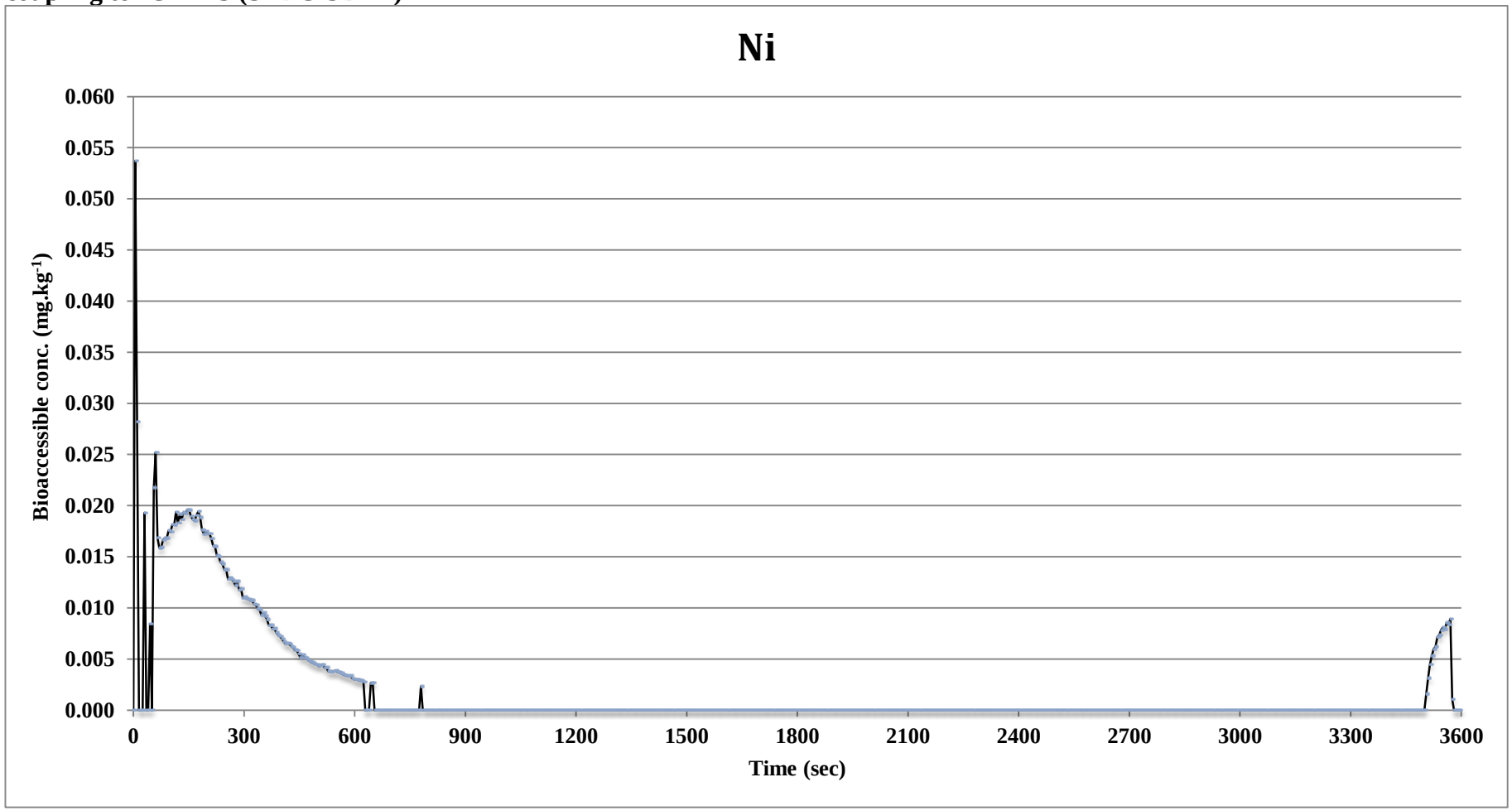

**Appendix E8. Bioaccessible Pb concentration (mg $kg^{-1}$) in simulated $PM_{10}$ samples, prepared using NIST SRM 2711A Montana II Soil, obtained by applying the single-pass dynamic model of the simplified bioaccessibility extraction test (SBET) with direct coupling to ICP-MS (SPDC-SBET)**

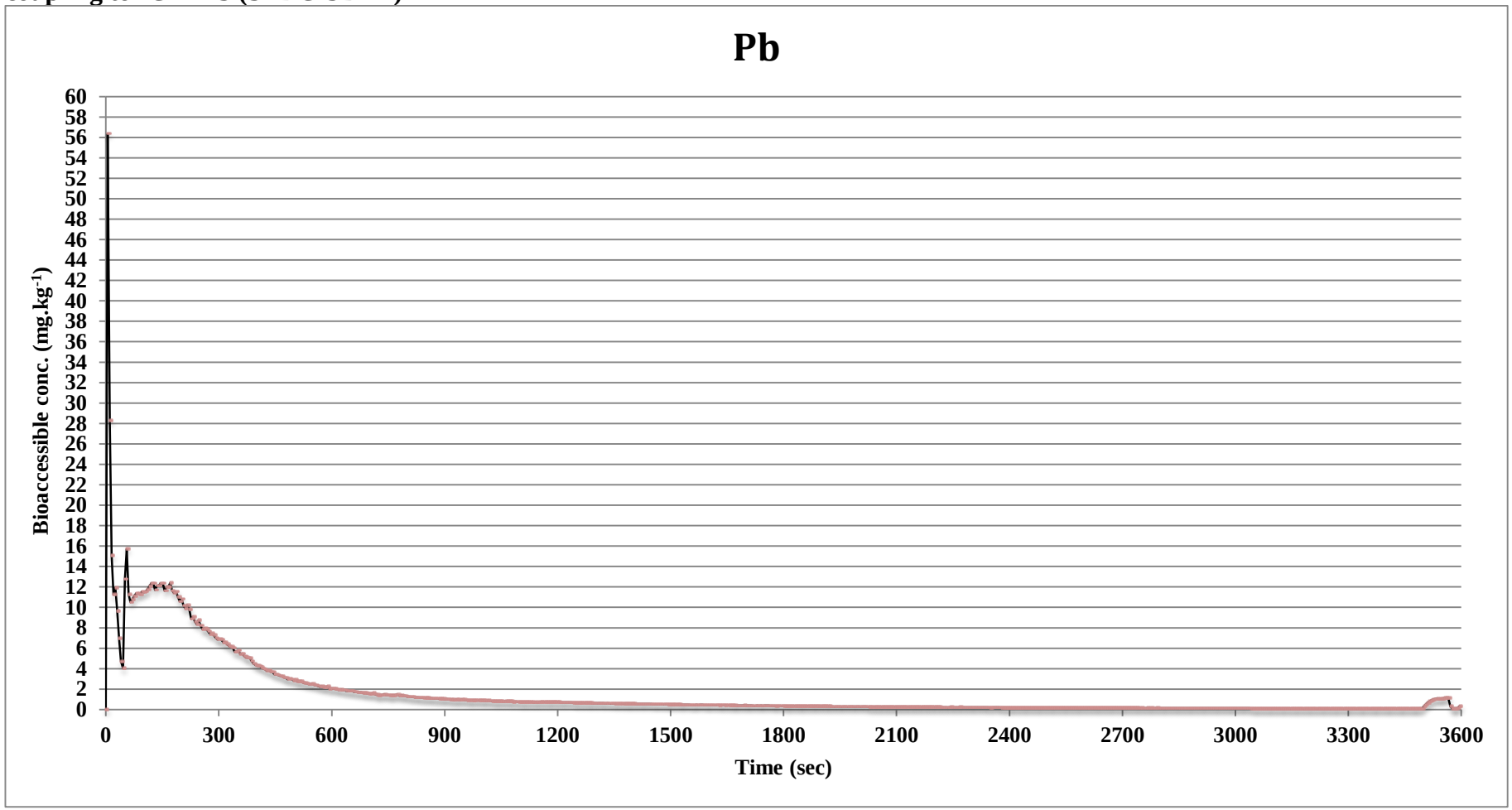

**Appendix E9. Bioaccessible Zn concentration (mg $kg^{-1}$) in simulated $PM_{10}$ samples, prepared using NIST SRM 2711A Montana II Soil, obtained by applying the single-pass dynamic model of the simplified bioaccessibility extraction test (SBET) with direct coupling to ICP-MS (SPDC-SBET)**

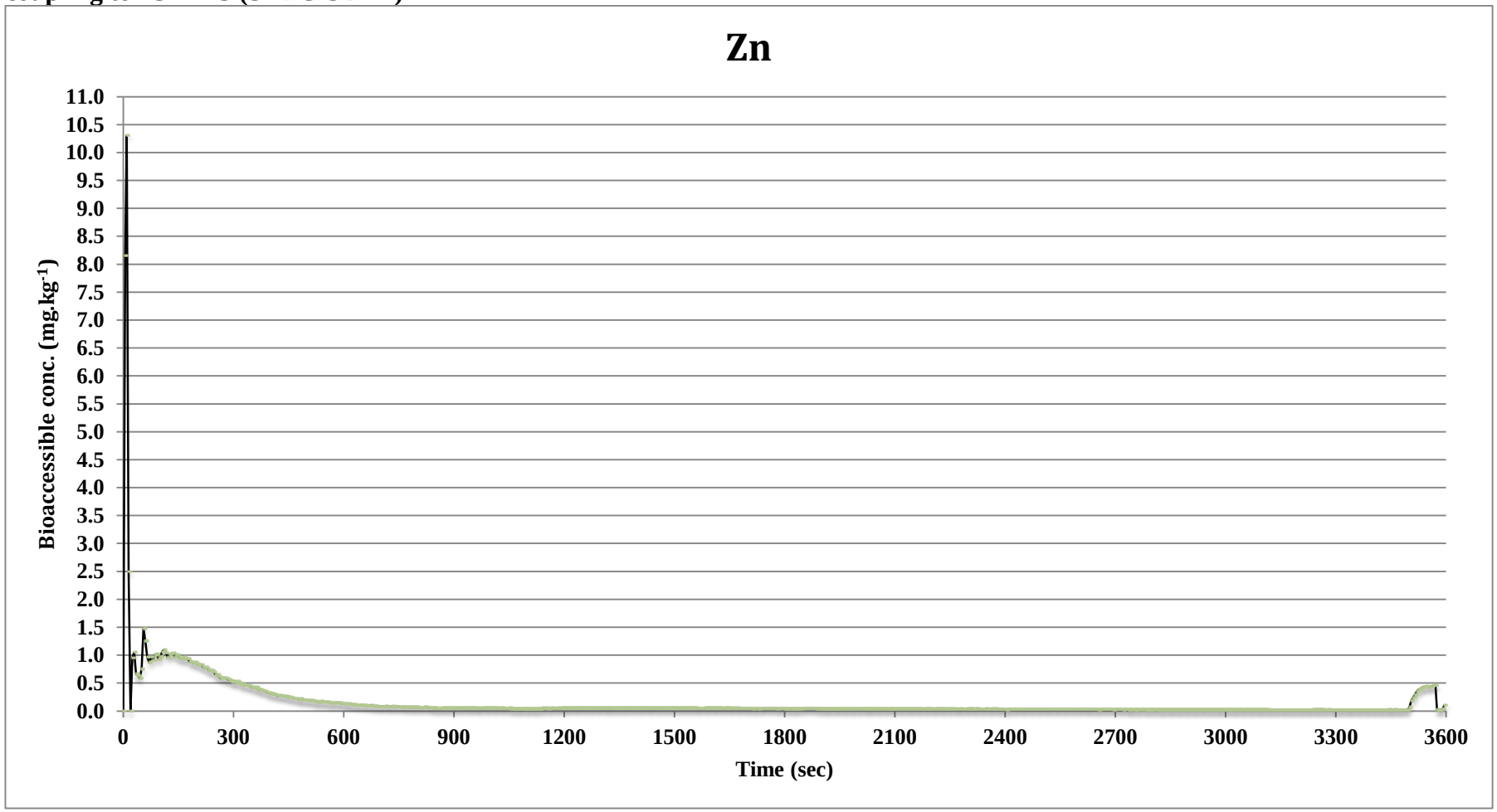

**Appendix F1. F test for the bioaccessible concentration of potentially toxic elements (PTE) in BGS RM 102 Ironstone Soil alone and in simulated $PM_{10}$ samples (BGS RM 102 Ironstone Soil on FDMS filters) by using artificial mucus fluid (AMF) only and by AMF sequentially with the simplified bioaccessibility extraction test (SBET2) or with the stomach phase of the unified bioaccessibility method (gastric fluid only) (UBMG) as well as for PTE bioaccessible concentration by using normal procedure of the SBET (*i.e.* SBET1) or the stomach phase of the UBM (UBMSG)**

| | AMF (Between soil alone and soil on FDMS filters) (ν =5) | | Between SBET1 and SBET2 (For soil alone) (ν =2) | | Between UBMSG and UBMG (For soil alone) (ν =2) | | Between SBET1 and SBET2 (For soil on FDMS filters) (ν =2) | | Between UBMSG and UBMG (For soil on FDMS filters) (ν =2) | |
|---|---|---|---|---|---|---|---|---|---|---|
| **PTE** | **F calculated** | **F critical** | **F calculated** | **F critical** | **F calculated** | **F critical** | **F calculated** | **F critical** | **F calculated** | **F critical** |
| **As** | 1.91 | 7.15 | 12.4 | 39.0 | 4.56 | 39.0 | 1.12 | 39.0 | 1.26 | 39.0 |
| **Cd** | - | - | 2.78 | 39.0 | 42.3 | 39.0 | 5.44 | 39.0 | 12.3 | 39.0 |
| **Cr** | - | - | 5.88 | 39.0 | 1.20 | 39.0 | 21.2 | 39.0 | 22.8 | 39.0 |
| **Cu** | 1.31 | 7.15 | 12.5 | 39.0 | 8.18 | 39.0 | 13.0 | 39.0 | 20.8 | 39.0 |
| **Fe** | - | - | 55.0 | 39.0 | 1.06 | 39.0 | 2.45 | 39.0 | 2.92 | 39.0 |
| **Pb** | - | - | 44.3 | 39.0 | 1.84 | 39.0 | 1.01 | 39.0 | 1.67 | 39.0 |
| **Mn** | 2.21 | 7.15 | 1.55 | 39.0 | 5.32 | 39.0 | 2.73 | 39.0 | 6.93 | 39.0 |
| **Ni** | 2.25 | 7.15 | 1.32 | 39.0 | 19.9 | 39.0 | 1.81 | 39.0 | 1.80 | 39.0 |
| **Zn** | - | - | 2.77 | 39.0 | 4.52 | 39.0 | 8.25 | 39.0 | 4.68 | 39.0 |

ν: degree of freedom; A significance level (α) =0.05

**Appendix F2. T test for the bioaccessible concentrations of potentially toxic elements (PTE) in BGS RM 102 Ironstone Soil only and in simulated $PM_{10}$ samples (BGS RM 102 Ironstone Soil on FDMS filters) by using artificial mucus fluid (AMF) only and by AMF sequentially with the simplified bioaccessibility extraction test (SBET2) or with the stomach phase of the unified bioaccessibility method (gastric fluid only) (UBMG) as well as PTE bioaccessible concentration by using normal procedure of the SBET (*i.e.* SBET1) or the stomach phase of the UBM (UBMSG)**

| | AMF (Between soil alone and soil on FDMS filters) (ν =10) | | Between SBET2 and SBET1 (For soil alone) (ν =4[a], 2[b]) | | Between UBMG and UBMSG (For soil alone) (ν =4[a], 2[b]) | | Between SBET2 and SBET1 (For soil on FDMS filters) (ν =4) | | Between UBMG and UBMSG (For soil on FDMS filters) (ν =4) | |
|---|---|---|---|---|---|---|---|---|---|---|
| **PTE** | **t calculated** | **t critical** | **t calculated** | **t critical** | **t calculated** | **t critical** | **t calculated** | **t critical** | **t calculated** | **t critical** |
| **As** | 2.22 | 2.23 | 41.84 | 2.78[a] | 1.39 | 2.78[a] | 37.44 | 2.78 | 4.19 | 2.78 |
| **Cd** | - | - | 10.40 | 2.78[a] | 0.00 | 4.30[b] | 9.78 | 2.78 | 0.16 | 2.78 |
| **Cr** | - | - | 18.95 | 2.78[a] | 3.22 | 2.78[a] | 11.08 | 2.78 | 0.91 | 2.78 |
| **Cu** | 0.58 | 2.23 | 7.33 | 2.78[a] | 7.67 | 2.78[a] | 9.60 | 2.78 | 4.30 | 2.78 |
| **Fe** | - | - | 5.72 | 4.30[b] | 7.39 | 2.78[a] | 2.48 | 2.78 | 14.92 | 2.78 |
| **Pb** | - | - | 32.74 | 4.30[b] | 7.42 | 2.78[a] | 16.95 | 2.78 | 3.20 | 2.78 |
| **Mn** | 4.44 | 2.23 | 7.19 | 2.78[a] | 1.32 | 2.78[a] | 1.44 | 2.78 | 1.96 | 2.78 |
| **Ni** | 0.93 | 2.23 | 8.91 | 2.78[a] | 1.74 | 2.78[a] | 0.48 | 2.78 | 6.88 | 2.78 |
| **Zn** | - | - | 7.30 | 2.78[a] | 3.53 | 2.78[a] | 2.52 | 2.78 | 1.93 | 2.78 |

ν: degree of freedom; A significance level (α) =0.05

**Appendix F3. The ratio of the sum of the bioaccessible concentrations of potentially toxic element (PTE) in simulated $PM_{10}$ samples (soil on FDMS filters) extracted by artificial mucus fluid (AMF) alone and by AMF sequentially with the simplified bioaccessibility extraction test (SBET2) to the PTE bioaccessible concentration by using the SBET (*i.e.* SBET1) procedure alone**

| PTE | AMF only (Mean ± SD) (n = 6) | SBET2 (Mean ± SD) (n = 3) | AMF+SBET2 (Mean ± SDc) | SBET1 (Mean ± SD) (n = 3) | ((AMF+SBET2)/SBET1) × 100 |
|---|---|---|---|---|---|
| **As** | 0.828 ± 0.021 | 2.98 ± 0.07 | 3.81 ± 0.07 | 1.66 ± 0.07 | 229 ± 11 |
| **Cd** | < IDL | 0.145 ± 0.003 | 0.145 ± 0.003 | 0.188 ± 0.007 | 77.1 ± 3.3 |
| **Cr** | < IDL | 30.5 ± 0.2 | 30.5 ± 0.2 | 23.3 ± 1.1 | 131 ± 6 |
| **Cu** | 1.90 ± 0.11 | 6.36 ± 0.08 | 8.26 ± 0.14 | 6.62 ± 0.29 | 125 ± 6 |
| **Fe** | < IDL | 1033 ± 14 | 1033 ± 14 | 1071 ± 22 | 96.5 ± 2.4 |
| **Mn** | 9.76 ± 1.19 | 1800 ± 26 | 1810 ± 26 | 1762 ± 43 | 103 ± 3 |
| **Ni** | 0.222 ± 0.033 | 7.79 ± 0.15 | 8.01 ± 0.15 | 7.93 ± 0.2 | 101 ± 3 |
| **Pb** | < IDL | 17.8 ± 0.3 | 17.8 ± 0.3 | 13.4 ± 0.3 | 133 ± 4 |
| **Zn** | < IDL | 21.9 ± 2.9 | 21.9 ± 2.9 | 34.8 ± 8.4 | 62.9 ± 17.3 |

SD: standard deviation; SDc: combined standard deviation; n: number of replicates; < IDL: less than instrumental detection limit

**Appendix F4. The ratio of the sum of the bioaccessible concentrations of potentially toxic element (PTE) in simulated $PM_{10}$ samples (soil on FDMS filters) extracted by artificial mucus fluid (AMF) alone and by AMF sequentially with the stomach phase (gastric fluid only) of the unified bioaccessibility method (UBMG) to the PTE bioaccessible concentration by using the UBMSG procedures alone**

| PTE | AMF only (Mean ± SD) (n = 6) | UBMG (Mean ± SD) (n = 3) | AMF+UBMG (Mean ± SDc) | UBMSG (Mean ± SD) (n = 3) | ((AMF+UBMG)/UBMSG) × 100 |
|---|---|---|---|---|---|
| **As** | 0.828 ± 0.021 | 3.38 ± 0.07 | 4.21 ± 0.07 | 4.41 ± 0.07 | 95.4 ± 2.2 |
| **Cd** | < IDL | 0.219 ± 0.021 | 0.219 ± 0.021 | 0.217 ± 0.006 | 101 ± 10 |
| **Cr** | < IDL | 33.9 ± 2.1 | 33.9 ± 2.1 | 35.0 ± 0.4 | 96.9 ± 6.1 |
| **Cu** | 1.90 ± 0.11 | 7.11 ± 0.80 | 9.01 ± 0.81 | 7.01 ± 0.18 | 129 ± 12 |
| **Fe** | < IDL | 842 ± 26 | 842 ± 26 | 1289 ± 45 | 65.3 ± 3.0 |
| **Mn** | 9.76 ± 1.19 | 2600 ± 144 | 2610 ± 144 | 2776 ± 55 | 94.0 ± 5.5 |
| **Ni** | 0.222 ± 0.033 | 10.4 ± 0.3 | 10.6 ± 0.3 | 12.2 ± 0.2 | 87.1 ± 2.9 |
| **Pb** | < IDL | 21.6 ± 1.1 | 21.6 ± 1.1 | 18.4 ± 1.4 | 117 ± 11 |
| **Zn** | < IDL | 30.9 ± 1.8 | 30.9 ± 1.8 | 35.6 ± 3.8 | 86.8 ± 10.6 |

SD: standard deviation; SDc: combined standard deviation; n: number of replicates; < IDL: less than instrumental detection limit